

ALEXANDRE GÓES MARTINI

RENIN SYNTHESIZING CELLS IN THE KIDNEY AND BEYOND  
“CÉLULAS PRODUTORAS DE RENINA NO RIM E ALÉM”

BRASÍLIA, 2018

**UNIVERSIDADE DE BRASÍLIA  
FACULDADE DE MEDICINA  
PROGRAMA DE PÓS-GRADUAÇÃO EM CIÊNCIAS DA SAÚDE**

**ALEXANDRE GÓES MARTINI**

**RENIN SYNTHESIZING CELLS IN THE KIDNEY AND BEYOND  
“CÉLULAS PRODUTORAS DE RENINA NO RIM E ALÉM”**

**Tese de Doutorado apresentada como requisito parcial para obtenção do título de Doutor em Ciências da Saúde pelo Programa de Pós-Graduação em Ciências da Saúde da Universidade de Brasília.**

**Orientador: Prof. Dr. Francisco de Assis Rocha Neves**

**BRASÍLIA  
2018**

**ALEXANDRE GÓES MARTINI**

**RENIN SYNTHESIZING CELLS IN THE KIDNEY AND BEYOND  
“CÉLULAS PRODUTORAS DE RENINA NO RIM E ALÉM”**

Tese de Doutorado apresentada como requisito parcial para obtenção do título de Doutor em Ciências da Saúde pelo Programa de Pós-Graduação em Ciências da Saúde da Universidade de Brasília.

Aprovada em: \_\_\_\_\_ de \_\_\_\_\_ de 2018.

**BANCA EXAMINADORA**

**Prof. Dr. Francisco de Assis Rocha Neves (presidente)  
Universidade de Brasília – UnB**

**Profa. Dra. Angélica Amorim Amato (membro)  
Universidade de Brasília – UnB**

**Profa. Dra. Dulce Elena Casarini (membro)  
Universidade Federal de São Paulo – UNIFESP**

**Profa. Dra. Maria Luiza de Moraes Barreto de Chaves (membro)  
Universidade de São Paulo – USP**

**Profa. Dra. Flora Aparecida Milton (suplente)  
Universidade Federal Fluminense – UFF**

*À minha mãe, Ana Góes, e às minhas tias por seu amor incondicional e princípios inabaláveis que regem minha vida.*

*À minha querida esposa, Luciana, por seu amor e paciência por todo o tempo que estive envolvido nesta tese*

## ACKNOWLEDGEMENT

It has been almost eight years since my arrival at the Laboratory of Molecular Pharmacology (Farmol) in the University of Brasilia (UnB). I must confess I arrived there very raw and inexperienced, despite my great passion on Science. The pathway was full of hurdles, but I had great people on my side all the time. I owe my success to everyone close to me in this long journey, with whom I have learned many lessons, which will be kept forever. Hence, I would like to acknowledge people who have supported me along this quest.

First, I would like to thank the mentor who has accompanied me since the beginning: Prof Dr. Francisco de Assis Rocha Neves. He was responsible to guide me into the reasearch, and without him, this journey would not be feasible. Besides, I must express all my gratitude to the members of Farmol for their help and priceless support along the years: Rilva, Luciano, Cristina, Flora, Maurício, Mariela, Caroline Lima, Carol, Isabela, Pedro, Cíntia, Dileesh, Henrique, Simone, Fernanda, Janice, Isadora and Sidney. In addition, my special thanks to the Farmol Professors, with whom I had the opportunity to work with: Angélica, Marie, Simeoni, Guilherme, Fátima, Adriana, Marília, Carine and Michela.

My profound gratitude to the ErasmusMC university, where I had the privilege to be and work for awhile. Particularly, I would like to thank my promotor in the Netherlands: Prof Dr AHJ Danser. His guidance was essential for this thesis. There are not enough words to express how grateful I am for everything he has done for me. Especially, I could not forget to mention Edith Friesema for the priceless support in Rotterdam, and also my mexican friends: Alejandro Labastida and Amada Eloisa Rubio-Beltran. They have become not only friends, but my family abroad.

Moreover, my special thanks for Prof Dr. Timothy Reudelhuber, which even retired, provided me the backbone project in Rotterdam, and Prof. Dr. Elena Casarini, who introduced me to Prof. Danser, and opened the doors for the renin-angiotensin system research to me.

Finally, my deepest gratitude to my family, especially my mother Ana, my aunties, Júlia e Socorro, and my wife Luciana for providing me the unbreakable determination to keep moving forward along the years.

*“Digo: o real não está na saída nem na chegada: ele se dispõe para a gente é no meio da travessia.”*

*(João Guimarães Rosa)*

## PREFACE

I decided to write a bit about the history behind this thesis. I have always been a great enthusiastic about science since my childhood. Indeed, during my graduation in Medicine, biochemistry and physiology were my favorite subjects. Unfortunately, as time went by, I have realized the emergence of an invisible barrier between the basic research and the clinical practice in Brazil. For some reason I could not fully understand, as the medical course progresses, all the subjects considered “basic” are set apart from the clinical practice. This partition is not totally evident, but the system that governs most of the medical courses in our country tends to commend the pragmatic point of view in detriment of the “basic” research. In other words, the medical doctor profile here is either someone able to work directly with patients, participating in their evaluation, propaedeutic and treatment, or the person involved in basic research, whose activity is delimited within the laboratory.

The truth is that the aforementioned partition between the basic research and clinical practice has always been present along the past years. However, this trend has been modified since the end of last century. The birth of the Translational Medicine enhances the importance of approximating the laboratory (lab) work with the practical medicine. Great efforts have been made to enable the future generations of medical doctors to work in both fields, in order to build up a faster result to the society. Nevertheless, this process in many universities of Brazil is still crawling. Truly, after my graduation, I completed my medical training in the Internal Medicine and Nephrology Residency Program in Brasilia. I have been taught to manage all sorts of situations in patients, however I had tiny knowledge in the basic research involved in Nephrology. Actually, neither me nor my colleagues and even preceptors were able to read, interpret and fully comprehend the papers published in the Nephrology basic research. None of us had received the proper training to do that, despite the ability to conduct in clinical practice any kidney disease.

As a person whose passion for kidney physiology was the main determinant to become a nephrologist, I was very disappointed with that situation. Therefore, I decided to apply for a Master degree in the University of Brasília, at the laboratory of Molecular Pharmacology, under the supervision of Prof. Dr. Francisco de Assis Rocha Neves. It was my first contact with the lab work and my first experience in performing molecular biology techniques by myself. At the end of 2012, I defended

my thesis entitled: “GQ-16, a partial PPAR $\gamma$  agonist, represses human mesangial cells proliferation”.

In 2013, I started my doctorate aiming to evaluate the regulation of renin transcription by the PPAR $\gamma$  agonist. In 2015, as part of sandwich PhD program, I moved to the Laboratory of Vascular Medicine and Pharmacology in the university of ErasmusMC, in Rotterdam, the Netherlands, under the supervision of Prof Dr. AHJ Danser. The study on the role of PPAR $\gamma$  full and partial agonist on renin synthesis could not be continued because our As4.1 cell model did not reproduce previous results showing that PPAR $\gamma$  interfere within renin production. Therefore, most of my studies were concentrated in the molecular mechanisms involved in the phenotypic plasticity of human juxtaglomerular cells (JGC).

Thus, this thesis represents the work I developed in the Netherlands, and which I also have used at my PhD defense in ErasmusMC, Rotterdam. In the first part, we will review the classical, new aspects and paradigms of the renin-angiotensin system (RAS). Then, we provide a broad review about the current knowledge on the renin-synthesizing cells (RPC). It summarizes not only classical concepts like the so-called “recruitment” phenomenon, growth and developmental processes, but also novel contexts such as inflammation, cell repair mechanisms and tissue regeneration.

The following section describes a new approach to understand RPC biology. It is the first report of a gene expression catalogue of human renin-producing tumors, or reninomas, that culminated in the discovery of 36 genes that are new to the RPC gene signature. Noteworthy, the cell models available to study RPC are mouse-derived, and therefore, proper knowledge of human RPCs is limited, relying on speculation on the basis of murine models. This fact makes our approach unique, and furthermore, among the genes identified, the platelet-derived growth factor (PDGF)  $\beta$  - PDGF  $\beta$  receptor signaling pathway was revealed as a promising RPC regulator.

Thereupon, we investigated the existence of the brain RAS, whose activity relies on the assumption that local renin synthesis by RPC would be a *sine qua non* condition, since the presence of the blood-brain barrier would preclude renin uptake from blood by central nervous system cells. We were unable to find evidence to support the aforementioned concept. Instead, our data suggest that renin in the brain represents trapped plasma renin and/or locally activated trapped plasma prorenin.

These findings uphold the conception that RPC in the kidney are the only renin source in the body.

The plausibility of 'open' prorenin (prorenin in an open conformation, capable of displaying angiotensin-generating activity) release by renin and/or prorenin-synthesizing cells was then investigated. After many decades, prorenin physiological role remains a riddle: is it just renin's inactive precursor or more than that? JGCs, i.e. RPC located at the juxtaglomerular apparatus, are the main source of prorenin and the only source of renin in circulation under unstressed conditions. In addition, other tissues are also able to synthesize and release prorenin. Under physiological conditions (pH 7.4, 37°C), prorenin is present in a 'closed' conformation, which cannot result in angiotensin generation. We hypothesized that prorenin might exert local angiotensin-generating effects, at the site of its release, provided that is released in an open conformation from prorenin-synthesizing cells, before returning to the closed conformation in the extracellular milieu. Our in-vitro study did not reveal any evidence to support this conjecture, and, thus, at least under cell culture conditions, RPC and other prorenin-synthesizing cells do not release open (active) prorenin.

Ultimately, we investigated renin and prorenin reabsorption by human conditionally immortalized proximal epithelial tubule cells (ciPTEC). The reabsorption of RAS components like angiotensinogen, renin and prorenin occurs in the kidney proximal tubule, in a megalin-dependent manner, and may underlie renal angiotensin production. Patients with Dent's disease or Lowe syndrome (resulting in impaired megalin function) exhibit an increase in urinary renin and angiotensinogen levels, suggestive for diminished reabsorption. Strikingly, the defective reabsorption also allowed the detection of urinary prorenin, which is normally undetectable. We demonstrated that ciPTEC bind and internalize renin and prorenin in a temperature-dependent manner, resulting in prorenin activation at 37°C. This process involved megalin and/or mannose-6-phosphate (M6P) receptors, and surprisingly, the M6P receptor antagonist, M6P, interfered with megalin endocytosis.

Here, I should also mention I had unfinished projects in Rotterdam, which still requires more experiments and work to be concluded, but certainly will result in future publications. It has been a long road so far, and I have learned considerably. My objective is not only to be a nephrologist, but also to become a skillful scientist,

with high expertise, able to contribute to the scientific research on the RAS field, and to help the development of the Translational Medicine in my country in the future.

## RESUMO

O benefício do bloqueio do sistema Renina Angiotensina (RAS) em doenças cardiovasculares e renais é incontestável, mas o que ainda é controverso, é o grau ideal deste bloqueio. Um alto grau de bloqueio do RAS pode ter efeitos benéficos adicionais, entretanto, também pode resultar em maior incidência de efeitos colaterais. Este bloqueio pode ser estimado a partir do aumento da renina circulante, representando o "recrutamento" de novas células produtoras de renina (RPC) ao longo das arteríolas aferentes. As consequências a longo prazo deste processo ainda são desconhecidas, bem como sua contribuição para insuficiência renal no futuro. Além da produção de renina, RPCs participariam diretamente na hipertrofia vascular concêntrica dos vasos renais, apesar do adequado controle dos níveis de pressão arterial. Esta tese enfoca os RPCs, seu conhecimento atual, novos aspectos, e uma nova abordagem para entender sua fisiologia. Além disso, analisamos o conceito de sítios extrarrenais de produção de renina, e a liberação de pró-renina ativa pelos rins. Nossos dados suportam o conceito de que as células Juxtaglomerulares, do aparato Juxtaglomerular, são a única fonte de renina no organismo, na qual depende a geração de angiotensina. A compreensão completa do "recrutamento" das RPCs e suas consequências adicionais, combinadas com uma compreensão completa da produção de angiotensina local (renal), em última análise, permitirão terapias anti-hipertensivas mais efetivas, além de melhores resultados em pacientes com patologias cardiovasculares e renais.

**Palavras-chave:** Renina. Pró-renina. Angiotensina. Sistema renina-angiotensina. Aparelho juxtaglomerular.

## ABSTRACT

The benefit of Renin-Angiotensin System (RAS) blockade in cardiovascular and renal disease is undisputed, but what is still controversial is the optimal degree of RAS blockade. A high degree of RAS blockade may have additional beneficial effects, but also results in a higher incidence of side effects. The degree of blockade can be estimated from the increase in circulating renin, depicting the “recruitment” of new renin-producing cells (RPC) along the afferent arterioles. The long-term consequences of this process are still unknown, nor do we know if it contributes to renal impairment in the future. Besides renin production, RPC would participate directly in the concentric vascular hypertrophy, despite the control of the blood pressure levels. This thesis focuses on the RPCs, their current knowledge, novel aspects, and a new approach to understand these cells biology. Furthermore, we have analyzed the concept of extrarenal sites of renin production, and the active prorenin release by the kidney. Our data support the Juxtaglomerular cells, in the Juxtaglomerular Apparatus, as only source of renin in the body, on which angiotensin generation depends. The complete understanding of the RPCs “recruitment” and its further consequences, combined with a full comprehension of local (renal) angiotensin production will ultimately allow more effective anti-hypertensive therapies, and better outcomes in patients with cardiovascular and renal pathologies.

**Keywords:** Renin. Prorenin. Angiotensin. Renin-angiotensin system. Juxtaglomerular apparatus.

## FIGURES LEGEND

Figure 1 –	Schematic illustration of the classical RAS.....	26
Figure 2 –	Schematic illustration of RAS axes.....	30
Figure 3 –	Schematic illustration of nephrogenesis.....	36
Figure 4 –	The “recruitment” phenomenon.....	38
Figure 5 –	Simplified scheme showing how cAMP and cGMP regulate renin	40
Figure 6 –	iFISH for renin in mouse kidney.....	58
Figure 7 –	Total renin levels, cell viability and qPCR.....	70
Figure 8 –	iFISH showing renin immunofluorescence in blue and in situ hybridization for Acta2 or PDGF $\beta$ .....	72
Figure 9 –	Concentration-dependent inhibition of angiotensin I-generating activity (AGA) by aliskiren.....	115
Figure 10 –	Renin and total renin levels in plasma and brain regions of mice before and after buffer perfusion (wash) of the brain.....	117
Figure 11 –	Renin and total renin levels in plasma and brain regions of untreated mice (WT), mice treated with DOCA-salt, mice infused with Ang II, and Ren1c <sup>-/-</sup> mice.....	118
Figure 12 –	Relationship between renin in plasma and renin in 3 different brain regions.....	119
Figure 13 –	Angiotensinogen mRNA expression in different brain regions.....	120
Figure 14 –	Ang I and II levels in plasma and brain of SHR treated with vehicle, olmesartan or lisinopril.....	122
Figure 15 –	Model displaying the closed and open prorenin conformations....	131
Figure 16 –	Angiotensin I generation in human plasma and renin IRMA.....	137
Figure 17 –	Renin, total renin and prorenin in the medium of HMC-1, HEK293 and decidua cells.....	139
Figure 18 –	Renin and total renin in medium obtained from HMC-1, HEK293 and decidua cells, incubated without cells.....	140
Figure 19 –	(Pro)renin immunoreactivity, measured by IRMA, F258 IRMA in the medium of HMC-1, HEK293 or decidua cells.....	141

Figure 20 – Total renin and angiotensin I levels in the medium of human decidua cells.....	142
Figure 21 – Angiotensin I levels in the medium of human decidua cells in the presence or absence of captopril.....	143
Figure 22 – Time-dependent increase in the cellular levels of total and activated prorenin after incubation with prorenin in the absence or presence of M6P at 37°C or 4°C.....	149
Figure 23 – Time-dependent increase in the cellular levels of renin after incubation with renin in the absence or presence of M6P at 37°C or 4°C.....	150
Figure 24 – Cellular levels of prorenin and renin in the presence or absence of M6P and/or RAP-GST in ciPTEC exposed to prorenin or renin at 37°C or 4°C.....	152
Figure 25 – Inhibition of BSA uptake in ciPTEC by M6P and RAP-GST, and fluorescence staining representing BSA accumulation.....	154
Figure S1 – Sequence coverage of the various reninoma RNAs.....	74
Figure S2 – Spearman pairwise comparison of the gene expression levels in the raw (unsubtracted) reads (FPKM) for each sample analyzed.	75
Figure S3 – Repeat Spearman pairwise comparison of the sample analyzed in Figure S2 after subtracting genes.....	76
Figure S4 – Venn diagram representing the overlap of the 100 most-expressed genes in the reninomas.....	77
Figure S5 – Representative iFISH results showing renin immunofluorescence and in situ hybridization for the indicated mouse mRNA in kidneys from 5 day-old mice, 10-12 week adult control mice and adult mice treated with captopril.....	78
Figure S6 – WB in HEK293 medium.....	100
Figure S7 – As4.1 morphology.....	100
Figure S8 – Secreted or intracellular renin.....	126

Figure S9 – B. Renin (secreted or intracellular), sRen and icRen mRNA expression in kidneys of wild-type (WT, n=6) and Ren1c<sup>-/-</sup> mice (n=4)..... 127

## TABLES LEGEND

Table 1 –	Quality control of sequenced reads.....	56
Table 2 –	Ratio of the number of renin reads (FPKM) obtained in the various biopsies versus those for the next most abundant transcript.....	57
Table 3 –	iFISH analysis on mouse kidney for the genes most highly expressed in the reninomas.....	60
Table S3 –	Rank order of the 100 most highly expressed genes in each of the reninomas.....	101
Table S4 –	Oligonucleotide sequences used to amplify the C57BL/6 mouse cDNA fragments for generation of the FISH probes.....	105
Table S5 –	Primer sequences used in qPCR (Ren, Akr1b7, SMA, IL6, RBPJ).	108
Table S6 –	Primer sequences and GenBank accession numbers.....	128
Table S7 –	Percent inhibition of angiotensin I-generating activity by aliskiren in brain nucleus homogenates before and after buffer perfusion...	129
Table S8 –	Angiotensin (Ang) metabolites in SHR plasma and brain during treatment with placebo, olmesartan or lisinopril.....	129

## ABBREVIATIONS

A2M	- Alpha-2-macroglobulin
AA	- Afferent arterioles
AC	- Adenylate cyclase
ACE	- Angiotensin converting enzyme
ACEi	- Angiotensin converting enzyme inhibitor
ACTA2	- Actin, alpha 2, smooth muscle, aorta
ADCY3	- Adenylate cyclase 3
AGA	- Angiotensin-generating activity
Akr1b7	- Aldo-keto reductase family 1, member B7
AMP	- Adenosine monophosphate
ANG	- Angiotensin
Aog	- Angiotensinogen
ARB	- Angiotensin receptor blocker
AT	- Angiotensin receptor
ATP	- Adenosine triphosphate
ATP1B2	- ATPase, Na <sup>+</sup> /K <sup>+</sup> transporting, beta 2 polypeptide
BGN	- Biglycan
BSA	- Bovine serum albumine
C4A	- Complement component 4A (Rodgers blood group)
CALD1	- Caldesmon 1
cAMP	- Cyclic AMP
CBLN4	- Cerebellin 4 precursor
CBP	- CREB-binding protein
CD	- Collecting duct
CD248	- CD248 molecule, endosialin
CD34	- CD34 molecule
cDNA	- Complementary deoxyribonucleic acid
CFP	- Cyan fluorescent protein
ciPTEC	- Conditionally immortalized proximal tubule epithelial cells
COL6A1	- Collagen, type VI, alpha 1

COL6A2	- Collagen, type VI, alpha 2
CPA3	- Carboxypeptidase A3 (mast cell)
CPE	- Carboxypeptidase E
CRE	- cAMP response element
CREB	- cAMP response element binding protein
CRIP1	- Cysteine-rich protein 1 (intestinal)
CSRP2	- Cysteine and glycine-rich protein 2
CXCL12	- Chemokine (C-X-C motif) ligand 12 (stromal cell-derived factor 1)
DBNDD2	- Dysbindin (dystrobrevin binding protein 1) domain containing 2
DCT	- Distal convolute tubule
DMEM	- Dulbecco's modified Eagle medium
DOCA	- Deoxycorticosterone acetate
EA	- Efferent arterioles
ECV	- Extracellular volume
EDTA	- Ethylenediamine tetraacetic acid
EKA	- Enzyme kinetic assay
ELISA	- Enzyme-linked immunosorbent assay
ERK	- Extracellular signal-regulated kinase
FCS	- Fetal calf serum
FISH	- Fluorescent
FKBP10	- FK506 binding protein 10, 65 kDa
FLNA	- filamin A, alpha (actin binding protein 280)
FOXD1	- Forkhead box D1
FPKM	- Fragments per kilobase of transcript per million
FXYD1	- FXYD domain containing ion transport regulator 1
GC	- Guanylate cyclase
GJA4	- Gap junction protein, alpha 4, 37kDa
GNAS	- GNAS complex locus
GPC1	- Glypican 1
GPR124	- G protein-coupled receptor 124
GPRC	- G protein-coupled receptor
GTP	- Guanosine triphosphate

HAT	- Histone acetyltransferase
HBSS	- Hank's Balanced Salt Solution
HCFC1R1	- Host cell factor C1 regulator 1 (XPO1 dependent)
HEK	- Human embryonic kidney
HIF	- Hypoxia inducible factor
HMC	- Human mastocytoma cells
HSPB6	- Heat shock protein, alpha-crystallin-related, B6
icREN	- Intracellular renin
IFITM1	- Interferon induced transmembrane protein 1 (9-27)
IFITM2	- Interferon induced transmembrane protein 2 (1-8D)
IFITM3	- Interferon induced transmembrane protein 3 (1-8U)
IGF2	- Insulin-like growth factor 2 (somatomedin A)
IL	- Interleukin
IRMA	- Immunoradiometric assay
ISYNA1	- Inositol-3-phosphate synthase 1
ITGA7	- Integrin, alpha 7
JAG1	- Jagged 1 (Alagille syndrome)
JG	- Juxtaglomerular
JGC	- Juxtaglomerular cells
KISS1	- KiSS-1 metastasis-suppressor
KO	- Knock-out
LBH	- Limb bud and heart development homolog (mouse)
LGALS1	- Lectin, galactoside-binding, soluble, 1
LH	- Loop of Henle
LM	- Loose mesenchyme
LRO	- Lysosome related organelles
LXR	- Liver X receptor
M6P	- Mannose 6-phosphate
MAPK	- Mitogen-activated protein kinases
MCAM	- Melanoma cell adhesion molecule
MDK	- Midkine (neurite growth-promoting factor 2)
MEF2C	- Myocyte enhancer factor 2C

MFGE8	- Milk fat globule-EGF factor 8 protein
miRNA	- Micro ribonucleic acid
MM	- Metanephric mesenchyme
MrgD	- Mas-related G-protein coupled receptor D
MSC	- Mesenchymal stem cells
MTT	- (3-(4,5-dimethylthiazol-2-yl)-2,5-diphenyl-2H-tetrazolium bromide
MXRA8	- Matrix-remodelling associated 8
MYL9	- Myosin, light chain 9, regulatory
NEP	- Neutral endopeptidase
NO	- Nitric oxide
NOTCH3	- Notch homolog 3 (Drosophila)
NPPC	- Natriuretic peptide precursor C
NRARP	- NOTCH-regulated ankyrin repeat protein
NT5DC2	- 5'-nucleotidase domain containing 2
OAZ2	- Ornithine decarboxylase antizyme 2
PBS	- Phosphate buffer saline
PCP	- Prolyl carboxipeptidase
PCT	- Proximal convolute tubule
PDE	- Phosphodiesterase
PDGFB	- Platelet derived growth factor $\beta$
PDGFR $\beta$	- Platelet-derived growth factor receptor, beta polypeptide
PEP	- Prolyl endopeptidase
PKA	- Protein kinase A
PLEKHH3	- Pleckstrin homology domain containing, family H (with MyTH4 domain) member 3
PRA	- Plasma renin activity
PTEC	- Proximal tubule epithelial cells
PTP4A3	- Protein tyrosine phosphatase type IVA, member 3
PVDF	- Polyvinylidene fluoride
qPCR	- Quantitative polymerase chain reaction
RAAS	- Renin angiotensin aldosterone system

RAP-GST	- Receptor-associated protein glutathione S-transferase
RAS	- Renin angiotensin system
RBPJ	- Recombination signal binding protein for immunoglobulin kappa J
REN	- Renin
RGS5	- Regulator of G-protein signaling 5
RNA	- Ribonucleic acid
RPC	- Renin-producing cells
RPMI	- Roswell park memorial institute
SERPINI1	- Serpin peptidase inhibitor, clade I (neuroserpin), member 1
SFRP4	- Secreted frizzled-related protein 4
SHR	- Spontaneous hypertensive rats
SLIT3	- Slit homolog 3 (Drosophila)
SM-MHC	- Smooth muscle myosin heavy chain
SMA	- Smooth muscle actin
SPARC	- Secreted protein, acidic, cysteine-rich (osteonectin)
SPARCL1	- SPARC-like 1 (hevin)
sREN	- Secreted renin
SRGN	- Serglycin
TAGLN	- Transgelin
TBC1D1	- TBC1 (tre-2/USP6, BUB2, cdc16) domain family, member 1
TBX2	- T-box 2
TGFBI	- Transforming growth factor, beta-induced, 68kDa
TGM2	- Transglutaminase 2 (C polypeptide, protein-glutamine-gamma-glutamyltransferase)
TIMP1	- TIMP metalloproteinase inhibitor 1
TINAGL1	- Tubulointerstitial nephritis antigen-like 1
TPM1	- Tropomyosin 1 (alpha)
TPM2	- Tropomyosin 2 (beta)
TPSB2	- Tryptase alpha/beta 1; tryptase beta 2
TUBA1A	- Tubulin, alpha 1a
UB	- Ureteric bud
VIM	- Vimentin

- VSMC - Vascular smooth muscle cells
- WB - Western blot
- WD - Wolfian duct
- WT - Wild type
- YFP - Yellow fluorescent protein

## TABLE OF CONTENTS

<b>1 INTRODUCTION</b> .....	<b>25</b>
1.1 CLASSICAL RENIN ANGIOTENSIN SYSTEM .....	25
1.2 RENIN, PRORENIN AND THEIR RECEPTORS .....	26
1.3 AXES OF RENIN ANGIOTENSIN SYSTEM.....	28
1.4 LOCAL/INTRARENAL RENIN ANGIOTENSIN SYSTEM.....	30
<b>2 AIM</b> .....	<b>33</b>
<b>3 JUXTAGLOMERULAR CELLPHENOTYPIC PLASTICITY</b> .....	<b>34</b>
3.1 JUXTAGLOMERULAR CELLS.....	34
3.2 JUXTAGLOMERULAR CELLS PROGENITORS AND THEIR EMBRYOLOGY.....	34
3.3 THE RECRUITMENT PHENOMENON .....	37
3.4 cAMP PATHWAY AND RECRUITMENT.....	39
3.5 ROLE OF CALCIUM AND CGMP .....	41
3.6 EPIGENETIC MECHANISMS AND MICRORNA.....	42
3.7 JGC SIGNATURE: THE MYO-ENDOCRINE PROFILE .....	43
3.8 NOTCH SIGNALING PATHWAY.....	44
3.9 PLASTICITY AND REGENERATION.....	46
3.10 CONCLUDING REMARKS.....	47
<b>4 TRANSCRIPTOME ANALYSIS OF HUMAN RENINOMAS AS AN APPROACH TO UNDERSTANDING JUXTAGLOMERULAR CELL BIOLOGY</b> .....	<b>49</b>
4.1 INTRODUCTION.....	49
4.2 METHODS .....	50
<b>4.2.1 Animals</b> .....	<b>50</b>
<b>4.2.2 Preparation and Sequencing of Reninoma RNA</b> .....	<b>51</b>
<b>4.2.3 Mapping and Transcript Quantification</b> .....	<b>51</b>
<b>4.2.4 Immunofluorescence/Fluorescent <i>In Situ</i> Hybridization</b> .....	<b>51</b>
<b>4.2.5 Cell Culture Studies</b> .....	<b>52</b>
<b>4.2.6 Plasmids</b> .....	<b>53</b>
<b>4.2.7 Transfection and Ligand Exposure of As4.1 Cells</b> .....	<b>53</b>
<b>4.2.8 Western Blot</b> .....	<b>54</b>
<b>4.2.9 (Pro)renin Measurement and Determination of Cell Viability</b> .....	<b>54</b>
<b>4.2.10 Quantitative PCR</b> .....	<b>55</b>

<b>4.2.11 Statistical Analysis</b> .....	<b>56</b>
4.3 RESULTS.....	56
4.4 DISCUSSION.....	66
4.5 SUPPLEMENT INFORMATION.....	74
<b>5 BRAIN RENIN-ANGIOTENSIN SYSTEM: DOES IT EXIST?</b> .....	<b>109</b>
5.1 INTRODUCTION.....	109
5.2 METHODS.....	110
<b>5.2.1 Brain Renin, Prorenin and Angiotensinogen Levels in Wild-Type Mice, Mice Treated with DOCA-Salt or Angiotensin II and Renin-Deficient Mice</b>	<b>110</b>
<b>5.2.2 Brain and Plasma Angiotensin Levels in Spontaneously Hypertensive Rats</b> .....	<b>111</b>
<b>5.2.3 Angiotensinogen Synthesis by Rat Primary Cortical Astrocytes</b> .....	<b>112</b>
<b>5.2.4 Measurement of Renin, Prorenin and Angiotensinogen</b> .....	<b>112</b>
<b>5.2.5 LC-MS/MS Based Quantification of Angiotensin Metabolites</b> .....	<b>112</b>
<b>5.2.6 Renin and Angiotensinogen Expression</b> .....	<b>113</b>
<b>5.2.7 Statistical Analysis</b> .....	<b>114</b>
5.3 RESULTS.....	115
<b>5.3.1 Aliskiren Inhibits Angiotensin I-Generating Activity in the Mouse Brain</b> .....	<b>115</b>
<b>5.3.2 Buffer Perfusion Reduces Mouse Brain Renin by &gt;60%</b> .....	<b>116</b>
<b>5.3.3 Comparable Reductions in Brain and Plasma (Pro)Renin after DOCA-Salt Treatment, Angiotensin II Infusion and Renin-Deficiency</b> .....	<b>117</b>
<b>5.3.4 Renin Expression in the Brain</b> .....	<b>118</b>
<b>5.3.5 Despite Angiotensinogen Expression, Angiotensinogen Protein is Undetectable in Mouse Brain and Rat Astrocytes</b> .....	<b>120</b>
<b>5.3.6 Angiotensins in the SHR Brain with and without RAS Blockade</b> .....	<b>121</b>
5.4 DISCUSSION.....	121
5.5 SUPPLEMENT INFORMATION.....	126
<b>6 DO PRORENIN-SYNTHESIZING CELLS RELEASE ACTIVE, 'OPEN' PRORENIN?</b> .....	<b>130</b>
6.1 INTRODUCTION.....	130
6.2 METHODS.....	132
<b>6.2.1 Human Samples</b> .....	<b>132</b>

6.2.2 Cell Culture Studies .....	133
6.2.3 Biochemical Assays.....	134
6.2.4 Data Analysis .....	135
6.3 RESULTS.....	136
6.3.1 Plasma Prorenin Displays Enzymatic Activity.....	136
6.3.2 VTP-27999 Increases Renin Immunoreactivity, but does not Unravel the Release of 'Open' Prorenin .....	137
6.3.3 Angiotensin Generation in Decidua Cells .....	140
6.4 DISCUSSION .....	141
<b>7 RENIN AND PRORENIN UPTAKE BY HUMAN PROXIMAL TUBULE CELLS: ROLE OF MEGALIN .....</b>	<b>145</b>
7.1 INTRODUCTION.....	145
7.2 METHODS .....	146
7.2.1 Cell Culture .....	146
7.2.2 Prorenin and Renin Binding Uptake .....	147
7.2.3 Albumin Uptake .....	147
7.2.4 Data Analysis .....	148
7.3 RESULTS.....	148
7.3.1 Prorenin and Renin Binding Uptake .....	148
7.3.2 Albumin Uptake .....	149
7.4 DISCUSSION .....	149
<b>8 CONCLUSIONS AND PERSPECTIVES.....</b>	<b>155</b>
<b>REFERENCES .....</b>	<b>158</b>

## 1 INTRODUCTION

### 1.1 CLASSICAL RENIN ANGIOTENSIN SYSTEM

In 1898, Robert Tigerstedt and Per Bergman performed a set of experiments, where they observed a rise in blood pressure after injecting rabbit kidney extracts in the jugular vein of rabbits. They characterized the substance as derived from the renal cortex, soluble in water and alcohol, thermolabile, and named it "renin" (1). This discovery remained dormant for more than 30 years, when Goldblatt et al. focus the research on hypertension, by renal artery clamping in dogs. They suggested the presence of a substance released by the kidney as the cause of hypertension, and they associated this substance with the renal hypoperfusion. Posteriorly, 2 independent groups, using the same aforementioned animal model, confirmed this concept. Furthermore, they also isolated a vasoconstrictor compound, later known as "angiotensin", and concluded that the substance released by the kidney was renin, capable of enzymatically act on a plasmatic protein to generate angiotensin (2).

The renin-angiotensin system (RAS) plays a central role in blood pressure regulation and fluid-electrolyte homeostasis. It involves an array of enzymes, peptides and receptors, whose actions are able to correct small extracellular volume (ECV) variations by increasing or decreasing RAS activity. According to the classical, endocrine view of the RAS, also known as the systemic or intravascular RAS, renin, synthesized in the kidneys, catalyzes cleavage of a 10-amino acid peptide, angiotensin I (Ang I), from the N-terminus portion of the circulating angiotensinogen, a protein produced by the liver. This decapeptide is subsequently hydrolyzed by angiotensin I-converting enzyme (ACE), a dicarboxyl-peptidase ubiquitously present on the plasma membrane of endothelial cells, yielding the octapeptide angiotensin II (Ang II), the active endproduct of the RAS cascade, which is responsible, among others functions, for sodium reabsorption in the proximal convolute tubule of the nephron, and vessel constriction, especially arterioles within the renal and systemic circulation (3, 4). This traditional axis was completed later, with the discovery of aldosterone. Angiotensin II stimulates the zona glomerulosa in the adrenal cortex to release aldosterone, which promotes sodium reabsorption coupled with potassium exchange in the distal convolute tubule of the nephron. The whole axis, named renin-

angiotensin-aldosterone system (RAAS), is now firmly linked to ECV adjustment and blood pressure regulation (4, 5).

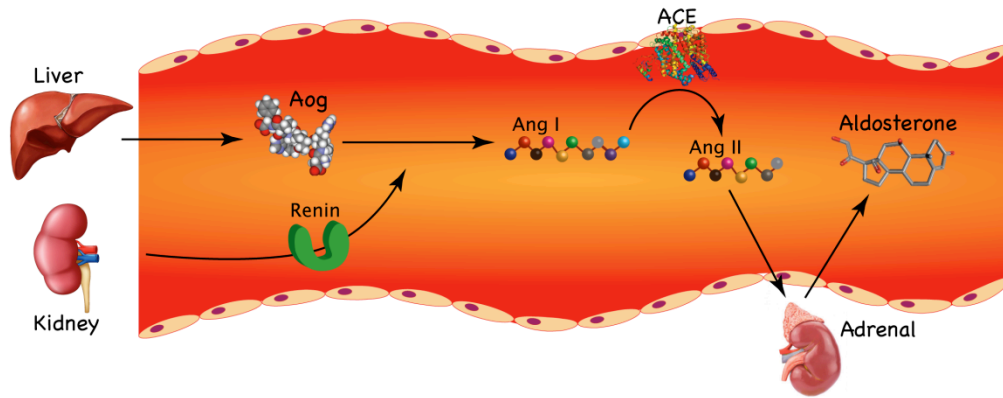


Figure 1. Schematic illustration of the classical RAS. Aog: Angiotensinogen; Ang: Angiotensin; ACE: Angiotensin converting enzyme. Modified from (4).

## 1.2 RENIN, PRORENIN AND THEIR RECEPTORS

Renin represents the first and the rate-limiting step of the RAS cascade. Overproduction and underproduction of renin result in severe disturbances of body fluid homeostasis. Precise regulation of renin release is therefore indispensable for proper RAS functioning (3, 6). Renin is an aspartyl protease synthesized as prorenin protein. Following its synthesis, the pre-part, which represents the signal peptide, is cleaved off inside the endoplasmic reticulum. The resulting molecule, prorenin, enters the Golgi apparatus to be glycosylated, and then proceeds to one of two different pathways. The first one involves clear vesicles containing prorenin which are secreted constitutively, while the second pathway involves prorenin tagging for regulated secretion, which is accompanied by proteolytic prorenin-renin conversion, and renin storage in dense cytoplasmic granules (7), awaiting release in response to various stimuli, such as sudden fall in blood pressure, low salt diet, or  $\beta$ -adrenergic stimulation (8).

The kidney secretes both renin and prorenin, but plasma levels of prorenin are, under normal conditions, about 10-fold higher than the plasma levels of renin (9). Renin consists of 2 homologous lobes, with a cleft in between, which contains the active site. Prorenin has a 43-amino acid N-terminal propeptide, the pro-segment, which covers the enzymatic cleft between the 2 lobes, thereby preventing the access of its specific and unique substrate, angiotensinogen (10). Prorenin is a glycoprotein,

which can be activated in 2 ways: proteolytically or non-proteolytically. The former is irreversible and involves removal of the pro-segment by a processing enzyme inside cytoplasmic granules, while the latter is reversible, inducible by certain conditions such as low temperature and pH, and results from a conformational alteration, i.e., unfolding of the propeptide from the enzymatic cleft (10). The proteases responsible to activate the prorenin enzymatically are not clearly known, although some candidates, like cathepsin B, have emerged (11).

Prorenin and renin (together denoted (pro)renin) are able to bind to the mannose-6-phosphate/insulin-like growth factor II (M6P/IGFII) receptors, which contain binding domains for IGFII and phosphomannosylated ligands such as (pro)renin. Following binding, (pro)renin is internalized, and the prorenin is enzymatically converted to renin (12). Interestingly, despite internalization, and the subsequent prorenin to renin conversion, no intracellular angiotensin generation has been demonstrated. Instead, their binding to the M6P receptors has led them to slow degradation, and hence, these receptors are currently accepted as clearance receptors for (pro)renin (12-14).

In 2002, a receptor that binds specifically to renin and prorenin was cloned: the (pro)renin receptor (15). Oppositely to the M6P receptor, the (pro)renin is not internalized or degraded. Instead, binding increases the renin catalytic activity, and surprisingly, it activates the prorenin non-proteolytically (16). Therefore, angiotensin generation would be feasible on cell surface, and the tissues would be able to uptake (pro)renin from the circulation. Interestingly, the (pro)renin receptor also plays some roles independently of Ang II generation. The (pro)renin binding triggers the activation of the MAPK (mitogen-activated protein kinases)/ERK (extracellular signal-regulated kinase) 1/2 signaling pathway, which result in the upregulation of genes related to inflammation, fibrosis and cell proliferation (17). Nevertheless, the receptor has a low affinity for both renin and prorenin, what implies that their binding to the receptor *in vivo* will most likely occur only in sites where (pro)renin levels are sufficiently high (18).

One question that still remains puzzling is the role of prorenin in modulating RAS system. Since prorenin is not an active enzyme, and does not generate angiotensin, why JGCs secrete more prorenin in the bloodstream than renin? In any circumstance, does prorenin contribute to Ang II generation or can display a specific pharmacological effect that is Ang II independent? In spite of the fact that different

studies have shown that prorenin has two different receptors, their role in the pharmacological action of (pro)renin is still unknown. Yet, the (pro)renin receptor gene has important role in the development of the brain, and it is considered an embryonic-essential gene. A specific mutation on this gene, which results in frame deletion of exon 4, has been associated to X-linked mental retardation and epilepsy in humans and mice (19).

### 1.3 AXES OF RENIN ANGIOTENSIN SYSTEM

The understanding of the RAS has built up with the aggregation of new peptides, receptors and enzymes to the system. Furthermore, novel functions associated with these recently described components allowed the inclusion of new axis in the RAS. It is no longer possible to conceive and accept the RAS as a linear, limited-proteolysis cascade, represented by a single and straightforward axis.

On the classical axis, the Ang II generated from the participation of renin and ACE binds to the angiotensin receptors type 1 (AT<sub>1</sub>) to exert the typical actions related to the blood pressure regulation. Furthermore, the axis ACE/Ang II/AT<sub>1</sub> is also linked to inflammation, proliferation and fibrosis (20). Nevertheless, many Ang II-derived peptides and angiotensin receptors have been described afterward. Indeed, Ang II can be hydrolyzed by different “angiotensinases”, such as aminopeptidases, carboxipeptidases, endopeptidases, neprilysin and angiotensin converting enzyme type 2 (ECA2). They are all proteolytic enzymes that cleaves the angiotensin molecules, yielding smaller fragments that may have similar or opposite effects to Ang II, according to the angiotensin receptor they bind (21). For instance, besides AT<sub>1</sub> receptor, at least 3 other more angiotensin receptors were described: angiotensin receptor type 2 (AT<sub>2</sub>), type 4 (AT<sub>4</sub>) and Mas receptor (22).

The first novel axis of the RAS involves the angiotensin (1-7), or Ang (1-7), pathway. Curiously, Ang (1-7) is the most studied angiotensin peptide since the seventies (23). It is an active heptapeptide that can be formed directly from Ang I by endopeptidases (neutral-endopeptidase (NEP) or prolyl-endopeptidase (PEP)), or from Ang II by PEP, prolyl-carboxipeptidase (PCP) or ACE2 (24). The latter is a transmembrane glycoprotein, homologue to ACE, but with a single active site domain that works as a monocarboxypeptidase, removing one amino acid not only from Ang II to yield Ang (1-7), but also from Ang I, resulting in Angiotensin (1-9), which can be

hydrolyzed to Ang (1-7) by ACE or NEP (25). Interestingly, the ACE inhibitors (ACEi) can not block the ACE2, only ACE, thereby favoring Ang II degradation and Ang (1-7) generation (26).

Ang (1-7) binds to the G protein-coupled receptor Mas, which is associated with cardiac, renal and cerebral protective responses (27). In fact, this angiotensin presents vasodilator and antihypertensive actions by stimulation of prostaglandins and nitric oxide (NO) (28). Furthermore, Ang (1-7) has been assumed to blunt important processes such as cell proliferation, hypertrophy, fibrosis and thrombosis (29). Thereupon, the discovery of the ACE2/Ang (1-7)/Mas axis depicts the complexity of the RAS, and the pathways involved in its regulation. The balance between the axes, displayed by ACE/Ang II vs. ACE2/Ang (1-7), will determine the subsequent outcomes, with the former promoting vasoconstriction/proliferation, while the latter upholds vasodilation/antiproliferation.

Angiotensin (2-8), or angiotensin III (Ang III), is another heptapeptide derived from Ang II by the aminopeptidase A, whose actions are similar to Ang II (30). The hydrolysis of Ang III by aminopeptidase N yields the angiotensin (3-8), or angiotensin IV (Ang IV). This angiotensin binds preferentially to the AT<sub>4</sub> receptor, recently identified as the transmembrane enzyme, the insulin-regulated membrane aminopeptidase, which can be found in adrenal gland, heart, brain, kidney and lung (31). Curiously, Ang IV also presents a wide range of effects, specially in the brain, where it enhances learning and memory recall and protects against cerebral ischemia (32). Conversely, Angiotensin A (Ang A) is another Ang II-derived fragment, which can be hydrolyzed by EAC2 to generate an heptapeptide known as Alamandine. Interestingly, this novel peptide has similar effects to Ang (1-7), by acting through the Mas-related G-coupled receptor type D (MrgD), representing another important counter-regulatory mechanism within RAS (33).

Another axis that has been described in the last decade is the (pro)renin/(pro)renin receptor/MAPK ERK1/2 pathway. Again, all the aforementioned actions related to this axis would be dependent upon the receptor binding, what is limited to specific tissue sites. The complexity involved in all these axes exposes different regulatory pathways that work in concert to preserve the homeostasis.



characterized by the generation of Ang II in situ has also emerged as an important pathway involved in the pathogenesis of CV disease (40). Local RAS has been demonstrated in tissues such as heart, adrenal gland (24, 41), kidney (23, 24), brain (42), vascular endothelium (24, 43) and reproductive system (44).

The best-described local RAS system is located in the kidneys, known as the intrarenal RAS. It harbors all the RAS components necessary for Ang II generation. Interestingly, the level of Ang II in the renal tissue is much higher than in plasma, sometimes 1000 times higher, what suggests selective local regulation, in a manner distinct from circulating RAS (23).

Traditionally, Ang II has a negative feedback loop on the renin release into the circulation, what leads to the subsequent decrease in the circulating Ang II (45). Notwithstanding, in Ang II-induced hypertension model, the tissue Ang II content is increased, possibly by 2 mechanisms: the AT<sub>1</sub> receptor-mediated uptake of circulating Ang II; and the presence of a positive feed-forward loop, in which circulating Ang II leads to the magnified production of local Ang II (23). Posteriorly, in that same experimental hypertension model, Navar et al. have demonstrated an augmented local expression of RAS components, including (pro)renin, angiotensinogen, and ACE (23). In 2010, Pohl et al. have shown the participation of the endocytotic receptor megalin in the uptake and internalization of RAS components such as angiotensinogen and renin in the proximal convolute tubule (PCT), thereby providing a novel aspect to the intrarenal RAS (46). Conversely, using an angiotensin receptor knockout (KO) mice, renal Ang II was located only extracellularly, which points toward the angiotensin production either in the interstitial space or bound to the cell surface (47).

The local production of angiotensins in different tissues is undisputed. Nevertheless, the expression of local RAS components does not prove their functional significance and/or clinical relevance (40). There is still no consensus whether intrarenal RAS could participate in hypertension etiology independently from the circulating RAS. To address this question, Gonzalez-Villalobos et al. generated a mouse model specifically lacking kidney ACE, and studied them under experimental hypertension. They have demonstrated that absence of intrarenal ACE blunts the hypertension under either low (nitric oxide synthesis inhibition) or high Ang II (Ang II infusion) circulating levels (48). In other words, that would be a robust evidence linking the participation of renal tissue RAS in the physiopathology of hypertension.

However, some caveats require better evaluation. The findings have been questioned, especially in what concerns the pattern of Ang II metabolism in the ACE KO mice. In these animals, the ACE-free tissues might exhibit alternative upregulated angiotensinases, resulting in reduced Ang II half-life. If so, the KO animals would have been exposed to lower Ang II concentrations, due to a diminished half-life, resulting in more modest hypertensive and renal responses compared to the control group (49). Additionally, Matsusaka et al., making use of either kidney-specific or liver-specific angiotensinogen knockout mice, have shown that renal Ang II production relies utterly on the hepatic angiotensinogen (50, 51). Further studies are required to elucidate the participation of the intrarenal RAS as an independent factor involved in the pathophysiology of hypertension.

## 2 AIM

- 1) To provide a review in the current literature about the new aspects and paradigms of the renin-angiotensin system and its relation with the renin-producing cells;
- 2) To validate a new approach to understand renin-producing cells biology, by using transcriptome analysis of human renin-producing tumors (reninoma);
- 3) To evaluate the occurrence of a brain renin-angiotensin system, and subsequently, the potential participation of renin-producing cells in this process;
- 4) To assess whether prorenin in an “open” conformation at the site of its release from renin-producing cells is capable of generating angiotensin locally;
- 5) To investigate renin and prorenin reabsorption in megalin-expressing human conditionally immortalized proximal tubule epithelial cells.

### 3 JUXTAGLOMERULAR CELL PHENOTYPIC PLASTICITY

#### 3.1 JUXTAGLOMERULAR CELLS

The JGC of the kidney are the only source of renin and the main source of prorenin in the circulation (3, 7). Several extrarenal tissues, such as the adrenal gland, ovary, testis, placenta and retina, additionally produce and secrete prorenin (9). Indeed, after a bilateral nephrectomy, prorenin, but not renin, can still be detected at low levels in blood (52).

JGC are part of the juxtaglomerular apparatus, a tight structure situated on the kidney glomerular hilum, composed mainly of specialized epithelial cells (macula densa cells of the ascending limb of the nephron loop), extraglomerular mesangial cells, the terminal portion of the afferent arterioles and the proximal portion of the efferent arterioles. JGC are within these vessels and exhibit an epithelioid appearance, with a prominent endoplasmic reticulum, Golgi apparatus, and renin granules, but also containing myofibrils and adhesion plaques, typical of smooth muscle cells (53).

Efforts to characterize JGC have historically been hampered by several factors: JGC lose their secretory granules and, concomitantly, their ability to proteolytically activate prorenin when placed in culture (54); JGC make up approximately 1/1000 of the total cell mass of the kidney, making it difficult to isolate sufficient quantities of pure cells for further characterization (55).

#### 3.2 JUXTAGLOMERULAR CELLS PROGENITORS AND THEIR EMBRYOLOGY

JGC represent one type of the so-called repertoire of renin-producing cells (RPC), a group of cells that at some moment in their lifespan produce renin. During kidney ontogeny in mammals, renin expression changes according to a pattern (Figure 3). It first appears in the undifferentiated metanephric blastema before vessel formation has begun. Once the vascularization begins, around the 14<sup>th</sup> embryonic day in mice and rats, RPC are distributed along the walls of the arteriolar vessels. As the process evolves, renin starts to be expressed in other cells along the distal portions of the newly formed vessels. Gradually, RPC disappear from the larger

vessels, shifting toward the afferent arterioles, and, finally, assuming their position on the juxtaglomerular apparatus (8). Gomez et al. showed that the ontogeny of renin expression by RPC depicts its own phylogenetic evolution pattern (56).

The expression of the renin gene is tissue-specific and developmentally regulated (57). Renal renin concentrations are high in early life, decreasing progressively as kidney maturation evolves (58). During this process, RPC are associated with assembling and branching of the developing kidney vasculature (59), and the ablation of these cells in mice during development results in a distinct kidney phenotype with peculiar vascular abnormalities (60). In vivo, vascularization of the kidney is synchronized with epithelial nephrogenesis (61). Epithelial branching morphogenesis is critical for the formation of various organs, including the vasculature and kidneys (62). The definitive kidney in mammals originates from a complex interaction between the ureteric bud and the metanephric mesenchyme, both derived from the intermediate mesoderm. These reciprocal actions lead the ureteric bud to elongate and bifurcate toward the metanephric mesenchyme, forming on its tip, an aggregate of mesenchyme cells, the cap mesenchyme. This condensate of cells generates a vesicle, which continues to form a comma-shaped body and later, a S-shaped body that gives rise to most of glomerulus and tubular epithelia. As nephrogenesis progresses, the newly formed S-shaped body is fused to the ureteric bud, from which the collecting ducts and ureter originate (63, 64).

Cap mesenchyme expresses the transcriptional factors *Six2* and *Cited1* and gives rise to Bowman's capsule, podocytes, the proximal and distal convoluted tubules and the loop of Henle. There is an outer layer of loose mesenchyme cells, adjacent to the cap mesenchyme, which expresses different transcriptional factors: *cKit* (endothelial precursors) or forkhead box D1 (*FoxD1*, stromal cells). The latter factor is responsible for the generation of RPC, mesangial cells and all mural cells, including vascular smooth muscle cells (VSMC), perivascular fibroblasts and pericytes (65-67).

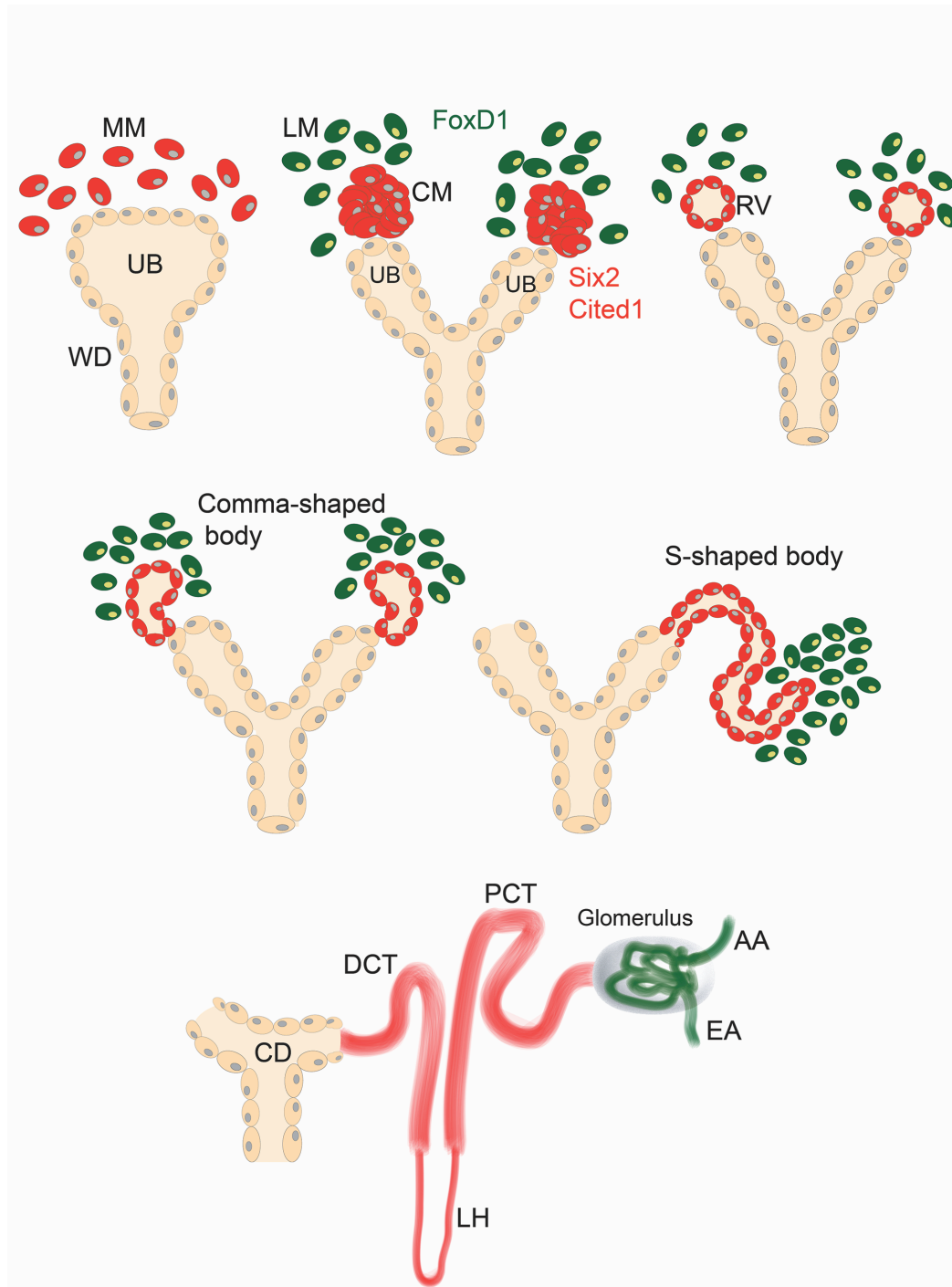


Figure 3. Schematic illustration of nephrogenesis. The ureteric bud (UB) interacts with the methanephric mesenchyme (MM), resulting in the subsequent formation of the cap mesenchyme (CM) and loose mesenchyme (LM). The CM harbors the transcription factors Six2 and Cited1 (in orange), and will give rise to the tubular system (proximal convoluted tubule (PCT), loop of Henle (LH) and distal convoluted tubule (DCT); the LM harbors the transcription factor FoxD1 (depicted in green), and will give rise to most of the glomeruli and vascular cells from the afferent arteriole (AA) and efferent arteriole (EA). The UB will evolve to form the collecting duct (CD) and ureter (61, 64, 68). WD: Wolfian duct.

### 3.3 THE RECRUITMENT PHENOMENON

JGC lineage involves differentiation of the above metanephric mesenchymal cells. This complex process generates hemangioblasts, which will evolve to endothelial cells, and RPC precursors, the latter harboring the transcriptional factor FoxD1. During kidney ontogeny, these precursors will give rise to JGC and a subset of VSMC (65, 67). In the adult, stress events that threaten body homeostasis, such as hypotension or extracellular fluid depletion, are normally corrected through renin release by JGC. Nevertheless, if this response does not suffice, or if renin expression is chronically stimulated, VSMC along the preglomerular arterioles undergo metaplasia to a renin cell phenotype in order to also synthesize renin, a phenomenon known as “recruitment” (69) (Figure 4). Importantly, the upregulation of renin synthesis and release following a homeostasis threat is due to a rise in the number of RPC (hyperplasia) rather than an elevation on the renin production per cell (hypertrophy) (70, 71).

The recruitment phenomenon is an indispensable mechanism to maintain homeostasis. In the 1970s, Cantin et al. observed metaplasia of VSMC into JGC in the arteries and arterioles of ischemic kidneys (72). Nowadays, it is known that this transformation involves differentiation of a non-renin-expressing cell into a phenotype that is able to synthesize renin, and occurs in the descendants of cells that previously expressed renin during development (73). Interestingly, once the stimulation perpetuates, the recruitment intensifies, and RPC may occur all along the extension of preglomerular arterioles, larger vessels, in the extraglomerular and intraglomerular mesangium, in a pattern that resembles the development of the embryonic kidney (73). In a recent review, Gomez emphasized that recruitment does not involve migration or replication of cells, but solely concerns a phenotype switch toward renin expression by cells whose capability to produce renin is latent, and re-acquired following appropriate stimulation (68).

Nevertheless, Dzau et al. identified liver X receptor alpha (LXR $\alpha$ ), a nuclear receptor, as an important player in the induction of renin expression in JGC. They showed that LXR $\alpha$  exerts its activity as a cAMP-responsive regulator, binding to a unique upstream region of the renin promoter (74). LXR $\alpha$  activation additionally upregulated a set of genes (e.g., c-myc) that are involved in cellular differentiation,

proliferation and migration. Accordingly, LXR $\alpha$  would induce JGC hypertrophy and hyperplasia, through its coordinate interaction on the renin and c-myc promoters (70).

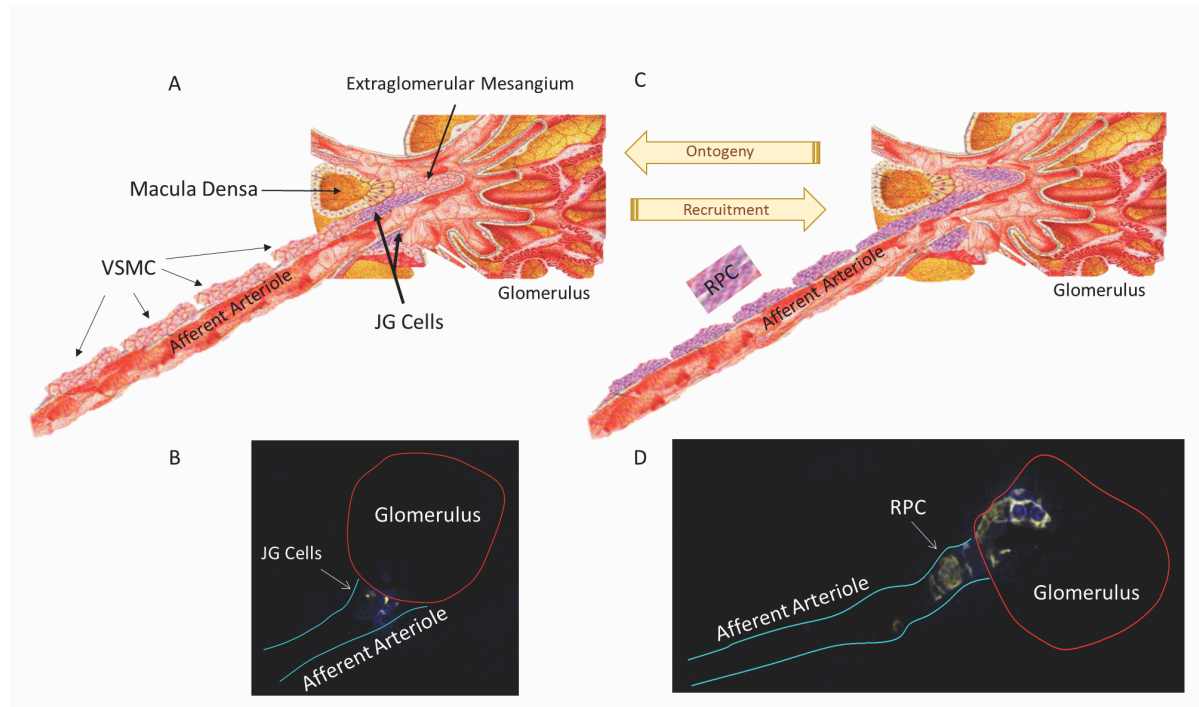


Figure 4. The “recruitment” phenomenon, illustrated by a schematic illustration (panels A and C) and immunofluorescence and fluorescent in situ hybridization data from control and captopril-treated mice (panels B and D, modified from (75)). In adult kidneys, renin is produced by the juxtaglomerular (JG) cells located within the afferent arterioles at the entrance of the glomeruli. However, under chronic renin stimulation (e.g., following captopril treatment), renin lineage cells (like the vascular smooth muscle cells (VSMC)) along the afferent arterioles may convert into a renin-producing cell (RPC) phenotype in order to maintain the homeostasis.

Moreover, mesenchymal stem cells (MSC) have also been suggested to play a pivotal role in the recruitment phenomenon. Matsushita et al. demonstrated that human and murine MSC are capable of synthesizing renin following LXR $\alpha$  activation. Indeed, MSC overexpressing LXR $\alpha$  and under continuous cAMP stimulation underwent differentiation to a RPC phenotype, which could also express  $\alpha$ -smooth muscle actin ( $\alpha$ SMA) (76). Thus, on the basis of these findings, it was speculated that MSC, which are normally resident within the glomerulus, might be the origin of the RPC (76). Wang et al. used cell lineage tracking models to further study the role of MSC in RPC recruitment. First, they isolated MSC from the adult mouse kidney and verified the expression of typical tissue stem/progenitor cell markers, including CD44, and of metanephric mesenchymal cell markers, such as FoxD1. CD44-positive MSC-like cells differentiated into RPC following exposure to an LXR $\alpha$  agonist, cAMP or a

phosphodiesterase inhibitor (77). Furthermore, mice submitted to a low salt diet and captopril treatment, conditions well-established to induce JGC recruitment, exhibited an expansion of RPC in the kidney, accompanied by CD44 cells, with co-localization of MSC markers and renin. These results could not be reproduced with bone marrow MSC, suggesting that only MSC resident in the adult kidney contribute to JGC recruitment (77). The prostaglandin E<sub>2</sub>/E-prostanoid receptor 4 pathway, also known for its involvement in tubuloglomerular feedback, played a key role in the activation of renal CD44-positive MSC during conditions of JGC recruitment (78).

However, the participation of adult renal MSC in JGC recruitment has been questioned. Gomez et al. reported that MSC at most have a very minor contribution in comparison with the already existing pool of arteriolar cells undergoing a phenotype switch (68). The latter authors ascertained that JGC also express CD44, so that it is questionable whether MSC truly represent a different cell group in the recruitment process, or are just simply descendants of the renin cell lineage, capable of switching their renin phenotype back and forth. Moreover, CD44 expression on MSC might be an *in vitro* artifact, since primary MSC from bone marrow lacked such expression, while it did occur after culturing the cells (79). Further studies are needed to unravel the precise role of MSC in JGC recruitment.

### 3.4 cAMP PATHWAY AND RECRUITMENT

Renin is a cAMP-inducible gene. In all species tested, there is a functional cAMP response element on the renin promoter (8). Among all the intracellular second messengers that control renin secretion, the cAMP signaling cascade appears to be the core pathway for the exocytosis of renin (7, 80, 81) (Figure 5). Thus, prostaglandins, kinins, and  $\beta$ -adrenergic agonists have a stimulatory effect on renin release, in all cases because they increase cAMP generation (82).

cAMP regulates a wide range of biological processes in cells. The binding of an extracellular signal molecule to a G-protein coupled receptor activates adenylyl cyclase (AC), an enzyme that generates cAMP from ATP, increasing its intracellular levels. This rise activates cAMP-dependent protein kinase A (PKA). PKA translocates to the nucleus to phosphorylate the gene regulatory protein CREB (cAMP responsive element binding protein). CREB recognizes a specific DNA sequence, called the cAMP response element (CRE), found in the regulatory region of many genes. Once

phosphorylated, CREB recruits the coactivator CBP (CREB-binding protein), which stimulates gene transcription (83).

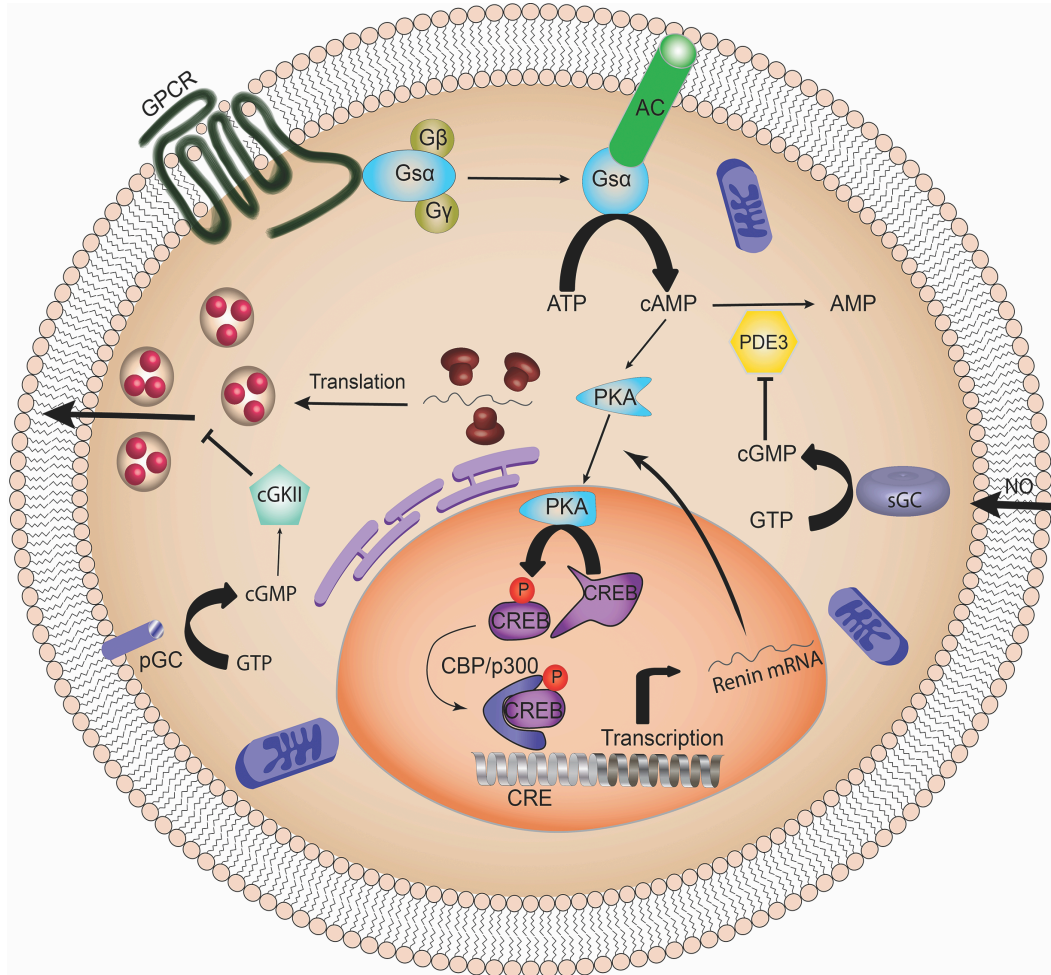


Figure 5. Simplified scheme showing how cAMP and cGMP regulate renin (modified from (68)). ATP, adenosine-triphosphate; GTP, guanosine-triphosphate; cAMP, cyclic adenosine-monophosphate; AC, adenylate cyclase; CBP, CREB-binding protein; CRE, cAMP response element; CREB, cAMP response element binding protein; cGMP, cyclic guanosine-monophosphate; PDE, phosphodiesterase; NO, nitric oxide; pGC, particulate guanylate cyclase; sGC, soluble guanylate cyclase; GPCR, G-protein-coupled receptor; G $\alpha$ , stimulatory G protein  $\alpha$ -subunit; G $\beta$ , inhibitory G protein  $\beta$ -subunit; G $\gamma$ , inhibitory G protein  $\gamma$ -subunit; PKA: protein kinase A; cGKII, cGMP-dependent protein kinase type II.

Interestingly, conditional deletion of G-protein subunits in RPC has a great impact on their function. Indeed, mice with protein G $\alpha$  (stimulatory subunit  $\alpha$ ) deficiency in JGC have very low plasma renin concentrations, with resulting low levels of aldosterone and arterial blood pressure. Moreover, such deletion also resulted in abnormalities in the glomerular arterial tree (84, 85).

Elegant evidence on the regulation of renin production by cAMP was obtained by Gomez et al., who labeled cells of renin lineage with cyan fluorescent protein (CFP), and cells producing renin with yellow fluorescent protein (YFP) (86). This yielded suitable amounts of cells which could still produce renin after several passages. CFP-labeled cells expressed VSMC markers like  $\alpha$ -SMA and smooth muscle myosin heavy chain (SM-MHC or Myh11), but not renin. However, after stimulation with forskolin (an AC stimulator) or cAMP analogs, they began to express YFP and renin, and decreased  $\alpha$ -SMA and Myh11 expression. This response was even bigger with more intense or longer stimuli, suggesting that the recruitment response is graded (86).

### 3.5 ROLE OF CALCIUM AND CGMP

Calcium plays an important role in the biology of secretory cells. In general, a rise in cytosolic calcium leads to the release of their content. However, the opposite occurs in parathyroid cells and JGC, where calcium inhibits renin exocytosis. This is known as the "calcium paradox", and it remained as a mystery for decades (82, 87).

JGC harbor 2 isoforms of AC (types V and VI), which are inhibited by cytosolic calcium. Thus, particularly in JGC, a decrease in cytosolic calcium would stimulate AC, resulting in cAMP synthesis and, consequently, renin release (88, 89). Initially, it had been reported that calcium inhibits renin gene transcription and destabilizes renin mRNA (90). More recently, it became clear that calcium stimulates, via the calcium sensing receptor, a calcium calmodulin-activated phosphodiesterase 1C (PDE1), an enzyme that degrades cAMP, thereby providing an additional explanation of the calcium paradox (91).

The contribution of cGMP to renin release is more complex, with both stimulatory and inhibitory effects (87). The cGMP and cAMP pathways are cross-linked. Nitric oxide (NO) activates soluble guanylate cyclase (GC) to generate cGMP, which in turn inhibits phosphodiesterase 3, a cAMP-degrading enzyme. Consequently, cAMP levels will go up, and renin release will rise (87, 92). However, ligands that increase cGMP via activation of particulate GC (like atrial natriuretic peptide) inhibit renin exocytosis through activation of cGMP-dependent protein kinase type II (7, 87). Interestingly, Neubauer et al. recently demonstrated that RPC recruitment is dependent on NO availability and the NO-GC signaling pathway (93).

### 3.6 EPIGENETIC MECHANISMS AND MICRORNA

Acetylation and deacetylation of histones are important epigenetics mechanisms involved in gene transcription regulation. Acetylation is mediated by histone acetyltransferase (HAT), which leads to the transfer of an acetyl functional group to histone molecules, promoting nucleosomal relaxation and transcriptional activation. Deacetylation is mediated by histone deacetylase (HDAC), and results in chromatin condensation and transcriptional repression (94).

Using the double-fluorescent reporter mouse model described above, Gomez et al. observed that chromatin remodeling contributes to the recruitment process, at the cAMP level, through histone H4 acetylation (86). The underlying mechanism involved the CREB-recruited cofactors CBP and p300, which exhibit HAT activity and, in the CRE region, promote nucleosomal relaxation and, consequently, transcriptional activation. In support of this concept, forskolin increased histone H4 acetylation in the CRE region (86). Studies carried out in mice with conditional deletion of CBP and p300 in RPC revealed that individual deletion of one of these cofactors did not affect renin expression, while simultaneous deletion reduced renin in adult life, and resulted in renal interstitial fibrosis (95). CBP/p300 were also indispensable for re-expression of renin in the arteriolar VSMC of mice exposed to low sodium + captopril (96). Taken together, RPC have a poised chromatin landscape suitable to respond properly to threats, allowing these cells to switch the renin phenotype on and off (68).

In addition to the epigenetic control mechanisms, microRNAs (miRNAs) also control JGC activity. miRNAs are endogenous small non-coding RNA molecules, containing around 18-22 nucleotides. They exert their function by targeting mRNA, inducing decay or translational repression (97). miRNA genes are phylogenetically conserved, and are involved in many cell processes such as developmental timing, death and proliferation (98). miRNA transcription, usually by RNA polymerase II, results in a long transcript, whose structure will be cleaved by the RNase III endonuclease Drosha and the cofactor DGCR8, yielding a miRNA precursor (pre-miRNA). This precursor is processed by the RNase III enzyme Dicer, and the product is incorporated into the RNA-induced silencing complex, where gene silencing proceeds (99).

Gomez et al. established the importance of Dicer for the JGC and, even further, for the morphologic and physiologic integrity of the kidney. They discovered that conditional deletion of Dicer in cells of the renin lineage in mice reduced the number of JGC and decreased renin gene expression, thus leading to reduced plasma renin and blood pressure levels. The animals also presented kidneys with vascular abnormalities and striped fibrosis (100). Noteworthy, this vascular pattern was quite similar to that found in mice with ablation of the RPC, through the expression of diphtheria toxin A chain driven by the renin promoter (60). Surprisingly, kidney vessels exhibited normal wall thickness and lumen size, in contrast to the concentric hypertrophy and thick vessel walls seen when RAS genes are deleted, including renin. Apparently, RPC are responsible for arterial wall thickening, by producing angiogenic and trophic factors (60, 61).

Furthermore, Medrano et al. identified two miRNA, miR-330 and miR-125b-5p, whose opposite actions are crucial for the recruitment phenomenon. miR-125b-5p is normally expressed in the VSMCs of the afferent arteriole, and responsible for sustaining a contractile phenotype. Yet, it is also expressed in JGC, in order to preserve their contractile function. However, under a homeostasis threat, miR-125b-5p expression diminishes in VSMC, allowing them to undergo a metaplastic transformation into a renin phenotype, and remains unaltered in JGC. miR-330 is expressed in JGC only, and inhibits contractile features, thus favoring renin production (101).

### 3.7 JGC SIGNATURE: THE MYO-ENDOCRINE PROFILE

Although several factors have been identified that regulate renin production and secretion, RPC-specific markers were limited to renin itself, and the gene *Zis* transcript (54). To overcome this problem, Brunskill et al. targeted YFP to mouse JGC and used fluorescence-activated cell sorting (FACS) to enrich tagged cells for transcriptome analysis. This approach yielded a set of 369 core genes, responsible for the JGC gene regulatory network (102). Furthermore, this distinct array of genes that governs JGC identity is unique when compared to other cell types in the kidney. Mainly, it encompasses genes highly expressed in both smooth muscle and endocrine cells (102).

Among the genes identified in the transcriptome analysis, renin was the highest transcribed gene. The second highest one was aldo-keto reductase family 1, member B7 (Akr1b7), responsible for detoxification of steroidogenesis products. Akr1b7 is a member of aldo-keto reductase superfamily, which reduces harmful aldehydes and ketones produced from the breakdown of lipid peroxides to their respective alcohols (103). Remarkably, despite its high expression on JGC, mice with Akr1b7-deficient kidneys had no abnormalities in renin production and secretion, while renin deletion also did not affect Akr1b7 expression (102, 104). Therefore, Akr1b7 gene might function as a novel JGC marker, independently of renin. Other highly expressed transcripts involved genes related to the smooth muscle phenotype, like  $\alpha$ -SMA, Myh11 and calponin (Cnn1) (102).

Interestingly, the aforementioned genetic regulatory network allows RPC to possess either an endocrine or a contractile phenotype. Hence, this bivalent profile sustains the ability of RPC to switch phenotype, depending on the situation. Therefore, during a homeostasis challenge, renin lineage cells have the gene program to differentiate into an endocrine cell, synthesizing and releasing renin, in order to reestablish the homeostasis. Moreover, due to their position, at the glomerular hilum, JGC should also retain contractile properties, allowing them to contract or relax and, subsequently, to adjust renal blood flow and glomerular filtration rate (68, 102).

### 3.8 NOTCH SIGNALING PATHWAY

The Notch signaling pathway is a highly conserved system, present in all animal species, which plays a pivotal role in local cell-cell communication, determining cell fate decisions and controlling patterns formation during ontogenesis. Its dysfunction is linked to severe developmental defects and pathologies (105). The Notch signaling cascade starts with the binding of specific ligands to the Notch transmembrane receptor, leading to cleavage of the intracellular Notch receptor domain (NIC). NIC translocates to the nucleus, where it binds to RBPJ (recombination signal binding protein for Ig-kJ region), a transcription factor that normally represses Notch target genes by recruiting a co-repressor complex. However, once it is coupled to NIC, RBPJ recruits cofactors that activate the transcriptional machinery (106).

Interestingly, among the 369 core genes that confer the JGC identity according to the approach performed by Brunskill et al., there are members of the Notch pathway, including RBPJ (102). In fact, RBPJ had already been related to RPC plasticity by Castellanos Rivera et al. (107). They generated a conditional knockout (cKO) of RBPJ in renin lineage cells. This resulted in a striking reduction in the JGC number and renin expression, with subsequently low plasma renin levels and a low blood pressure. Furthermore, under conditions that trigger the recruitment phenomenon, such as sodium depletion and captopril treatment, RBPJ-cKO mice were unable to exhibit renin expression along the afferent arterioles, i.e., the ability of their VSMCs to regain the renin phenotype was impaired.

Additionally, mice with RBPJ-cKO in renal cells of FoxD1 lineage displayed significant renal abnormalities, including a decline in the arteries and arterioles number, with a thinner smooth muscle cell layer and renin depletion, further upholding the concept that RBPJ is a major determinant of the transformation of FoxD1 cells progenitors into a healthy kidney vasculature (108). Experiments in transgenic renin reporter zebrafish fully support the essential role of the Notch signaling pathway for developmental renin expression and its association with proper angiogenesis (109).

RBPJ also has a pivotal role in the maintenance of the JGC myo-endocrine gene program. Using a bacterial artificial chromosome reporter, it was observed that RBPJ activates the renin promoter directly (55). A double-fluorescent mice reporter model subsequently revealed that RBPJ deletion does not affect RPC endowment. RPC were at their proper location, although unable to express renin and *Akr1b7*, and, surprisingly, also did not express the VSMC markers  $\alpha$ -SMA, *Myh11* and *Cnn1*. Yet, they displayed an upregulation of genes related to the immunological system, such as *lipocalin-2*, *lysozyme-2*, *chemokine ligand-9* and *interleukin-6* (55). Furthermore, Belyea et al. identified renin progenitors in mouse bone marrow, and found that in the presence of RBPJ-cKO in the renin cell lineage, those progenitors gave rise to a very aggressive lymphoblastic leukemia (110).

JGC are surrounded by multiple cell types, including pericytes, endothelial cells, epithelial cells, VSMCs, mesangial cells, and macula densa cells. Direct cell-to-cell interaction will undoubtedly contribute to normal RPC functioning. It is therefore not surprising that, among the highly expressed transcripts identified by Brunskill et al. in JGC, is *connexin 40* (102). Connexins are transmembrane proteins, six of

which assemble to mold a hemichannel. When 2 hemichannels of adjacent cells align, a channel is formed which allows the cytoplasm of both cells to connect. A set of these channels in parallel builds a gap junction, a structure that permits the cells to share small molecules and, therefore, to respond to extracellular signals in a coordinated way (56). Unexpectedly, in mice lacking connexin 40, RPC were found in the periglomerular interstitium, and not at their normal juxtaglomerular location. Besides, the recruitment phenomenon (following severe sodium depletion) did not occur at its usual location, i.e., in the wall of the upstream preglomerular arterioles (111). Apparently therefore, cell-to-cell communication via gap junctions is essential for the correct juxtaglomerular positioning and recruitment of RPC.

### 3.9 PLASTICITY AND REGENERATION

More than 100 years have passed since renin's discovery, and the RAS now turns out to have multiple effects beyond its role in blood pressure regulation. As outlined in this review, renin cells function as pluripotent progenitors for other kidney cells types (73, 112). Normally, a low perfusion pressure leads to an expansion of RPC. Kurt et al. investigated to what degree this relates to hypoxia per se, by deleting the von Hippel-Lindau protein in JGC, i.e., the negative regulator of the hypoxia-inducible transcriptional factor-2 (HIF-2 $\alpha$ ). Remarkably, following the upregulation of HIF-2 $\alpha$  by this procedure, RPC started to express erythropoietin instead of renin, and the normal renin upregulation after low salt was no longer seen. In fact, JGC were reprogrammed into fibroblast-like cells, expressing collagen I and PDGF receptor  $\beta$  (PDGFR $\beta$ ) (113, 114). Clearly therefore, hypoxia-inducible genes are essential for normal development and physiologic adaptation of RPC. The upregulated PDGFR $\beta$  expression in these cells is in full agreement with the results from the human reninoma studies showing that the PDGFB- PDGFR $\beta$  pathway downregulates renin expression (115).

Pippin et al. proposed that cells of renin lineage present alongside the preglomerular arteries participate in the glomerular regeneration after podocyte injury (116). In support of this concept, renin cells from the juxtaglomerular apparatus were shown to migrate to the glomerular tuft, in order to replace podocytes (117). This is

quite striking, since podocytes are normally derived from a different embryonic structure, the cap mesenchyme cells.

Easier to understand is the participation of renin progenitors in glomerular mesangium regeneration, since mesangium cells, considered as specialized pericytes, are derived from FoxD1 stromal cells present at the loose mesenchyme. Indeed, in a mesangiolytic murine model, renin lineage cells repopulated the intraglomerular mesangium (118). Interestingly, these cells stopped producing renin and expressed PDGFR $\beta$ , i.e., the receptor linked to renin downregulation (115). Furthermore, Stefanska et al. established that pericytes are RPC in the human kidney (119). Traditionally, pericytes are perivascular cells that wrap around blood capillaries. They are highly plastic cells contributing to multiple processes like angiogenesis, tumorigenesis and vasculopathy progression (120). The concept that RPC are or derive from pericytes is very interesting, since pericytes possess regenerative potential and are additionally known for the fact that they express the PDGFR $\beta$  (119). In fact, in zebrafish, Rider et al. observed that renin cells express this marker (121).

### 3.10 CONCLUDING REMARKS

How exactly renin cells are able to differentiate into many different phenotypes remains to be clarified. The signals allowing RPC to shift phenotype, or to migrate to an injury site are now only beginning to be unraveled. Many questions still need to be answered, most importantly, whether regeneration would eventually allow a restoration of normal function. This is of particular relevance in chronic glomerulopathies, where glomerular cells are destroyed, with subsequent overproduction of extracellular matrix, fibrosis and architectural disruption, all leading to physiological impairment. Apparently, under such severe pathological conditions, tissue regeneration by RPCs either does not occur or is insufficient. One possibility is that RPCs under pathological conditions transform to fibroblast-like cells, thus contributing to renal fibrosis themselves. Currently, RAS blockade is the cornerstone of renal and cardiovascular diseases. Simultaneously, it is well known that RAS blockers, like most anti-hypertensive drugs, induce RPCs recruitment. The long-term effect of this chronic activation is still unknown, nor do we know to what degree it contributes to (further) impairment of renal function. Detailed knowledge of this

process would lead to better treatment options and more favorable outcomes. Clearly, this whole area not only illustrates the complexity of the renin cell, but also represents an exciting new field that needs to be explored in the coming years.

## 4 TRANSCRIPTOME ANALYSIS OF HUMAN RENINOMAS AS AN APPROACH TO UNDERSTANDING JUXTAGLOMERULAR CELL BIOLOGY

### 4.1 INTRODUCTION

The aspartyl protease renin catalyzes the rate-limiting step in the renin-angiotensin system (RAS). Renin is produced almost exclusively by so-called juxtaglomerular (JG) cells that line the afferent arterioles at their point of entry into the kidney glomeruli. JG cells convert renin from its inactive precursor (prorenin) by proteolysis and store the resulting active renin in lysosome-like dense cytoplasmic granules whose content can be rapidly released in response to such stimuli as a sudden drop in the perfusion pressure of the afferent arteriole or beta-adrenergic stimulation. During kidney development, renin-producing cells are more broadly distributed along the lumen of the nascent arterioles (59) and gradually become restricted to the glomerular poles after birth. Prolonged exposure to stimuli, such as blood pressure-lowering medication, a low-salt diet or ischemia results in an apparent recruitment of new renin-producing cells along the afferent arterioles (122), which has been proposed to represent a partial return to the developmental pattern of JG cell distribution. Altogether, renin-producing JG cells display many unique biological features and because of their central role in modulating blood pressure and fluid balance, there has been long-standing interest in obtaining a better understanding of their origins and biology.

Efforts to characterize JG cells have historically been hampered by two factors: First, JG cells rapidly de-differentiate when placed in culture, losing their secretory granules and, concomitantly, their ability to proteolytically activate prorenin. As a result, attempts to immortalize both mouse and human renin-producing cells have resulted in the establishment of cell lines that have lost the ability to secrete renin (123, 124). Second, JG cells make up only approximately 1/1000 of the cell mass of the kidney, making it difficult to isolate sufficient quantities of pure cells for further characterization. As an alternative approach, Brunskill et al. (102) targeted yellow fluorescent protein to mouse JG cells and used fluorescence-activated cell sorting (FACS) to enrich tagged cells for expression analysis. The resulting study

proposed a 369 gene “signature” that characterizes mouse JG cells, although few of these have been verified in subsequent studies.

In an effort to extend these studies and to determine if the genes identified in the mouse also characterize human renin-producing cells, we have catalogued the gene expression pattern of biopsies derived from 4 human renin-producing tumors, or reninomas. Reninomas are rare, benign tumors arising from a proliferation of JG cells in the kidney cortex (125, 126) and are often detected due to the appearance of fulminant hypertension in relatively young patients (mean age under 30 years) with no obvious explanatory risk factors. RNA sequencing (RNA-Seq) revealed a set of 54 highly expressed genes that are common to all four tumors and another 30 expressed in 3 of the 4 biopsies tested. In situ hybridization of mouse kidney sections subsequently confirmed JG cell expression of 44 of these genes, the vast majority of which have not previously been reported to be expressed in JG cells. Finally, hypothesizing that the highly expressed reninoma genes affect renin-synthesizing capacity, we selected 10 ligands (based on known relevance for blood pressure and kidney disease) and studied their effects on (pro)renin release by As4.1 cells. These cells are derived from a transgene-induced mouse kidney tumor, and do not store renin. They may thus be considered as de-differentiated JG cells which have lost their capacity to secrete lysosomes. Consequently, As4.1 cells might serve as a model to study the effect of reninoma-specific ligands on JG cell plasticity. Results revealed an unexpected suppressant role for platelet-derived growth factor B (PDGFB).

## 4.2 METHODS

### 4.2.1 Animals

The mice used in this study were housed in a 10/14 hour light/dark cycle with free access to normal mouse chow and water. All of the experiments described herein were approved by the institutional Animal Ethics Committee and are in compliance with guidelines issued by the Canadian Council on Animal Care (CCAC). C57BL/6 mice were obtained commercially from Harlan Teklad (Lachine, Quebec, Canada) and bred in a specific pathogen free facility. Where indicated, 10-12 week old male mice were treated for 7 days with the ACE inhibitor captopril (Sigma-Aldrich,

Oakville, Ontario, Canada) at a dose of 10 mg/kg/day in drinking water, as described before (127).

#### **4.2.2 Preparation and Sequencing of Reninoma RNA**

These studies were approved by the Human Ethics committee of the IRCM (protocol 2013-31). Biopsies of histologically proven reninomas from patients with history of severe hypertension associated with high plasma active and inactive renin (i.e., renin and prorenin) concentrations were obtained at surgery from 4 anonymous patients (Paris1, Paris2, Montreal, Rotterdam) and snap frozen in liquid nitrogen. Total RNA was isolated using Trizol (Invitrogen) from 10 mg pieces of each tumor or biopsy, and was further purified using RNeasy MinElute Cleanup spin (#74204, Qiagen, Toronto, Canada) according to manufacturer's instructions and eluted in a final volume of 10  $\mu$ L. Eight  $\mu$ L of RNA was used as input, and library preparation conducted according to manufacturer's instructions ("Low-Throughput (LT) Protocol" TruSeq RNA Sample Preparation Guide, Illumina). Resulting library preps were assessed for quality and concentration using the Agilent 2100 Bioanalyzer (Agilent Technologies). Fifty base pair paired end sequencing was conducted by the McGill University Genome Quebec Discovery Center using the HiSeq2000 (Illumina).

#### **4.2.3 Mapping and Transcript Quantification**

Low quality bases (any leading or trailing base with a quality below 3, and any window of 4 bases with an average quality below 15) were removed with Trimmomatic (v0.22) (128). After trimming, the sequences were aligned mapped to the human reference genome hg19 using Tophat (v2.0.6) (129), with a reference annotation downloaded from the UCSC Genome Browser (<http://genome.ucsc.edu/>). Transcript assembly and abundance were determined computed using Cufflinks (v2.0.2). The gene expression levels are represented as Fragments Per Kilobase of transcript per Million mapped reads (FPKM). The normalized data are deposited in <<http://www.ncbi.nlm.nih.gov/geo/query/acc.cgi?acc=GSE57401>>.

#### **4.2.4 Immunofluorescence/Fluorescent *In Situ* Hybridization**

iFISH was carried out as described (130). Mice (5 day old, 10-12 week old and 10-12 week old treated with captopril for 7 days) were sacrificed and kidneys were rapidly removed and de-capsulated before being snap frozen in isopentane on dry ice. Eight to ten micron sections were cut on a cryotome, and slide-mounted sections were post-fixed with 4% paraformaldehyde for 1 hour at room temperature. Total cDNA was generated from C57BL/6 mouse kidney and an approximate 1000 bp fragment for each of the targeted transcripts was amplified by polymerase chain reaction (PCR) using the oligonucleotides shown in Table S4, and subsequently sequenced to verify identity. An engineered T7 polymerase promoter on the double-stranded cDNAs was used as a template to transcribe a cRNA containing UTP labeled with disoxygenin (DIG). The cRNAs were hybridized to the kidney sections and after washing the slides were incubated with biotin-conjugated mouse monoclonal anti-DIG (0.25  $\mu\text{g}/\text{slide}$ ) and rabbit anti-mouse renin (Molecular Innovation), diluted 0.15  $\mu\text{g}$  in 100  $\mu\text{L}$ . After thorough washing, the slides were incubated with streptavidin- HRP (Biolegend # 405210) diluted 1/100 and goat anti-rabbit IgG conjugated to Alexa 488 (Invitrogen, A11008) diluted 1/400 followed by incubation with Cyanine3-tyramide reagent pack (PerkinElmer) and mounted in Mowiol. All samples were scanned with an LSM700 confocal laser scanning microscope (Carl Zeiss, Inc) linked to an AxioObserver Z.1 (Carl Zeiss, Inc) set with the same parameters. We used a 40x oil objective with a numerical aperture of 1.3. The 488 laser (reflected on the main beam splitter 405/488/555/639) was used to excite the Alexa-Fluor 488 probe and the fluorescent signal was detected by filter through the low-pass adjustable dichroic set to 542nm. The 555 laser (reflected on the main beam splitter 405/488/555/639) was used to excite the Alexa-fluor 555 probe and the fluorescent signal was detected by filter through the high-pass portion of the adjustable dichroic set to 559nm. The image pixel size was 0.078 $\mu\text{m}$  collected with 2048x2048 pixels at 8bit depth with a pixel dwell time of 0.39 $\mu\text{s}$  and averaging lines 16 times. The DIC image was acquired using the transmitted photo-multiplier tube (PMT).

#### **4.2.5 Cell Culture Studies**

Human Embryonic Kidney (HEK) 293 cells and the mouse kidney tumor cell line As4.1 (ATCC, Manassas, VA) were cultured in 75  $\text{cm}^2$  culture flasks using

Dulbecco's Modified Eagle Medium (DMEM Media - GlutaMAX™-I; Thermo Fisher Scientific, The Netherlands), supplemented with 10% heat-inactivated Fetal Bovine Serum (FBS; Thermo Fisher Scientific), 100 U/mL penicillin and 100 U/mL streptomycin (Lonza Benelux, The Netherlands), and maintained in a humidified atmosphere at 37°C with 5% CO<sub>2</sub>.

#### **4.2.6 Plasmids**

Ten highly expressed reninoma genes encoding for ligands were selected from the 100 most upregulated genes present in the transcriptome analysis, focusing on genes involved in blood pressure regulation and renal disease. Their corresponding mouse cDNAs were cloned with a c-myc epitope. One Shot® TOP10 Chemically Competent E. coli (Thermo Fisher Scientific) cells were used for plasmid propagation, according to the manufacturer's instructions. The plasmid extraction was achieved using the Qiagen® Plasmid Mini Kits (Qiagen).

#### **4.2.7 Transfection and Ligand Exposure of As4.1 Cells**

HEK293 cells were transfected with the mammalian expression vector pcDNA3, containing each of the 12 selected mouse cDNAs. The transfection was performed with X-tremeGENE™ 9 DNA Transfection Reagent (Sigma-Aldrich, The Netherlands), according to the manufacturer's instructions. Once HEK293 and As4.1 cells were confluent in the culture flasks (90-100%), they were trypsinized and resuspended in 10 mL of DMEM, supplemented with 10% FBS, 100 U/mL penicillin and 100 U/mL streptomycin. Then, HEK293 and As4.1 cell suspensions (500 and 200 µL of each, respectively) were transferred to a 6-well plate with 1.5 mL of DMEM. Twenty-four hours later, the medium of the HEK293 cells was refreshed with 900 µL of DMEM, and the transfection mix prepared in a proportion of 1 µg of plasmid to 3 µL of transfection reagent. The final volume was adjusted to 100 µL, and this was added to the HEK293 6-well plates. Forty-eight hours later, the conditioned medium from the transfected HEK293 cells was transferred to the 6-well plates seeded with As4.1 cells, and incubated for another 48 hours. Thereafter, medium and cells were collected, cells were lysed with RIPA buffer (50 mmol/L Tris HCl, 150 mmol/L NaCl, 1% Triton X-100, 0.5% sodium deoxycholate, 0.1% SDS and 1 mmol/L EDTA)

supplemented with protease inhibitor (Phosphatase Inhibitor Cocktail 3 plus cOmplete™, Mini Protease Inhibitor Cocktail, Sigma-Aldrich), and all samples were stored at -80°C.

#### **4.2.8 Western Blot**

In order to test the HEK293 transfection efficiency for each of the cDNAs, WB experiments were carried out with the medium obtained at 24 or 48 hours after transfection. The medium was collected and treated with protease inhibitor (Phosphatase Inhibitor Cocktail 3 plus cOmplete™, Mini Protease Inhibitor Cocktail, Sigma-Aldrich), and protein measurements were performed using the Pierce™ BCA Protein Assay Kit (Thermo Fisher Scientific). Samples were prepared with a 4X Laemmli buffer (4% SDS, 20% glycerol, 10% 2-mercaptoethanol, 0.004% bromophenol blue and 0.125 mol/L Tris HC; Bio-Rad, Veenendaal, The Netherlands) and heated at 95°C for 5 minutes. The protein electrophoresis was performed with Mini-PROTEAN® Precast Gels (Bio-Rad), with a 16-µL of final volume for all samples. The bands were transferred by electroblotting to a PVDF membrane, which was blocked thereafter in a 5% Blotting Grade Blocker casein solution (Bio-Rad) for 1 hour, and then incubated overnight with the primary antibody (anti-Mouse c-myc-tag monoclonal antibody, 1:1500; Cell Signaling Technology, Leiden, The Netherlands) under agitation at 4°C. On the next day, the secondary antibody was applied for 1 hour at room temperature (Goat anti-mouse IgG (H+L)-HRP conjugate, 1:8000; Bio-Rad). The membrane was then washed and incubated with home-made peroxidase substrate for enhanced chemiluminescence for 2 minutes, and pictures were taken with the ImageQuant LAS 4000 (GE Healthcare Life Sciences, Eindhoven, The Netherlands).

#### **4.2.9 (Pro)renin Measurement and Determination of Cell Viability**

Renin and prorenin were determined in medium and cell lysates 48 hours after the treatment of the As4.1 cells with the conditioned medium from the transfected HEK293 cells, making use of an in-house enzyme-kinetic assay, applied both before and after prorenin activation with trypsin (131).

As4.1 cell viability following PDGFB exposure was evaluated by (3-(4,5-dimethylthiazol-2-yl)-2,5-diphenyl-2H-tetrazolium bromide (MTT, Sigma Aldrich)

assay according to the manufacturer's instructions. In brief, confluent cells were trypsinized, resuspended in DMEM at a density of  $3 \times 10^6$  cells/mL, and incubated in 96-well plates at 100  $\mu$ L/well with or without PDGFB (Sigma-Aldrich). Twenty hours later, 10  $\mu$ L MTT (5 mg/mL in PBS) was added to each well, and incubated for 4 hours. Then, the medium was replaced by 230  $\mu$ L 0.04 mol/L HCl in isopropanol, and following 30 min of agitation at room temperature, absorbance was determined at 570 nm, with background subtraction determined at 650 nm.

#### 4.2.10 Quantitative PCR

To extract total RNA from As4.1 cells, cells were washed twice with cold PBS, and homogenized with 500  $\mu$ L of TRI reagent (Sigma-Aldrich). Next, 200  $\mu$ L chloroform (Sigma-Aldrich) was added, and centrifugation was performed at 14000 rpm. Supernatants were collected and mixed with 250  $\mu$ L isopropanol (Sigma-Aldrich), centrifuged, and the pellet was washed in 500  $\mu$ L of 75% ethanol, re-centrifuged and suspended in diethylpyrocarbonate (Invitrogen, Groningen, The Netherlands) water. RNA concentration and purity were determined by NanoDrop 2000 Spectrophotometer (Thermo Fisher Scientific). RNA was stored at  $-80^\circ\text{C}$ . cDNA was generated using the QuantiTect Reverse Transcription Kit (Qiagen) according to the manufacturer's instructions. The amount of RNA used per reaction was up to 1  $\mu$ g, and the final cDNA concentration was assessed by NanoDrop 2000 Spectrophotometer. cDNAs were stored at  $-20^\circ\text{C}$ . Primers for the genes of interest were designed in the Ensembl genome browser (<<http://www.ensembl.org>>) or obtained from public database (<<http://www.rtpimerdb.org>>). Sequences were evaluated with the Blast tool in the NCBI platform (<<http://www.ensembl.org/Multi/Tools/Blast>>). Primers (see Table S5) were ordered from Integrated DNA Technologies (IDT, Belgium). Reactions were prepared in 384-well plates, with the reagents: 7.5  $\mu$ L KAPA SYBR® Green FAST (KapaBiosystems), 0.3  $\mu$ L of each primer (Forward and Reverse), 0.3  $\mu$ L High ROX, and 10 ng of cDNA. Nuclease-free water (IDT) was added to set the final volume reaction at 15  $\mu$ L. The reaction protocol was identical for all qPCR experiments: 3 minutes at  $95^\circ\text{C}$  for DNA polymerase activation, 40 cycles of  $95^\circ\text{C}$  for 3 seconds for denaturation, and  $60^\circ\text{C}$  for 25 seconds for primer annealing and extension. Standard curves were constructed on the Applied Biosystems StepOnePlus™ Real-Time PCR Systems, and data were

analyzed with the Software StepOne v2.2. Gene expression quantification experiments were carried out on the Bio-Rad CFX384™ IVD Real-Time PCR Systems, and data analyzed with the Bio-Rad CFX Manager 3.0.

#### 4.2.11 Statistical Analysis

Results are expressed as mean±SEM. Data were analyzed for normal distribution using a Shapiro-Wilk's test ( $P>0.05$ ). Differences were tested using one-way or two-way ANOVA, followed by Holm-Sidak's or Dunnett's multiple comparison test.  $P<0.05$  was considered significant.

### 4.3 RESULTS

Deep sequencing of RNA (RNA-Seq) was performed on three biopsies of a first reninoma from Paris (Par1B1-B3), one biopsy from a reninoma from Montréal (Mon), two biopsies from a reninoma from Rotterdam (RotB1, B2), and a second reninoma from Paris (Par2) along with a biopsy from adjacent supposedly normal tissue from the same patient (Par2N) (Table S1). We obtained from 45-100 million reads per sample (Table 1) with comparable overall sample quality (Figure S1). Remarkably, the Fragments Per Kilobase of transcript per Million (FPKM) mapped reads values for renin were quite similar in the four tumor samples and, in each tumor, renin was expressed at 15-41 times the level of the next most abundant transcript, confirming the diagnosis of bona fide reninomas (Table 2).

Table 1 – Quality control of sequenced reads.

Sample	Number of Reads Before Trimming	Number of Reads After Trimming	% Reads Post-Filtering	Exonic Alignment Rate
Par1B1	88058080	83611860	94.95	0.811
Par1B2	88713782	84187709	94.90	0.803
Par1B3	74683086	71782557	96.12	0.813
Mon	76131363	73212125	96.17	0.760
Rot1B1	117331030	109192033	93.06	0.753
Rot1B2	95468148	88616034	92.82	0.766
Par2	55053372	47536436	86.35	0.766
Par2N	117480551	101148769	86.10	0.647

Table 2 – Ratio of the number of renin reads (FPKM) obtained in the various biopsies versus those for the next most abundant transcript. Also shown is the ratio of renin reads obtained between the putative tumor and normal adjacent tissue (Par2N) biopsies for the Par2 samples. Data are drawn from Table S1.

<b>Sample</b>	<b>Par1 (ave.)</b>	<b>Mon</b>	<b>Rot (ave.)</b>	<b>Par2</b>	<b>Par2N</b>	<b>Par2/Par2N</b>
Ren FPKM	74372	110034	110062	117805	541	217
2nd transcript (FPKM)	GNAS (2218)	GNAS (2652)	KISS1 (6830)	KISS1 (8110)		
<b>Ratio</b>	<b>33.53</b>	<b>41.49</b>	<b>16.11</b>	<b>14.53</b>		

Results obtained from the three independently analyzed biopsies of the Paris1 reninoma demonstrated an inter-sample Spearman correlation of  $>0.98$  (Figure S2, red outlines) and similar results were obtained with the two biopsies of the reninoma from Rotterdam (Figure S2, green outlines) suggesting that the sample preparation and results obtained were reliable and reproducible. In the one case in which we had biopsies of both tumor and adjacent tissue from a single patient (Paris 2), there was a 217-fold increase in the number of renin reads in the reninoma versus the “normal” sample (Table 2) although the samples overall were very highly correlated (0.92 for all genes; see Figure S2, blue outlines). By limiting the gene set analyzed in all the samples to those that were expressed at least 4-fold higher in the reninoma versus the “normal” biopsies for Paris 2, we reduced the gene set to just over 1000 (Table S2) and this resulted in the removal of low reads (which are commonly unreliable) and many “housekeeping” genes from the analysis. Using this limited gene set, we identified the 100 most-expressed genes in each biopsy (Table S3). Re-calculation of the Spearman correlation using these highly expressed genes revealed a higher discrimination between samples (Figure S3). Although the repeat biopsies continued to exhibit a correlation  $>0.98$ , the correlation between the reninomas varied between a low of 0.46 (Par1 versus Par2) and a high of 0.74 (RotB1 and Par2). Surprisingly, the highest correlation is between the Par2 and Par2N samples (0.81, Figure S3), raising the possibility that the supposedly normal sample from this patient contains some reninoma. A Venn diagram reveals that 54 of the 100 most expressed genes were common to all 4 reninomas (Table S3 and Figure S4) and another 30 genes

were highly expressed in 3 out of 4 of the tumors analyzed. Functional annotation clustering analysis (DAVID) did not reveal any statistically significant correlation for cellular function using the genes most commonly expressed in the reninomas (data not shown).

To test if these reninoma-enriched genes were also expressed in JG cells, we performed iFISH for 71 of the above 84 common reninoma transcripts (excluding, among others, genes that have no mouse equivalent) in kidney sections from C57BL/6 mice using the equivalent mouse probes (Table 3 and Figure S5). As expected, combined in situ hybridization and immunofluorescence for renin reveals perfect co-localization in the JG cells of adult mice (Figure 6A-1D). Furthermore, treatment of the mice with captopril for one week resulted in the expected recruitment of JG cells along the afferent arterioles (Figure 6E), while co-localization was also observed throughout the maturing arterioles of 5 day-old mice (Figure 6F). These results confirm the validity of this approach to assess the co-localization of the transcripts from the reninoma in the mouse JG cells.

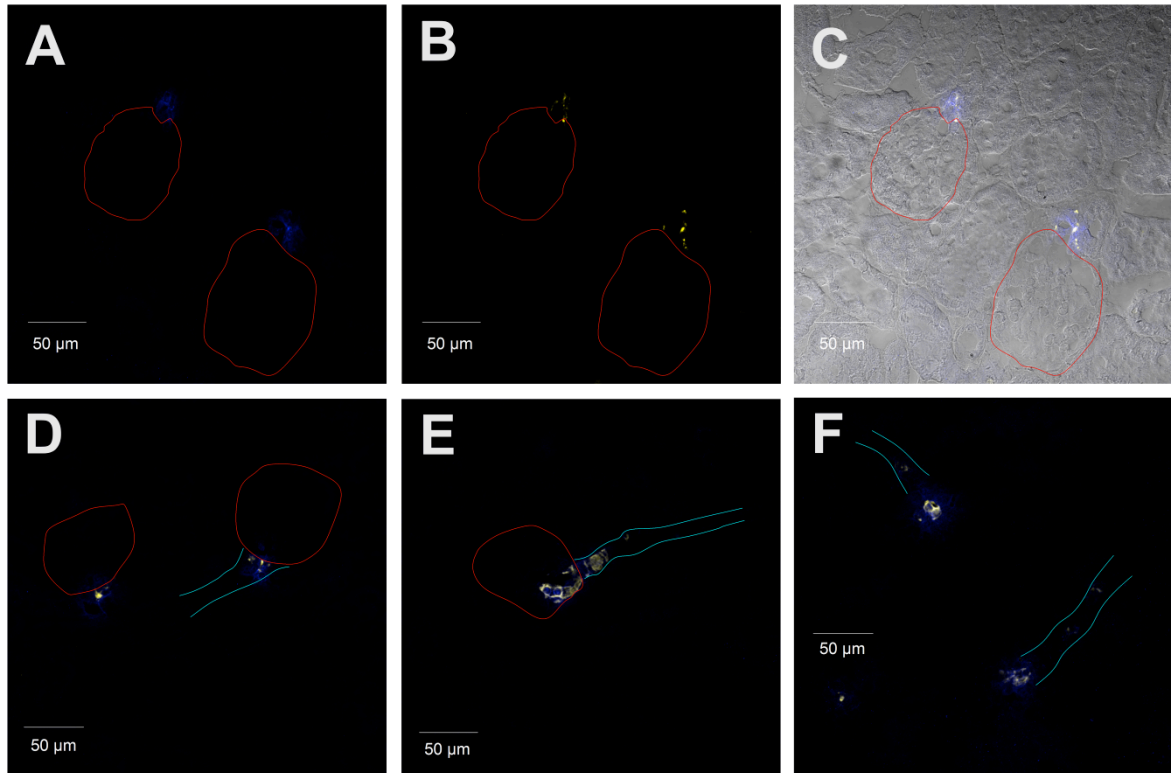


Figure 6. iFISH for renin in mouse kidney. Where possible, glomeruli are outlined in red and vessels in light blue. (a) Immunofluorescence for renin in adult mouse kidney is shown in blue; (b) In situ hybridization for renin in the same section is shown in yellow; (c) merged image from panels a and b, including phase contrast microscopy showing that renin is expressed at the base of the glomeruli as

expected; (d) iFISH overlay for renin in kidneys from adult; (e) 5 day-old mouse, and (f) adult mouse treated for one week with captopril. Original magnification X 20. Scale bar=50 $\mu$ m.

In order to obtain a semi-quantitative comparison of gene expression levels in renin-producing cells, all confocal microscopy images were taken using the same parameters and a ranking from 0 (for no expression observed) to 4 (highly expressed) was assigned for each gene under each condition tested (Table 3). Among the 71 genes tested, 44 genes are expressed in both reninomas and mouse JG cells. Twenty-four of these were detected in all three conditions (5 day-old, adult and adult treated with captopril kidneys) while the remainder showed preferential expression in one or more of the conditions (Figure S5 and Table 3). Functional annotation clustering analysis using the 44 genes expressed in both the reninomas and mouse JG cells identified “developmental processes” as the most likely gene ontology (data not shown).

From the top 100 highly expressed genes, focusing on blood pressure regulation and renal disease, we selected 10 genes coding for ligands (FSTL1, IGF2, LGALS1, MDK, MFGE8, NPPC, PDGFB, SPARC, SPARCL1, WFDC2) in order to investigate their potential role in JG recruitment. The corresponding mouse cDNAs were cloned with a c-myc epitope and transfected into HEK293 cells to obtain high concentrations of these ligands in the supernatant of the culture medium. WB experiments confirmed the presence of the proteins of each of the transfected genes in the HEK293 cell medium at 48 hours after transfection (Figure S6). Since all ligands were tagged with a c-myc epitope, the same primary antibody could be used.

Table 3 – Summary of the iFISH analysis on mouse kidney for the genes most highly expressed in the reninomas. The genes found to express in renin-producing cells (RPC) are listed in their order of expression in the reninomas from highest to lowest (see Table S1) and their relative expression in each sample is estimated on a scale of 0 (no detectable expression) to 4 (highest expression), based upon the data in Figure S5. \*Described as part of a 369 gene list that makes up a renin-producing cell signature, according to Brunskill et al. (102); #Reported as reninoma marker. Of the genes confirmed by iFISH, 36 have not been reported before in relationship to renin-producing cells. (to be continued)

Gene symbol	Gene ID	Expression in Mouse Renin-producing Cells (iFISH)			Notes
		Developing Kidney	Adult Kidney	Adult Kidney + Captopril	
<b>Present in all 4 Reninomas</b>					
REN*#	Renin	4	2	4	
KISS1	KISS-1 metastasis-suppressor	1	0	2	
GNAS	GNAS complex locus	4	1	4	
A2M	alpha-2-macroglobulin	3	0	0	
PTP4A3*	protein tyrosine phosphatase type IVA, member 3	1	0	4	
SPARCL1	SPARC-like 1 (hevin)	4	4	4	
C4A	complement component 4A (Rodgers blood group)	0	1	2	
VIM#	vimentin	4	2	4	also in mesangial cells and arterioles
MYL9	myosin, light chain 9, regulatory	4	3	3	strongest in developing arterioles
NOTCH3	Notch homolog 3 (Drosophila)	1	1	2	
MFGE8	milk fat globule-EGF factor 8 protein	2	2	4	
ITGA7	integrin, alpha 7	0	0	2	
SPARC	secreted protein, acidic, cysteine-rich (osteonectin)	2	2	0	mostly in cells adjacent to JG

Table 3 – Summary of the iFISH analysis on mouse kidney for the genes most highly expressed in the reninomas. The genes found to express in renin-producing cells (RPC) are listed in their order of expression in the reninomas from highest to lowest (see Table S1) and their relative expression in each sample is estimated on a scale of 0 (no detectable expression) to 4 (highest expression), based upon the data in Figure S5. \*Described as part of a 369 gene list that makes up a renin-producing cell signature, according to Brunskill et al. (102); #Reported as reninoma marker. Of the genes confirmed by iFISH, 36 have not been reported before in relationship to renin-producing cells. (continuation)

Gene symbol	Gene ID	Expression in mouse renin-producing cells (iFISH)			Notes
		Developing Kidney	Adult Kidney	Adult Kidney + Captopril	
<b>Present in all 4 Reninomas</b>					
JAG1	jagged 1 (Alagille syndrome)	0	1	1	mostly in arterioles adjacent to JG
SERPINI1*	serpin peptidase inhibitor, clade I (neuroserpin), member 1	0	0	1	
TBC1D1	TBC1 (tre-2/USP6, BUB2, cdc16) domain family, member 1	0	0	1	
CXCL12	chemokine (C-X-C motif) ligand 12 (stromal cell-derived factor 1)	3	0	1	mostly in cells adjacent to RPC in developing arterioles
TPM2	tropomyosin 2 (beta)	1	0	1	
SLIT3	slit homolog 3 (Drosophila)	3	0	1	only in some RPC 5 day and recruited JG capto (faint)?
PDGFRB	platelet-derived growth factor receptor, beta polipeptide	3	2	2	
GJA4	gap junction protein, alpha 4, 37kDa	1	0	2	
DBNDD2	dysbindin (dystrobrevin binding protein 1) domain containing 2	3	2	2	
FLNA	filamin A, alpha (actin binding protein 280)	3	2	4	

Table 3 – Summary of the iFISH analysis on mouse kidney for the genes most highly expressed in the reninomas. The genes found to express in renin-producing cells (RPC) are listed in their order of expression in the reninomas from highest to lowest (see Table S1) and their relative expression in each sample is estimated on a scale of 0 (no detectable expression) to 4 (highest expression), based upon the data in Figure S5. \*Described as part of a 369 gene list that makes up a renin-producing cell signature, according to Brunskill et al. (102); #Reported as reninoma marker. Of the genes confirmed by iFISH, 36 have not been reported before in relationship to renin-producing cells. (continuation)

Gene symbol	Gene ID	Expression in mouse renin-producing cells (iFISH)			Notes
		Developing Kidney	Adult Kidney	Adult Kidney + Captopril	
<b>Present in all 4 Reninomas</b>					
ISYNA1	inositol-3-phosphate synthase 1	1	1	2	
CALD1	caldesmon 1	4	2	4	also mesangial cells?
NRARP	NOTCH-regulated ankyrin repeat protein	0	1	1	
MXRA8	matrix-remodelling associated 8	1	1	2	
OAZ2	ornithine decarboxylase antizyme 2	2	2	3	
TIMP1	TIMP metalloproteinase inhibitor 1	0	0	1	
ADCY3	adenylate cyclase 3	1	1	0	
LBH	limb bud and heart development homolog (mouse)	1	1	4	
TINAGL1	tubulointerstitial nephritis antigen-like 1	1	2	4	
IGF2	insulin-like growth factor 2 (somatomedin A)	0	0	0	
IFITM3	interferon induced transmembrane protein 3 (1-8U)	0	0	0	
SFRP4	secreted frizzled-related protein 4	0	0	0	

Table 3 – Summary of the iFISH analysis on mouse kidney for the genes most highly expressed in the reninomas. The genes found to express in renin-producing cells (RPC) are listed in their order of expression in the reninomas from highest to lowest (see Table S1) and their relative expression in each sample is estimated on a scale of 0 (no detectable expression) to 4 (highest expression), based upon the data in Figure S5. \*Described as part of a 369 gene list that makes up a renin-producing cell signature, according to Brunskill et al. (102); #Reported as reninoma marker. Of the genes confirmed by iFISH, 36 have not been reported before in relationship to renin-producing cells. (continuation)

Gene symbol	Gene ID	Expression in mouse renin-producing cells (iFISH)			Notes
		Developing Kidney	Adult Kidney	Adult Kidney + Captopril	
<b>Present in all 4 Reninomas</b>					
CSRP2	cysteine and glycine-rich protein 2	0	0	0	
IFITM1	interferon induced transmembrane protein 1 (9-27)	0	0	0	
COL6A2	collagen, type VI, alpha 2	0	0	0	
CPE	carboxypeptidase E	0	0	0	
LGALS1	lectin, galactoside-binding, soluble, 1	0	0	0	
TGM2	transglutaminase 2 (C polypeptide, protein-glutamine-gamma-glutamyltransferase)	0	0	0	
CBLN4	cerebellin 4 precursor	0	0	0	
SRGN	serglycin	0	0	0	
TBX2	T-box 2	0	0	0	
COL6A1	collagen, type VI, alpha 1	0	0	0	in extraglomerular cells surrounding JG
NT5DC2	5'-nucleotidase domain containing 2	0	0	0	weak expression in cells adjacent to JG
TPM1	tropomyosin 1 (alpha)	0	0	0	
GPR124	G protein-coupled receptor 124	0	0	0	

Table 3 – Summary of the iFISH analysis on mouse kidney for the genes most highly expressed in the reninomas. The genes found to express in renin-producing cells (RPC) are listed in their order of expression in the reninomas from highest to lowest (see Table S1) and their relative expression in each sample is estimated on a scale of 0 (no detectable expression) to 4 (highest expression), based upon the data in Figure S5. \*Described as part of a 369 gene list that makes up a renin-producing cell signature, according to Brunskill et al. (102); #Reported as reninoma marker. Of the genes confirmed by iFISH, 36 have not been reported before in relationship to renin-producing cells. (continuation)

Gene symbol	Gene ID	Expression in mouse renin-producing cells (iFISH)			Notes
		Developing Kidney	Adult Kidney	Adult Kidney + Captopril	
<b>Present in all 4 Reninomas</b>					
HSPB6	heat shock protein, alpha-crystallin-related, B6	0	0	0	
CD34#	CD34 molecule	0	0	0	
HCFC1R1	host cell factor C1 regulator 1 (XPO1 dependent)	0	0	0	
PLEKHH3	pleckstrin homology domain containing, family H (with MyTH4 domain) member 3	0	0	0	
<b>Present in 3 out of 4 Reninomas</b>					
MDK	midkine (neurite growth-promoting factor 2)	1	1	4	
CPA3	carboxypeptidase A3 (mast cell)	1	2	0	
RGS5*	regulator of G-protein signaling 5	4	4	2	
ACTA2	actin, alpha 2, smooth muscle, aorta	4	0	2	mostly in VSMC in adult
CD248	CD248 molecule, endosialin	3	2	4	
IFITM2*	interferon induced transmembrane protein 2 (1-8D)	0	0	1	
TUBA1A	tubulin, alpha 1a	2	3	4	
BGN	biglycan	1	2	4	

Table 3 – Summary of the iFISH analysis on mouse kidney for the genes most highly expressed in the reninomas. The genes found to express in renin-producing cells (RPC) are listed in their order of expression in the reninomas from highest to lowest (see Table S1) and their relative expression in each sample is estimated on a scale of 0 (no detectable expression) to 4 (highest expression), based upon the data in Figure S5. \*Described as part of a 369 gene list that makes up a renin-producing cell signature, according to Brunskill et al. (102); #Reported as reninoma marker. Of the genes confirmed by iFISH, 36 have not been reported before in relationship to renin-producing cells. (conclusion)

Gene symbol	Gene ID	Expression in mouse renin-producing cells (iFISH)			Notes
		Developing Kidney	Adult Kidney	Adult Kidney + Captopril	
<b>PRESENT IN 3 OUT OF 4 RENINOMAS</b>					
ATP1B2*	ATPase, Na <sup>+</sup> /K <sup>+</sup> transporting, beta 2 polypeptide	2	2	2	
MCAM	melanoma cell adhesion molecule	2	2	3	
TAGLN	transgelin	3	2	3	also in adjacent arterioles
CRIP1*	cysteine-rich protein 1 (intestinal)	0	1	4	
MEF2C	myocyte enhancer factor 2C	0	0	0	
TGFBI	transforming growth factor, beta-induced, 68kDa	0	0	0	
TPSB2	tryptase alpha/beta 1; tryptase beta 2	0	0	0	
NPPC	natriuretic peptide precursor C	0	0	0	
GPC1	glypican 1	0	0	0	
FKBP10	FK506 binding protein 10, 65 kDa	0	0	0	
FXYP1*	FXYP domain containing ion transport regulator 1	0	0	0	

After adding the 48-hour conditioned HEK293 medium (containing the highest level of the desired protein) to (pro)renin-producing As4.1 cells for 2 days, we studied As4.1 cell morphology and quantified (pro)renin in the medium. Only PDGFB altered

As4.1 cell morphology, in that the cells after exposure to this ligand displayed a more elongated densely packed and aligned shape (Figure S7). Moreover, PDGFB also induced parallel decreases in the medium and cellular (pro)renin levels, by  $64\pm 5\%$  and  $53\pm 10\%$ , respectively ( $n=11$ ), although only the former was significant ( $P=0.03$ ; Figure 7A). Under control conditions, the medium contained predominantly ( $>95\%$ ) prorenin. In contrast, the cell lysate contained renin only, at levels corresponding to  $<1\%$  of the total amount of renin+prorenin in the medium. qPCR experiments revealed that the reduction in (pro)renin also occurred at the expression level, decreasing its level by  $84\pm 5\%$  ( $P=0.005$ ,  $n=5$ ; Figure 7A). Furthermore, when applying commercially obtained PDGFB directly to As4.1 cells, it lowered (pro)renin concentration-dependently (Figure 7B), and from these data, it could be estimated that the PDGFB level in the conditioned HEK293 medium was  $>100$  ng/mL. MTT assays confirmed that the effect of PDGFB was not due to a reduction in cell viability (Figure 7B). Moreover, PDGFB did not affect total protein content, suggesting that its effect was also not due to a decrease in cell number (data not shown).

Finally, we evaluated the effect of PDGFB-containing HEK293 medium on the expression of markers that illustrate the occurrence of a smooth muscle, endocrine and/or immunological phenotype, i.e., aldo-keto reductase family 1, member B7 (Akr1b7),  $\alpha$ -smooth muscle actin (Acta2), interleukin-6 (IL-6), and Recombination signal binding protein for immunoglobulin kappa j (Rbpj). Figure 7C illustrates that PDGFB upregulated IL-6 ( $P<0.0001$ ,  $n=4$ ), and downregulated Acta2 ( $P=0.01$ ,  $n=6$ ) in As4.1 cells. Non-significant increases in Akr1b7 ( $P=0.06$ ,  $n=4$ ) and Rbpj ( $P=0.06$ ,  $n=5$ ) expression were also observed.

#### 4.4 DISCUSSION

The aim of this study was to gain insight into human JG cell biology. Given their rapid de-differentiation in culture, such knowledge is currently lacking. Instead, information on renin synthesis is largely derived from renin-producing tumor-derived cell lines, like As4.1 (mouse), Calu-6 (human) and human mastocytoma cells (HMC-1). In an attempt to catalogue the genes expressed in JG cells, Brunskill et al. (102) used a fluorescent reporter mouse model, in which they have used cell sorting to enrich for gene-tagged renin-expressing cells in the mouse kidney. Comparison of gene expression arrays from the sorted cells versus the whole kidney led to the

identification of 369 core genes whose expression was proposed to constitute a “gene signature” for the mouse JG cell. In the current study, we have used direct RNA sequencing (RNA-Seq) of human reninomas to independently quantify gene expression levels in each of the biopsies we obtained, and to test for correlation of the gene expression patterns between mouse and human renin-expressing cells. This approach has the additional advantage that a control tissue to which expression can be compared was not required. This was an important consideration since our samples were derived from frozen pathology specimens, and only one of them had a corresponding biopsy of adjacent, presumed non-tumor, tissue. The high reproducibility and sequence “depth” achieved confirm that this approach is valid, robust and applicable to archival samples and the comparison of the reninoma transcriptomes allowed us to derive a gene expression “fingerprint” for the tumors. In addition, the high expression of renin, CD34, and vimentin, all of which have been previously reported as markers of reninomas (126, 132), confirms the diagnosis of bona fide reninoma in all of the tumors.

At least 3 of the 4 reninomas expressed genes at relatively high levels that were also reported to be highly expressed in mouse renin-expressing cells (102) including, in addition to renin, RGS5, CRIP1, and ATP1B2. Conversely, a number of the most highly expressed transcripts previously identified in the mouse JG cell preparations were not detected in the 100 most-expressed genes in the reninomas including *Syne2*, *Plac9*, *Myh11*, *Jph2*, *Myo18*, *Akr1b7* and *Mgp*. Interestingly, *Akr1b7*, a member of the alpha-keto reductase gene family was previously found to be highly enriched in mouse JG cell preparations and to serve as a specific marker for JG cells in the mouse kidney (102). Even though *Akr1b7* does not have a homologue in humans, its closest human analogues, *AKR1B10* and *AKR1B15*, are not expressed at detectable levels in the reninomas (data not shown). Since more recent results have shown that targeted deletion of *Akr1b7* in mouse JG cells does not affect renin production (133), it is possible that the expression of *Akr1b7* in mouse JG cells is unrelated to renin synthesis.

Indeed, of the extended list of 369 core genes previously reported to be enriched in the mouse renin cell preparations (102), only 8 were among the 84 genes expressed in at least 3 of the 4 reninomas (Table 3 and Table S3). Although the exact reason for these differences is unclear, they could be due to several factors. First, some of the highly-expressed transcripts in the reninomas might be related to

the tumoral transformation of the renin-producing cells. For example, the expression of neither CD34, a commonly reported marker of reninomas and myelo-lymphopoietic precursors, nor insulin-like growth factor 2 (IGF2) was detected in the mouse JG cells. IGF2 also did not affect (pro)renin release by As4.1 cells. Alternatively, the differences could be due to the fact that in both the current study and that of Brunskill et al. (102), the gene expression patterns were obtained from impure populations of renin-producing cells and could reflect expression of a gene in a contaminating non-JG cell. Finally, they could reflect true differences between mouse and humans.

To overcome some of these limitations, we used iFISH to test whether the commonly expressed genes in the reninomas were also expressed in mouse JG cells (Figure S5). Even though the sensitivity of this analysis is limited by the level of expression of the candidate genes, it nevertheless confirmed that 44 of the gene transcripts expressed in the reninomas were also detected in mouse JG cells (Table 3) and thereby significantly extends the list of potential markers for this unique cell type.

Previous studies have reported that JG cells express contractile proteins, are related to pericytes (134) and, like pericytes, are derived from FoxD1-expressing lineages (135). Simultaneously, renal CD44(+) mesenchymal stem cell-like cells, whose differentiation is triggered by LXR stimulation (136), have been suggested to differentiate into JG-like renin-expressing cells (77). The current analysis confirmed the expression of a number of contractile proteins in both reninomas and JG cells, including myosin light chain 9 (MYL9), tropomyosin 2 (TPM2), transgelin (TAGLN), myocyte enhancer factor 2C (MEF2C), caldesmon (CALD1) and very low levels of ACTA2, as well as some pericyte markers including RGS5 and osteonectin (SPARC). We also confirmed the expression of vimentin (VIM), a marker of mesenchyme-derived cells, in both the reninomas and JG cells, but did not detect expression of either LXR receptor or CD44 in the tumors.

Our data also call into question the model that “recruited” JG cells (e.g., after captopril treatment) represent a return to the embryonic stage of renin-producing cells. The ACTA2 gene codes for  $\alpha$ -smooth muscle actin, a marker for smooth muscle cells. Consistent with what has been previously reported (137) there is a demarcation in Acta2 expression with the expected higher expression in smooth muscle cells of the afferent arteriole and very low expression in adjacent JG cells of adult mice (Figure 8A). This demarcation persists after recruitment of new JG cells

following captopril treatment (Figure 8B). In contrast, there appear to be 2 populations of renin-expressing cells in the developing kidney: one population that exists in clusters similar to the JG apparatus in adult kidney (Figure 8C, arrow) and which express only very low levels of ACTA2 and others which line the vessels of the developing kidney and exhibit significant overlap of renin staining and ACTA2 expression (Figure 8C, light blue outline). Other genes whose expression was detected almost exclusively in renin-producing cells of the developing kidney include A2m, Slit3 and Cxcl12. Conversely, a number of genes appeared to be preferentially expressed in the JG cells of adult control and captopril-treated mice including Ptp4a3, C4a, Tinagl1, Lbh, Mdk, Bgn and Crip1. Taken together, these results suggest that JG recruitment does not simply involve a return to the embryonic renin-producing cell, but may rather reflect differentiation of smooth muscle to either an intermediate or alternative phenotype.

KISS1, which codes for a metastasis suppressor and is the second to third most abundant transcript in each of the four of the reninomas (Table 3), also presents a major difference in expression in the reninomas and mouse kidney. The KISS1 gene is located immediately adjacent to the renin gene on chromosome 1 in both mice and humans (<http://www.ncbi.nlm.nih.gov/gene/3814>). When large chromosomal fragments containing both genes are used to generate transgenic mice, coordinate expression of renin and KISS1 is detected in brain, kidney, lung and placenta (138). While we detected some expression of Kiss1 in the JG cells of captopril-treated mice (Figure S5), we did not detect its expression in adult mouse JG cells, raising the possibility that the neighboring Kiss1 gene is expressed only in conditions of very high renin gene expression. Whether it explains the fact that intra-renal reninomas rarely metastasize is currently unknown.

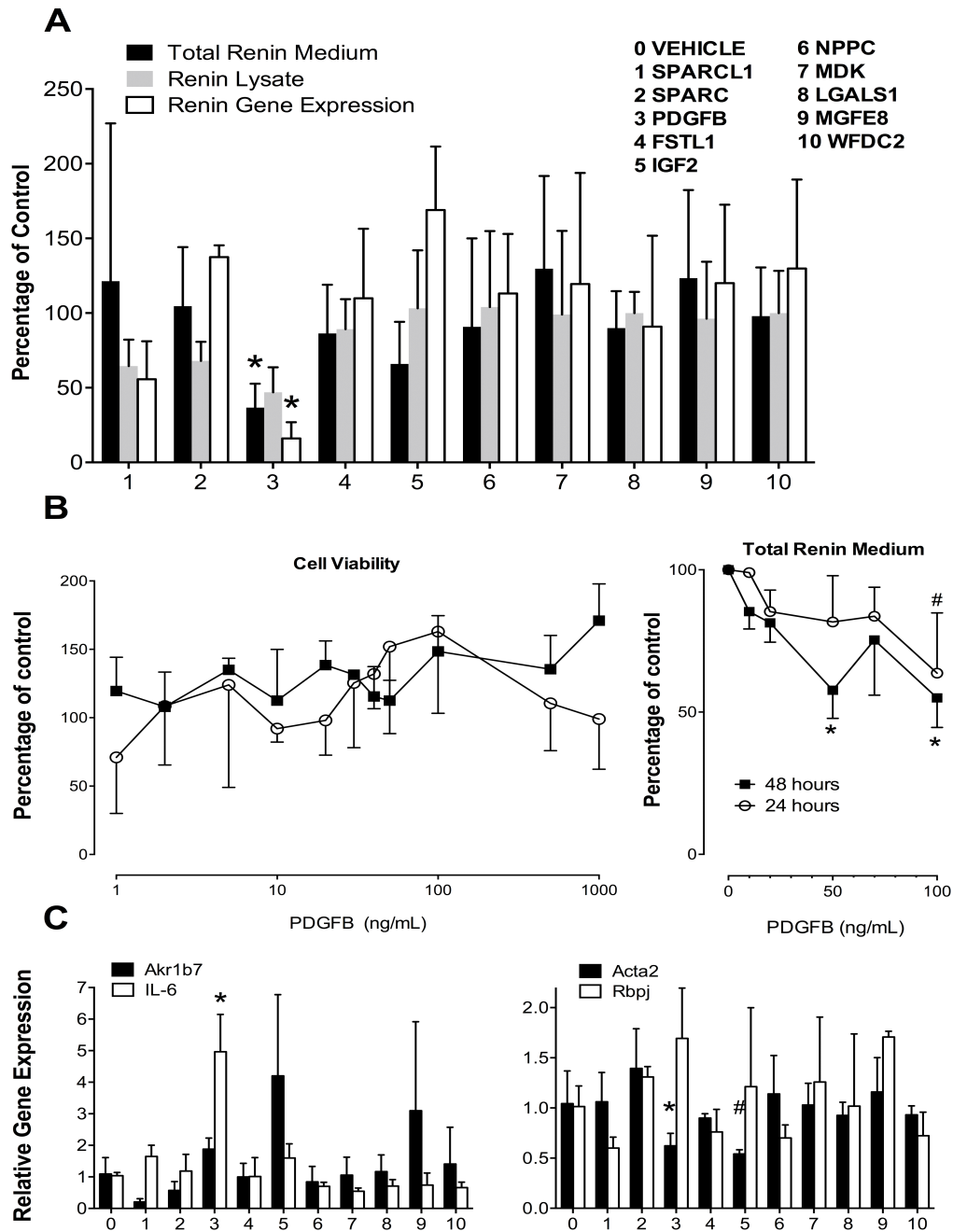


Figure 7. A) Total renin (i.e., renin + prorenin) levels in the medium, and renin levels in the cell lysate obtained from As4.1 cells incubated for 48 hours with medium obtained from HEK293 cells transfected with 10 genes expressing ligands that were upregulated in the 4 reninomas. Renin gene expression is also provided. Data are mean  $\pm$ SEM of 5-11 experiments and have been expressed as a percentage of the levels in cells exposed to medium of control-transfected cells, i.e., cells treated with the transfection mix, but without cDNA. \* $P < 0.01$ . B) Cell viability and total renin levels in the medium of As4.1 cells exposed to PDGFB for 24 or 48 hours. Data are mean  $\pm$ SEM of 3 experiments and have been expressed as a percentage of the levels in cells not exposed to PDGFB ('control'). \* $P < 0.01$ , # $P < 0.05$  vs. 100%. C) Aldo-keto reductase family 1, member B7 (Akr1b7),  $\alpha$ -smooth muscle actin (Acta2), interleukin-6 (IL-6), and recombination signal binding protein for immunoglobulin kappa j (Rbpj) expression in As4.1 cells incubated for 48 hours with medium obtained from HEK293 cells transfected with 10 genes expressing ligands that were upregulated in the 4 reninomas. Data are mean  $\pm$ SEM of 4-6 experiments and have been expressed as fold change versus the levels in cells exposed to medium of control-transfected cells, i.e., cells treated with the transfection mix, but without cDNA ('vehicle'). \* $P < 0.01$ , # $P < 0.05$  vs. 1.0.

Also among the most highly expressed genes in all 4 reninomas is *DBNDD2* (Table S3), a paralog of the gene *DTNBP1*, which is a component of the BLOC-1 complex that is required for normal biogenesis of lysosome-related organelles (LRO), such as platelet dense granules and melanosomes. Thus, *DBNDD2* might be an interesting candidate to explain the high content of LROs found in the JG cells.

A number of ligands and receptors were also found to be highly expressed in the reninomas and in mouse renin-producing cells, some of which might play a role in either the maintenance of the JG cell phenotype or in JG cell recruitment. Of particular interest is the high level of expression of the Notch3 receptor and PDGF receptor  $\beta$  (PDGFR) in the reninomas and JG cells. Indeed, *RBPJ*, the main effector involved in Notch receptor signaling, activates the myo-endocrine program of the JG cell, and conditional deletion of *Rbpj* in renin-producing cells results in a dramatic decrease in the number of JG cells seen in adult mice (55). Yet, in humans mutations in *NOTCH3* have been identified as the underlying cause of cerebral autosomal dominant arteriopathy with subcortical infarcts and leukoencephalopathy (CADASIL), with no known effects on renin. In the current study we observed that PDGFB suppressed (pro)renin synthesis in As4.1 cells, and altered their morphology. The concomitant suppression of *Acta2* and upregulation of IL-6 suggests an As4.1 phenotype change from myo-endocrine to inflammatory. IL-6 upregulation by PDGFB is well-known, and occurs in a *RBPJ*-independent manner (139). No significant alterations were observed in *Akr1b7* and *Rbpj*, nor did PDGFB affect cell viability. Classically, endothelium-derived PDGFB recruits pericytes and promotes VSMC proliferation (140). Importantly, pericytes in the human kidney were recently reported to produce renin (119). Hypoxia transforms renin-producing cells into erythropoietin-producing cells (114), and erythropoietin-expressing cells are assumed to be derived from capillary pericytes (141). Finally, following severe mesangial injury, renin-positive precursor cells moved into intraglomerular sites and differentiated into (renin-negative), PDGFR $\beta$ -expressing mesangial cells (118). As shown in Figure 8 (panels D-F), PDGFR $\beta$  modestly overlapped with renin in kidneys of adult, young, and captopril-treated adult mice, in addition to its well-known expression in interstitial cells. Moreover, Rider et al. observed that renin cells in the zebrafish kidney express both *Acta2* and *Pdgfr $\beta$*  (121). Given the well-known role of endothelial PDGFB as a

facilitator of mesangial cell proliferation and migration, an additional effect of PDGFB might now be suppression of renin expression. Here it should be mentioned that neither conditional deletion of the PDGFR $\beta$  in renin-producing cells nor deletion of endothelial PDGFB production affected the normal development of renal renin-expressing cells (142). This may not be too surprising, given the fact that PDGFB actually is a negative regulator of renin expression, possibly coming into play only under pathological conditions.

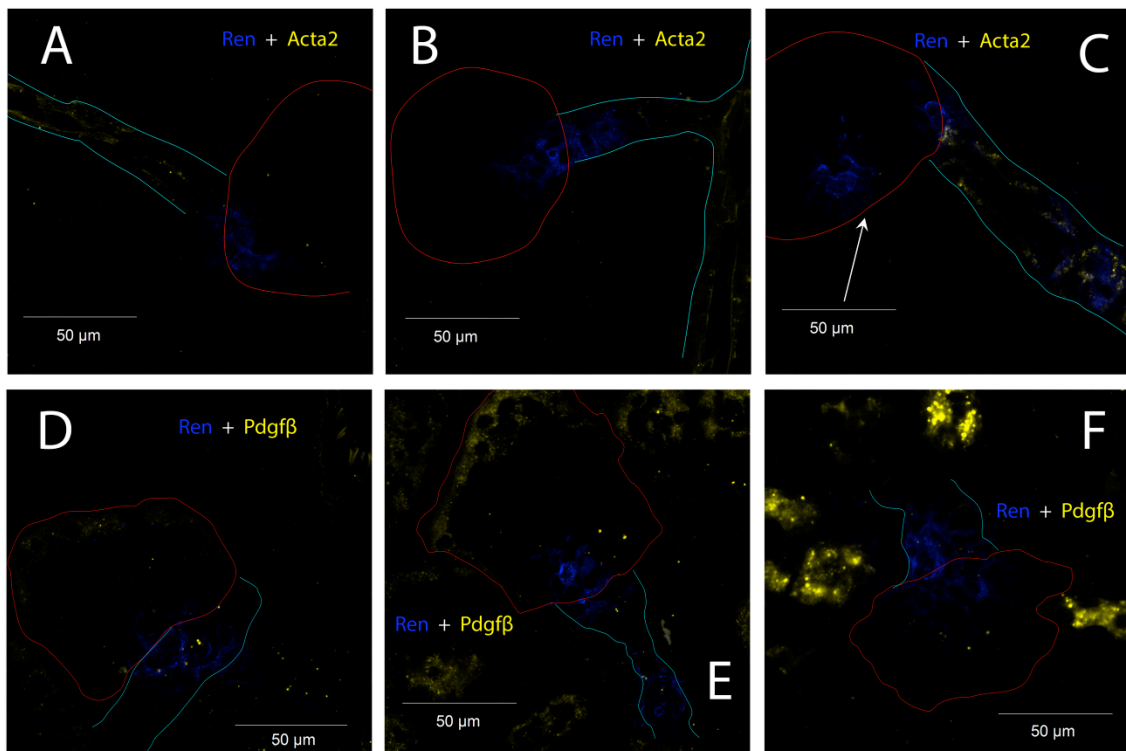


Figure 8. iFISH showing renin immunofluorescence in blue and in situ hybridization for Acta2 or PDGF $\beta$  in yellow in kidneys from adult (A,D), 5 day-old (B,E) and captopril-treated (C,F) mice. Note the existence of 2 types of renin-producing cells in the 5 day-old mouse: those that co-express Acta2 (outlined in the vessel in light blue) and those that don't (arrow). Original magnification X 40. Scale bar=50 $\mu$ m.

Besides the high level of PDGFR $\beta$  expression in the reninomas and the JG cells, both also express the genes for SPARC, SPARCL1 (SPARC-like 1 or hevin) and MFGE8 (lactadherin) at relatively high levels. It has been reported that SPARC can both prevent the binding of PDGF to its receptor (143) and potentiate its profibrotic effects (142), while lactadherin potentiates PDGFR $\beta$  signaling (144). This raises the possibility that a more complex interplay between SPARC, SPARCL1, MFGE8 and PDGF regulates either the recruitment or other physiological responses

of JG cells in their natural setting. In agreement with this concept, the current study revealed no effect of either SPARC, SPARCL1 or MGE8 alone on (pro)renin synthesis by As4.1 cells. Additionally, ligands that are known to be involved in blood pressure regulation (NPPC, or natriuretic peptide precursor C), diabetic nephropathy (LGALS1 or galectin-1) (145), nephrogenesis (MDK or midkine)(146), renal fibrosis (WFDC2, or WAP four-disulfide core domain protein 2)(147), and renal injury prevention (FSTL1, or follistatin-related protein 1) (148) also did not directly affect (pro)renin synthesis by As4.1 cells.

Somewhat surprisingly, no proteases were included in the 100 most expressed genes in the reninomas (Table S3) where we might have expected to find one or more candidate prorenin processing enzymes (PPE) necessary for proteolytic activation of the renin secreted by these tumors. However, examination of the gene lists before subtraction of the genes expressed in the Par2N “normal” biopsy (Table S1) reveals that the rank of Cathepsin B (CTSB) expression varies from the 8<sup>th</sup> (Par1B1) to the 78<sup>th</sup> (Par2) position in the reninomas, although these expression levels did not appear to correlate with the apparent renin expression levels in each sample (not shown). However, because CTSB was only expressed 1.1-fold more in the Par2 reninoma than in the Par2N control kidney biopsy, it was eliminated from our gene list. Nevertheless, because CTSB has been co-localized with renin in JG cells secretory granules (149) and shown to accurately process human prorenin in vitro (150), it is quite possible that it fulfills the role of the PPE in the reninomas, even though it is a ubiquitously distributed protease. This analysis also reveals one of the potential shortcomings of our approach since by focusing on genes whose expression was consistently enriched in tumor biopsies we may have eliminated consideration of genes that play an important functional role in the biology of the JG cell, but whose expression is more widely distributed.

The present study is the first to use a reninoma transcriptome analysis as an approach to understand human JG cell biology. It has yielded multiple new candidates that might play a role in the developmental plasticity of these cells and, among them, raises the PDGFB-PDGFR $\beta$  signaling pathway as a promising novel pathway that controls renin-expressing cells.

## 4.5 SUPPLEMENT INFORMATION

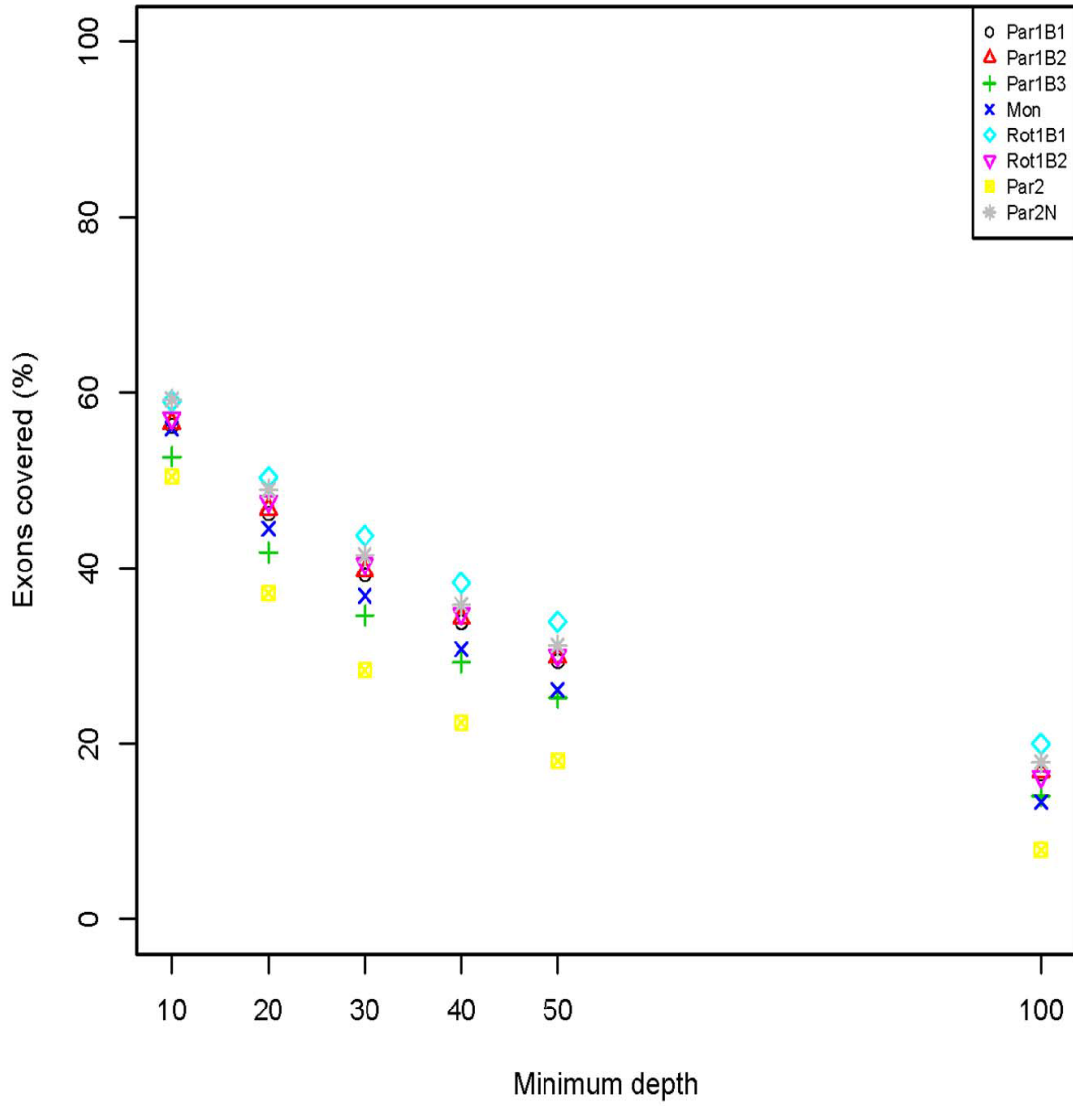


Figure S1. Sequence coverage of the various reninoma RNAs.

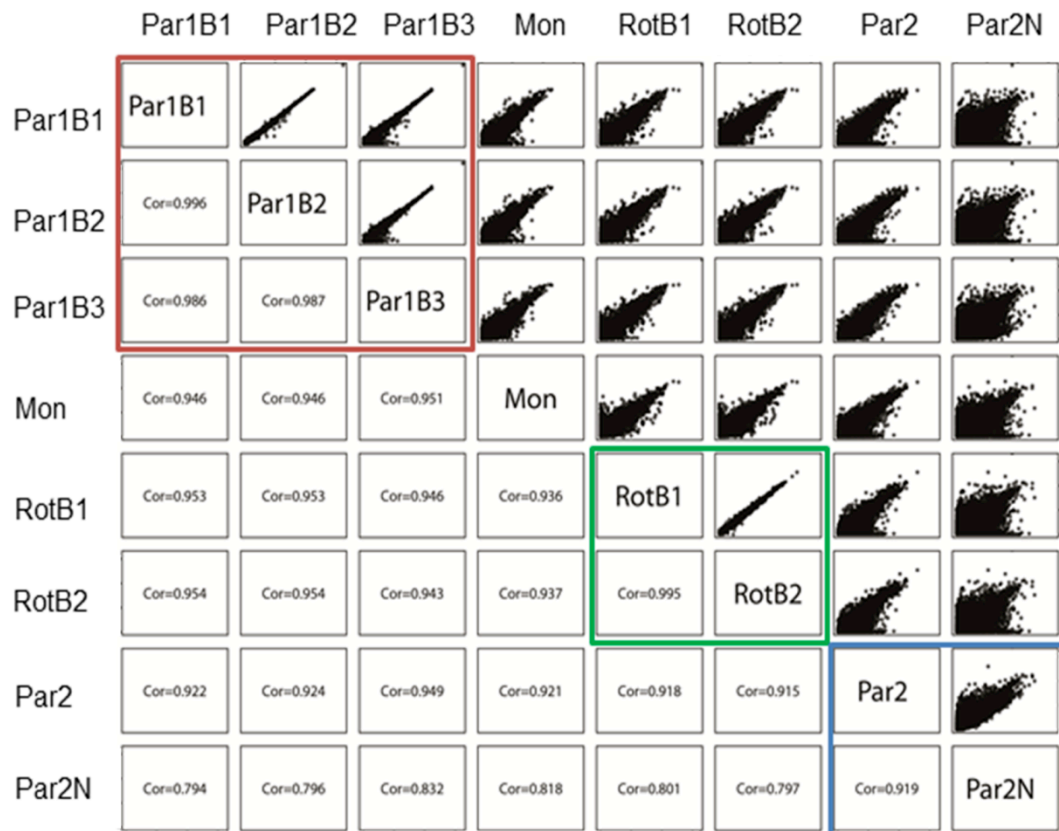


Figure S2. Spearman pairwise comparison of the gene expression levels in the raw (unsubtracted) reads (FPKM) for each sample analyzed. The sample displayed on the X-axis is shown above the graphs, while that displayed on the Y-axis is shown at left. The correlation coefficient for overlap is shown in each reciprocal position. Par1B1-3 are biopsies 1-3 of the Paris 1 reninoma (bordered by a red box). Mon; Montreal. RotB1, 2 are the 2 biopsies analyzed from the Rotterdam reninoma (bordered by a green box). Par2 is the second Paris reninoma and Par2N is a biopsy of supposedly unaffected adjacent kidney tissue (bordered by a blue box).

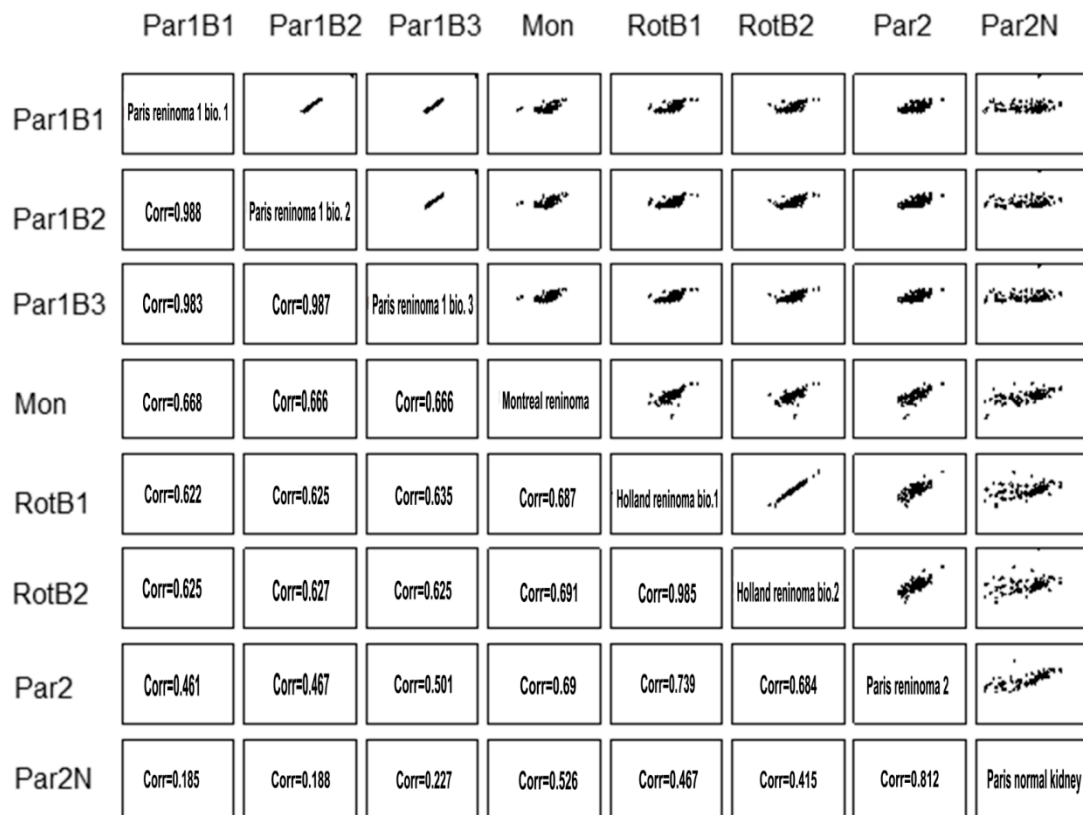


Figure S3. Repeat Spearman pairwise comparison of the sample analyzed in Figure S2 after subtracting genes that differed less than 4-fold between the Par2 and Par2N samples. See Figure S2 legend for details.

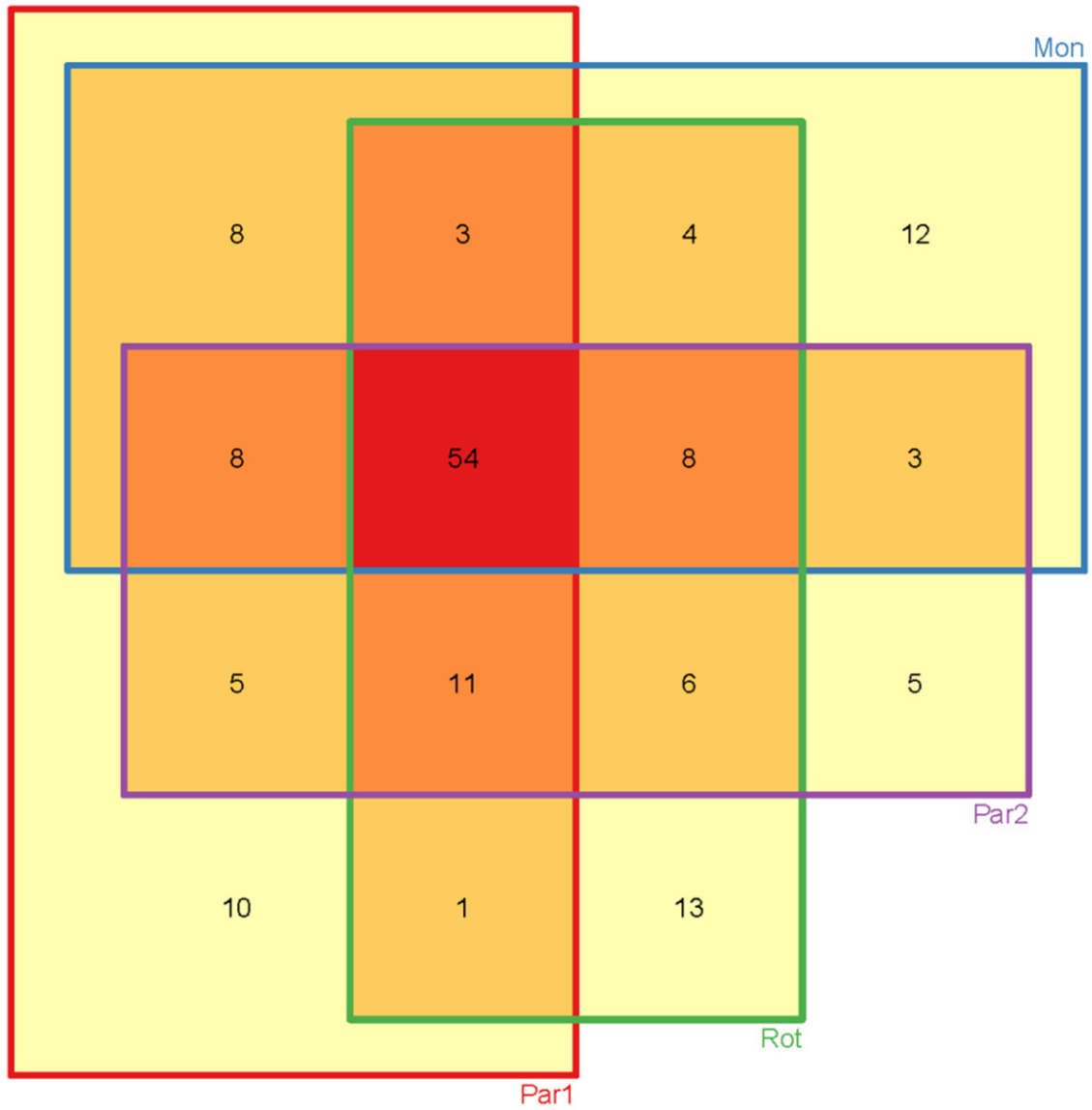


Figure S4. Venn diagram representing the overlap of the 100 most-expressed genes in the reninomas (from Table S3).

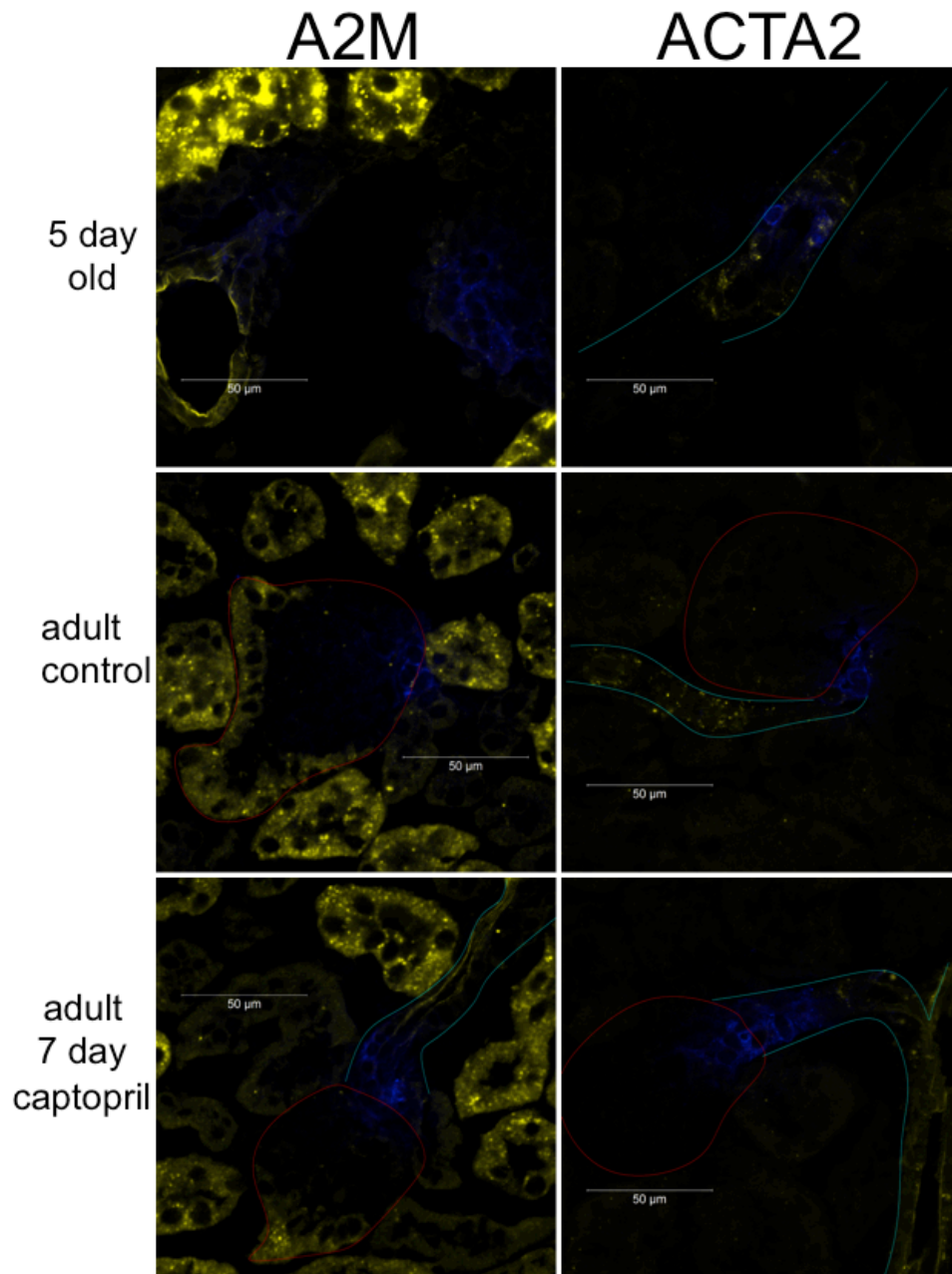


Figure S5. Representative iFISH results showing renin immunofluorescence (in blue) and in situ hybridization for the indicated mouse mRNA (in yellow) in kidneys from 5 day-old mice (upper panel) 10-12 week adult control mice (middle panels) and adult mice treated for 7 days with the ACE inhibitor captopril (lower panels). The results from each probe is presented on one page in alphabetical order. Where possible, glomeruli are outlined in red and vessels in light blue. Overlapping expression of renin and any of the corresponding genes in renin-producing cells (RPC) of the 5 day old (developing) kidney or juxtaglomerular (JG) cells of the adult kidney is seen as white dots. Signal in the tubules represents some degree of non-specific background. Results are summarized in Table 3 of the text. (to be continued)

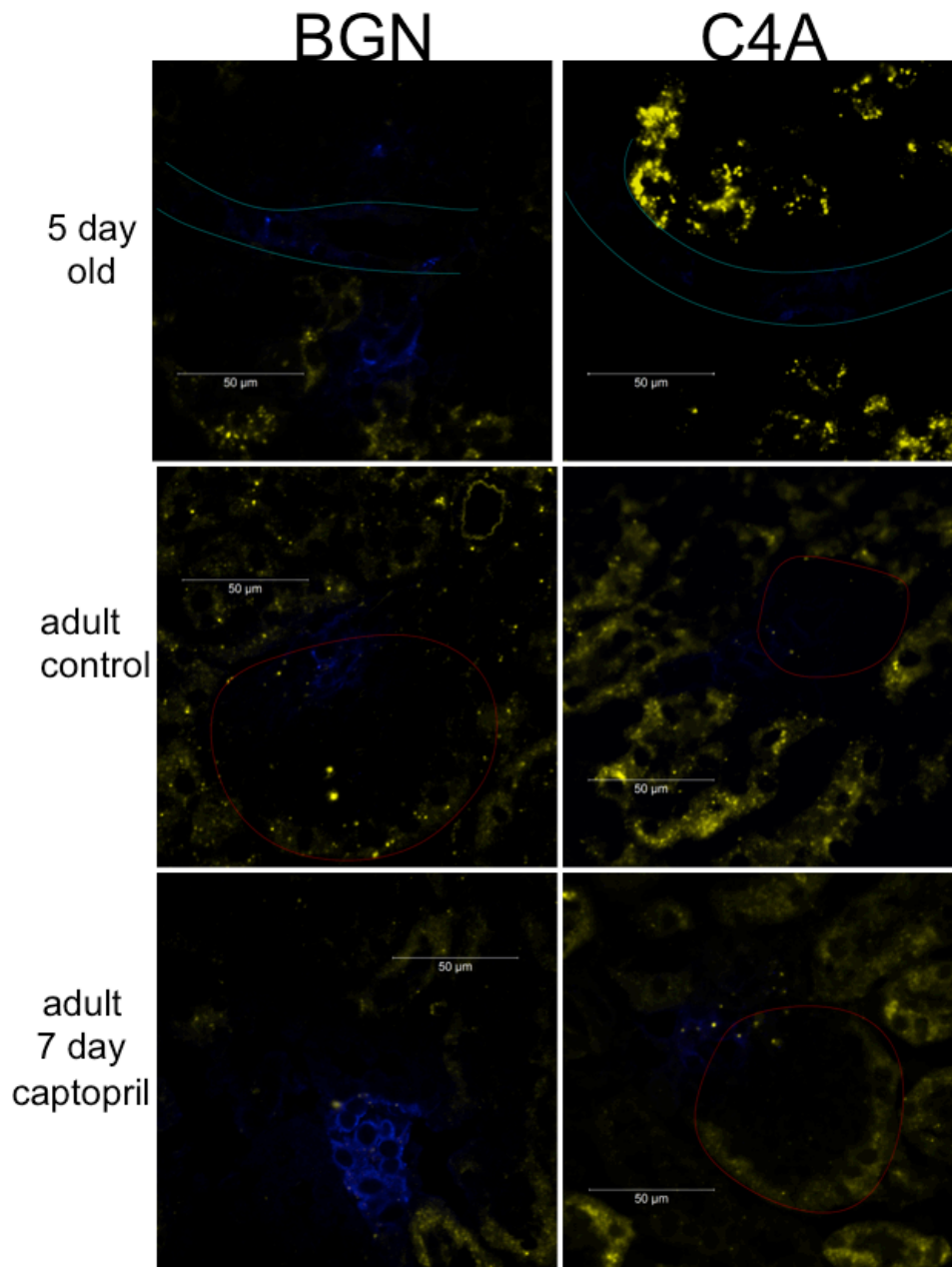


Figure S5. Representative iFISH results showing renin immunofluorescence (in blue) and in situ hybridization for the indicated mouse mRNA (in yellow) in kidneys from 5 day-old mice (upper panel) 10-12 week adult control mice (middle panels) and adult mice treated for 7 days with the ACE inhibitor captopril (lower panels). The results from each probe is presented on one page in alphabetical order. Where possible, glomeruli are outlined in red and vessels in light blue. Overlapping expression of renin and any of the corresponding genes in renin-producing cells (RPC) of the 5 day old (developing) kidney or juxtaglomerular (JG) cells of the adult kidney is seen as white dots. Signal in the tubules represents some degree of non-specific background. Results are summarized in Table 3 of the text. (continuation)

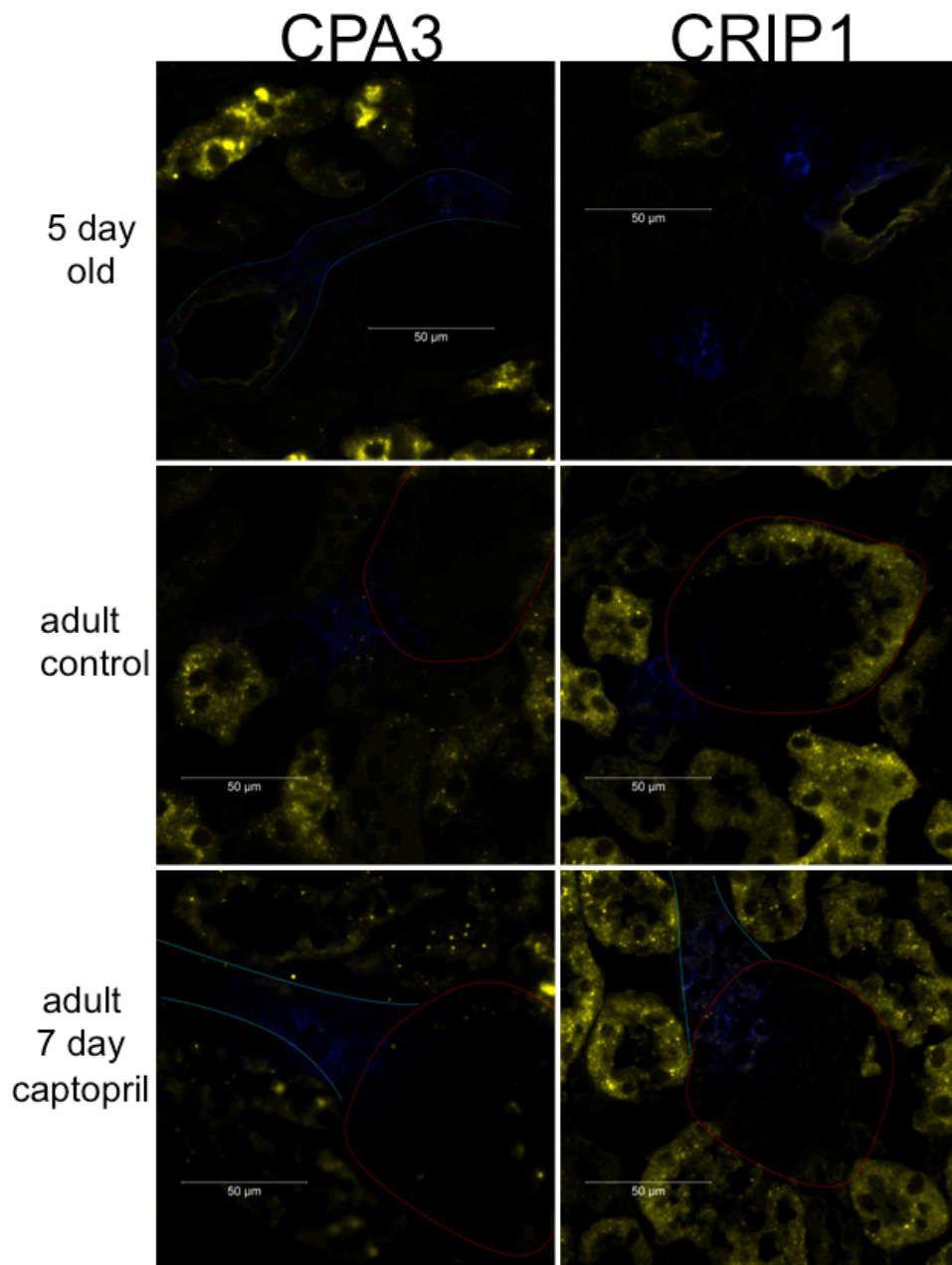


Figure S5. Representative iFISH results showing renin immunofluorescence (in blue) and in situ hybridization for the indicated mouse mRNA (in yellow) in kidneys from 5 day-old mice (upper panel) 10-12 week adult control mice (middle panels) and adult mice treated for 7 days with the ACE inhibitor captopril (lower panels). The results from each probe is presented on one page in alphabetical order. Where possible, glomeruli are outlined in red and vessels in light blue. Overlapping expression of renin and any of the corresponding genes in renin-producing cells (RPC) of the 5 day old (developing) kidney or juxtaglomerular (JG) cells of the adult kidney is seen as white dots. Signal in the tubules represents some degree of non-specific background. Results are summarized in Table 3 of the text. (continuation)

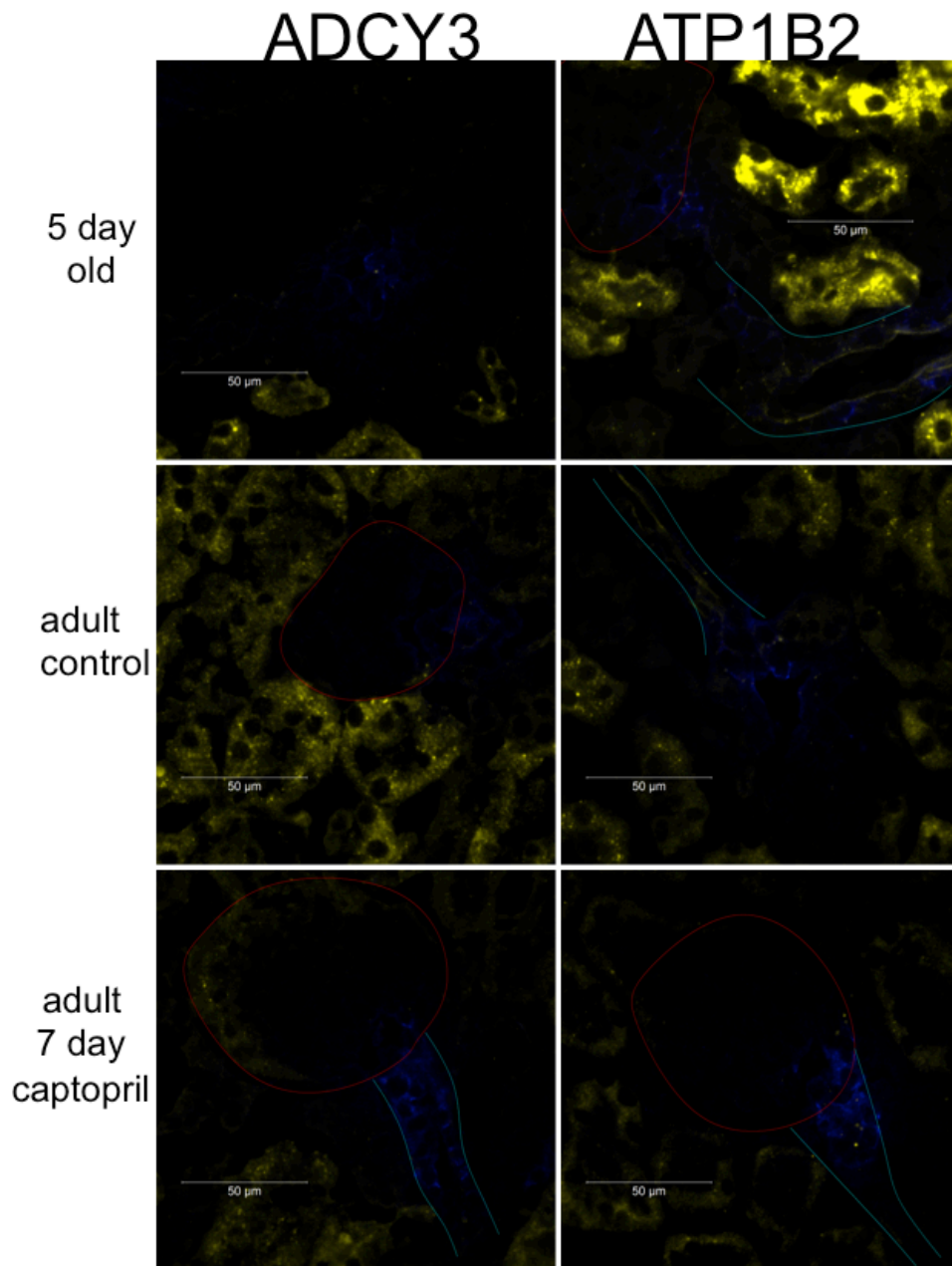


Figure S5. Representative iFISH results showing renin immunofluorescence (in blue) and in situ hybridization for the indicated mouse mRNA (in yellow) in kidneys from 5 day-old mice (upper panel) 10-12 week adult control mice (middle panels) and adult mice treated for 7 days with the ACE inhibitor captopril (lower panels). The results from each probe is presented on one page in alphabetical order. Where possible, glomeruli are outlined in red and vessels in light blue. Overlapping expression of renin and any of the corresponding genes in renin-producing cells (RPC) of the 5 day old (developing) kidney or juxtaglomerular (JG) cells of the adult kidney is seen as white dots. Signal in the tubules represents some degree of non-specific background. Results are summarized in Table 3 of the text. (continuation)

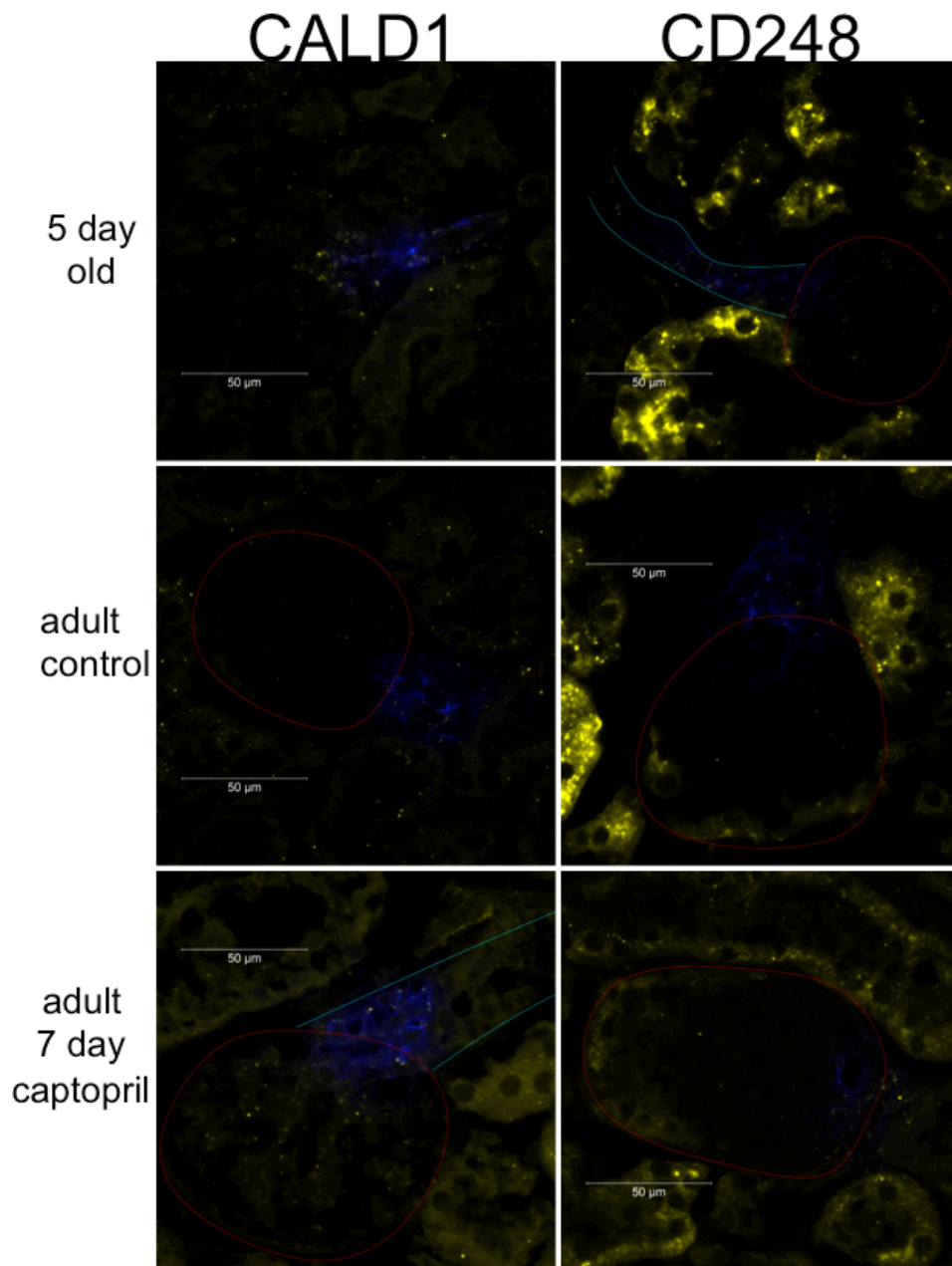


Figure S5. Representative iFISH results showing renin immunofluorescence (in blue) and in situ hybridization for the indicated mouse mRNA (in yellow) in kidneys from 5 day-old mice (upper panel) 10-12 week adult control mice (middle panels) and adult mice treated for 7 days with the ACE inhibitor captopril (lower panels). The results from each probe is presented on one page in alphabetical order. Where possible, glomeruli are outlined in red and vessels in light blue. Overlapping expression of renin and any of the corresponding genes in renin-producing cells (RPC) of the 5 day old (developing) kidney or juxtaglomerular (JG) cells of the adult kidney is seen as white dots. Signal in the tubules represents some degree of non-specific background. Results are summarized in Table 3 of the text. (continuation)

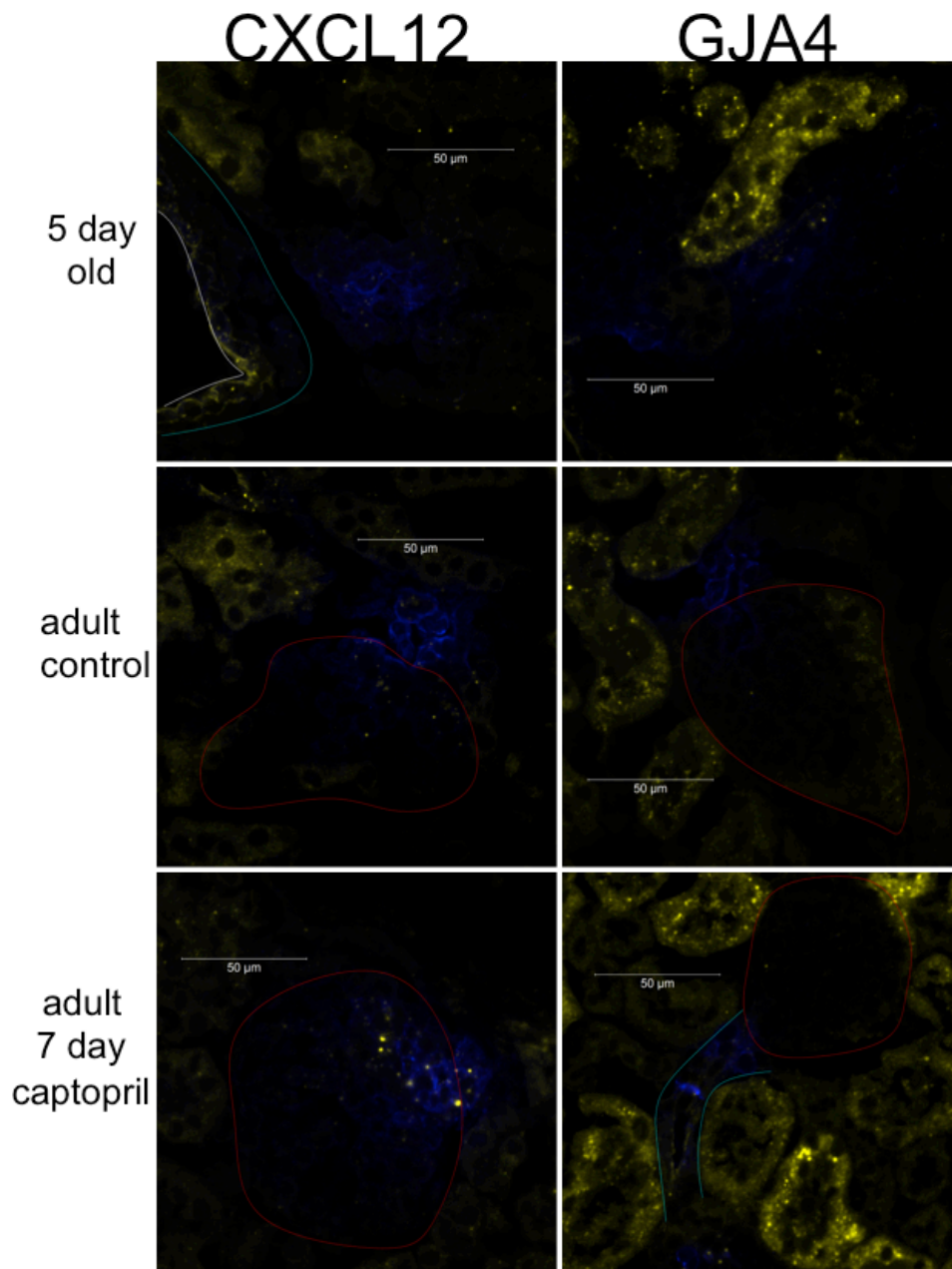


Figure S5. Representative iFISH results showing renin immunofluorescence (in blue) and in situ hybridization for the indicated mouse mRNA (in yellow) in kidneys from 5 day-old mice (upper panel) 10-12 week adult control mice (middle panels) and adult mice treated for 7 days with the ACE inhibitor captopril (lower panels). The results from each probe is presented on one page in alphabetical order. Where possible, glomeruli are outlined in red and vessels in light blue. Overlapping expression of renin and any of the corresponding genes in renin-producing cells (RPC) of the 5 day old (developing) kidney or juxtaglomerular (JG) cells of the adult kidney is seen as white dots. Signal in the tubules represents some degree of non-specific background. Results are summarized in Table 3 of the text. (continuation)

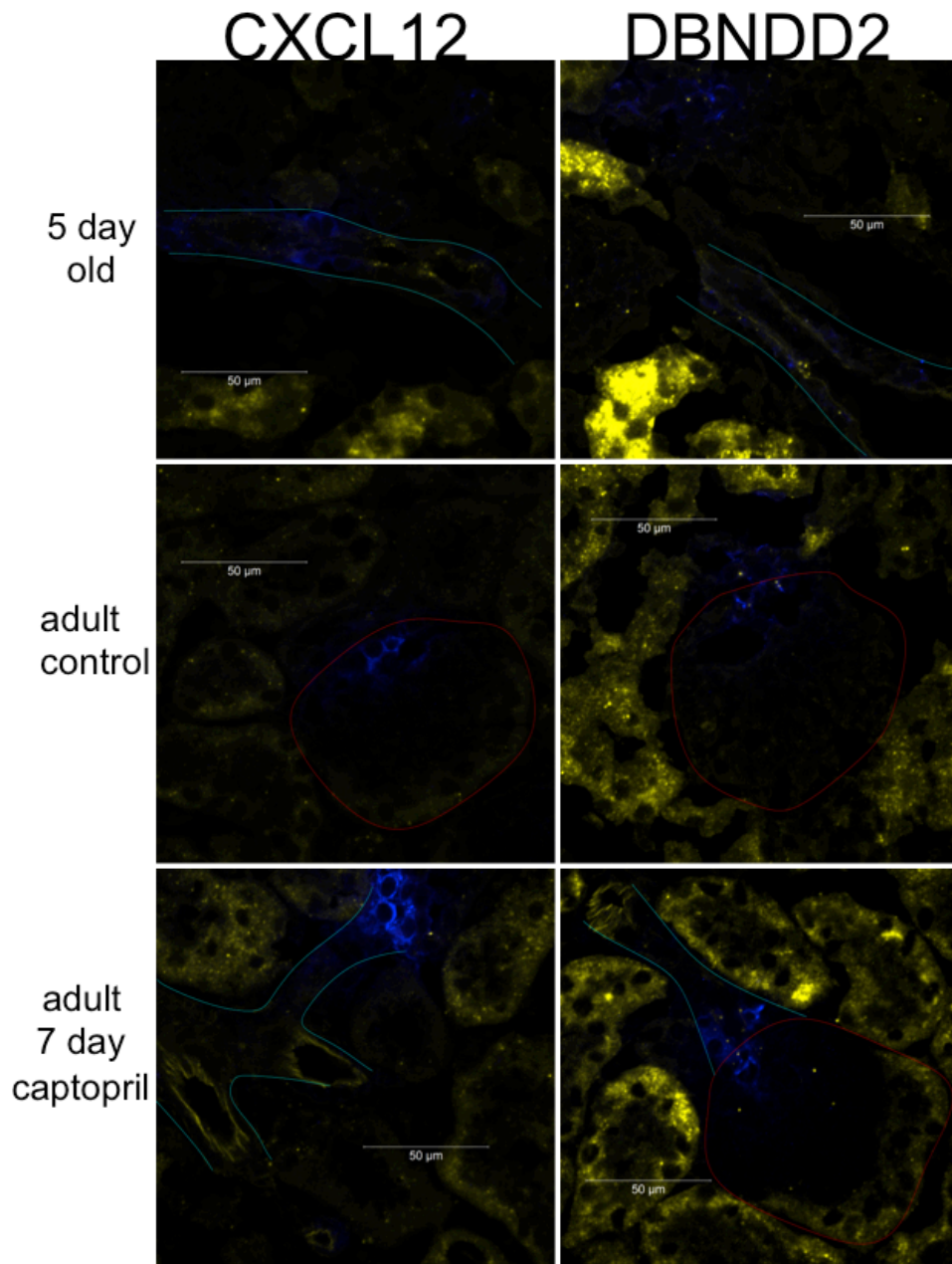


Figure S5. Representative iFISH results showing renin immunofluorescence (in blue) and in situ hybridization for the indicated mouse mRNA (in yellow) in kidneys from 5 day-old mice (upper panel) 10-12 week adult control mice (middle panels) and adult mice treated for 7 days with the ACE inhibitor captopril (lower panels). The results from each probe is presented on one page in alphabetical order. Where possible, glomeruli are outlined in red and vessels in light blue. Overlapping expression of renin and any of the corresponding genes in renin-producing cells (RPC) of the 5 day old (developing) kidney or juxtaglomerular (JG) cells of the adult kidney is seen as white dots. Signal in the tubules represents some degree of non-specific background. Results are summarized in Table 3 of the text. (continuation)

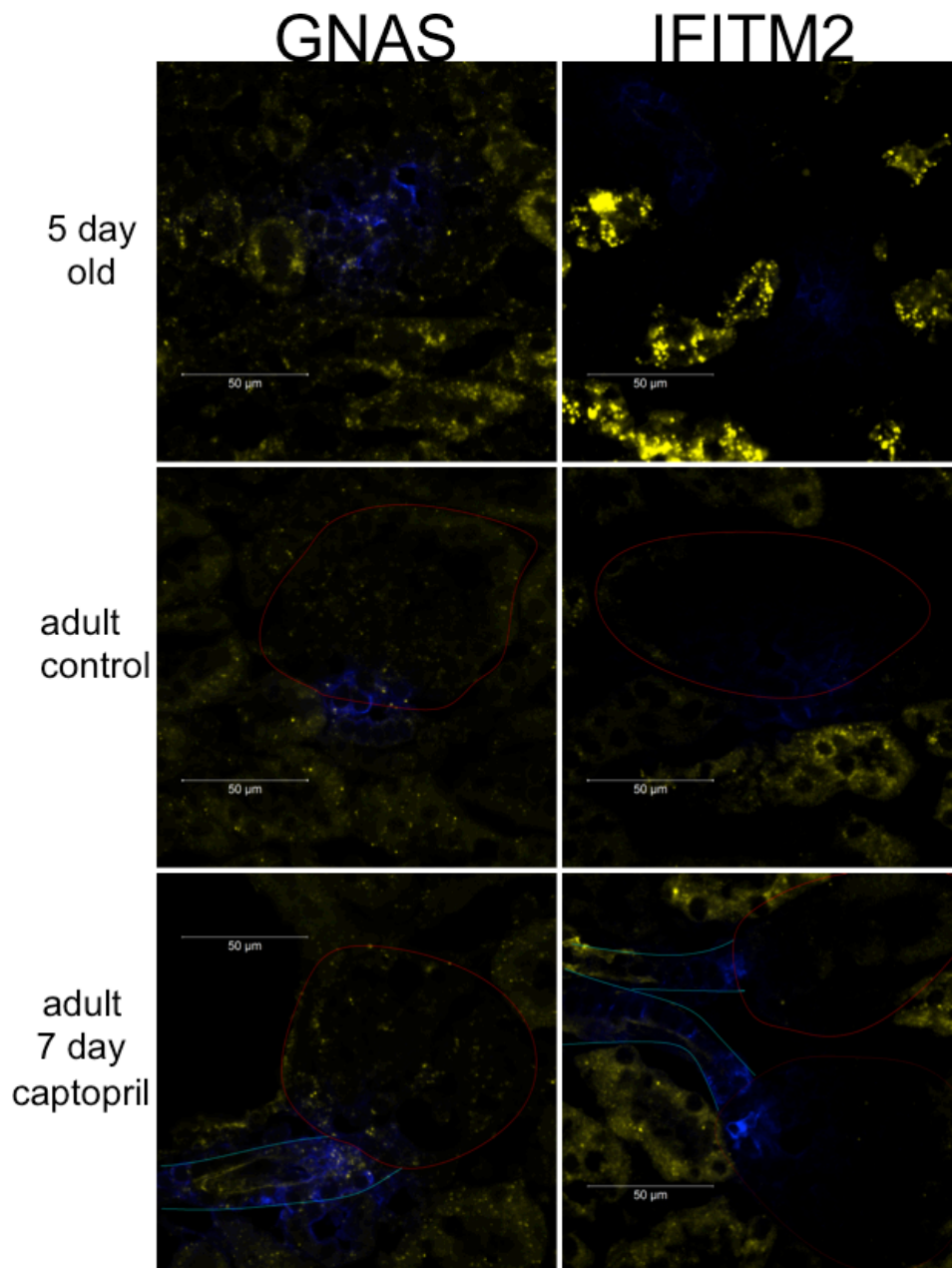


Figure S5. Representative iFISH results showing renin immunofluorescence (in blue) and in situ hybridization for the indicated mouse mRNA (in yellow) in kidneys from 5 day-old mice (upper panel) 10-12 week adult control mice (middle panels) and adult mice treated for 7 days with the ACE inhibitor captopril (lower panels). The results from each probe is presented on one page in alphabetical order. Where possible, glomeruli are outlined in red and vessels in light blue. Overlapping expression of renin and any of the corresponding genes in renin-producing cells (RPC) of the 5 day old (developing) kidney or juxtaglomerular (JG) cells of the adult kidney is seen as white dots. Signal in the tubules represents some degree of non-specific background. Results are summarized in Table 3 of the text. (continuation)

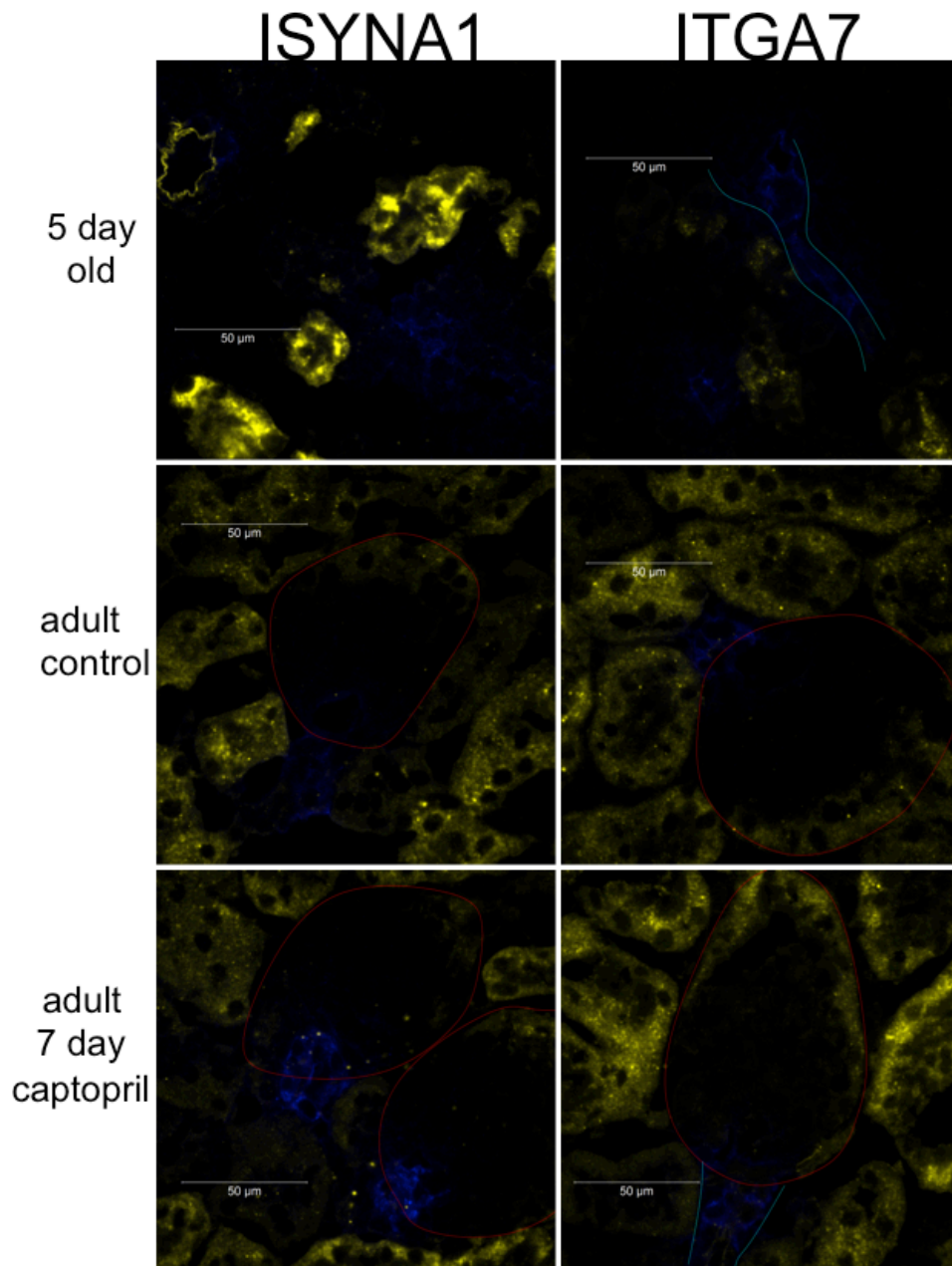


Figure S5. Representative iFISH results showing renin immunofluorescence (in blue) and in situ hybridization for the indicated mouse mRNA (in yellow) in kidneys from 5 day-old mice (upper panel) 10-12 week adult control mice (middle panels) and adult mice treated for 7 days with the ACE inhibitor captopril (lower panels). The results from each probe is presented on one page in alphabetical order. Where possible, glomeruli are outlined in red and vessels in light blue. Overlapping expression of renin and any of the corresponding genes in renin-producing cells (RPC) of the 5 day old (developing) kidney or juxtaglomerular (JG) cells of the adult kidney is seen as white dots. Signal in the tubules represents some degree of non-specific background. Results are summarized in Table 3 of the text. (continuation)

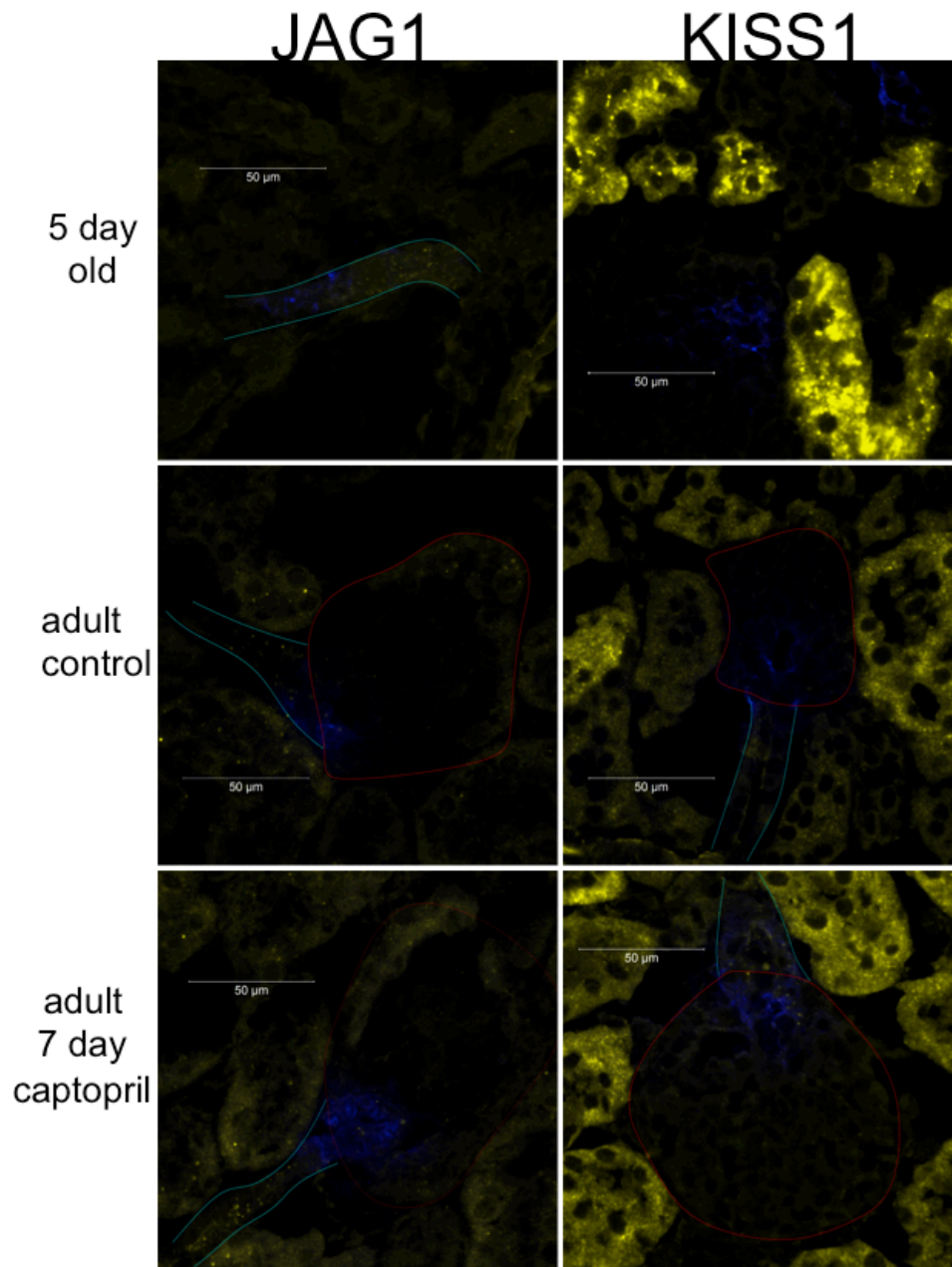


Figure S5. Representative iFISH results showing renin immunofluorescence (in blue) and in situ hybridization for the indicated mouse mRNA (in yellow) in kidneys from 5 day-old mice (upper panel) 10-12 week adult control mice (middle panels) and adult mice treated for 7 days with the ACE inhibitor captopril (lower panels). The results from each probe is presented on one page in alphabetical order. Where possible, glomeruli are outlined in red and vessels in light blue. Overlapping expression of renin and any of the corresponding genes in renin-producing cells (RPC) of the 5 day old (developing) kidney or juxtaglomerular (JG) cells of the adult kidney is seen as white dots. Signal in the tubules represents some degree of non-specific background. Results are summarized in Table 3 of the text. (continuation)

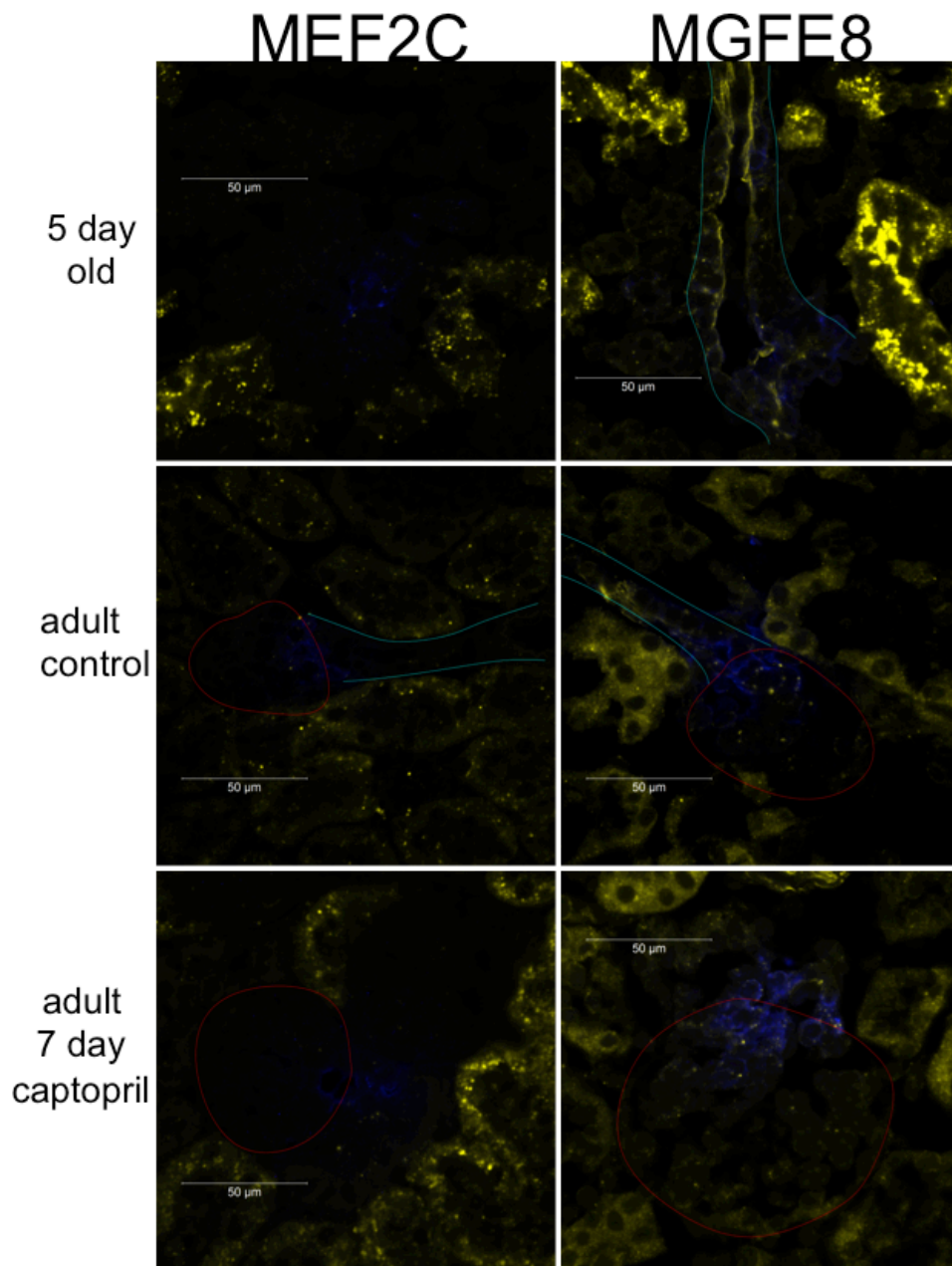


Figure S5. Representative iFISH results showing renin immunofluorescence (in blue) and in situ hybridization for the indicated mouse mRNA (in yellow) in kidneys from 5 day-old mice (upper panel) 10-12 week adult control mice (middle panels) and adult mice treated for 7 days with the ACE inhibitor captopril (lower panels). The results from each probe is presented on one page in alphabetical order. Where possible, glomeruli are outlined in red and vessels in light blue. Overlapping expression of renin and any of the corresponding genes in renin-producing cells (RPC) of the 5 day old (developing) kidney or juxtaglomerular (JG) cells of the adult kidney is seen as white dots. Signal in the tubules represents some degree of non-specific background. Results are summarized in Table 3 of the text. (continuation)

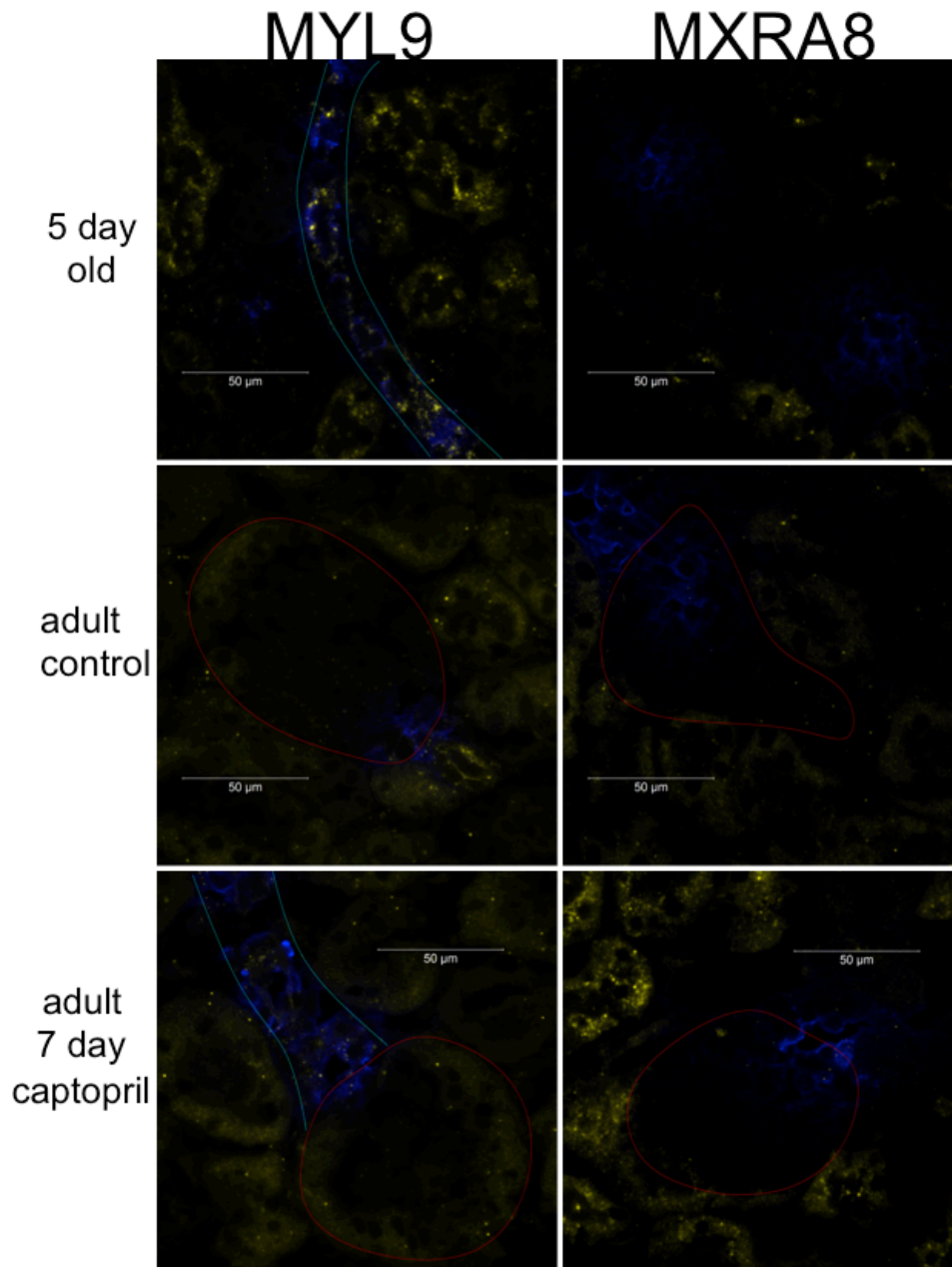


Figure S5. Representative iFISH results showing renin immunofluorescence (in blue) and in situ hybridization for the indicated mouse mRNA (in yellow) in kidneys from 5 day-old mice (upper panel) 10-12 week adult control mice (middle panels) and adult mice treated for 7 days with the ACE inhibitor captopril (lower panels). The results from each probe is presented on one page in alphabetical order. Where possible, glomeruli are outlined in red and vessels in light blue. Overlapping expression of renin and any of the corresponding genes in renin-producing cells (RPC) of the 5 day old (developing) kidney or juxtaglomerular (JG) cells of the adult kidney is seen as white dots. Signal in the tubules represents some degree of non-specific background. Results are summarized in Table 3 of the text. (continuation)

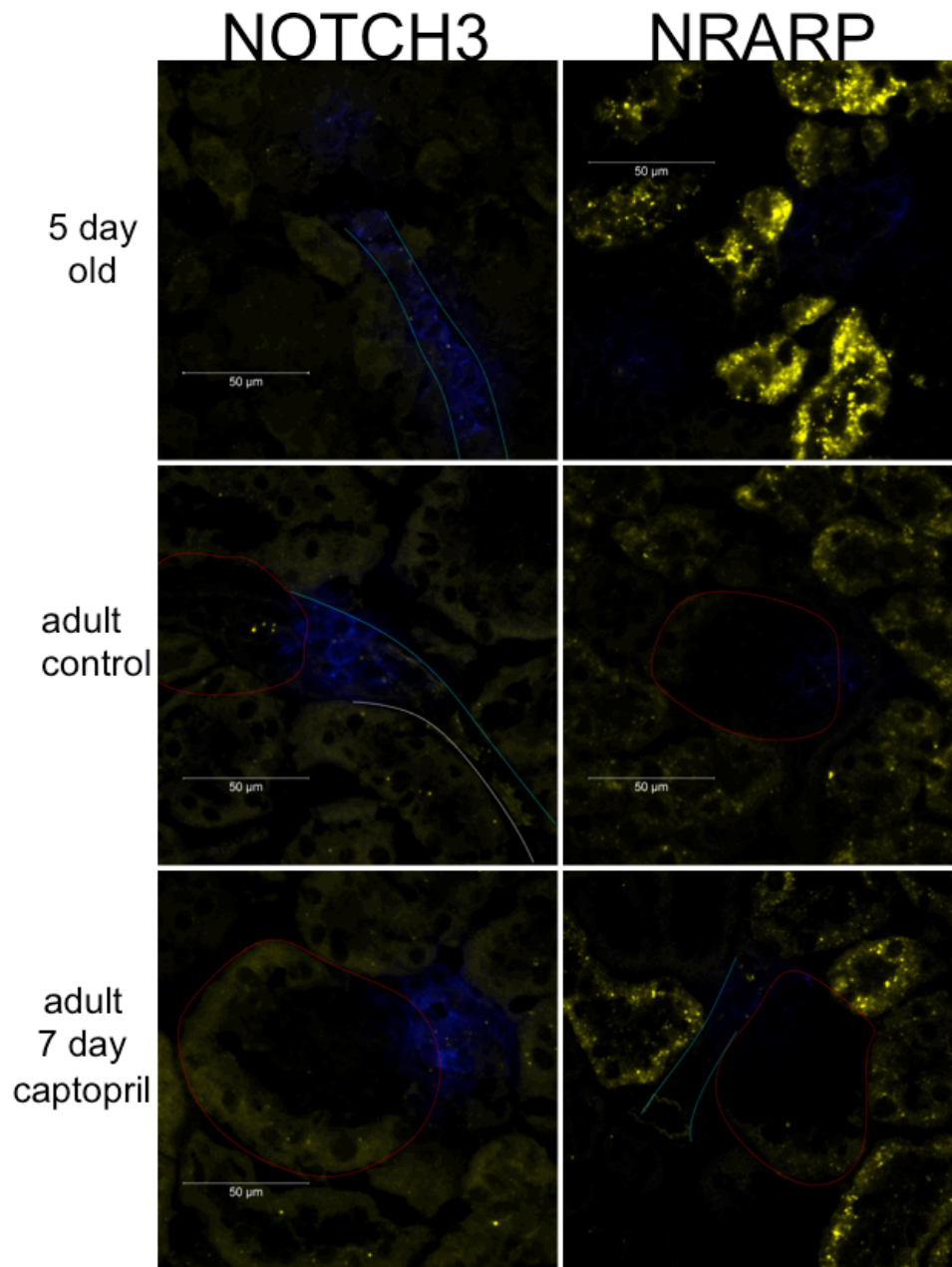


Figure S5. Representative iFISH results showing renin immunofluorescence (in blue) and in situ hybridization for the indicated mouse mRNA (in yellow) in kidneys from 5 day-old mice (upper panel) 10-12 week adult control mice (middle panels) and adult mice treated for 7 days with the ACE inhibitor captopril (lower panels). The results from each probe is presented on one page in alphabetical order. Where possible, glomeruli are outlined in red and vessels in light blue. Overlapping expression of renin and any of the corresponding genes in renin-producing cells (RPC) of the 5 day old (developing) kidney or juxtaglomerular (JG) cells of the adult kidney is seen as white dots. Signal in the tubules represents some degree of non-specific background. Results are summarized in Table 3 of the text. (continuation)

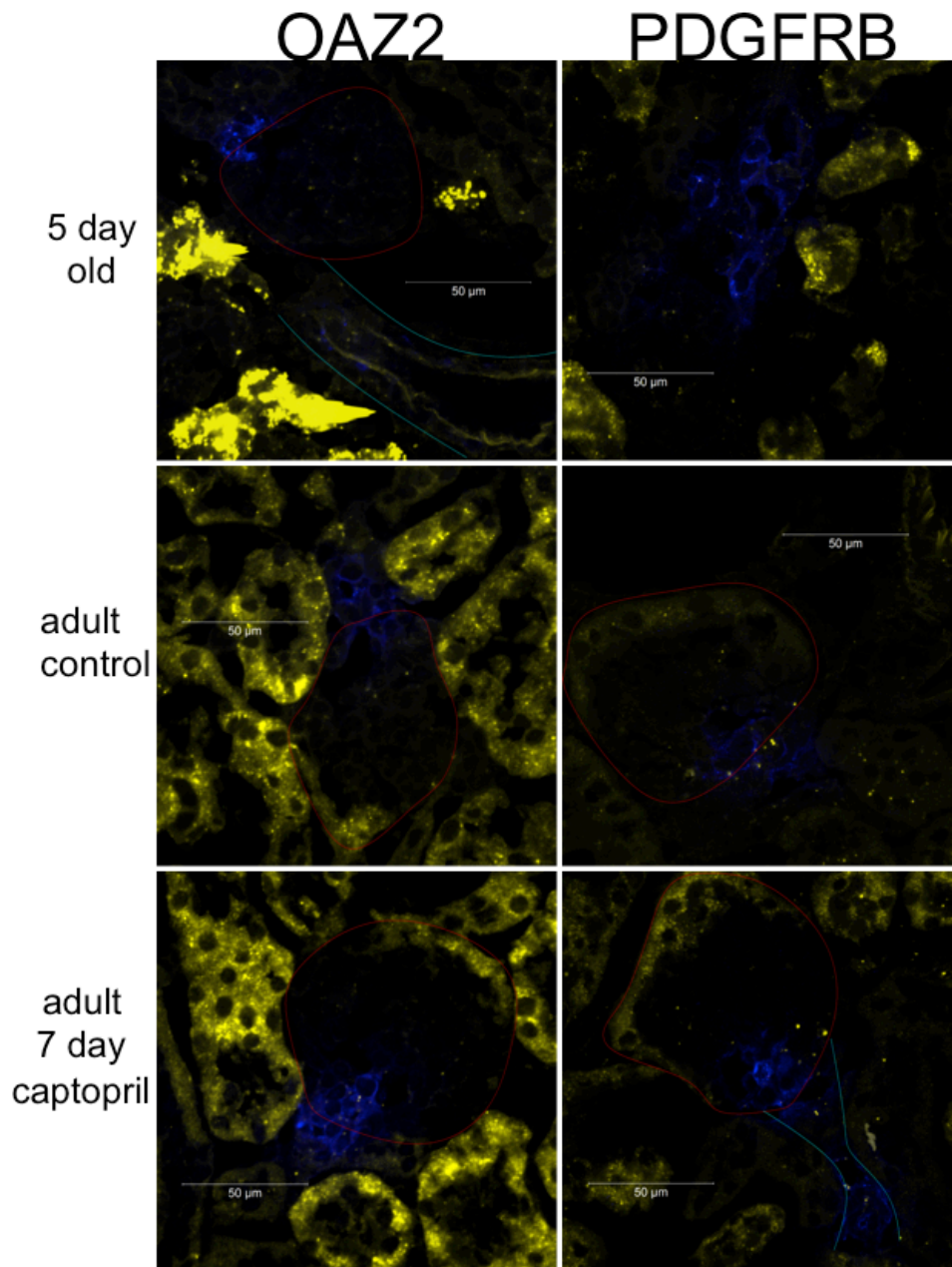


Figure S5. Representative iFISH results showing renin immunofluorescence (in blue) and in situ hybridization for the indicated mouse mRNA (in yellow) in kidneys from 5 day-old mice (upper panel) 10-12 week adult control mice (middle panels) and adult mice treated for 7 days with the ACE inhibitor captopril (lower panels). The results from each probe is presented on one page in alphabetical order. Where possible, glomeruli are outlined in red and vessels in light blue. Overlapping expression of renin and any of the corresponding genes in renin-producing cells (RPC) of the 5 day old (developing) kidney or juxtaglomerular (JG) cells of the adult kidney is seen as white dots. Signal in the tubules represents some degree of non-specific background. Results are summarized in Table 3 of the text. (continuation)

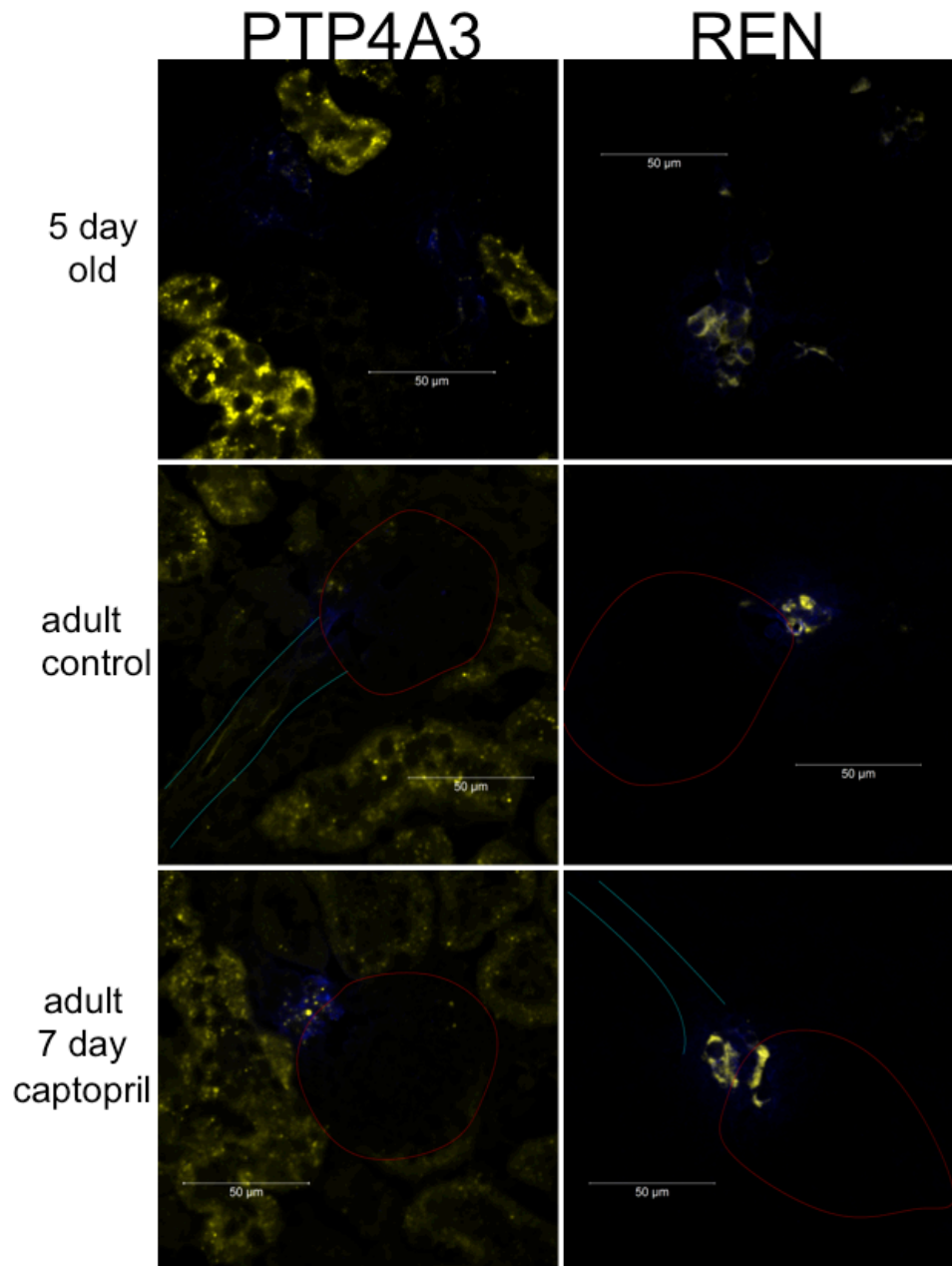


Figure S5. Representative iFISH results showing renin immunofluorescence (in blue) and in situ hybridization for the indicated mouse mRNA (in yellow) in kidneys from 5 day-old mice (upper panel) 10-12 week adult control mice (middle panels) and adult mice treated for 7 days with the ACE inhibitor captopril (lower panels). The results from each probe is presented on one page in alphabetical order. Where possible, glomeruli are outlined in red and vessels in light blue. Overlapping expression of renin and any of the corresponding genes in renin-producing cells (RPC) of the 5 day old (developing) kidney or juxtaglomerular (JG) cells of the adult kidney is seen as white dots. Signal in the tubules represents some degree of non-specific background. Results are summarized in Table 3 of the text. (continuation)

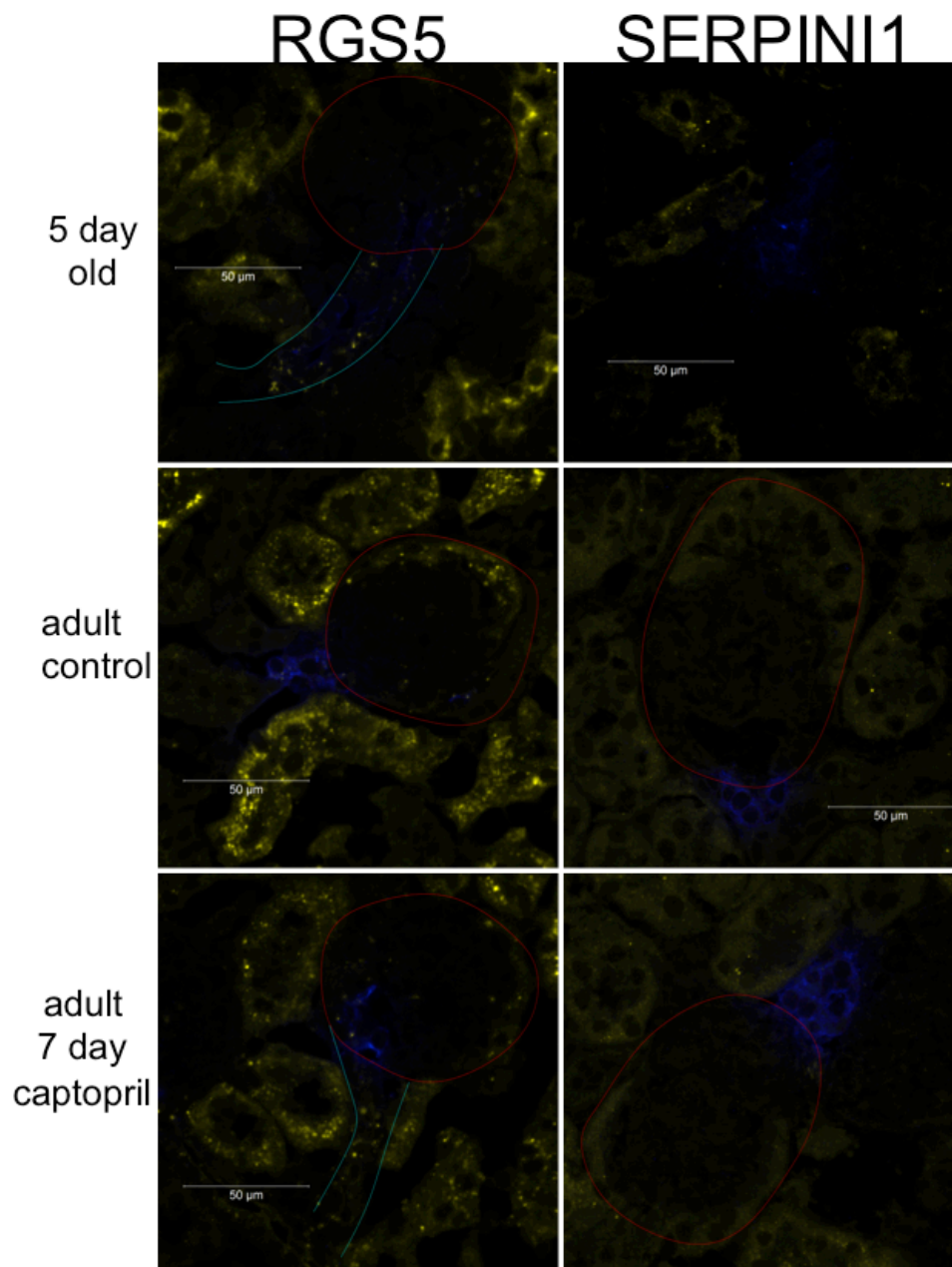


Figure S5. Representative iFISH results showing renin immunofluorescence (in blue) and in situ hybridization for the indicated mouse mRNA (in yellow) in kidneys from 5 day-old mice (upper panel) 10-12 week adult control mice (middle panels) and adult mice treated for 7 days with the ACE inhibitor captopril (lower panels). The results from each probe is presented on one page in alphabetical order. Where possible, glomeruli are outlined in red and vessels in light blue. Overlapping expression of renin and any of the corresponding genes in renin-producing cells (RPC) of the 5 day old (developing) kidney or juxtaglomerular (JG) cells of the adult kidney is seen as white dots. Signal in the tubules represents some degree of non-specific background. Results are summarized in Table 3 of the text. (continuation)

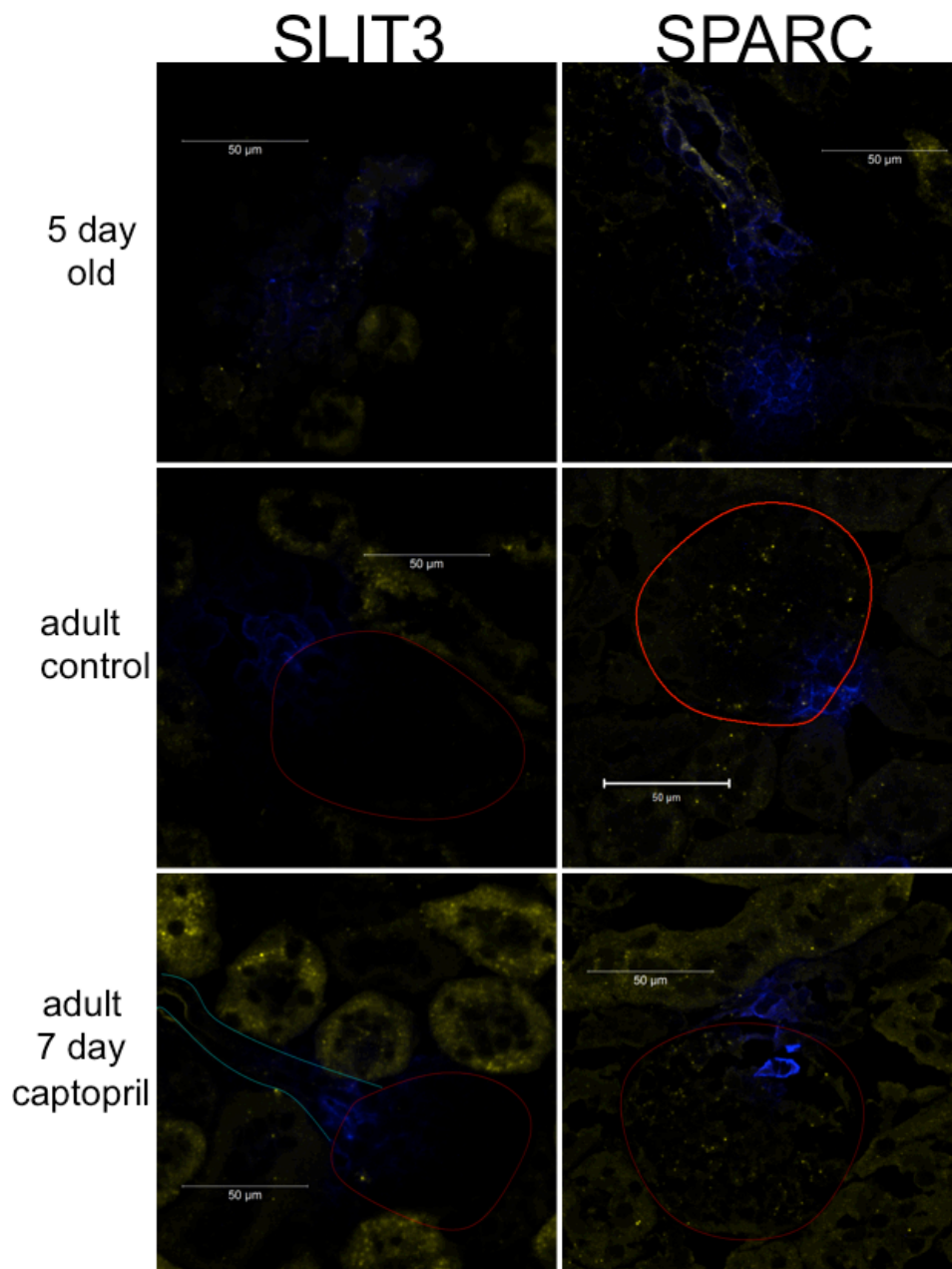


Figure S5. Representative iFISH results showing renin immunofluorescence (in blue) and in situ hybridization for the indicated mouse mRNA (in yellow) in kidneys from 5 day-old mice (upper panel) 10-12 week adult control mice (middle panels) and adult mice treated for 7 days with the ACE inhibitor captopril (lower panels). The results from each probe is presented on one page in alphabetical order. Where possible, glomeruli are outlined in red and vessels in light blue. Overlapping expression of renin and any of the corresponding genes in renin-producing cells (RPC) of the 5 day old (developing) kidney or juxtaglomerular (JG) cells of the adult kidney is seen as white dots. Signal in the tubules represents some degree of non-specific background. Results are summarized in Table 3 of the text. (continuation)

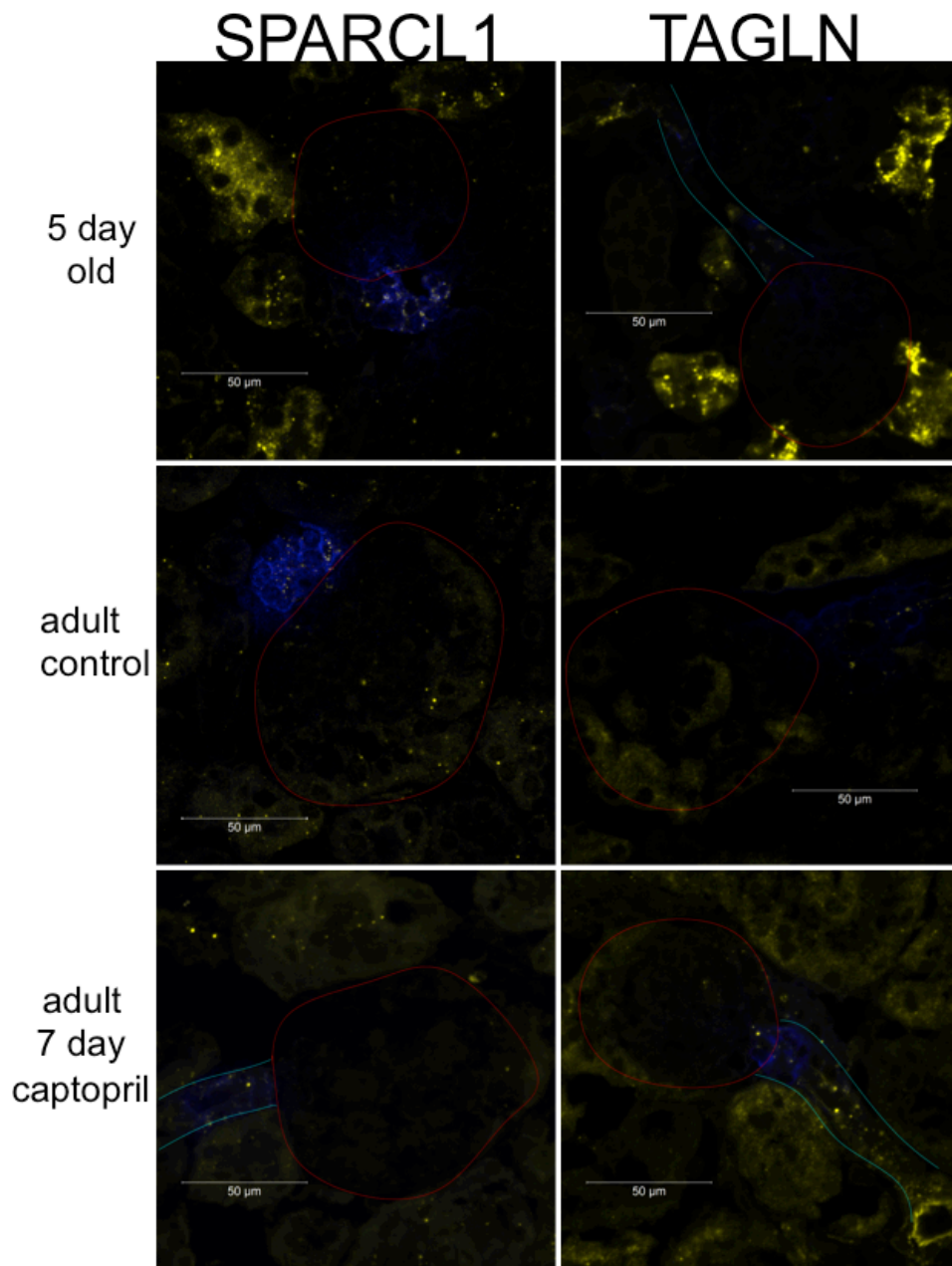


Figure S5. Representative iFISH results showing renin immunofluorescence (in blue) and in situ hybridization for the indicated mouse mRNA (in yellow) in kidneys from 5 day-old mice (upper panel) 10-12 week adult control mice (middle panels) and adult mice treated for 7 days with the ACE inhibitor captopril (lower panels). The results from each probe is presented on one page in alphabetical order. Where possible, glomeruli are outlined in red and vessels in light blue. Overlapping expression of renin and any of the corresponding genes in renin-producing cells (RPC) of the 5 day old (developing) kidney or juxtaglomerular (JG) cells of the adult kidney is seen as white dots. Signal in the tubules represents some degree of non-specific background. Results are summarized in Table 3 of the text. (continuation)

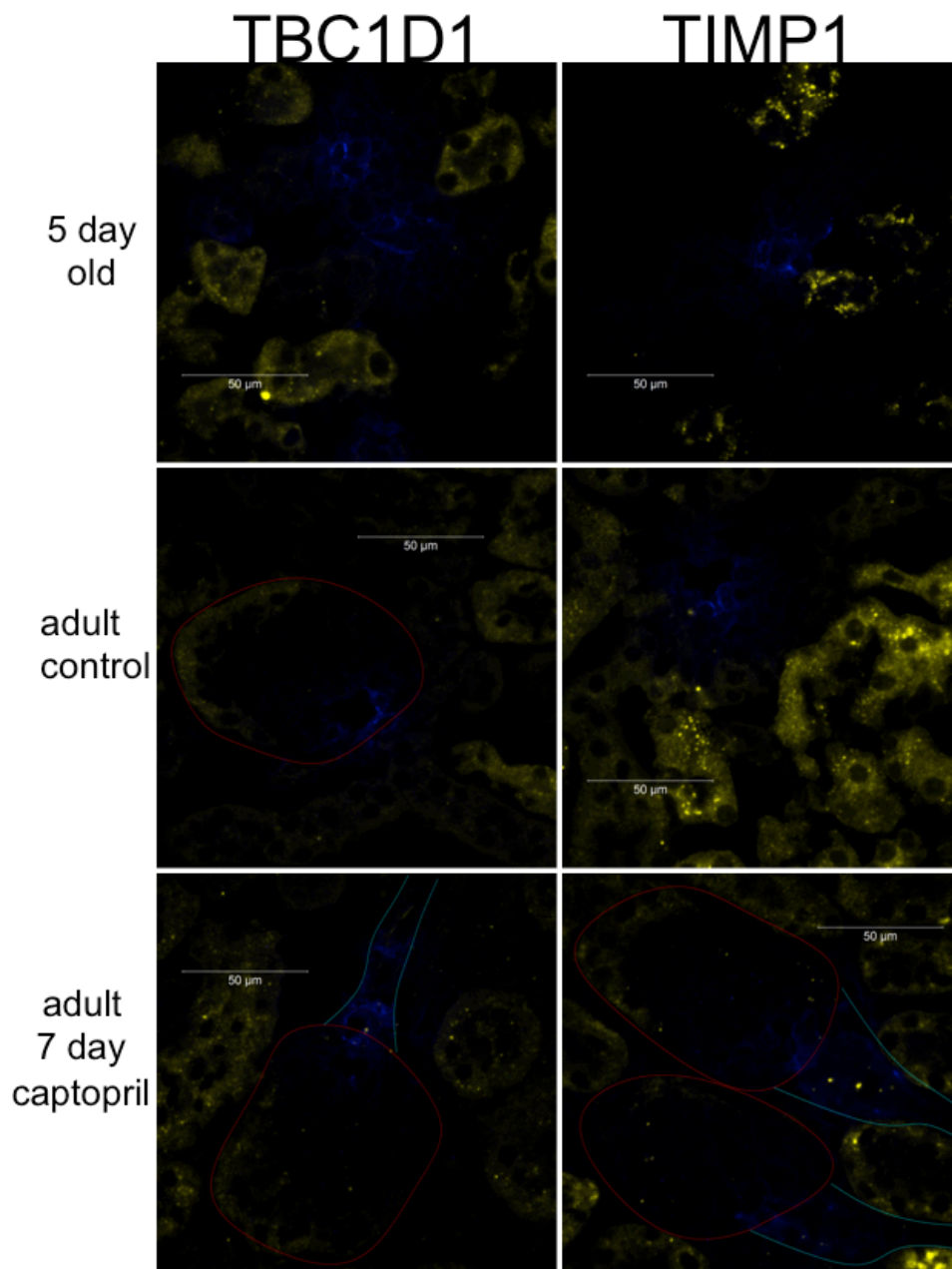


Figure S5. Representative iFISH results showing renin immunofluorescence (in blue) and in situ hybridization for the indicated mouse mRNA (in yellow) in kidneys from 5 day-old mice (upper panel) 10-12 week adult control mice (middle panels) and adult mice treated for 7 days with the ACE inhibitor captopril (lower panels). The results from each probe is presented on one page in alphabetical order. Where possible, glomeruli are outlined in red and vessels in light blue. Overlapping expression of renin and any of the corresponding genes in renin-producing cells (RPC) of the 5 day old (developing) kidney or juxtaglomerular (JG) cells of the adult kidney is seen as white dots. Signal in the tubules represents some degree of non-specific background. Results are summarized in Table 3 of the text. (continuation)

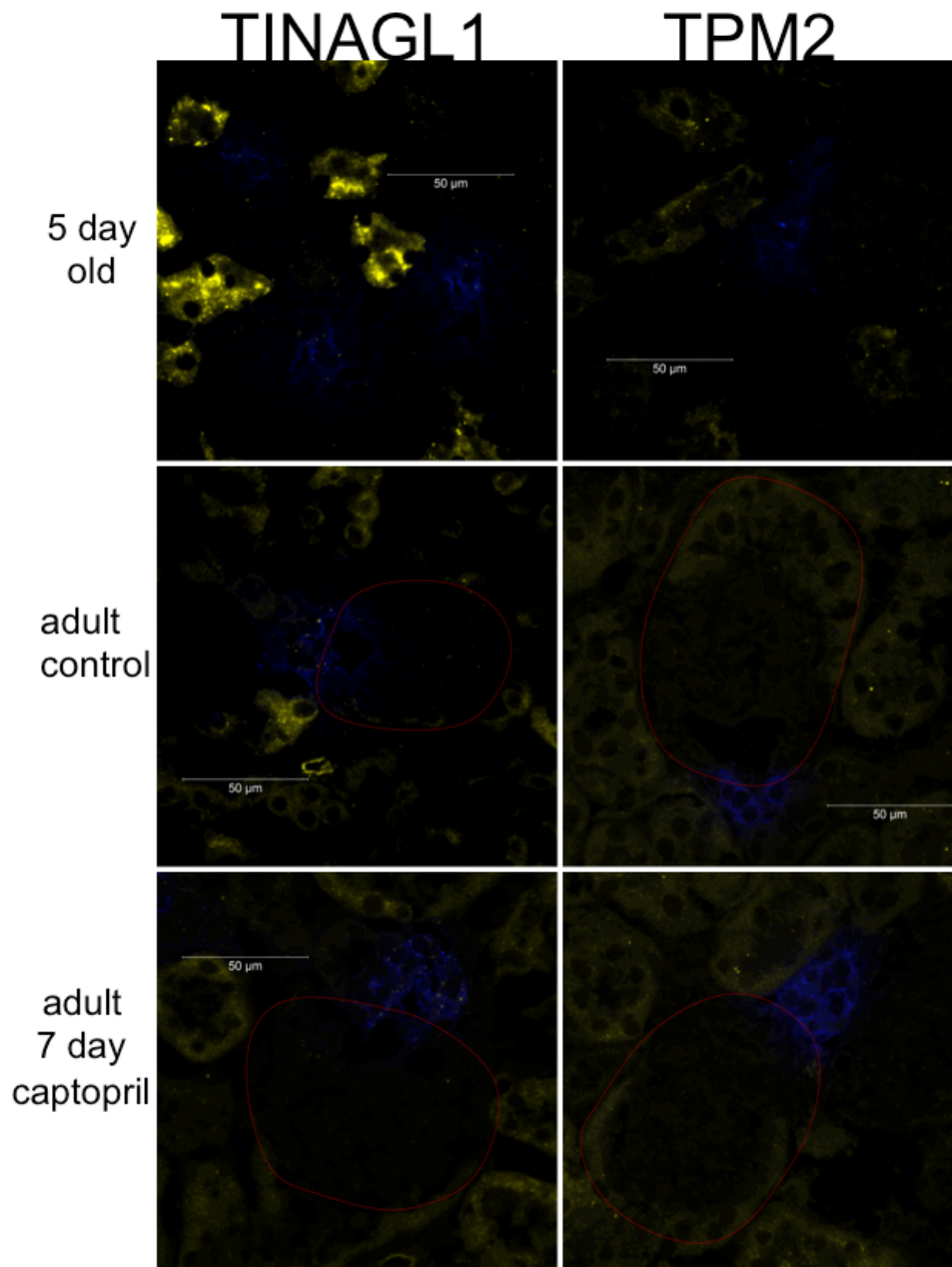


Figure S5. Representative iFISH results showing renin immunofluorescence (in blue) and in situ hybridization for the indicated mouse mRNA (in yellow) in kidneys from 5 day-old mice (upper panel) 10-12 week adult control mice (middle panels) and adult mice treated for 7 days with the ACE inhibitor captopril (lower panels). The results from each probe is presented on one page in alphabetical order. Where possible, glomeruli are outlined in red and vessels in light blue. Overlapping expression of renin and any of the corresponding genes in renin-producing cells (RPC) of the 5 day old (developing) kidney or juxtaglomerular (JG) cells of the adult kidney is seen as white dots. Signal in the tubules represents some degree of non-specific background. Results are summarized in Table 3 of the text. (continuation)

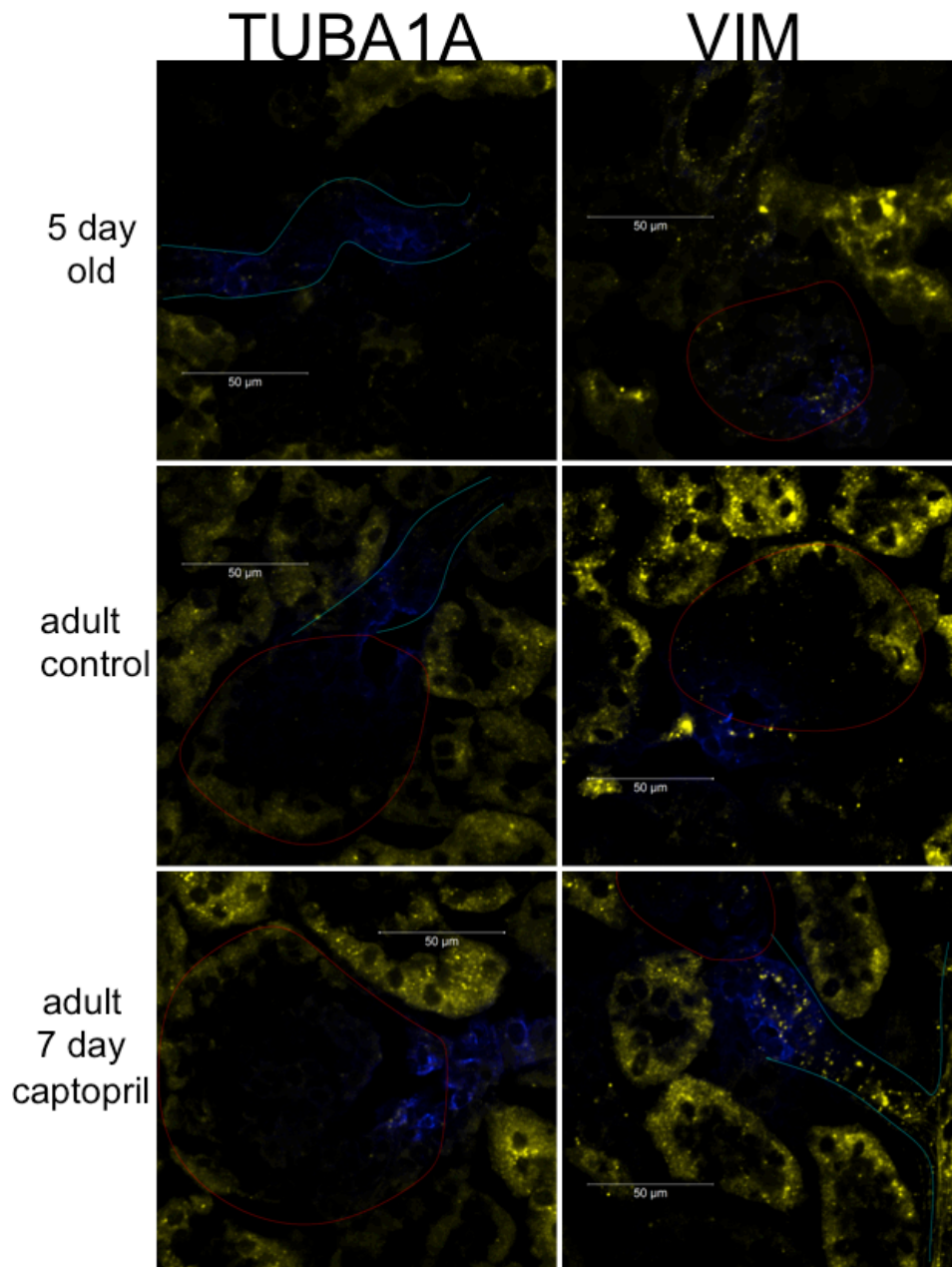


Figure S5. Representative iFISH results showing renin immunofluorescence (in blue) and in situ hybridization for the indicated mouse mRNA (in yellow) in kidneys from 5 day-old mice (upper panel) 10-12 week adult control mice (middle panels) and adult mice treated for 7 days with the ACE inhibitor captopril (lower panels). The results from each probe is presented on one page in alphabetical order. Where possible, glomeruli are outlined in red and vessels in light blue. Overlapping expression of renin and any of the corresponding genes in renin-producing cells (RPC) of the 5 day old (developing) kidney or juxtaglomerular (JG) cells of the adult kidney is seen as white dots. Signal in the tubules represents some degree of non-specific background. Results are summarized in Table 3 of the text. (continuation)

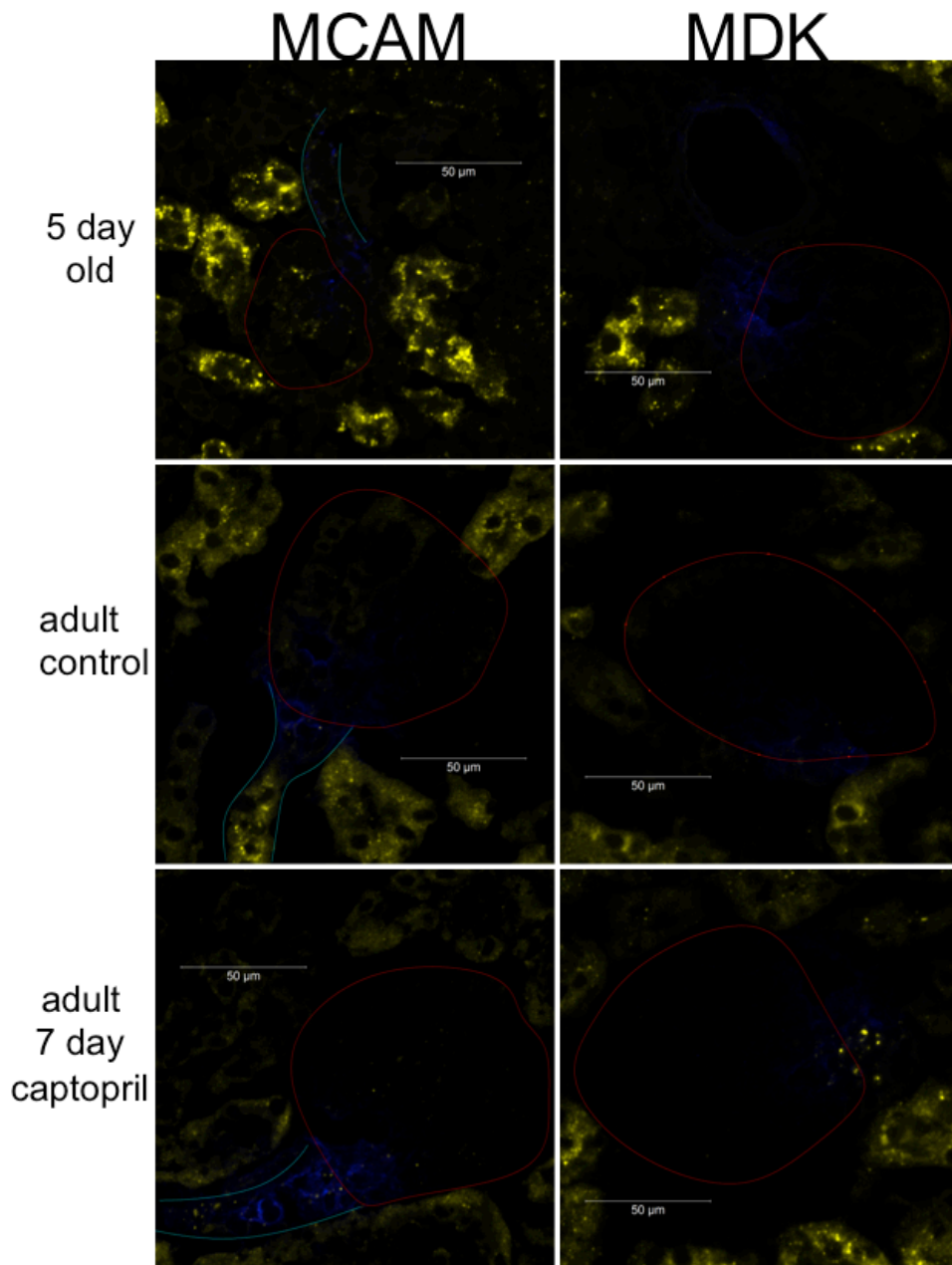


Figure S5. Representative iFISH results showing renin immunofluorescence (in blue) and in situ hybridization for the indicated mouse mRNA (in yellow) in kidneys from 5 day-old mice (upper panel) 10-12 week adult control mice (middle panels) and adult mice treated for 7 days with the ACE inhibitor captopril (lower panels). The results from each probe is presented on one page in alphabetical order. Where possible, glomeruli are outlined in red and vessels in light blue. Overlapping expression of renin and any of the corresponding genes in renin-producing cells (RPC) of the 5 day old (developing) kidney or juxtaglomerular (JG) cells of the adult kidney is seen as white dots. Signal in the tubules represents some degree of non-specific background. Results are summarized in Table 3 of the text. (conclusion)

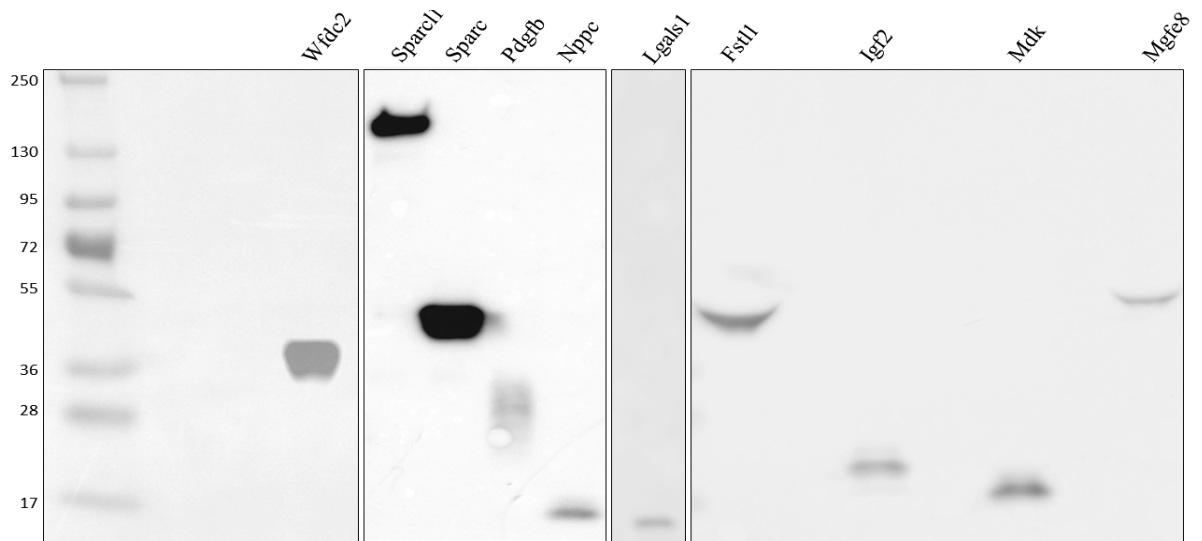


Figure S6. WB experiments confirmed the presence of each of the transfected genes in the HEK293 cells medium at 48 hours after transfection.

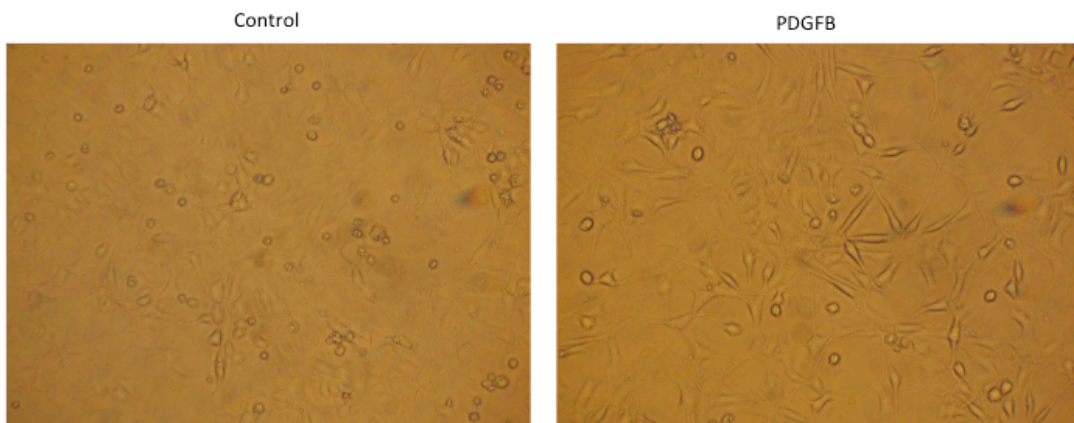


Figure S7. PDGFB altered As4.1 morphology, in that the cells after exposure to this ligand displayed a more elongated, densely packed and aligned shape.

Table S3 – Rank order of the 100 most highly expressed genes in each of the reninomas. Genes in yellow are part of a 369 gene list that makes up a renin-producing cell signature, according to Brunskill et al. (102) (to be continued)

Rank	Par1	Mon	Rot	Par2
1	REN	REN	REN	REN
2	GNAS	GNAS	KISS1	KISS1
3	KISS1	KISS1	GNAS	GNAS
4	IGF2	IGF2	IGF2	IFITM3
5	IFITM3	A2M	C4A	PTP4A3
6	A2M	IFITM3	PTP4A3	IGF2
7	SFRP4	SPARCL1	CSRP2	CSRP2
8	PTP4A3	PTP4A3	IFITM3	ACTA2
9	SPARCL1	TGFBI	A2M	A2M
10	TGFBI	C4A	MYL9	MYL9
11	CSRP2	CSRP2	TPM2	TPM2
12	C4A	JAG1	SPARCL1	IFITM1
13	VIM	NOTCH3	C10orf116	TAGLN
14	TPSB2	PDGFRB	TAGLN	C10orf116
15	MYL9	IGLL5	ACTA2	C4A
16	IFITM1	SERPINI1	ISYNA1	SPARCL1
17	MDK	WFDC2	TPSB2	VIM
18	TPSAB1	IFITM1	TPSAB1	LGALS1
19	COL6A2	SRGN	COL6A2	SPARC
20	CPE	HSPB6	HSPB6	LBH
21	NOTCH3	ISYNA1	JAG1	SFRP4
22	MFGE8	NPPC	SRGN	COL6A2
23	LGALS1	SFRP4	MYBPH	TPM1
24	PDGFRB	LBH	CPE	JAG1
25	TGM2	ECEL1	CALD1	CPE
26	SPARC	GPC1	IFITM1	ISYNA1
27	JAG1	MXRA8	LGALS1	TBX2
28	CBLN4	TBC1D1	NOTCH3	TPSB2
29	SRGN	ADCY3	VIM	IFITM2
30	SERPINI1	VIM	LBH	CALD1
31	TBC1D1	ITGA7	TBX2	SRGN
32	ECEL1	TBX2	FLNA	MCAM
33	TBX2	CPE	IFITM2	TBC1D1
34	CXCL12	TGM2	CXCL12	MXRA8

Table S3 – Rank order of the 100 most highly expressed genes in each of the reninomas. Genes in yellow are part of a 369 gene list that makes up a renin-producing cell signature, according to Brunskill et al. (102) (continuation)

Rank	Par1	Mon	Rot	Par2
35	TPM2	COL6A1	TPM1	MDK
36	CPA3	ATP1B2	COL6A1	COL6A1
37	RGS5	CALD1	ITGA7	C11orf96
38	ACTA2	CBLN4	TBC1D1	CXCL12
39	NPPC	SPARC	MXRA8	TGFBI
40	SLIT3	NT5DC2	TGM2	OAZ2
41	CD248	LGALS1	CPA3	NOTCH3
42	FABP5	APLP1	BCKDHB	PDGFRB
43	IFITM2	MDK	C1QB	BGN
44	ITGA7	FLNA	HCFC1R1	TPSAB1
45	TUBA1A	SLIT3	NRIP2	GJA4
46	LBH	C20orf27	TM4SF1	WFDC2
47	C20orf27	HRC	TINAGL1	RERGL
48	BGN	TUBA1A	SFRP4	NT5DC2
49	COL6A1	C1QB	C1QA	TINAGL1
50	ATP1B2	COL6A2	ADCY3	COL13A1
51	GPC1	CXCL12	GJA4	CRIP1
52	CD55	DBNDD2	SPARC	TUBA1A
53	MXRA8	PDE4C	C20orf27	SERPINI1
54	MCAM	GPR133	C1QC	ADCY3
55	C10orf116	FSTL1	PDGFRB	TM4SF1
56	FKBP10	RASAL1	SLC5A7	UBA2
57	FXD1	WISP1	ATP1B2	MFGE8
58	OAZ2	C10orf116	NR2F1	C1QA
59	NT5DC2	OAZ2	WFDC2	C1QB
60	FSTL1	GJA4	COL13A1	NRARP
61	GJA4	TPM2	C11orf96	TPM4
62	DBNDD2	FABP5	FLRT2	FLNA
63	TAGLN	NRARP	DBNDD2	HCFC1R1
64	FLNA	CD34	UBA2	CBLN4
65	IGLL5	HCFC1R1	NT5DC2	NRIP2
66	ISYNA1	MMP7	SLC7A2	ENO3
67	CALD1	GPAT2	OAZ2	CPA3
68	SGCA	FKBP10	SERPINI1	RGS5

Table S3 – Rank order of the 100 most highly expressed genes in each of the reninomas. Genes in yellow are part of a 369 gene list that makes up a renin-producing cell signature, according to Brunskill et al. (102) (conclusion)

Rank	Par1	Mon	Rot	Par2
69	CRIP1	C1QC	FXYD1	DBNDD2
70	PLTP	MYL9	CASQ2	C1QC
71	KLHDC8B	UBA2	PEAR1	NPPC
72	ADCY3	ADAMTS9	SLIT3	CD248
73	TPM1	C1QA	ADAM33	CD34
74	RERGL	CD248	MFGE8	HSPB6
75	GPR124	MFGE8	MYOM2	C10orf10
76	TIMP1	HES4	MCAM	ITGA7
77	HSPB6	FABP4	NRARP	PLEKHH3
78	COX4I2	PLEKHH3	CD34	HES4
79	FABP4	TIMP1	PDLIM7	SEPT4
80	DAAM2	DDIT4	HES4	COX4I2
81	HRC	ADAM33	TIMP1	NR2F1
82	RET	LIMCH1	MYH11	CCR10
83	PCOLCE	KLHDC8B	LEFTY1	BCKDHB
84	TINAGL1	TBX3	BGN	FKBP10
85	CSPG4	TNFRSF1B	MEIS1	TGM2
86	DKK3	PEAR1	LMOD1	CCL14
87	CD34	TINAGL1	TYROBP	SGCA
88	GUCY1B3	CRIP1	CBLN4	TIMP1
89	UNC5B	TPM1	MEF2C	PPP1R12C
90	HCFC1R1	PPP1R12C	GPR124	NDUFA4L2
91	PLEKHH3	GRK5	TNFRSF1B	C20orf27
92	TPM4	TPM4	GUCY1B3	DKK3
93	COL15A1	COL13A1	GPC1	GPR124
94	NRARP	NRIP2	SEPT7	GRK5
95	ADRA2C	HIC1	PLEKHH3	GUCY1B3
96	MEF2C	EMILIN1	ENO3	FXYD1
97	ARHGEF17	GPR124	RGS5	SLIT3
98	EMILIN1	MEF2C	DDIT4	PDE4C
99	NDUFA4L2	NPTX1	ARHGEF17	PTPN12
100	POSTN	COL5A3	PDE1A	SLC5A7

Table S4 – Oligonucleotide sequences used to amplify the C57BL/6 mouse cDNA fragments for generation of the FISH probes. F; forward. R; reverse. Shown in the right-hand column is the expected length of the amplified fragment. (to be continued)

Gene	Sense	Sequence	size (bp)
A2m	F	ATGGAGTCTGTCCGTGGGA	1066bp
	R	GTTAGGGACGTGCCCATGAT	
Acta2	F	GCTATGTGTGAAGAGGAAGA	1028bp
	R	CCAGACAGAGTACTTGCCT	
Adcy3	F	CAAAATGGCCTCAACGGCTC	1014bp
	R	AGTACTTGGAAGGCACCAGG	
Atp1b2	F	CCCCTTTCTATCGCAGTCGG	1088bp
	R	ATCCGGAGTTTGAAGGCCAC	
Bgn	F	GCATCAATGACTTCTGTCCTA	1017bp
	R	ACCTTCCAGCTTCCTCCAG	
C4a	F	CCCGGGGCGAAGGTCACAGACGCTGTG	1007bp
	R	GGCCGCGGCTGCTGAACTCCATCAGGA	
Cald1	F	TGCCTATCAGAGAAATGATGAT	982bp
	R	CGATCTCTTCCTTTAACCTC	
Cbln4	F	CTAGCCACCTTTGCTAGCGT	1063bp
	R	CATCACGGAGAAGTCGGGTT	
Cd34	F	ATGCAGGTCCACAGGGAC	959bp
	R	CCTTTCTCCTGTAGGGCTC	
Cd248	F	CCCGGGGCGTGATCTCTGCCACTCGACC	1012bp
	R	GGCCGCGGTGTGGTCTCAGCCATGTGTC	
Col6a1	F	GGTGAAGCTGGAGCAGAC	999bp
	R	GCGCTTCTCCGGTGAATG	
Col6a2	F	ACATGGGTGAACCAGGAGA	999bp
	R	CAGCATCCACAGGTCTCC	
Cpa3	F	CCCGGGGCCATCCTGAGATGGTTTCAAG	996bp
	R	GGCCGCGGCTGTTGGGAGTAAATAGAAAC	
Cpe	F	GCTGTCATTCCTGGATCAT	1015bp
	R	CGGTTGACTTCTTCATGGC	
Crip1	F	GGTCCCTGAAAAGCGCGG	443bp
	R	TTCCAAAGATCAGGTTTATTAA	
Csrp2	F	AGTCTCCGGATCCGCC	840bp
	R	TAAGAGGTGGTACCCAAATC	
Cxcl12	F	GCCATGGACGCCAAGGTC	1064bp
	R	CCAGAGCACATCTATCCTC	

Table S4 – Oligonucleotide sequences used to amplify the C57BL/6 mouse cDNA fragments for generation of the FISH probes. F; forward. R; reverse. Shown in the right-hand column is the expected length of the amplified fragment. (continuation)

Gene	Sense	Sequence	size (bp)
Dbn2	F	GCTGACATGGACCCAAATC	1054bp
	R	CAATGCCTTGCGGAGATGAA	
Fkbp10	F	CATGTTCTTGTGGGGTCCTC	1056bp
	R	CCATTCTCCCCGTAGGCA	
FlnA	F	TATGGTGGTCACCAAGTGCC	1055bp
	R	CTGGTCACATCCAGCCCATT	
Fxyd1	F	GGGTGGAGCATCCAGTTCT	559bp
	R	TTATCAAGAAGGAAAACCGAG	
Gja4	F	AGCACACCCACCCTGATCTA	1006bp
	R	AGTCAAGAGCACTCCCACCT	
Gnas	F	GCGATGGTGAGAAGGCCA	1022bp
	R	CTATGGTGGGTGACCAACT	
Gpc1	F	GCCATGGAActCCGGACC	1008bp
	R	CTGTGAGTGTGTCCTTGTTG	
Gpr124	F	TGGGAGGCCCAACATTTCTC	1006bp
	R	AATCAACGCCACCGGTATGT	
Hcfc1r1	F	CCCGGGCGAGCCGTAATGATCCTGCAA	858bp
	R	GGCCGCGGTTATTGTGGGATAATGTTTGG	
Hspb6	F	CAGCGTAGGAACAGGATGGAG	1098bp
	R	TTGAGTTTGGGGTTCCTGGT	
Ifitm1	F	TTAACTCCGCAGCCCCTAA	700bp
	R	GGCAGAAAGTCACAGCACG	
Ifitm2	F	CCAGAGTCAGTACCATGAGCC	589bp
	R	CCACCCCGTGCACTTTATTGA	
Ifitm3	F	GGAAACTTCTGAGAAACCGA	640bp
	R	GGTGGTTATCAAGTGCACTT	
Igf2	F	GAAGTCGATGTTGGTGCTTC	1017bp
	R	CCAAGTCTTAGCCAATTTGAC	
Isyna1	F	GTGGTCTACAGCCCCGAAAC	1043bp
	R	TCCACCACACTGCTCTTTGT	
Itga7	F	GCAGACCTGATTGTGGGTG	999bp
	R	TGGGCAGAGCCTGGAAct	
Jag1	F	GAGATCCTGTCCATGCAGA	1036bp
	R	CAGTTATTTGGAGAACAGTCA	

Table S4 – Oligonucleotide sequences used to amplify the C57BL/6 mouse cDNA fragments for generation of the FISH probes. F; forward. R; reverse. Shown in the right-hand column is the expected length of the amplified fragment. (continuation)

Gene	Sense	Sequence	size (bp)
Kiss1	F	CCTGGAAGGAGACTGTAGA	496bp
	R	GACGGCAGCATTGCTTTTAT	
Lbh	F	GAAGCTGGCTAGCGGGCT	1005bp
	R	CTCAGACAGCACATGGTTG	
Lgals1	F	GTCTCTCGGGTGGAGTCT	800p
	R	TTAGTGGTTTCTGGCTTTTATT	
Mcam	F	ATATGAGCACCGCCTTAGCC	1040bp
	R	CCATCCATGGGGACCCAAAA	
Mdk	F	CCCGGGGCGCTCCCTGCCACATCAGA	997bp
	R	GGCCGCGGCTTAATAACAAGTATCAGGGT	
Mef2c	F	CCCGGGGCGTCTGATGGGCGGAGATC	1019bp
	R	GGCCGCGGCTCAAGTGCTAAGCGTATCT	
Mfge8	F	CTACACAGCTGGGCATGGAA	1047bp
	R	AAGGTCGTCAGCCACAGAAG	
Mxra8	F	TGTGGACCCAAGACCGGC	999bp
	R	ACAGCAAACCTCCACCATGT T	
MyI9	F	GGCAAGATGTGCGAGCAAGA	1013bp
	R	CAGCCTTGATTAAAGAGACTG	
Notch3	F	GCTGCCAGTGTCTCTTG	1050bp
	R	CTGACGGCTATGAGTGTGCG	
Nppc	F	GCACAGCAGTAGGACCTGT	961bp
	R	CATTACAATGGTTGGCTTCTT	
Nrarp	F	CCCGGGGCGCAACATGAGCCAAGCCG	1038bp
	R	CCCGGGGCGCAACATGAGCCAAGCCG	
Nt5dc2	F	AAGTGATCGACCTGTACGGC	1000bp
	R	CGCGGGTAGAAGGTGAAGTC	
Oaz2	F	AGAGCCACCGAGGATGATAAA	1046bp
	R	AAAGCCTATACTCAGGAGCCC	
Pdgfrb	F	GACACCAGCTCTGTTCTCT	1018bp
	R	CTATCACAGGGGTGGACAA	
Plekhh3	F	CATGGTTACTCCCACGCAGA	1024bp
	R	GCTCCTCGCTGCTCATACAA	
Ptp4a3	F	GGACCTGAAGAAGTACGGG	1014bp
	R	CCACTGAAAGTTCCAAGTGA	

Table S4 – Oligonucleotide sequences used to amplify the C57BL/6 mouse cDNA fragments for generation of the FISH probes. F; forward. R; reverse. Shown in the right-hand column is the expected length of the amplified fragment. (continuation)

Gene	Sense	Sequence	size (bp)
Ren	F	ACATGACCAGGCTCAGTGC	1004bp
	R	ACTTGCGGATGAAGGTGGC	
Rgs5	F	ATGTGTAAGGGACTGGCAG	1008bp
	R	CTAACCAAATTCTGAAGCCAT	
Serpini1	F	GCACAGCTGATCGAAGAATG	1071bp
	R	CATGTGGCATATTGGTTCA	
Sfrp4	F	GCTCCATCCTGGTGGCGT	1064bp
	R	CCATCACAGAAAGTAATTAGCT	
Slit3	F	GAACCTCTGTCAGCACGAG	1000bp
	R	CTGCAGCTGTGACCAAGG	
Sparc	F	GTCCTGGTCACCTTGTACG	1018bp
	R	CCTAAGAGTCGAGAAGACAG	
Sparcl1	F	GAGCAACCTGTAAGTGACTC	1015bp
	R	CAAGCTCCGAAGTAATCCAG	
Srgn	F	GCTAATCCAGAGGCTGAGT	894bp
	R	GAGGCCACTGTGTTTCACT	
Tagln	F	TTTAAACCCCTCACCCAGCC	1003bp
	R	TCGATATCAAGGACAGTGGGC	
Tbc1d1	F	ATGGAGGCAATCACATTCAC	994bp
	R	GAGCACTCTCGGCAGATGA	
Tbx2	F	CACCCAGGACAATTCGCCAT	1024bp
	R	TCCTGGGATGCTTTCCGAAG	
Tgfbi	F	GTATGTGCTGTGCAGAAGG	1029bp
	R	CAGTGGAGACGTCAGATTC	
Tgm2	F	GGAGAGGTGTGATTTGGAGA	995bp
	R	TCCACCCAGCAGTGGAAGT	
Timp1	F	TGGGTGGATGAGTAATGCGT	800bp
	R	AGGCTTCAGTTTTTCCTGGGG	
Tinagl1	F	GAAGTGCTACCCACTGCCTT	1033bp
	R	CTGCAGTTTTCAAACAGGGC	
Tpm1	F	CACCATGGACGCCATCAAGA	1003bp
	R	TAGAAAGCAGTCTGTGCCTGG	
Tpm2	F	TGGACGCCATCAAGAAGAAG	863bp
	R	TCAGAGGGAAGTGATGTCAT	

Table S4 – Oligonucleotide sequences used to amplify the C57BL/6 mouse cDNA fragments for generation of the FISH probes. F; forward. R; reverse. Shown in the right-hand column is the expected length of the amplified fragment. (conclusion)

Gene	Sense	Sequence	size (bp)
Tpsb2	F	GCAGCTAAGATGCTGAAGCG	1009bp
	R	GAACCGGAATGGCTAGGGAC	
Tuba1a	F	GTCTCCAGGGCTTCTTGTTTT	1000bp
	R	CATCCCTGTGGAAGCAGCAC	
Vim	F	GAGCTCGAGCAGCTCAAG	1026bp
	R	CTGTTGCACCAAGTGTGTG	

Table S5 – Primer sequences used in quantitative real-time PCR.

Gene	Primer Forward	Primer Reverse
renin	AGCTACATGGAGAACGGGTC	TTCCACCCACAGTCACCGAG
aldo-keto reductase family 1, member B7	CCCTCACGCATACAGGAGAA	GCCATGTCCTCCTCACTCAA
$\alpha$ -smooth muscle actin	CCTGGCTTCGCTGTCTACCT	TTGCGGTGGACGATGGA
interleukin-6	TCCAGTTGCCTTCTTGGGAC	GTGTAATTAAGCCTCCGACTT
recombination signal binding protein for immunoglobulin kappa j	CAGACAAGGCCGAGTACAC	GTTTCGGCTTCTACATCCC

## 5 BRAIN RENIN-ANGIOTENSIN SYSTEM: DOES IT EXIST?

### 5.1 INTRODUCTION

Since the discovery of renin in the brain nearly 50 years ago (151), numerous studies have proposed that a so-called brain renin-angiotensin system (RAS) exists. Given the presence of the blood-brain barrier, brain RAS activity should depend on the local synthesis of (pro)renin in the brain rather than uptake from blood. In support of this concept, an intracellular, non-secreted form of renin (icREN) has been shown to occur exclusively in the brain. This renin isoform is derived from an alternative transcript of the renin gene, lacking the signal peptide and part of the prosegment (152, 153). To what degree this truncated prorenin truly generates angiotensin (Ang) I remains elusive. Lee-Kirsch et al. detected low Ang I-generating activity (AGA) levels in cell lysates of AtT20 cells transfected with icREN during incubation with excess angiotensinogen, but failed to demonstrate to what degree this AGA was renin-mediated (e.g., by making use of a renin inhibitor). Peters et al. showed increased AGA in cardiac homogenates of transgenic rats overexpressing icREN and were able to block this with the renin inhibitor CH732 (154). Yet, unexpectedly, the AGA increase was observed only after prosegment removal with trypsin, in disagreement with the fact that truncated prorenin does not require prosegment removal to display activity (155). Moreover, icREN overexpression in the heart, if anything, resulted in effects that were unrelated to angiotensin formation (156).

DOCA-salt treatment is widely believed to stimulate brain RAS activity. Confusingly, it lowers icREN expression, but increases the expression of the classical, secreted form of renin in brain tissue (sREN) (157), possibly because, icREN, via an unknown mechanism, inhibits sREN expression (158). Li et al. proposed that DOCA-salt selectively increases brain prorenin, which, in the absence of a prosegment-cleaving enzyme in the brain, requires interaction with the (pro)renin receptor to allow Ang I generation locally (159, 160). The underlying assumption of this concept is that prorenin binding to the (pro)renin receptor results in a conformational change in the prorenin molecule, allowing it to display enzymatic activity without prosegment cleavage (161). Yet, the low (nanomolar) affinity of the

(pro)renin receptor implies that very high prorenin levels are required for receptor binding (161), for which there currently is no evidence (160).

Given these uncertainties, in the present study we set out to re-evaluate the occurrence of (pro)renin in the brain. We quantified brain (pro)renin in a wide variety of brain regions, derived from control mice, mice exposed to DOCA-salt or Ang II, and renin-deficient mice. Under all conditions, a comparison was made with plasma (pro)renin, and the renin inhibitor aliskiren was applied in the assay to evaluate whether AGA was truly renin-mediated. Mice were studied given the fact that their (pro)renin levels are several orders of magnitude higher than those in humans or rats, thereby facilitating the detection of renin-dependent AGA, even in areas with low (pro)renin levels. To obtain a more complete understanding of the brain RAS, we also quantified brain angiotensinogen, and we studied the changes in brain angiotensin generation making use of brainstem tissue obtained from control spontaneously hypertensive rats (SHR) and SHR treated with the AT<sub>1</sub> receptor blocker (ARB) olmesartan or the ACE inhibitor lisinopril for 4 weeks.

## 5.2 METHODS

All animal experiments were performed under the regulation and permission of the Animal Care Committee, conforming to the Guide for the Care and Use of Laboratory Animals published by the US National Institutes of Health (NIH Publication No. 8523, revised 1985).

### **5.2.1 Brain Renin, Prorenin and Angiotensinogen Levels in Wild-Type Mice, Mice Treated with DOCA-Salt or Angiotensin II and Renin-Deficient Mice**

Male and female C57BL/6J mice (wild-type, WT) were obtained by in-house breeding or purchased from Charles River (Sulzfeld, Germany). Mice (age 3-4 months) were either untreated, treated with deoxycorticosterone acetate (DOCA)-salt (150 mg, 60-day release pellet [Innovative Research of America, Sarasota, USA]) for 4 weeks, or infused with Ang II (490 ng/kg/min by osmotic minipump [Alzet, model 2004, DURECT, Cupertino, USA](162)) for 2 weeks. Ren1c homozygous null mice (Ren1c<sup>-/-</sup>; 3 females and 1 male) were generated as described before (C57BL/6J background) (163) and sacrificed at the age of 3-6 months. All mice were housed

under standard laboratory conditions (temperature  $23\pm 1^\circ\text{C}$ , 12-hour light-dark cycle) and maintained on standard chow (Special Diets Services, Essex, UK) with ad libitum access to tap water. DOCA-salt-treated mice had ad libitum access to 0.15 mol/L (0.9%) NaCl solution. At the end of the treatment period, mice were sacrificed with an overdose of isoflurane and blood was collected by cardiac puncture into EDTA-coated tubes. Blood was centrifuged at 4600 rpm for 10 minutes and plasma was stored at  $-80^\circ\text{C}$  until analysis. Five untreated mice were perfused transcardially with PBS to wash away blood from the brain vasculature. Brains were rapidly removed from all mice and the desired regions (cerebellum, brainstem, cortex, hippocampus, midbrain, striatum and thalamus) were dissected, frozen in liquid nitrogen, and stored at  $-80^\circ\text{C}$  until analysis.

### **5.2.2 Brain and Plasma Angiotensin Levels in Spontaneously Hypertensive Rats**

Male 10-week old SHR (Janvier Labs, Le Genest St. Isle, France) were treated with either vehicle (tap water), the ACE inhibitor lisinopril (15 mg/kg body weight; Sigma-Aldrich, Darmstadt, Germany) or the  $\text{AT}_1$  receptor blocker olmesartan (10 mg/kg body weight, Daiichi Sankyo Co., Ltd., Japan) once daily per gavage for four weeks. Animals were housed under standard laboratory conditions (temperature  $23\pm 1^\circ\text{C}$ , 12-hour light-dark cycle), they were fed a standard pellet diet (1.8% NaCl; Velaz, Prague, Czech Republic), and drank tap water ad libitum. At the end of treatment period, the animals were sacrificed in terminal isoflurane anesthesia (2-3%) by being bled out. Blood was collected in the presence of an inhibitor cocktail containing ethylenediaminetetraacetic acid (EDTA), pepstatin A, p-hydroxymercuribenzoic acid, phenanthroline and specific inhibitors for renin and aminopeptidases to a final concentration of 5% v/v (Attoquant Diagnostics, Vienna, Austria) and immediately cooled on ice.(164) Plasma was isolated by centrifugation at  $4^\circ\text{C}$  and frozen at  $-80^\circ\text{C}$  until analysis. Brains were sampled via skull trepanation followed by removal of the hemispheres and cerebellum. The brainstem was isolated, rapidly frozen in liquid nitrogen and preserved at  $-80^\circ\text{C}$  until analysis.

### **5.2.3 Angiotensinogen Synthesis by Rat Primary Cortical Astrocytes**

Rat primary cortical astrocytes (Invitrogen, Thermo Fisher, Waltham, USA) were grown in 6-well plates (Corning Incorporated, Corning, USA) in DMEM medium (85% Dulbecco's Modified Eagle Medium containing high glucose 4.5 g/L, 15% FCS (Gibco, Thermo Fisher) and L-glutamine (600 mg/L; Flow Lab, UK)) in an incubator at 37°C and 5% CO<sub>2</sub> until confluency. Medium and cells were collected after 24, 48, 72 or 96 hours. For the determination of angiotensinogen, the culture medium was removed and stored at -80°C, while cells were gently washed with PBS, lysed with RIPA buffer (50 mmol/L Tris-HCl, 150 mmol/L NaCl, 1% Triton x-100, 0.5% sodium deoxycholate, 0.1% SDS, 1 mmol/L EDTA), and frozen at -80°C until analysis.

### **5.2.4 Measurement of Renin, Prorenin and Angiotensinogen**

Mouse plasma renin and prorenin were measured as described before (165). Brain tissue was homogenized in 0.01 mol/L phosphate buffer, pH 7.4, containing 0.15 mol/L NaCl, and the homogenates were used to measure renin, total renin (i.e., renin plus prorenin), and angiotensinogen. AGA was measured by enzyme-kinetic assay in the presence of excess sheep angiotensinogen, both without and with the renin inhibitor aliskiren (10 pmol/L-10 µmol/L) (166). Total renin was measured identically after conversion of prorenin to renin by acidification (166). Angiotensinogen was measured in mouse plasma, mouse brain homogenate, rat astrocyte cell culture medium and astrocyte cell lysate (after its centrifugation at 8000 x g for 10 min) as the maximum quantity of Ang I that was generated during incubation with excess recombinant rat renin (161).

### **5.2.5 LC-MS/MS Based Quantification of Angiotensin Metabolites**

Plasma was thawed on ice, and samples were spiked with 200 pg of stable isotope-labeled internal standards for Ang I, Ang II, Ang-(1-7) and Ang-(2-8). Following C18-based solid-phase-extraction, samples were subjected to LC-MS/MS analysis using a reversed-phase analytical column (Acquity UPLC® C18, Waters,

Milford, USA) operating in line with a XEVO TQ-S triple quadrupole mass spectrometer (Waters) in MRM mode. Internal standards were used to correct for peptide recovery of the sample preparation procedure for each angiotensin metabolite in each individual sample. Angiotensin peptide concentrations were calculated considering the corresponding response factors determined in matrix calibration curves, on condition that integrated signals exceeded a signal-to-noise ratio of 10. Brain tissue samples were grinded under liquid nitrogen (pestle and mortar) and the resulting frozen tissue powder was rapidly dissolved in ice cold 6 mol/L guanidine hydrochloride supplemented with 1 % (v/v) TFA at a concentration of 100 mg tissue/mL (167). Resulting homogenates were spiked with 200 pg of stable isotope-labelled internal standard for each angiotensin metabolite analyzed and subjected to solid phase based peptide extraction and subsequent LC-MS/MS analysis. The lower limits of quantification for Ang I, Ang II, Ang-(1-7) and Ang-(2-8) in plasma were 2.1, 0.9, 1.9 and 1.1 pg/mL, and in brain 8.1, 6.7, 12.7 and 8.0 pg/g tissue, respectively.

### **5.2.6 Renin and Angiotensinogen Expression**

Total RNA was isolated from kidney and liver tissue, using Tri Reagent (Sigma-Aldrich, Darmstadt, Germany), and from brain tissue (cerebellum, brainstem, cortex, hippocampus, midbrain, striatum and thalamus), using the RNeasy Lipid kit (Qiagen, Venlo, The Netherlands). RNA concentration was quantified using microspectrophotometry (NanoDrop Technologies, Wilmington, USA). Single stranded complementary DNA was synthesized using the genomic DNA-free total RNA using the Quantitect Reverse Transcription kit (Qiagen) according to the manufacturer's protocol. Quantitative real-time PCRs were conducted in 10  $\mu$ L and 100 ng of cDNA, using the CFX384 Touch™ Real-time PCR detection system (BioRad, Hercules, USA), followed by measurement using either IQ™ SYBR® Green Supermix (BioRad) or Taqman probes (IDT, Coralville, USA). The exon-exon junction spanning oligonucleotide primers for qPCR were designed with NCBI (Primer-BLAST). Primer sequences and GenBank accession numbers for the sequences used to design the primers are listed in Table S6. Regarding mouse renin, primers were designed to selectively detect sREN and icREN, as well as to detect renin independently of its signal peptide and prosegment ('secreted + intracellular renin'; Figure S8A). The

following cycling conditions were used [95°C for 3 min, (95°C for 3 sec, 60°C for 25 sec) × 40 cycles] for the KAPA SYBR® FAST qPCR Master Mix, [95°C for 5 min, (95°C for 10 sec, 59-72°C for 40 sec) × 40 cycles] for the IQ™ SYBR® Green Supermix, and [95°C for 3 min, (95°C for 15 sec, 60°C for 1 min) × 45 cycles] for the Taqman assay. Expression levels in kidney, liver and brain tissue were normalised to the housekeeping genes B2M and TubG2, respectively. The  $2^{-\Delta\Delta C_t}$  method was used for relative quantification of gene expression.

Renin expression in brain tissue was also explored by using Ingenuity Pathway Analysis (IPA). In IPA, tissue expression datasets were created based on expression annotations from the GNF Body Atlas (expression calls were made from microarray data from dissection of healthy, adult, untreated C57/BL6 mouse tissues). Data was also available in Gene Expression Omnibus (<<http://www.ncbi.nlm.nih.gov/geo/query/acc.cgi/acc=GSE1133>>). Published (168) cases where a gene was marked "Present" in a particular tissue (based upon the Affymetrix MAS5 Absence/ Presence call) were used as evidence of mRNA expression, and were incorporated into the tissue expression dataset for that particular tissue. The criteria used to define a gene as expressed in the body atlas data in IPA correspond to an average concentration of 3 transcripts per cell (10 transcripts per million). Additional mRNA expression calls were derived from findings in the Ingenuity Knowledge Base that describes observations of mRNA expression in normal, healthy, adult mammalian tissue (human, mouse, rat and mammalian orthologs). Only findings where high quality mRNA detection methods were used (e.g. Northern Blots, quantitative RT-PCR, etc.) were included. Additional information is provided at the following link: <<http://ingenuity.force.com/ipa/IPATutorials?id=kA250000000TN5CCAW>>.

### 5.2.7 Statistical Analysis

Data are expressed as mean±SEM. To determine the minimum number of animals needed for this study, we reasoned that, if renin is synthesized locally in certain brain areas, the majority of this renin (>50%) should not be washed away by buffer perfusion. Moreover, Grobe et al. (157) have suggested that brain sREN expression doubles after DOCA-salt. On the basis of these 2-fold changes, at an SD of 40% (as observed in brainstem, see Results), with  $\alpha = 0.05$  and  $\beta = 80\%$ , the

minimum n-number is 3. Univariate linear associations between plasma and brain renin levels were assessed by calculation of Pearson's coefficient of correlation. Differences between groups were evaluated by Student's t-test or ANOVA, and corrected for multiple testing by post-hoc Bonferroni analysis when needed.  $P < 0.05$  was considered significant. Statistical analysis was performed with IBM SPSS Statistics version 21.0 (IBM, Armonk, New York, USA).

## 5.3 RESULTS

### 5.3.1 Aliskiren Inhibits Angiotensin I-Generating Activity in the Mouse Brain

Aliskiren identically inhibited AGA in mouse plasma ( $n=2$ ), mouse kidney homogenate ( $n=2$ ) and mouse brain homogenate ( $n=3$ ) (Figure 9). Its  $IC_{50}$  was in the nanomolar range, as has been reported before for mouse renin. (169, 170) These data suggest that AGA in mouse brain homogenates is due to renin. All subsequent AGA measurements were performed both in the absence and presence of  $10 \mu\text{mol/L}$  aliskiren in order to correct for non-renin (i.e., non-aliskiren-inhibitable) AGA.

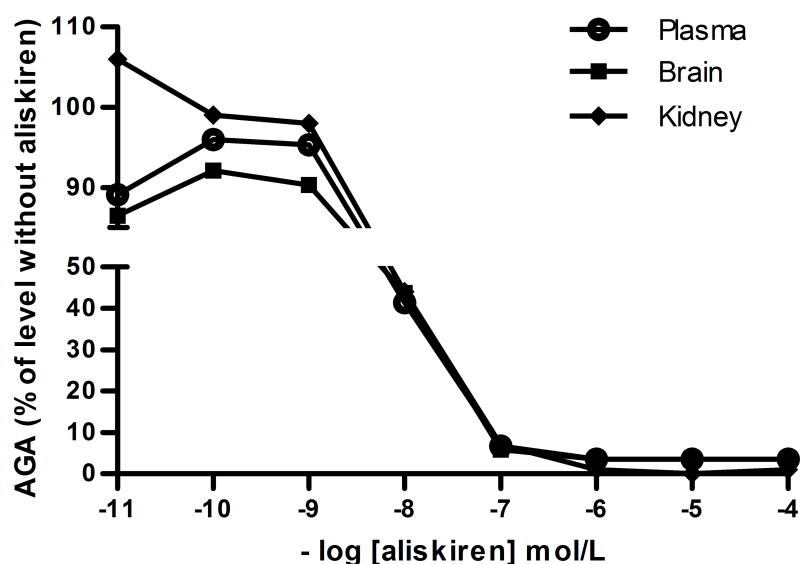


Figure 9. Concentration-dependent inhibition of angiotensin I-generating activity (AGA) by aliskiren in mouse plasma ( $n=2$ ), mouse kidney homogenate ( $n=2$ ) and mouse brain homogenate ( $n=3$ , representing pooled brainstem, cortex and midbrain regions, respectively, from 3-4 mice each).

### 5.3.2 Buffer Perfusion Reduces Mouse Brain Renin by >60%

Renin-dependent (i.e., aliskiren-inhibitable) AGA was readily detectable in brain regions, the highest AGA being present in brainstem (>thalamus ≈cerebellum ≈striatum ≈midbrain >hippocampus ≈cortex) (Figure 10, n=5/group). AGA increased in each individual brain region after prorenin activation, but only when analyzing all brain regions together by multivariate ANOVA did this increase reach significance ( $P<0.05$ ). Applying the prorenin activation procedure to 3 mouse brain homogenates (cortex, midbrain and brainstem, respectively) to which recombinant human prorenin had been added yielded values in a renin IRMA ( $211\pm 12$  pg/mL) that were similar to those when activating the same amount of recombinant human prorenin in buffer with aliskiren(171) ( $169\pm 6$  pg/mL). This confirms that our prorenin activation procedure was appropriate. PBS perfusion of the mouse brain reduced AGA in all brain areas by >60% (Figure 2;  $P<0.01$ ), and diminished the percentage of AGA that could be blocked by aliskiren (Table S7). These data suggest that blood removal predominantly washes away renin, but not non-renin enzymes that are also capable of reacting with angiotensinogen. Plasma renin (expressed per mL plasma) was 40-800x higher than brain renin (expressed per g tissue), and, as expected, identical in mice that were exposed to buffer perfusion. Plasma prorenin levels were of the same order of magnitude as plasma renin levels, as demonstrated earlier in mice (127).

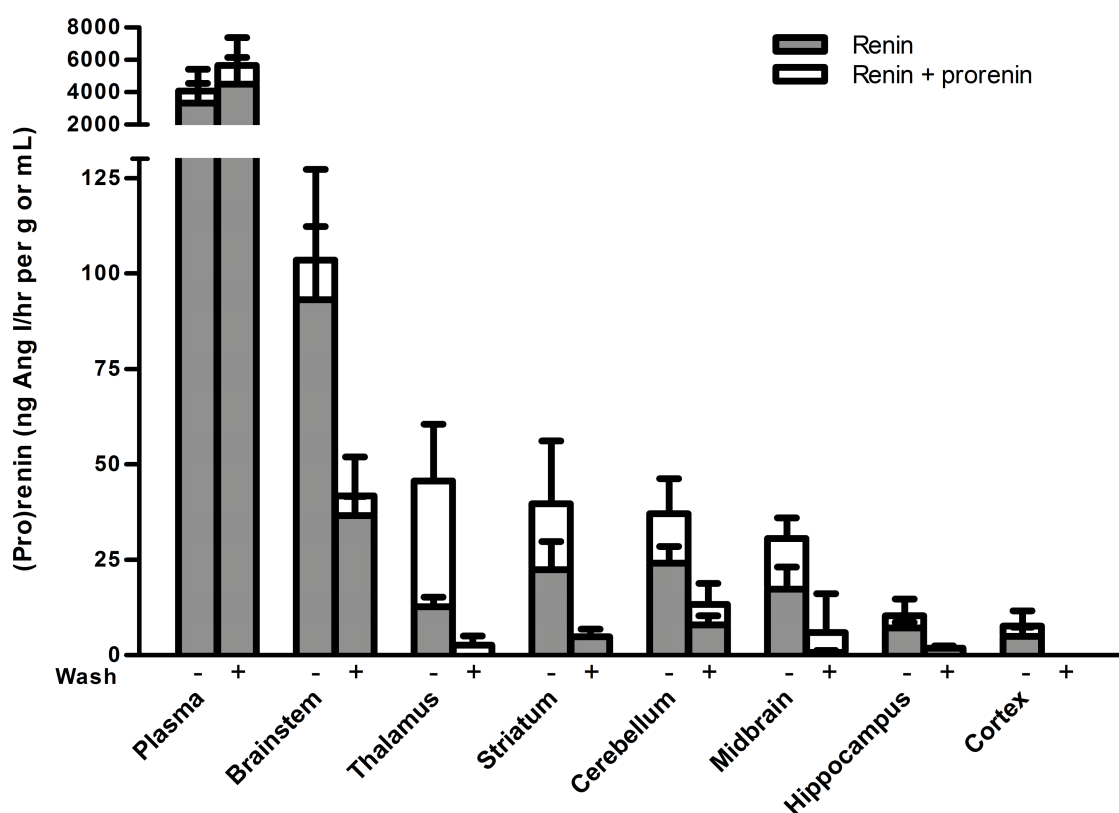


Figure 10. Renin and total renin (=renin + prorenin) levels in plasma and brain regions of mice before and after buffer perfusion (wash) of the brain. Data are mean $\pm$ SEM of  $n=5$ . Multivariate ANOVA showed that total renin levels were higher than renin levels ( $P<0.05$ ), and that buffer perfusion reduced renin by  $>60\%$  in all regions ( $P<0.01$ ).

### 5.3.3 Comparable Reductions in Brain and Plasma (Pro)Renin after DOCA-Salt Treatment, Angiotensin II Infusion and Renin-Deficiency

DOCA-salt ( $n=6$ ) and Ang II ( $n=7$ ) suppressed plasma renin versus WT ( $n=6$ ), and parallel decreases were observed for brainstem, midbrain and cortex renin (Figure 11), although significance was not reached in all cases. Nevertheless, brain renin levels (expressed per g tissue) correlated significantly with plasma renin levels (expressed per mL plasma) in all 3 brain regions (Figure 12). The different slopes may reflect the different blood content of each brain region. Plasma prorenin levels were comparable to plasma renin levels, and prorenin activation in brain regions non-significantly increased brain AGA. Plasma renin and prorenin were undetectable in  $Ren1c^{-/-}$  mice ( $n=4$ ), and renin (i.e., aliskiren-inhibitable AGA) was also undetectable

in the 3 brain regions obtained from Ren1c<sup>-/-</sup> mice. However, low levels of aliskiren-inhibitable AGA were present in brainstem (1 out of 4) midbrain (3 out of 4) and cortex (2 out of 4) after prorenin activation in the Ren1c<sup>-/-</sup> mice. Since this cannot represent prorenin, these data imply that our prorenin activation procedure occasionally activated a renin-like enzyme, capable of reacting with angiotensinogen, the activity of which can be blocked by 10  $\mu$ mol/L aliskiren.

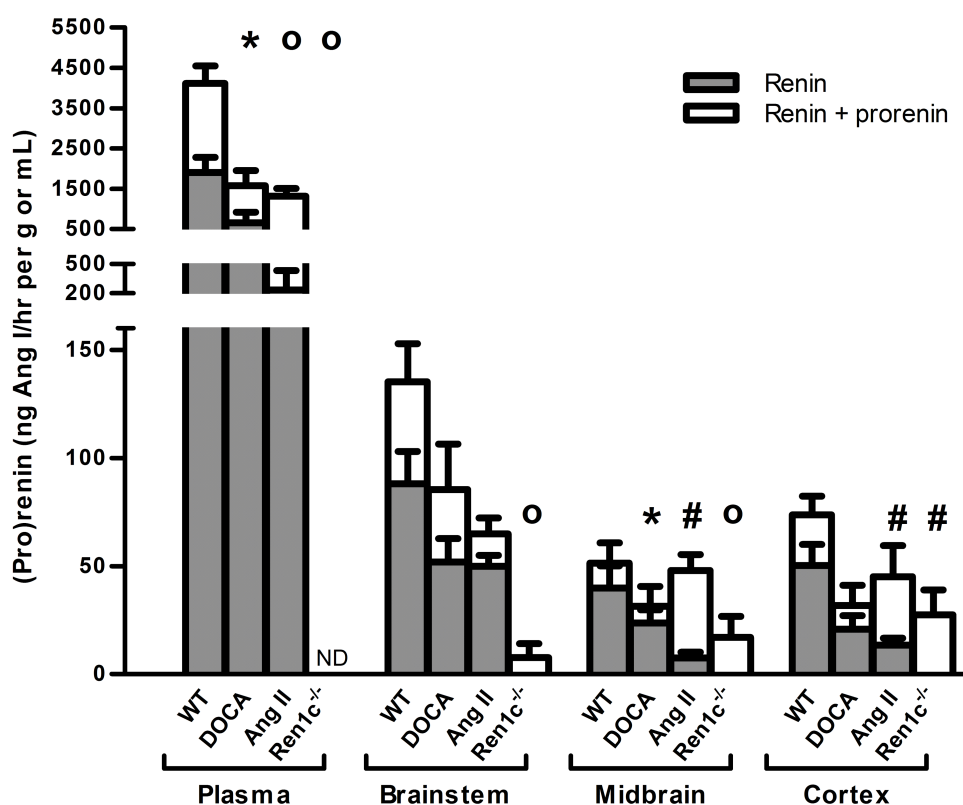


Figure 11. Renin and total renin (=renin + prorenin) levels in plasma and brain regions of untreated mice (WT), mice treated with DOCA-salt, mice infused with Ang II, and Ren1c<sup>-/-</sup> mice. Data are mean $\pm$ SEM of n=4-7. Differences in renin levels were assessed by one-way ANOVA, followed by correction for multiple testing by post-hoc Bonferroni analysis. \*P<0.05, #P<0.01, <sup>o</sup>P<0.001 vs. WT.

### 5.3.4 Renin Expression in the Brain

Renin (secreted + intracellular), sREN or icREN mRNA expression levels were undetectable in all brain regions in WT, DOCA-salt-treated and Ang II-infused mice. Primer specificity for renin (secreted + intracellular) and sREN was validated by measuring renal renin expression in Ren1c<sup>-/-</sup> mice (Figure S8B). In the IPA tissue

expression data sets, renin expression was found in cerebellum, hypothalamus and pituitary, but only in 3 out of 9 different datasets examined (data not shown).

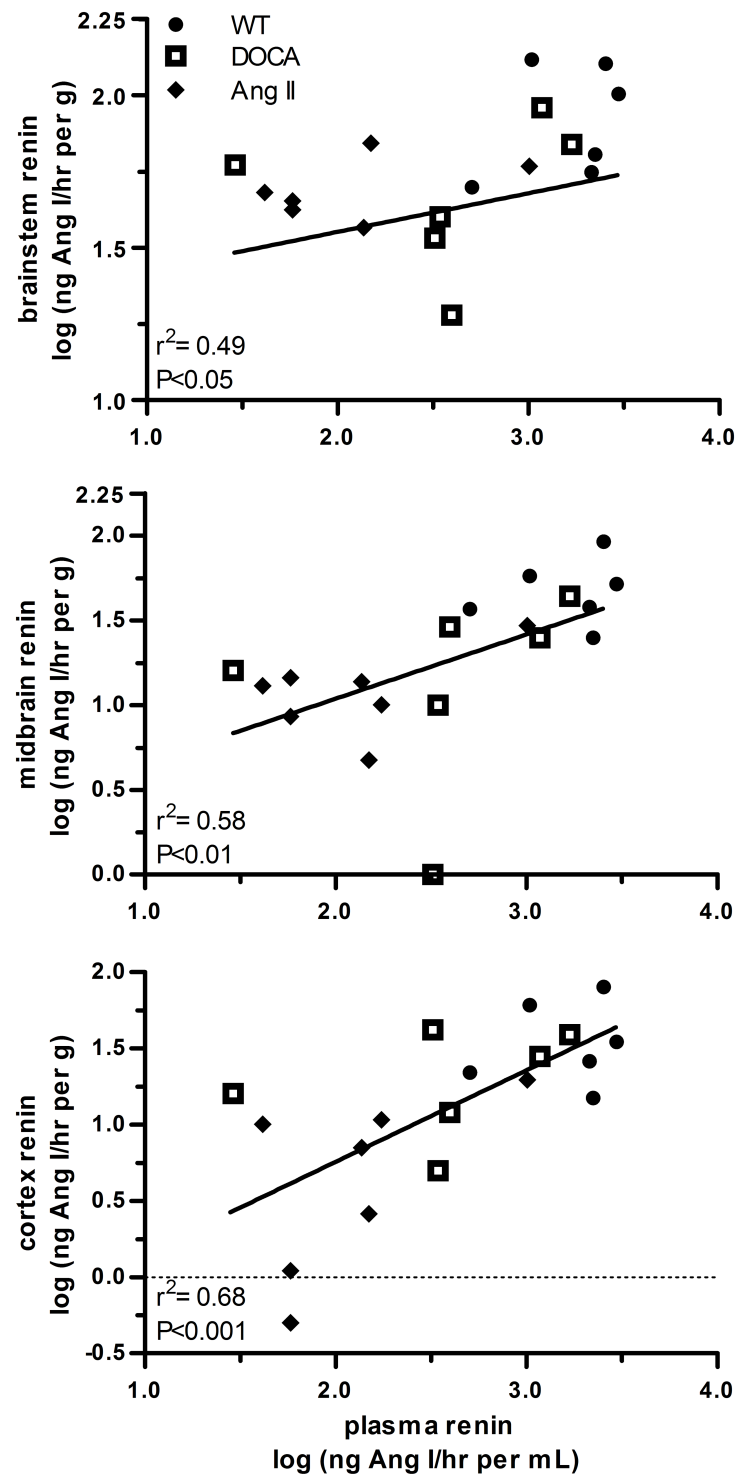


Figure 12. Relationship between renin in plasma and renin in 3 different brain regions in untreated mice (WT, n=6), mice treated with DOCA-salt (n=6) and mice infused with Ang II (n=7).

### 5.3.5 Despite Angiotensinogen Expression, Angiotensinogen Protein is Undetectable in Mouse Brain and Rat Astrocytes

Mouse plasma contained detectable levels of angiotensinogen ( $28 \pm 5$  pmol/mL). Angiotensinogen mRNA expression was observed in different brain regions (Figure 13), at  $C_t$  values of 23 (cerebellum), 22 (thalamus), 25 (hippocampus) and 27 (striatum) versus  $\approx 18$  in the liver. Brain expression levels changed inconsistently after DOCA-salt, Ang II and renin deficiency: an increase was observed in the thalamus after DOCA-salt ( $P < 0.05$ ), while decreases occurred in the cerebellum after DOCA-salt ( $P < 0.05$ ), and in the hippocampus after Ang II ( $P < 0.05$ ). Yet, angiotensinogen protein was undetectable ( $< 1$  pmol/g) in mouse cortex and brainstem ( $n = 4$  of each). Angiotensinogen was also undetectable in the medium of cultured rat astrocytes ( $< 0.3$  pmol/mL), cultured for 24, 48, 72 or 96 hours ( $n = 4$  for each condition), or the accompanying cell lysates ( $< 0.3$  pmol/mg protein).

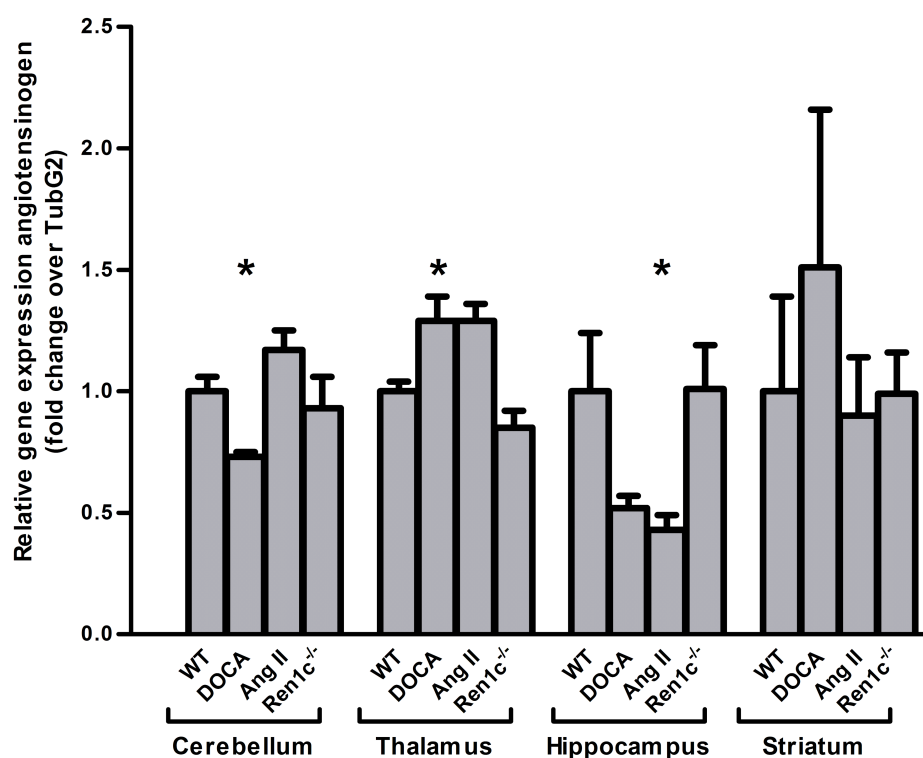


Figure 13. Angiotensinogen mRNA expression in different brain regions in untreated mice (WT), mice treated with DOCA-salt, mice infused with Ang II, and Ren1c<sup>-/-</sup> mice. Data, presented as fold change over TubG2 relative to WT levels, are mean±SEM of n=3-6. Differences were assessed by one-way ANOVA, followed by correction for multiple testing by post-hoc Bonferroni analysis. \*P<0.05 vs. WT.

### 5.3.6 Angiotensins in the SHR Brain with and without RAS Blockade

Ang I, Ang-(1-7) and Ang-(2-8) were below detection limit in brain tissue of untreated SHR (n=6), while Ang II could be detected in the rat brain at levels corresponding with ≈25% of the Ang II levels in blood plasma (Table S8 and Figure 14). Ang I and Ang-(2-8), but not Ang-(1-7), were detectable in plasma in untreated SHR. Brain Ang-(1-7) and Ang-(2-8) remained undetectable after olmesartan (n=6) or lisinopril (n=4), while Ang I became detectable in the rat brain after both types of RAS blockade (P<0.001 for both). Since plasma Ang I increased ≈20-fold after olmesartan and lisinopril (P<0.001 for both), it could be calculated that, during both types of RAS blockade, brain Ang I levels corresponded with ≈1% of the Ang I levels in plasma. Olmesartan increased brain Ang II ≈5-fold (P<0.001) and plasma Ang II ≈25-fold (P<0.001), so that after AT<sub>1</sub> receptor blockade, the brain/plasma ratio of Ang II decreased by ≈80% (P<0.05). Lisinopril decreased plasma Ang II by >90% (P<0.001), and diminished brain Ang II to undetectable levels (P<0.001). Lisinopril also decreased plasma Ang-(2-8) to undetectable levels, and greatly increased plasma Ang-(1-7), while olmesartan increased both plasma Ang-(2-8) and plasma Ang-(1-7). Taken together, given that brain Ang I levels correspond with ≈1% of the circulating Ang I levels, 10 μL plasma per g brain tissue is sufficient to explain the entire brain Ang I content. Brain Ang II levels, relative to plasma Ang II levels, are higher, suggesting either local synthesis or an active uptake mechanism. The massive decrease in the Ang II brain/plasma ratio after olmesartan supports the latter.

## 5.4 DISCUSSION

The present study confirms that renin-dependent AGA can be detected in virtually every region of the mouse brain. Yet, as compared to plasma, brain renin levels were very low, corresponding with the amount of renin in 1-25 μL blood plasma

per g brain tissue ( $\approx 0.1$ - $2.5$  % (v/v)). This volume mimics the amount of blood plasma in various brain regions determined with tritiated inulin or Evans blue dye (172, 173). Moreover, perfusing the brain with PBS prior to the collection of the various regions, reduced brain renin uniformly by  $>60\%$ . Had local renin synthesis occurred in one or more specific brain regions, the washout percentage should have been much lower in these regions, similar to the fact that in the kidney one cannot wash away stored renin (165, 174), while this does happen in non-renin producing organs like the heart (175). Furthermore, DOCA-salt, like Ang II, reduced circulating renin, and, contrary to our expectations, did not increase brain prorenin. In fact, if anything, both DOCA-salt and Ang II lowered brain renin in parallel with plasma renin. Aliskiren-inhibitable AGA was entirely absent in the brain of  $Ren1c^{-/-}$  mice, supporting the validity of our brain renin measurement. Taken together, our data do not support the presence of kidney-independent (pro)renin synthesis in the brain, nor the concept that this occurs particularly in the DOCA-salt model. In fact, brain renin levels are so low that the accumulation of renin at brain tissue sites outside the blood compartment seems unlikely. This greatly differs from other organs (e.g., the heart), where renin diffuses freely into the interstitium and/or binds to a receptor, thereby reaching tissue levels that are, on a gram basis, at least as high as the renin levels in blood plasma (on a mL basis) (175-177). Clearly, the presence of the blood-brain barrier prevents such distribution.

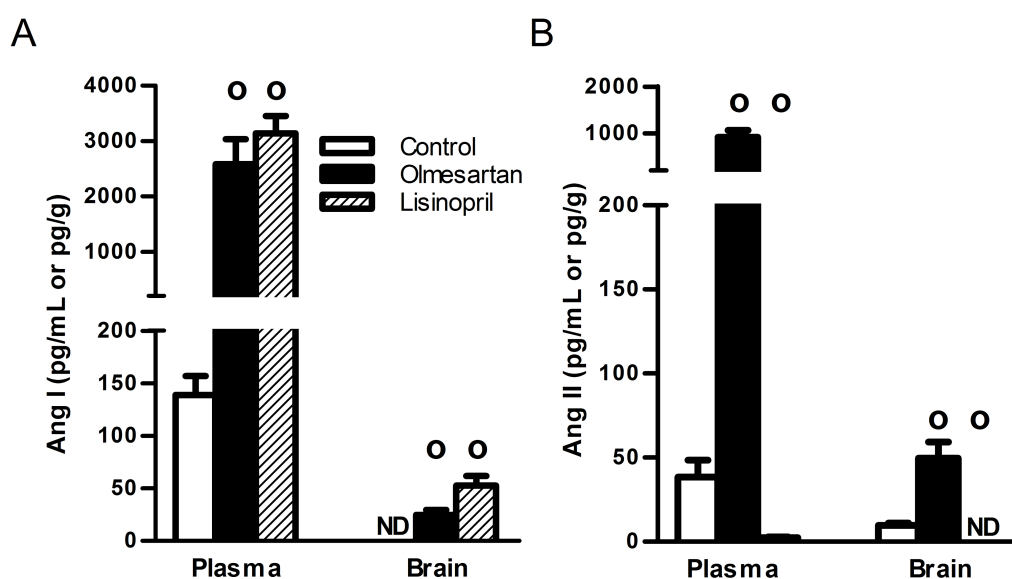


Figure 14. Ang I and II levels in plasma and brain of SHR treated with vehicle (control), olmesartan or lisinopril. ND, not detectable. Data are mean $\pm$ SEM of  $n=4-6$ . Differences were assessed by one-way

ANOVA, followed by correction for multiple testing by post-hoc Bonferroni analysis.  $^{\circ}P < 0.001$  vs. control.

Prorenin activation resulted in modest AGA increases in all brain regions, and significance for this increase was only obtained by analyzing all regions together. Applying recombinant human prorenin to brain homogenates prior to the prorenin activation procedure (on the basis of acid activation (177)) confirmed that this procedure resulted in complete prorenin activation. However, small rises in aliskiren-inhibitable AGA were also observed in brain homogenates from  $Ren1c^{-/-}$  mice after their exposure to acid. Since  $Ren1c^{-/-}$  mouse brain tissue cannot contain prorenin, this implies that the brain contains a non-renin proenzyme, which is activated by acid exposure, and which is capable of cleaving Ang I from angiotensinogen in an aliskiren-inhibitable manner. A possible candidate is pro-cathepsin D. Indeed, renin inhibitors, at high micromolar concentrations, do inhibit cathepsin D (178). Our difficulty to demonstrate prorenin in the brain is reminiscent of earlier studies in organs not synthesizing prorenin themselves, like the heart (177). Obviously, blood plasma contains prorenin, and thus some prorenin should be detected in the blood-containing homogenates derived from such tissues. Yet only under conditions where circulating prorenin levels were greatly elevated, like in heart failure in humans, did we reliably detect prorenin in cardiac tissue (166). In mice, in contrast to humans, circulating prorenin levels are relatively low (versus renin), making it even more difficult to show a rise in AGA on top of already low renin-mediated AGA. A further complicating factor is that tissue homogenization per se may result in (partial) prorenin activation. In summary, given the presence of prorenin in blood plasma, brain homogenates should minimally contain the amount of prorenin present in a few  $\mu\text{L}$  of blood. The rises in AGA after prorenin activation are consistent with this view, but should still be interpreted with caution given the fact that non-renin enzymes also came into play after acid activation. Brain-selective prorenin rises, e.g. after DOCA-salt, were not observed. This implies that prorenin-(pro)renin receptor interaction is unlikely to occur in the mouse brain, particularly after DOCA-salt (which lowers brain (pro)renin), although it may obviously occur after intracerebroventricular infusion of pharmacological prorenin doses into the brain (160).

Most, if not all, studies on brain renin relied on the detection of renin mRNA in the brain, either under normal conditions, or after deleting/overexpressing sREN or icREN. Deleting sREN in neurons or glia did not affect blood pressure, heart rate, water intake, or metabolic rate (179), while preservation of icREN did not compensate for the consequences of whole body sREN-deficiency (hypotension, renal defects, lethality) (180). Surprisingly, brain-selective deletion of icREN even caused neurogenic hypertension, possibly because icREN inhibits sREN (158). These data seem to argue against icREN as an Ang I-generating enzyme. Yet, overexpressing either human icREN or sREN in astrocytes, if combined with human angiotensinogen, resulted in Ang II-dependent hypertension and an increase in drinking volume (181). Since icREN under the latter conditions was not detectable in cerebrospinal fluid (CSF), it was concluded that this phenomenon involved intracellular Ang II formation. We attempted to detect renin mRNA, using either specific assays for sREN or icREN, or a non-specific assay that detects both sREN and icREN. Under no condition were we able to show renin (secreted + intracellular), sREN or icREN gene expression in any of the different regions of the brain: the expression level was below the detection threshold of the RT-PCR assay, even with the use of the highly sensitive Taqman probes. The specificity of our renin primers was validated by making use of the kidneys of *Ren1c<sup>-/-</sup>* mice. Of course, poor renin expression in the brain has been noted before (182-184). Because of the technical limitations inherent in any RT-PCR assay, we could not load more than 100 ng of total RNA. Our results therefore indicate that, if renin is expressed in the brain, its expression is  $>2^{18}$ -fold lower than that in the kidney (no signal after 40 cycles, with renin detection in the kidney at  $C_T \approx 22$ ). The IPA expression data sets confirm this view. Yet, Kubo et al. observed a blood pressure drop after intraventricular renin antisense injection in SHR (185). In their hands only one of three tested antisense oligonucleotides acted hypotensive, and this response was accompanied by a 20% drop in renin mRNA (detected after 45 cycles of RT-PCR). These authors did not measure renin levels in brain or plasma, and were unable to rule out antisense leakage to the kidney. Therefore, these data cannot be taken as definitive proof for the existence of an independent brain RAS.

The mouse RAS differs from the human RAS, in that the circulating renin levels in mice are up to 1000-fold higher (on a ng Ang I/ml.hr basis) than in humans. As a consequence, circulating angiotensinogen levels in mice are far below  $K_m$

range, as confirmed in the present study. Nevertheless, despite these differences, mouse angiotensin levels in blood and tissue are comparable to those in humans, rats and pigs (164, 186-188). We attempted to measure angiotensinogen in the mouse brain, both at the mRNA and protein level. Although we did observe angiotensinogen mRNA expression in different regions of the brain, in full agreement with previous work (189, 190), expression was up to 500-fold lower than in the liver. Under no condition were we able to detect angiotensinogen protein in the brain. Given the detection limit of our assay (1 pmol/g), this implies that brain angiotensinogen, if present, occurs at levels (per g tissue) that are <3% of the levels in plasma (per mL plasma). Such low levels have been reported before in the rat brain, as well as in human and rat CSF (172, 191-193), and thus our data entirely agree with the literature. Clearly, mice, given their low angiotensinogen levels, are not the optimal species to study brain angiotensinogen. As astrocytes are assumed to be the source of brain angiotensinogen (194, 195), we additionally studied angiotensinogen synthesis by rat primary cortical astrocytes, but again failed to detect any angiotensinogen. Nevertheless, data from Schink et al. (193) do support the functional presence of angiotensinogen in the rat brain. These authors artificially elevated renin in the brain by either intracerebroventricular renin infusion (in Sprague-Dawley rats) or by making use of transgenic hypertensive rats overexpressing mouse Ren2. The responses to both approaches (drinking and blood pressure reduction, respectively) were greatly diminished after lowering brain angiotensinogen by brain-selective expression of an antisense RNA against angiotensinogen mRNA.

Finally, given our observation that brain renin is confined to the plasma compartment, while brain angiotensinogen is extremely low (if not also confined to the plasma compartment), an urging question is what degree local angiotensin generation truly occurs in the brain. We therefore collected brainstem tissue (i.e., the brain region with the highest renin level) from SHR under control conditions and during RAS blockade with olmesartan or lisinopril. Rats rather than mice were used here, because at identical angiotensin levels in both species, the larger rat brainstem would allow a more reliable quantification of angiotensins. Without treatment, brain Ang I was undetectable, while Ang II occurred at levels that were  $\approx 25\%$  of the levels in plasma (per gram tissue weight). This contrasts with other organs where Ang II is usually much higher than in plasma, while Ang I is easily detectable (167, 196-198).

RAS blockade induced the usual rise in Ang I levels in plasma, and now brain Ang I became detectable, however, at only 1% (v/v) of its plasma levels. It seems reasonable to assume that also in the untreated animals brain Ang I levels were in the 1% range of plasma Ang I, and therefore too low to be detected with our assays. If so, this implies that under all conditions, brain Ang I at most represented the amount of Ang I that is inherently present in brain tissue because it contains a small amount ( $\approx 1\%$ ) of blood (172). Lisinopril decreased brain Ang II to undetectable levels, while olmesartan reduced the brain/plasma Ang II ratio by  $>80\%$ . The latter finding suggests that, normally, circulating Ang II accumulates in brain tissue via binding to  $AT_1$  receptors. Such uptake occurs in multiple organs (199), and facilitates the intracellular accumulation of Ang II (200). Without receptors (i.e., in AT receptor-deficient mice), tissue Ang II levels drop dramatically (47), suggesting that tissue Ang II levels do not originate intracellularly. If Ang II binding to  $AT_1$  receptors is the only source of Ang II in the brain, one would expect angiotensin metabolites that do not (or only with low affinity) bind to this receptor to be undetectable in the brain. This is indeed what we observed for both Ang-(2-8) and Ang-(1-7). An olmesartan-induced reduction in brain Ang II levels was also observed in Dahl-sensitive hypertensive rats, albeit in the absence of an effect on blood pressure (201). Clearly therefore, the changes observed in brain Ang II are blood pressure-independent.

## 5.5 SUPPLEMENT INFORMATION

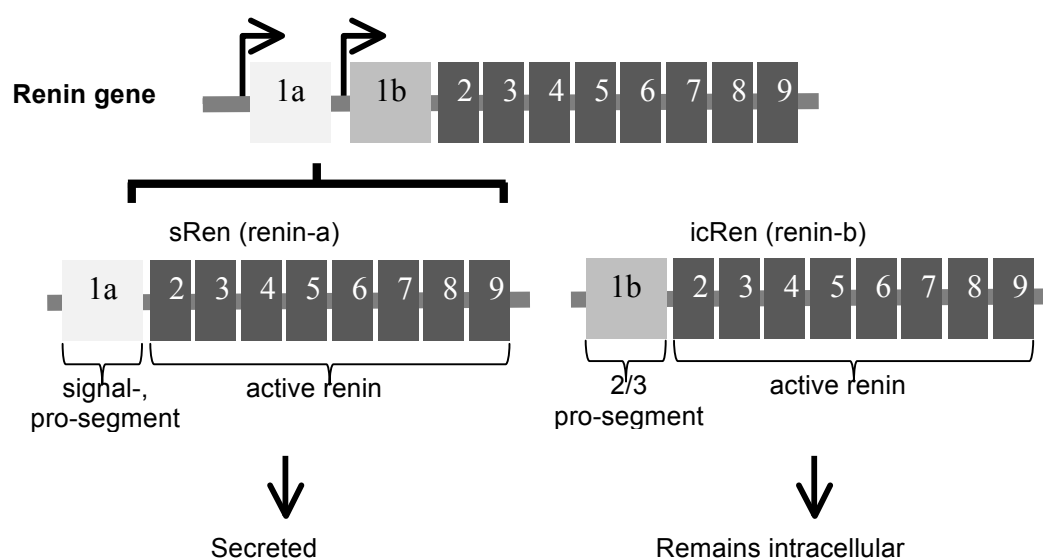


Figure S8 A. Proposed pathway for secreted renin and intracellular renin. It is hypothesized that in the brain, a different mRNA, renin-b, is transcribed that result in a novel transcript lacking exon 1a. This

renin isoform lacks the signal peptide and part of the prosegment, and is believed to remain intracellular. Adapted from Grobe et al. (155)

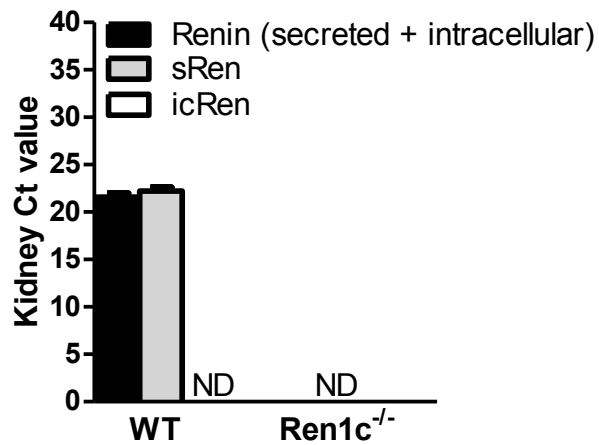


Figure S9. B. Renin (secreted or intracellular), sRen and icRen mRNA expression in kidneys of wild-type (WT, n=6) and *Ren1c*<sup>-/-</sup> mice (n=4). icRen was undetectable under all conditions, while renin (secreted + intracellular) and sRen were undetectable in kidneys of *Ren1c*<sup>-/-</sup> mice. C<sub>t</sub> values were generated with the SYBR Green assay.

Table S6 – Primer sequences and GenBank accession numbers.

<b>Kidney and Brain Tissue (Mus musculus)</b>		
<b>SYBR green assay</b>		
Beta-2 microglobulin (B2M)	CTCACACTGAATTCACCCCA GTCTCGATCCCAGTAGACGGT	>NM_009735.3
Tubulin gamma-2 chain (TubG2)	CAGACCAACCACTGCTACAT AGGGAATGAAGTTGGCCAGT	>NM_134028.2
Renin (secreted + intracellular)	AGCTACATGGAGAACGGGTC TTCCACCCACAGTCACCGAG	>NM_031192.3
Secreted renin (sRen)	GCACCTTCAGTCTCCCAACAC TCCCGGACAGAAGGCATTTTC	>NM_031192.3
Intracellular renin (icRen)	CCGGCTGCTTTGAAGATTTGAT ATGCCAATCTCGCCGTAGTA	-
Angiotensinogen (Aog)	ACCCCGAGTGGGAGAGGTTTC GCCAGGCTGCTGGACAGACG	>NM_007428.3
<b>Taqman assay</b>		
Beta-2 microglobulin (B2M)	Assay ID-Mm.PT.58.10497647 (IDT)	NM_009735(1)
Tubulin gamma-2 chain (TubG2)	Assay ID-Mm.PT.58.41559687 (IDT)	NM_134028(1)
Renin (secreted + intracellular)	FW: TCAGCAAGACTGACTCCTGGC Rev: GCACAGCCTTCTTCACATAGC Probe: TCACGATGAAGGGGGTGTCTGTGGG	
Secreted renin (sRen)	FW: GCACCTTCAGTCTCCCAACAC Rev: TCCCGGACAGAAGGCATTTTC Probe: CCTTTGAACGAATCCC	
Intracellular renin (icRen)	FW: CCGGCTGCTTTGAAGATTTGAT Rev: CAGGTAGTTGGTGAAGACCAC Probe: TCACAAAGAGGCCTTCCTTGACCA	

Table S7 – Percent inhibition of angiotensin I-generating activity by aliskiren in brain nucleus homogenates before and after buffer perfusion. Data are mean±SEM of n=5.

Brain Nucleus	Before Buffer Perfusion		After Buffer Perfusion	
	Renin	Total Renin	Renin	Total Renin
Brainstem	96±1	91±3	92±3	87±3
Thalamus	81±6	81±9	18±20	28±19
Cerebellum	86±4	92±2	73±12	54±18
Striatum	71±2	60±18	51±16	34±20
Midbrain	83±10	84±6	37±19	30±19
Hippocampus	49±6	48±22	47±15	13±13
Cortex	50±23	36±17	15±17	0±0

Table S8 – Angiotensin (Ang) metabolites in SHR plasma and brain during treatment with placebo, olmesartan or lisinopril. Data are mean±SEM of n=4-6, and if undetectable, were based on the detection limit.

Treatment	Ang I (pg/mL or g)	Ang II (pg/mL or g)	Ang-(2-8) (pg/mL or g)	Ang-(1-7) (pg/mL or g)
<b>Plasma</b>				
Placebo	139±20	39±11	8±2	<2±0
Olmesartan	2579±497	911±171	223±57	9±2
Lisinopril	3142±362	2±1	<1±0	58±14
<b>Brain</b>				
Placebo	<8±1	9±2	<9±0	<13±1
Olmesartan	25±5	50±11	<8±0	<13±1
Lisinopril	53±10	<7±1	<8±0	<13±1

## **6 DO PRORENIN-SYNTHEZING CELLS RELEASE ACTIVE, 'OPEN' PRORENIN?**

### **6.1 INTRODUCTION**

Renin belongs to the A1 family of aspartic proteases. Its 3D structure consists of two  $\beta$ -sheet domains, the N- and C-domain. Renin has an inactive precursor, prorenin, in which the catalytic binding site is covered by the N-terminal part of mature renin that, in turn, is covered by the prosegment (202). After removal of the prosegment, this N-terminal part becomes part of a six-stranded  $\beta$ -sheet on the back of the mature renin molecule, previously occupied by the prosegment. This requires a conformational change that fully exposes the active cleft (202).

Prosegment unfolding occurs in a pH- and temperature-dependent manner, and, if not followed by cleavage, results in two prorenin conformations (Figure 15): a 'closed', inactive form, and an 'open' form that displays full enzymatic activity (203, 204). In addition, an intermediate form exists where the prosegment has moved away from the cleft, but where the renin part still has to undergo the afore-mentioned conformational changes. Under physiological conditions (pH 7.4, 37°C), <2% of prorenin is in the open conformation. The renin inhibitor aliskiren binds to prorenin in the open conformation as well as to the intermediate form of prorenin (203, 204). Binding to the intermediate form induces prorenin unfolding. Due to the tight binding of the renin inhibitor, the refolding step (i.e., the return to the closed conformation) is now no longer possible, and thus, the equilibrium between the closed and open conformation will shift in favor of the open conformation. Eventually, all prorenin molecules may be open ('non-proteolytic activation'), allowing its recognition by the active site-directed antibodies used in renin immunoradiometric assays (IRMAs), despite the fact that the prosegment is still present and aliskiren is bound to the active site (171, 205).

Unexpectedly, VTP-27999, a new, active site-directed renin inhibitor with an  $IC_{50}$  (0.3 nmol/L) that is comparable to that of aliskiren, did not induce prorenin unfolding (206). Yet, it blocked the aliskiren-induced unfolding of prorenin. This suggests that VTP-27999 does bind to the intermediate form of prorenin, but that such binding has no conformational consequences. Furthermore, VTP-27999 increased

renin immunoreactivity. This may relate to the observation, based on crystallization studies, that there are 2 renin conformations (207). Aliskiren and VTP-27999 bind to both conformations, but only in the case of VTP-27999, the conformations of the two monomers are nearly identical (206). These conformational differences are likely to affect the affinity of the active site-directed antibodies applied in renin IRMAs. As a consequence, the renin IRMA yields higher levels in the presence of VTP-27999 than without this inhibitor.

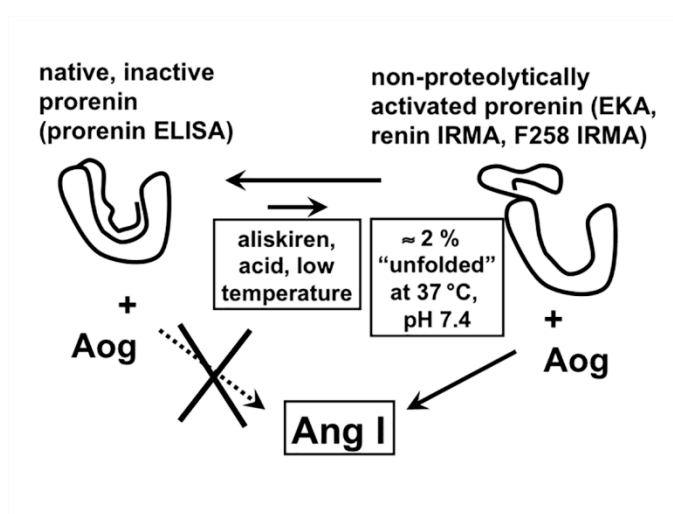


Figure 15. Model displaying the closed and open prorenin conformations, as well as the assays allowing the detection of these prorenin variants. Normally, <2% of prorenin is in the open conformation. Aliskiren, acid and low temperature shift the equilibrium to the right, allowing the detection of prorenin in a renin IRMA, on the basis of its prosegment (F258 IRMA), or by enzyme-kinetic assay (EKA). Only a direct prorenin ELISA allows the detection of intact, closed prorenin.

A long-standing question concerns the function of prorenin. As mentioned above, it displays limited activity in plasma. Nguyen et al. proposed that it binds to the so-called (pro)renin receptor at nanomolar affinity (15). This resulted in a conformational change, allowing prorenin to display full activity. Theoretically, this would result in angiotensin generation, at least in (pro)renin receptor-expressing tissues, by receptor-bound prorenin. Initially, this finding was received with great enthusiasm, since it finally provided a role for prorenin: although synthesized in only a limited number of organs, given the wide occurrence of the (pro)renin receptor, prorenin might now contribute to angiotensin generation in virtually every organ of the body. However, although in-vitro studies applying high prorenin concentrations confirmed this concept, the prorenin concentrations in vivo are many orders below its  $K_d$  for the (pro)renin receptor, thereby making this possibility unlikely (161, 208). As a

consequence, this concept is now being abandoned, and we need alternative hypotheses to explain the function (if any) of prorenin. One possibility is that prorenin acts exclusively at its site of synthesis. For this to occur, prorenin-synthesizing cells should release prorenin in an open conformation, allowing it to display local activity in the immediate vicinity of the cells, before it returns to its inactive, closed conformation, e.g., when reaching blood plasma. If true, renin inhibitors capable of interfering with open prorenin might have an advantage over other RAS blockers, since they can specifically suppress angiotensin generation in prorenin-synthesizing tissues. Possibly, novel inhibitors need to be developed to optimally exert this effect.

To test this concept in the present study, we made use of human prorenin-synthesizing cells. For comparison, renin-releasing cells were also evaluated. We used 3 approaches. First, we incubated the cells with VTP-27999. This inhibitor, like aliskiren, would bind to prorenin if it is released in an open conformation, thus preventing its return to the closed conformation, allowing its detection in a renin IRMA. VTP-27999, unlike aliskiren, would not additionally convert all closed prorenin molecules into the open conformation, and thus this renin inhibitor is ideal to quantify the percentage of prorenin molecules released in the open conformation. We applied renin-, prorenin-, and prosegment-specific assays (available for human (pro)renin only) to verify this concept. Second, we studied angiotensin I generation during prorenin release by adding angiotensinogen to the medium, the underlying assumption being that only open prorenin would be able to display enzymatic activity. Finally, we verified to what degree prorenin in human plasma displays angiotensin I-generating activity.

## 6.2 METHODS

### 6.2.1 Human Samples

All studies were approved by the Medical Ethical Review Board, and performed in accordance with the Declaration of Helsinki and Good Clinical Practice. Informed consent was obtained from each subject. Blood samples were obtained from 6 healthy controls (4 men, 2 women; age 23-45 years, mean 31 years). Blood was collected in polystyrene tubes containing 6.25 mmol/L EDTA (final concentration). The samples were centrifuged at room temperature at 3000 g for 10

minutes, and plasma was either used immediately or stored at -20°C. Placenta's were harvested from 7 women after delivery (age 26-41, mean 34 years). Renin- and prorenin-synthesizing human mast cells (HMC-1) were a gift from Dr. J.H. Butterfield (Mayo Clinic, Rochester, MN, USA) (131).

### 6.2.2 Cell Culture Studies

Cell culture studies were performed at 37°C in a humidified 5% CO<sub>2</sub> incubator (Sanyo, Panasonic Biomedical Sales Europe B.V., Etten-Leur, The Netherlands).

HMC-1 cells were cultured in 75 cm<sup>2</sup> culture flasks using Iscove's modified Dulbecco's medium (Lonza, Verviers, Belgium), supplemented with 10%, iron-supplemented bovine calf serum (Hyclone, Thermo Fisher Scientific, Breda, The Netherlands), 1% Penicillin Streptomycin (PS; Invitrogen, Bleiswijk, The Netherlands) and 1.2 mmol/L  $\alpha$ -thio-glycerol (Sigma, Zwijndrecht, The Netherlands).

HEK293 cells were transfected with the mammalian expression vector pRhR1100, containing human prorenin (209), a gift from Dr. Reudelhuber (IRCM, Montréal, Canada). In short, cells were transfected with Lipofectamine2000 (Invitrogen), according to the manufacturers protocol, and put on selection using 0.6 mg/mL G418 (Invitrogen). The clone with the highest expression of prorenin was isolated, and used for further experiments. Cells were cultured in DMEM-F12 (GIBCO, Breda, The Netherlands) medium supplemented with 10% fetal calf serum (FCS; Lonza), 1% PS, and 0.6 mg/mL G418.

Decidua cells were harvested from the maternal side of the placenta according to Markoff et al. (210). In short, tissue was chopped and washed twice with DPBS (GIBCO), alternated by centrifugation steps of 10 minutes at 700 rpm. The pellet was resuspended in 5 mL RPMI-1640 (GIBCO) per gram tissue, supplemented with 1% FCS, 0.1% collagenase and 0.1% hyaluronidase (Sigma) in a tissue culture flask, and put on an orbital shaker (150 rpm) for two hours at 37°C. This suspension was filtered using a sieve with a mesh of 40  $\mu$ m. The filtered solution was centrifuged for 10 minutes at 700 rpm, after which the pellet was washed with RPMI-1640, and centrifuged again. The pellet was then exposed to 20 mL RBC lysis solution (5PRIME, Hilden, Germany) for 10 minutes, followed by another 10 minutes of centrifugation. This was followed by another two wash steps with RPMI. Next, cells were cultured in RPMI-1640 containing 10% FCS, 12.5 mmol/L HEPES (GIBCO), 50

$\mu\text{g/mL}$  gentamycin (Sigma) and  $5 \mu\text{g/mL}$  fungizone (Sigma). Medium was changed every 24 hours in the first 72 hours.

For experiments verifying the release of open prorenin, cells were seeded in 6- or 12-well plates at a concentration of  $0.5 \times 10^6$  cells/mL in fresh medium in the presence or absence of VTP-27999 (0.1-1000 nmol/L). After 2 to 5 days, medium was collected, and spun down 5 minutes at 2500 rpm to remove remaining cells. Supernatant was stored at  $-20^\circ\text{C}$ .

To study prorenin-induced angiotensin generation, decidua cells were incubated for 24 hours in the presence of 150 nmol/L human angiotensinogen (Sigma). Cells incubated without angiotensinogen served as control. Medium samples ( $75 \mu\text{L}$ ) for the determination of renin and prorenin were collected at 4, 8 and 24 hr. Medium samples ( $500 \mu\text{L}$ ) for the determination of angiotensin I were collected at 24 hours with  $25 \mu\text{L}$  inhibitor stock solution (containing 0.1 mmol/L aliskiren, 200 mmol/L EDTA and 0.2 mmol/L lisinopril), frozen in liquid  $\text{N}_2$ , and stored at  $-70^\circ\text{C}$ . The first-order rate constant for angiotensin I elimination was determined by incubating the cells with 100 nmol/L angiotensin I for maximally 4 hrs in the presence or absence of 100 nmol/L captopril. Medium samples ( $50 \mu\text{L}$ ) for the determination of angiotensin I were collected at 0, 0.5, 1 and 4 hr, mixed with  $2.5 \mu\text{L}$  inhibitor stock solution, and stored as described above.

### 6.2.3 Biochemical Assays

Renin and prorenin were determined either indirectly, by enzyme-kinetic assay (i.e., quantifying angiotensin I-generating activity) or directly, by IRMA (i.e., quantifying renin or prorenin immunoreactively).

Enzyme-kinetic assays were applied to human plasma samples only, to verify prorenin activity. The sample was incubated with excess sheep angiotensinogen in the presence of angiotensinase inhibitors, either directly after its removal from the patient, after freezing and thawing, or after keeping it for 18 hours at  $37^\circ\text{C}$ . Imidazole buffer (final concentration 0.1 mol/L) was added to the incubation mixture to keep pH at 7.4.

Immunoreactive renin was measured with the Renin III (Cisbio, France) IRMA. This assay, which makes use of a monoclonal antibody (4G1) (211) directed against renin's active site, also recognizes intact, open prorenin (203, 212). This implies that intact prorenin can be measured with this assay after incubating it with acid (pH=3.3) or after exposing it for 48 hours at 4°C to 10 µmol/L aliskiren, since both procedures induce the conversion of all prorenin molecules into the open conformation (171).

Intact, closed prorenin was measured with an enzyme-linked immunosorbent assay (ELISA) that recognizes residues 32-39 of the prosegment (Molecular Innovations, Novi, MI, USA) (204). This prorenin assay was performed according to the instructions of the manufacturer, making use of human recombinant prorenin to construct the standard curve.

In a select set of samples, intact, open prorenin was measured on the basis of its prosegment, replacing the <sup>125</sup>I-labeled active site-directed monoclonal antibody of the Cisbio kit by a prosegment-directed <sup>125</sup>I-labeled monoclonal antibody (F258-37-B1) in the IRMA ('F258 IRMA'). F258-37-B1 is directed against the C-terminal part (p20-p43) of the propeptide and does not react (<0.1%) with renin. F258-37-B1 also does not react (<0.1%) with intact, closed prorenin (13). However, it does react with prorenin after the converting all prorenin molecules into the open conformation by incubation with acid. Thus, the acid-induced non-proteolytic conformational change, causing the propeptide to move to the surface of the molecule, allows the recognition of prorenin by both the active site-directed antibody of the Cisbio kit, and the prosegment-directed antibody of the prorenin IRMA.

The levels of Angiotensin I and II in the medium were measured by radioimmunoassay after SepPak extraction and reversed-phase high performance liquid chromatography separation (188).

#### **6.2.4 Data Analysis**

Results are shown as mean±SEM. Differences were tested using one-way ANOVA, followed by Dunnett's multiple comparison test; P<0.05 was considered significant. Angiotensin I-generating activities obtained in the enzyme-kinetic assay were converted to renin concentrations based on the fact that 1 ng of angiotensin I per milliliter per hour corresponds with 2.6 pg of human renin per milliliter (213).

## 6.3 RESULTS

### 6.3.1 Plasma Prorenin Displays Enzymatic Activity

When incubating freshly obtained plasma samples from 6 healthy controls with excess angiotensinogen at 37°C, angiotensin I generation was linear over time (Figure 16, left panel). Results obtained in the same samples after they had been frozen and thawed were identical. However, when performing the assay after the samples had been kept for 18 hours at 37°C (to inactivate open prorenin) the degree of angiotensin I generation was lower ( $P < 0.05$ ). This was not due to (pro)renin degradation, since total renin levels (determined by immunoreactive assay) did not change over the 18 hour-period (Figure 16, right panel). The average decrease in angiotensin I-generating activity after 18 hours ( $\approx 1$  ng angiotensin I/mL.hr) corresponded with  $\approx 3\%$  of the immunoreactive prorenin levels. This confirms that both blood handling/centrifugation (at room temperature) and freezing/thawing induce a conformational change in prorenin, allowing a small percentage of the prorenin molecules to display enzymatic activity in the enzyme-kinetic assay. Prolonged incubation at 37°C reversed this phenomenon.

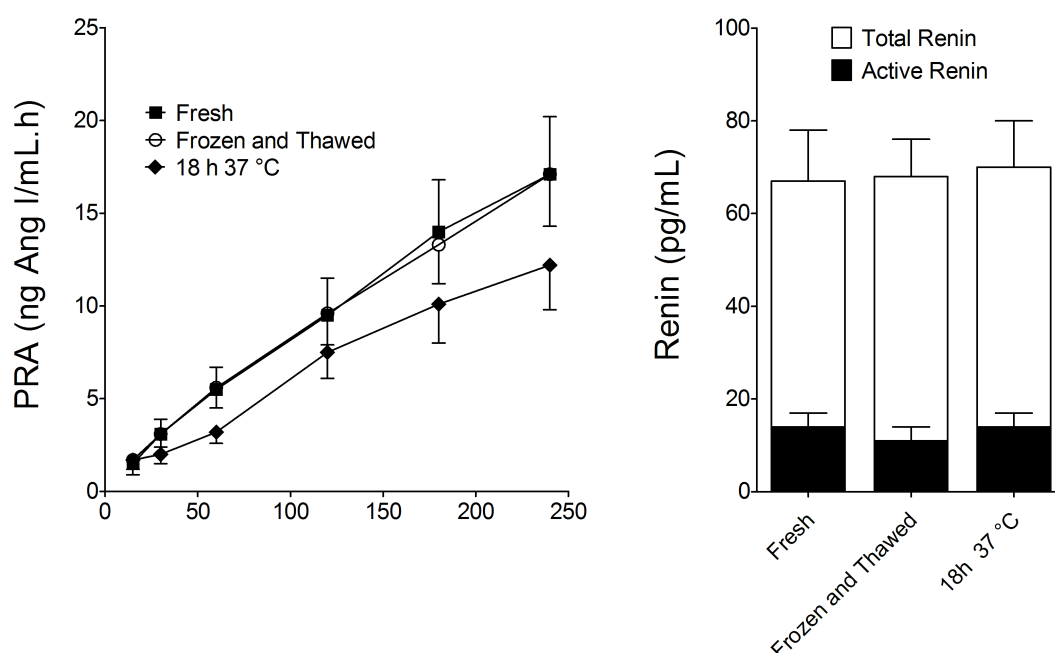


Figure 16. Left, angiotensin I generation in human plasma during its incubation with excess sheep angiotensinogen, either immediately after collecting the plasma samples (fresh), after keeping the samples for 18 hours at 37°C, or after freezing and thawing the samples. Right, renin and total renin levels measured by renin IRMA after 4 hours of incubation. Data are mean±SEM of n=6.

### 6.3.2 VTP-27999 Increases Renin Immunoreactivity, but does not Unravel the Release of ‘Open’ Prorenin

Open prorenin release was studied in cells that synthesize both renin and prorenin (HMC-1 cells) and in cells that exclusively synthesize prorenin (human prorenin-expressing HEK293 cells and decidua cells).

In medium samples obtained from HMC-1 cells incubated without inhibitor, renin was measured by renin IRMA, both before and after activating prorenin with aliskiren (i.e., converting all closed prorenin molecules to open prorenin molecules). Aliskiren exposure increased renin immunoreactivity ≈3-fold (Figure 17, left panel; n=7), illustrating that the cells predominantly released prorenin. Total renin measurements after aliskiren exposure did not change significantly following incubation of the cells with increasing concentrations of VTP-27999, nor did prorenin immunoreactivity (determined by prorenin ELISA) change in the presence of this inhibitor. This implies that VTP-27999 did not affect (pro)renin release per se. Yet, renin immunoreactivity (expressed as a % of the total renin levels without VTP-27999) almost tripled following incubation of the cells with VTP-27999 (Figure 17 left

panel; n=6). Given the absence of changes in the release of (pro)renin, these data suggest that VTP-27999 affects the renin assay itself (i.e., yields higher renin levels for a given amount of renin).

Aliskiren increased renin immunoreactivity in the medium of control (i.e., incubated without inhibitor) HEK293 and decidua cells >10-fold (Figure 17, middle and right panels; n=5). This is in agreement with the fact that these cells exclusively release prorenin, and that, at pH=7.4 and 37°C, only a few percent of prorenin is in the open conformation (i.e., can be recognized in a renin IRMA). Total renin measurements after aliskiren exposure did not change following incubation of the cells with increasing concentrations of VTP-27999, nor did prorenin immunoreactivity change in the presence of this inhibitor. Thus, as in HMC-1 cells, VTP-27999 did not affect prorenin release in either HEK293 cells or decidua cells. Yet, VTP-27999 doubled renin immunoreactivity in both cell types.

The latter increase in renin immunoreactivity might be suggestive for the release of open prorenin. To verify this further, we first repeated the studies in (pro)renin-containing medium (obtained from control cells) incubated with VTP-27999 in the absence of cells. Results were identical (Figure 18; n=5-7). Second, we exposed (pro)renin-containing medium of the 3 cell types to acid, to induce the open (renin-like) conformation in all prorenin molecules. Under this condition, the prosegment is still present, but folded away from the active site (allowing prorenin detection both by renin - and prosegment IRMA). Next, pH was returned to pH=7.4 in the absence or presence of either 10  $\mu\text{mol/L}$  aliskiren or VTP-27999. Without renin inhibitor, prorenin will rapidly return to its closed conformation, no longer allowing its detection by renin - or prosegment IRMA. But with renin inhibitor, prorenin will be trapped in its open conformation, allowing its detection in both IRMAs.

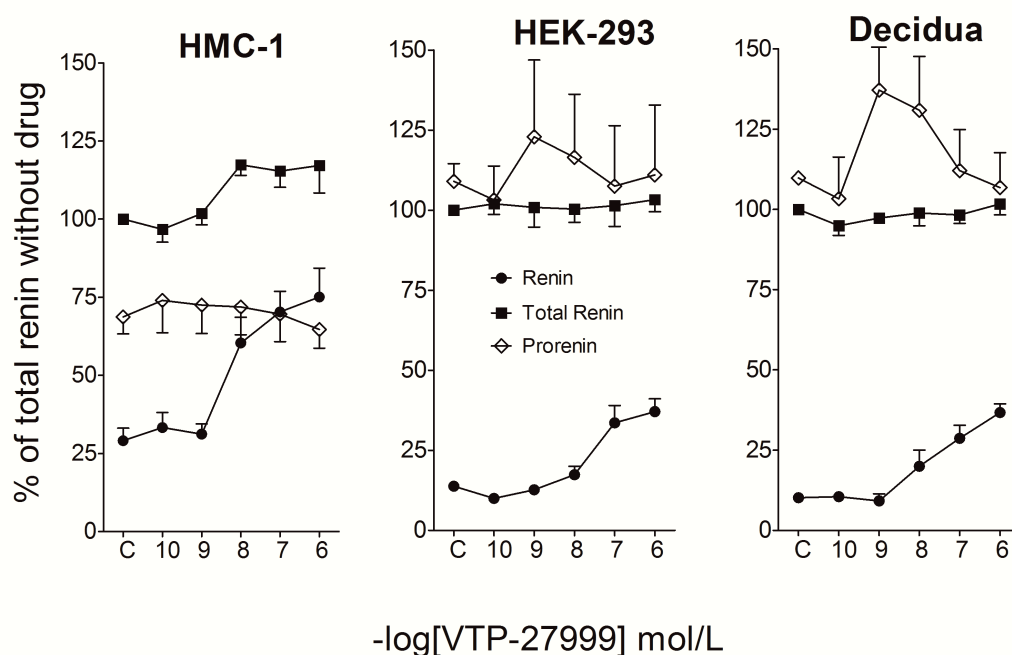


Figure 17. Renin, total renin (measured following after aliskiren pretreatment) and prorenin in the medium of renin+prorenin-secreting HMC-1 cells or exclusively prorenin-secreting HEK293 and decidua cells, cultured in the presence of increasing concentrations VTP-27999. Renin and total renin were measured by renin IRMA, prorenin was measured by direct prorenin ELISA. Data are mean $\pm$ SEM of n=5-7, and have been expressed as a percentage of the total renin levels without VTP-27999.

Results show that both renin inhibitors greatly increased renin and prosegment immunoreactivity (Figure 19, n=3 for all conditions), confirming their capacity to trap prorenin in its open conformation. Importantly, the increases in renin immunoreactivity after VTP-27999 were  $\approx 20$ -fold, i.e. double those seen after aliskiren. In contrast, the increases in prosegment immunoreactivity were identical for both inhibitors. This implies that VTP-27999 increases renin immunoreactivity, but not prosegment immunoreactivity.

Taken together, these data show that incubation of all 3 cell types with VTP-27999 yields higher renin immunoreactivity levels in the medium. Yet, this is due to the fact that VTP-27999, for a given amount of renin or open prorenin, increases renin immunoreactivity in the renin IRMA 2-3 fold. It is not due to the release of open prorenin, since a) results were identical in the absence of cells, and b) renin immunoreactivity rises in the medium of prorenin-releasing cells were far below the 20-fold that would have been expected had all prorenin been released in the open conformation.

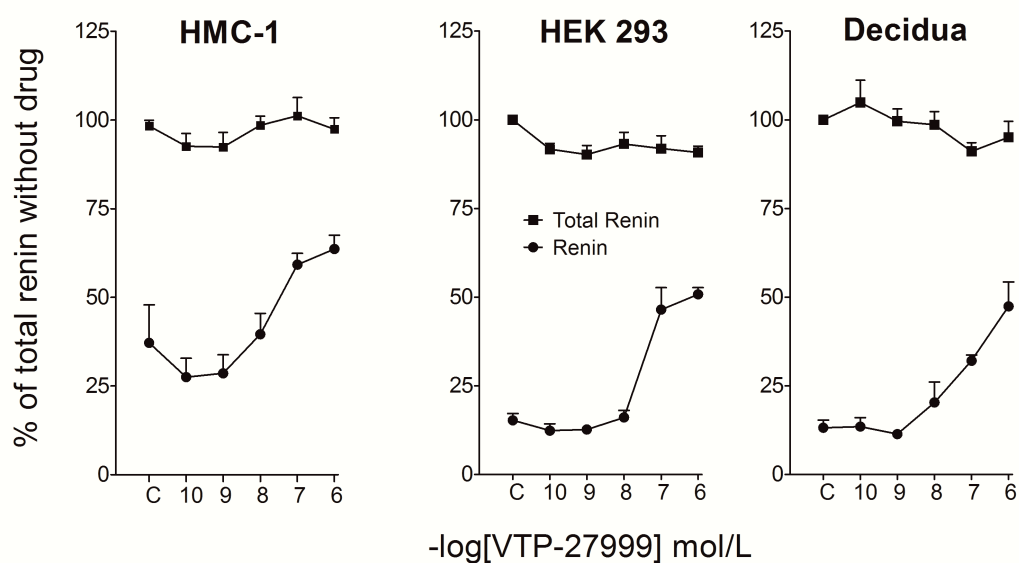


Figure 18. Renin and total renin (measured following after aliskiren pretreatment) in medium obtained from renin+prorenin-secreting HMC-1 cells or exclusively prorenin-secreting HEK293 and decidua cells, incubated without cells in the presence of increasing concentrations VTP-27999. Renin and total renin were measured by renin IRMA. Data are mean $\pm$ SEM of n=5-7, and have been expressed as a percentage of the total renin levels without VTP-27999.

### 6.3.3 Angiotensin Generation in Decidua Cells

The medium prorenin levels of decidua cells continuously rose during a 24 hour-incubation (Figure 20, left panel; n=3-7). Angiotensin I, when added to these cells, disappeared with a half life ( $t_{1/2}$ ) of  $0.45\pm 0.04$  hr (n=7). In the presence of captopril, the angiotensin I half life increased to  $1.41\pm 0.13$  hr ( $P<0.01$ ), implying that  $66\pm 4\%$  of the angiotensin I metabolism was due to conversion by ACE (Figure 21, left panel). Importantly, the angiotensin I disappearance was identical when repeating these studies in (serum-containing) medium in the absence of cells (n=5), suggesting that the majority of the angiotensin I metabolism involved serum-derived ACE (Figure 21, right panel). In other words, we found no evidence for the presence of decidual ACE. Consequently, when investigating angiotensin generation after adding angiotensinogen, we only focused on angiotensin I, and not angiotensin II. Angiotensin I levels in the medium at 24 hours after adding angiotensinogen were 4-5 times higher than the (background) levels measured in the absence of angiotensinogen (Figure 20, right panel; n=7). Normally, 2.6 pg/mL renin corresponds with 1 ng angiotensin I/ml.hr ( $v_{max}$ ), at least when activity is determined at angiotensinogen levels above  $K_m$  ( $=1200$  nmol/L). However, our experiments were

performed at angiotensinogen levels 8 times below  $K_m$  (150 nmol/L). This implies that angiotensin I generation in our experimental set-up occurred at a rate  $v$  corresponding with  $v = 150/(150+1200) \times v_{max}$ . Given the angiotensin I half life of 0.45 hr, the expected steady-state level of angiotensin I level can be calculated as  $v \times t_{1/2}/\ln 2$ . Had all prorenin detected at 24 hours been active, this steady-state angiotensin I level would have been  $12109 \pm 4488$  fmol/mL. In reality, the steady-state angiotensin I levels at that time point amounted to only  $1.3 \pm 0.7\%$  of this level. This suggests that  $\approx 1\%$  of prorenin displayed enzymatic activity under our experimental conditions. This is comparable to the percentage of ‘active’ prorenin in human plasma, and thus opposes the concept that prorenin-synthesizing cells release open prorenin.

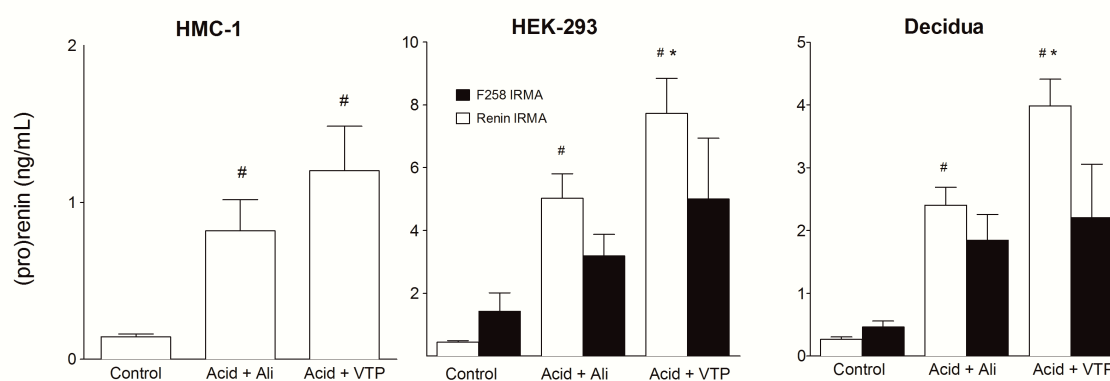


Figure 19. (Pro)renin immunoreactivity, measured by renin IRMA (open bars) or prosegment (F258) IRMA (closed bars) in the acid-pretreated medium of HMC-1 cells, HEK293 cells or decidua cells, followed by a 1-hour incubation with buffer (control), 10  $\mu$ mol/L aliskiren (acid+ali), or 10  $\mu$ mol/L VTP-27999 (acid+VTP). #  $P < 0.05$  vs. control. \* $P < 0.05$  vs. aliskiren. Data are mean  $\pm$  SEM of  $n=3$ .

## 6.4 DISCUSSION

The current study, making use of human prorenin-releasing cells, does not provide evidence for the concept that such release occurs in an ‘open’ conformation, subsequently allowing prorenin to display (full) activity at the site of its release. Theoretically, given the low pH conditions under which (pro)renin synthesis/release occurs(214), this might have happened, given that a low pH shifts the equilibrium between the open and closed conformation of prorenin into the direction of the former. Our data in acid-pretreated medium samples (containing 100% open prorenin (215)) confirm that the renin inhibitor VTP-27999 would have kept prorenin in this

open conformation, allowing its detection in a renin assay, or an assay detecting the prosegment.

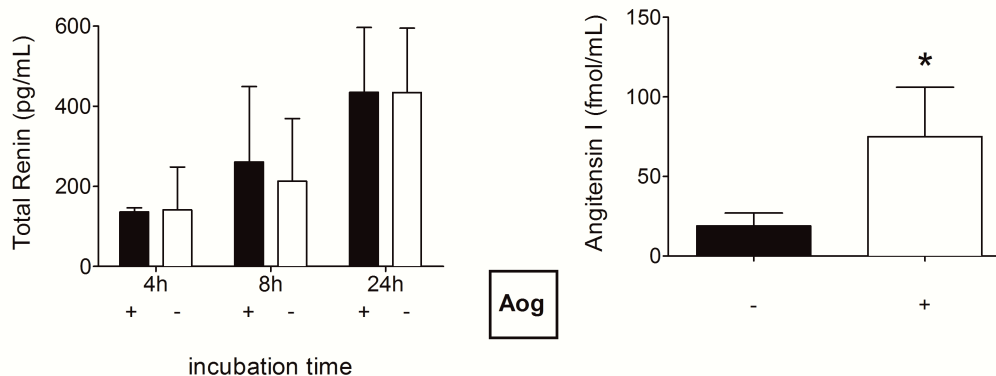


Figure 20. Left, total renin levels in the medium of human decidua cells after 4, 8 and 24 hours (mean $\pm$ SEM of n=3-7) in the absence (open bars) or presence (closed bars) of 150 nmol/L human angiotensinogen. Levels were measured by renin IRMA after prorenin activation with aliskiren. Right, angiotensin I levels in the medium of human decidua cells after 24 hours (mean $\pm$ SEM of n=7) in the absence (open bars) or presence (closed bars) of 150 nmol/L human angiotensinogen.

The renin inhibitor aliskiren would have done the same. However, this inhibitor, unlike VTP-27999, also affects the equilibrium between the open and closed conformation by inducing a conformational change in prorenin (171). Therefore, aliskiren, if applied at sufficiently high concentrations, would have converted all closed prorenin molecules into the open conformation. This would have resulted in an overestimation of the number of open prorenin molecules, and thus aliskiren cannot be used to quantify the release of open prorenin.

When applying VTP-27999 to cells that release renin (HMC-1 cells), we observed that this inhibitor increased renin immunoreactivity 2-3-fold. This has been observed before in human plasma (206), and is related to the existence of 2 renin conformations (207), and the different affinity of the active site-directed antibody for these 2 conformations. The immunoreactivity increase also occurred when applying VTP-27999 to acid-activated prorenin, i.e., prorenin that has the open conformation. This confirms that the 3D structure of open prorenin resembles that of renin, despite the fact that the prosegment is still present (203). Since VTP-27999 did not affect the outcome of the prosegment assay (F258 IRMA), it can be concluded that the binding of VTP-2799 to renin's active site selectively affected the affinity of the active site-directed antibody.

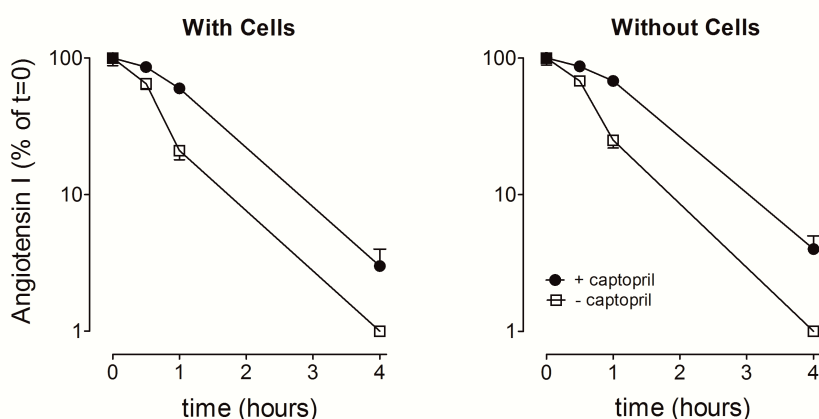


Figure 21. Left, angiotensin I levels in the medium of human decidua cells in the presence (closed circles) or absence of 100 nmol/L captopril (open squares) after adding 100 nmol/L angiotensin I at  $t=0$ . Right, angiotensin I levels in medium alone (i.e., without cells), in the presence or absence of 100 nmol/L captopril after adding 100 nmol/L angiotensin I at  $t=0$ . Data are mean $\pm$ SEM of  $n=5-7$ , and have been expressed of the levels of angiotensin I at  $t=0$ .

Under physiological conditions, only a small percentage of prorenin is in the open conformation (203). This was also the case in the medium of our HEK293 and decidua cells (i.e., cells that exclusively released prorenin). Therefore VTP-27999 should have minimally bound to this percentage of the prorenin molecules, and, given its effect on the affinity of the active site-directed antibody, it might subsequently marginally have increased renin immunoreactivity in the renin IRMA. This is indeed what happened: no substantial rises in renin immunoreactivity were observed after VTP-27999, although a >20-fold rise would have been feasible (Figure 19) in case all prorenin molecules would have been released in an open conformation. Moreover, the rises observed in prorenin-containing medium incubated with VTP-27999 in the absence of cells were identical to those observed with cells. These data therefore strongly argue against the release of open prorenin.

In addition, our angiotensin measurements after applying human angiotensinogen to the medium of human decidua cells also do not support the release of open, active prorenin. At most, the generated levels of angiotensin I in the medium of these cells support the idea that  $\approx 1\%$  of prorenin displayed activity, i.e., is in the open conformation. Such low percentages are in the range occurring in human blood plasma, and simply represent the open/closed equilibrium at  $\text{pH}=7.4$  and  $37^\circ\text{C}$ , i.e., our cell culture conditions (10, 215, 216). Lowering temperature will increase this percentage, as confirmed by our measurements in human plasma, and only keeping the samples for a prolonged time at  $37^\circ\text{C}$  allowed prorenin to refold into its closed,

inactive conformation. Clearly, depending on the assay conditions, prorenin may be detected as renin, and given its much higher levels than those of renin, this should be taken into account when quantifying renin in patients with low renin levels (217). Decidua cells neither released angiotensinogen themselves, nor generated ACE. Yet, these components are present in the 10% FCS added to the medium (218), and obviously this should be corrected for when studying angiotensin generation by decidua cells.

In summary, the function of prorenin, if any, remains elusive. The discovery of the (pro)renin receptor (15) caused a lot of excitement, but recent studies have revealed that its in-vivo function in reality is largely, if not entirely, prorenin-independent (219-221). All studies investigating prorenin binding to this receptor applied highly non-physiological concentrations, which have no relevance in vivo (161, 222). Our current studies do not reveal evidence for the release of open, active prorenin by prorenin-synthesizing cells. This argues against prorenin activity at the site of its release, at least when applying cell culture conditions, but does not exclude that there are sites where prorenin may display activity. At such sites, either a prorenin-activating enzyme should be present, or conditions favouring prorenin unfolding, e.g. a low pH or a novel, high-affinity prorenin-binding receptor. Finally, to minimize the contribution of prorenin in renin assays, samples should not be exposed to low temperatures and preferably be incubated immediately. However, since this is not feasible in daily clinical practice, the best is to centrifuge them at room temperature (i.e., not at 4°C), to freeze and thaw the samples only once, and to incubate them as long as possible at 37°C in the assay.

## **7 RENIN AND PRORENIN UPTAKE BY HUMAN PROXIMAL TUBULE CELLS: ROLE OF MEGALIN**

### **7.1 INTRODUCTION**

The kidney is a major player in the maintenance of the body fluid-electrolyte homeostasis. This is achieved by complex mechanisms, in which 3 major processes occur: glomerular filtration, tubular secretion, and tubular reabsorption (223). Kidney proximal tubular epithelial cells (PTEC) are responsible for 60-70% of the reabsorption of water, NaCl, NaHCO<sub>3</sub>, and for the majority of the reabsorption of nutrients in the glomerular ultrafiltrate (224). Fluid and electrolyte reabsorption by the proximal tubule (PT) is the result of transcellular and paracellular fluxes, with the participation of both active transport and passive paracellular electrochemical diffusion (225). The uptake of proteins filtered by the glomerulus in the PT largely relies on the endocytic receptors megalin and cubilin (226). For instance, albumin as well as the renin-angiotensin system (RAS) components renin and angiotensinogen are reabsorbed in the PT by endocytotic uptake in a megalin-dependent manner (46).

Megalyn is a large glycosylated receptor of 600 kDa that belongs to the low-density lipoprotein receptor family, encoded by the LRP2 gene. More than 40 ligands have been identified that bind to megalin by its large extracellular domain. It works in concert with cubilin, a 460-kDa glycosylated extracellular protein, forming a multireceptor complex with the bound ligands, driving their internalization and subsequent endocytosis (226-228). Both megalin and cubilin are abundantly coexpressed in the PT apical (brush-border) membrane, and the physiological and pathological roles of these multiligand receptors have been detected in animal models and human allelic syndromes (227). For instance, the loss-of-function mutations in either the CLCN5 gene, responsible for Dent-1 disease, or the OCRL gene, responsible for Dent-2 disease and Lowe syndrome, lead to dysfunctional receptor-mediated endocytosis and lysosomal function, in which the expression or trafficking of receptors (including megalin and cubilin) is impaired (229). This results in low-molecular weight (LMW) proteinuria, hypercalciuria with nephrolithiasis, nephrocalcinosis, and other variable proximal tubular defects (229). Interestingly, in patients with Dent or Lowe syndrome, both renin and angiotensinogen rise 20-40 fold

in urine, supporting impaired reabsorption (230). Moreover, in such patients prorenin becomes detectable in urine, while normally this precursor of renin is entirely undetectable in urine, even in patients with elevated plasma prorenin levels, like diabetics, or in transgenic animals with prorenin levels that are >1000-fold above normal (230).

To investigate megalin-mediated renin and prorenin reabsorption in further detail, we used human conditionally immortalized proximal tubules cells (ciPTEC), a cell line that is highly suitable to study the effect of ligands on PTEC function, since, unlike other cell lines, it expresses multiple influx and efflux transporters, in addition to the whole endocytosis machinery (231, 232). Cells were incubated with recombinant human renin or prorenin at 37°C (allowing binding and internalization) or 4°C (allowing binding only), in the presence or absence of the megalin inhibitor recombinant receptor-associated protein bound to glutathione-S-transferase (RAP-GST). Because renin and prorenin are also known to be internalized via mannose 6-phosphate (M6P) receptors, binding and uptake were additionally studied in the presence of the M6P receptor antagonist M6P. Finally, we evaluated to what degree M6P interferes with megalin-mediated processes, making use of the fact that ciPTEC internalize bovine serum albumin (BSA) exclusively via megalin (231).

## 7.2 METHODS

### 7.2.1 Cell Culture

The ciPTEC line was derived from a healthy donor (231). Cells were cultured in phenolred-free DMEM/F12 (Invitrogen, Breda, the Netherlands) supplemented with 10% (v/v) FCS (MP Biomedicals, Uden, The Netherlands), containing insulin (5 µg/mL), transferrin (5 µg/mL), selenium (5 ng/mL), hydrocortisone (36 ng/mL), epithelial growth factor (10 ng/mL), and tri-iodothyronine (40 pg/mL). The cells were seeded at a density of 55000 cells per cm<sup>2</sup> in 96- or 24-wells plates (Costar, Corning, New York, USA). They were cultured for 24 hours at 33°C and matured for 7 days at 37°C, in 5% CO<sub>2</sub>.

### 7.2.2 Prorenin and Renin Binding Uptake

To study prorenin and renin binding and internalization by ciPTECs, cells were incubated at 4°C or 37°C with 1000 U/L recombinant human prorenin and renin (a gift from Actelion Pharmaceuticals, Alschwill, Switzerland) diluted in phosphate buffer. Incubations lasted up to 24 hours, and were performed in 24-well plates in the absence or presence of M6P (10 mmol/L) and/or recombinant RAP-GST (100 µg/L). After incubation, the medium was removed, and the cells were washed three times with ice-cold Hank's Balanced Salt Solution (HBSS). Then, the cells were lysed with ice-cold 0.2% triton X-100, and centrifuged for 15 minutes at 4°C at 14000 rpm. Supernatants were collected and stored at -20°C. Immunoreactive renin in the supernatants was measured with the Renin III (Cisbio, Gif-sur-Yvette, France) immunoradiometric assay. Prorenin was also measured with this assay, after its conversion to the renin conformation (allowing its detection in the assay) by incubating it with aliskiren (233, 234). Prorenin measurements were performed both before and after aliskiren incubation, with levels being detected before aliskiren exposure representing prorenin that had been activated by the cells, and levels after aliskiren exposure representing the total amount of prorenin.

### 7.2.3 Albumin Uptake

To study whether M6P interferes with megalin-mediated uptake, cells were incubated in a 96-well plate setup at 37°C with 10 µg/mL fluorescently labelled BSA (BSA Alexa Fluor™ conjugate, Invitrogen, Carlsbad, USA), in the absence or presence of M6P (1 µmol-10 mmol/L) or RAP-GST 1.5-200 µg/mL) for 4 hours (231). During the last 10 minutes, the Hoechst33342 stain (Life Technologies, Carlsbad, USA) was added to dye the nucleus. Then, the medium was removed, and the wells were washed with HBSS at room temperature. Florescence readings were performed using a CV7000S high-content imager (Yokogawa, Tokyo, Japan).

#### 7.2.4 Data Analysis

Results are shown as mean $\pm$ SEM. Differences were tested using two-way ANOVA, followed by Bonferroni multiple comparison test.  $P < 0.05$  was considered significant. Data below detection limit were assumed to equal the detection limit.

### 7.3 RESULTS

#### 7.3.1 Prorenin and Renin Binding Uptake

Incubating ciPTEC with either prorenin (Figure 22) or renin (Figure 23) at 37°C resulted in a time-dependent increase in their cellular levels, a plateau being reached after 6-8 hours. The majority of cellular prorenin (up to 90%) was recognized as renin, suggestive for prorenin activation upon binding and/or internalization. In contrast, following incubation at 4°C, the majority of prorenin was in its inactive form, and the steady-state levels of both renin and prorenin were  $\approx$ 5-10-fold lower than those at 37°C (Figures 1 and 2). At 37°C, M6P reduced cellular prorenin ( $P < 0.05$ ) and renin ( $P < 0.01$ ) accumulation by  $>80\%$ , without altering the degree of prorenin activation. At 4°C, the blocking effect of M6P was much more modest, significance being reached in the case of renin only ( $P < 0.05$ ).

At 37°C, RAP-GST reduced cellular prorenin and renin accumulation after 8 hours by  $>80\%$ , both in the absence and presence of M6P (Figure 24). At 4°C, its blocking effects were more modest, particularly in the presence of M6P.

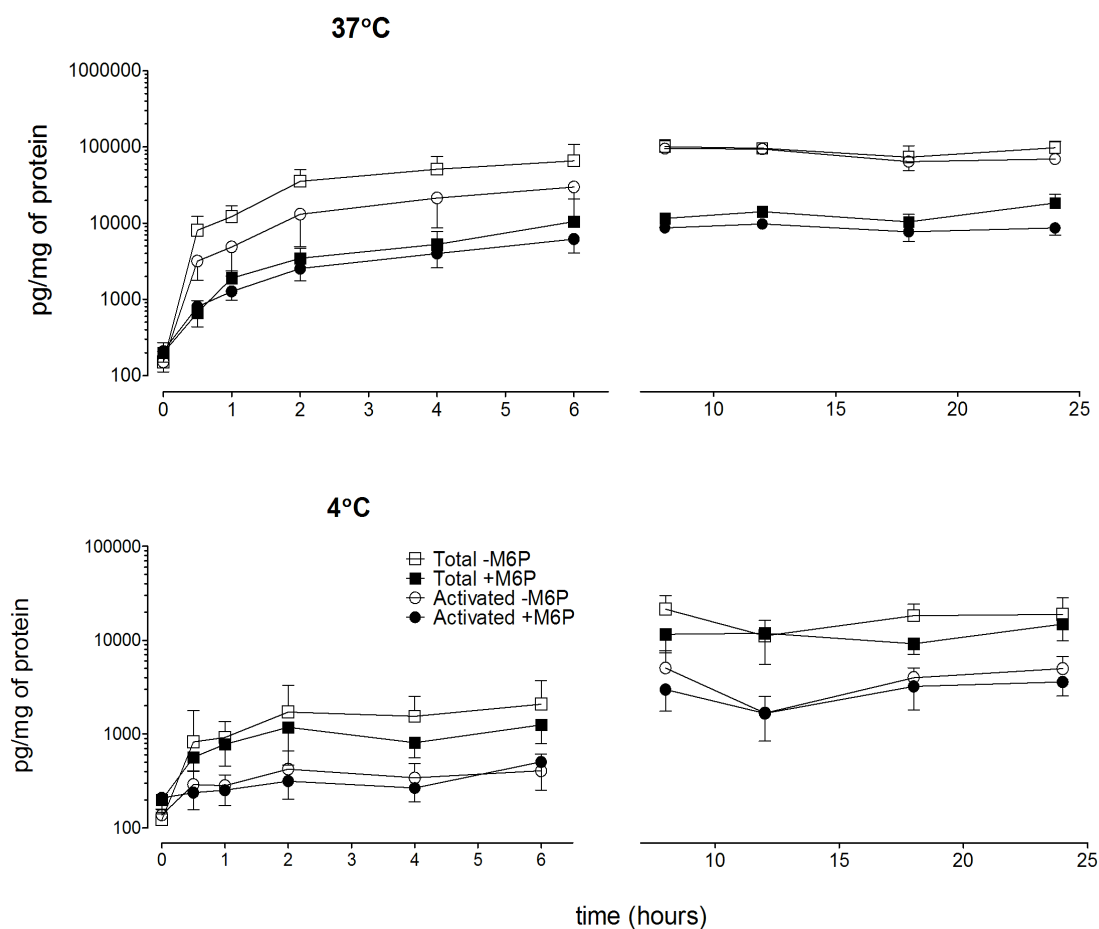


Figure 22. Time-dependent increase in the cellular levels of total and activated prorenin after incubation with 1000 U/L of prorenin in the absence or presence of 10 mmol/L M6P at 37°C or 4°C. Data (mean±SEM of 3-5 experiments) are expressed per mg of protein. Please note the difference in scale for the 37°C or 4°C data.

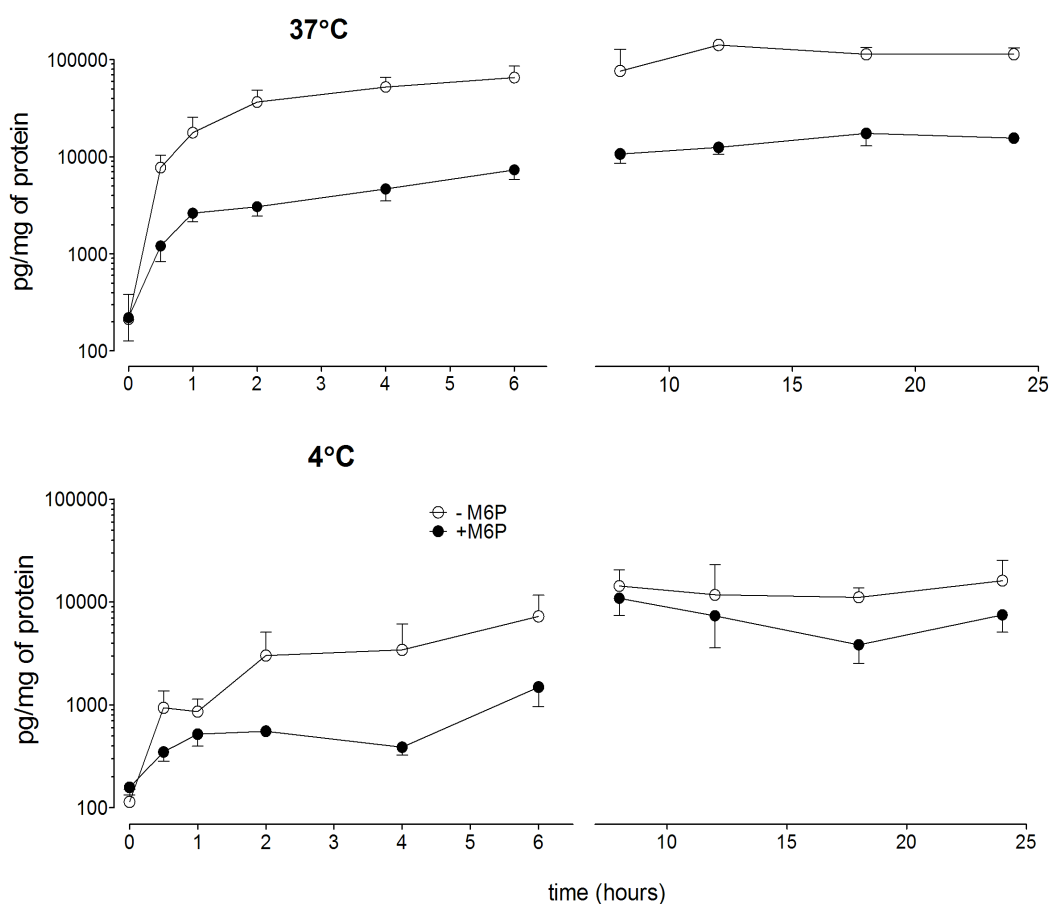
### 7.3.2 Albumin Uptake

Both M6P and RAP-GST blocked the uptake of labelled BSA at 37°C in a concentration-dependent manner, with  $IC_{50}$ 's of  $\approx 10$  mmol/L and 140  $\mu$ g/mL (corresponding with 21  $\mu$ mol/L), respectively (Figure 25).

## 7.4 DISCUSSION

The aim of this study was to investigate megalin-mediated renin and prorenin uptake by ciPTEC. PT physiology involves complex mechanisms for substance transporting. Until now, information about such transport arose from cell lines

expressing at most a few of the many transporters physiologically present in the PT, while megalin endocytosis has been investigated predominantly in non-human cells (232). ciPTEC express most of these transporters and efflux pumps, and possess the complete endocytosis machinery, thus making these cells a more appropriate model



to study PT physiology (232).

Figure 23. Time-dependent increase in the cellular levels of renin after incubation with 1000 U/L of renin in the absence or presence of 10 mmol/L M6P at 37°C or 4°C. Data (mean $\pm$ SEM of 3-5 experiments) are expressed per mg of protein.

The RAS is essential to maintain fluid-electrolyte homeostasis and blood pressure regulation. Moreover, the RAS also participates in the pathophysiology of cardiovascular and renal diseases, and consequently, its blockade is currently the crux in the treatment of these pathologies (37, 38). Recently, it has been suggested that urinary levels of RAS components, specifically renin and angiotensinogen, correlate to intrarenal RAS activity, thus making it possible to monitor hypertension worsening and kidney function deterioration by simply measuring renin and/or angiotensinogen in urine (235, 236). Yet, confusingly, although multiple studies

suggest that angiotensinogen is synthesized in the PT (supporting the existence of an independent intrarenal RAS), renal angiotensin II generation turned out to depend exclusively on liver-derived angiotensinogen (51), i.e., it was not affected by renal angiotensinogen KO, both under normal and pathological conditions. If so, a renal angiotensinogen uptake process might be a prerequisite for renal angiotensin production, e.g. involving megalin-mediated endocytosis (46). Curiously, prorenin, which is undetectable in urine, has been detected by Roksnoer et al. in urine of patients with Dent disease and Lowe syndrome, two disorders that are characterized by mutations that impair receptor-mediated endocytosis in the PT (230). This suggests that, normally, prorenin is completely reabsorbed from urine via the megalin pathway. This is not the case for renin, since renin can be detected in urine at levels corresponding to 6-7% of its plasma levels (236). Nevertheless, renin levels rose 20-40 fold in urine of patients with Dent disease and Lowe syndrome, in parallel with the levels of angiotensinogen. This finding, together with the close correlation between angiotensinogen and albumin levels in urine (230, 236, 237), argues against tubular secretion of renin and angiotensinogen, and rather suggests that these urinary components are derived from blood via glomerular filtration.

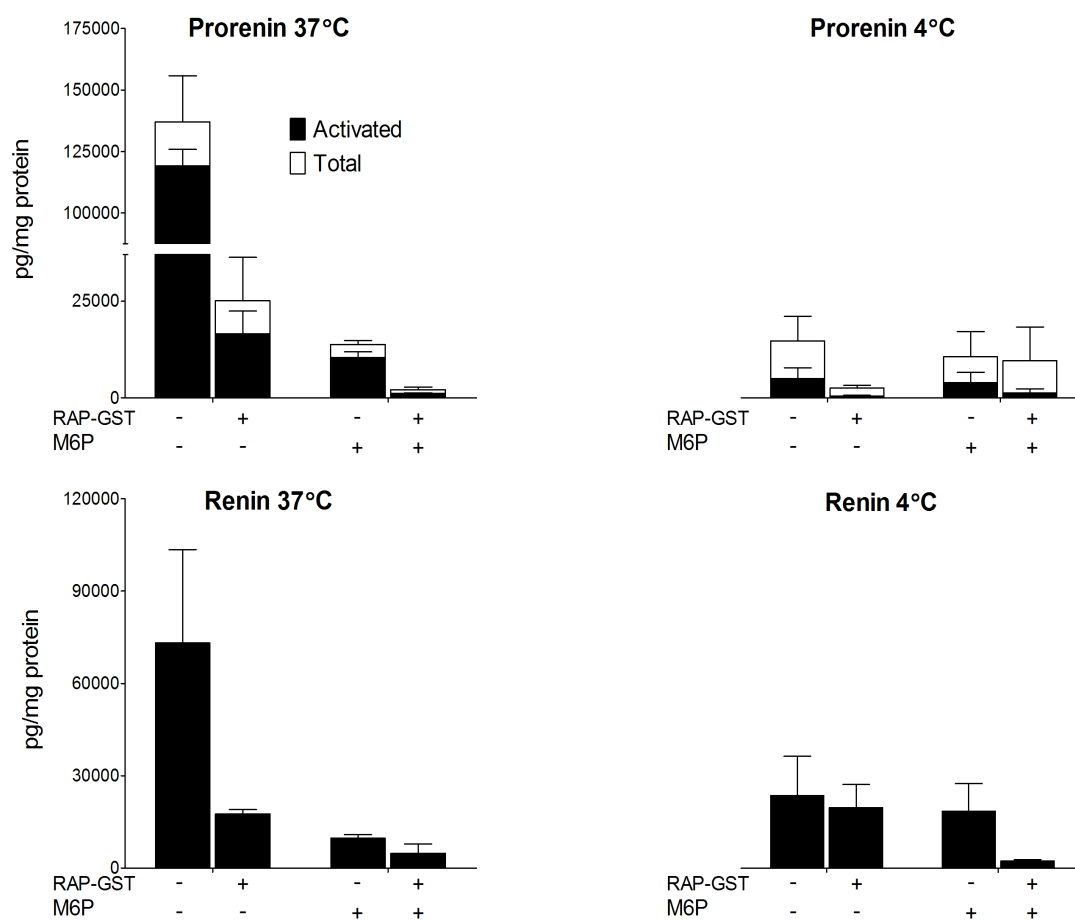


Figure 24. Cellular levels of prorenin (activated and total) and renin in the presence or absence of 10 mmol/L M6P and/or 100  $\mu$ g/mL RAP-GST in ciPTEC exposed to prorenin or renin (both 1000 U/L) at 37°C or 4°C. Data (mean $\pm$ SEM of 3 experiments) are expressed per mg of protein

In many studies with different cell types such as rat vascular smooth muscle cells, cardiomyocytes, fibroblasts, and human endothelial cells, it has been demonstrated that besides megalin, M6P receptors also bind and internalize renin and prorenin (238-240). Moreover, M6P receptor-mediated prorenin uptake resulted in prorenin activation, most likely as part of an intracellular clearance process, evidenced by the fact that we were unable to link this to intracellular angiotensin generation (239, 241). In the current study, the M6P-induced decrease in prorenin and renin uptake by ciPTEC suggests that these cells also display M6P receptor-mediated uptake of renin and prorenin. Not surprisingly, the effect of M6P was best seen at 37°C, since at this temperature (but not at 4°C), M6P receptors cycle continuously between the cell surface and the intracellular compartment, thus allowing substantial (pro)renin accumulation in the cells. In contrast, at 4°C, renin and

prorenin can only bind to cell surface M6P receptors, without being internalized (242), nor can prorenin activation occur. Thus, at 4°C, cellular renin/prorenin accumulation is very limited, making it more difficult to show blockade of this effect by M6P.

Two different M6PRs have been identified: the cation-independent type (or insulin-like growth factor II [IGFII] receptor) and the cation-dependent type. The IGFII/M6P receptor harbours two M6P binding sites, and is therefore able to bind to M6P-containing proteins, like renin and prorenin (238). Interestingly, this receptor was also described as a ligand for the megalin receptor (243). To what degree M6P itself acts as a ligand for the megalin receptor is unknown. Our results now show that the megalin inhibitor RAP-GST exerted identical effects as M6P (up to 90% inhibition of renin/prorenin uptake at 37°C, and a comparable, but much smaller effect at 4°C), and that both antagonists still exerted effects when added on top of each other. These data are suggestive for an interaction between megalin and M6P receptors and/or imply that M6P additionally blocks megalin-mediated pathways. To evaluate the latter, we studied the effect of M6P on the uptake of BSA, a widely accepted megalin ligand (228). Importantly, M6P not only blocked BSA uptake to the same degree as RAP-GST, but it also decreased RAP-GST endocytosis (data not shown). This therefore strongly suggests that M6P is a megalin receptor blocker.

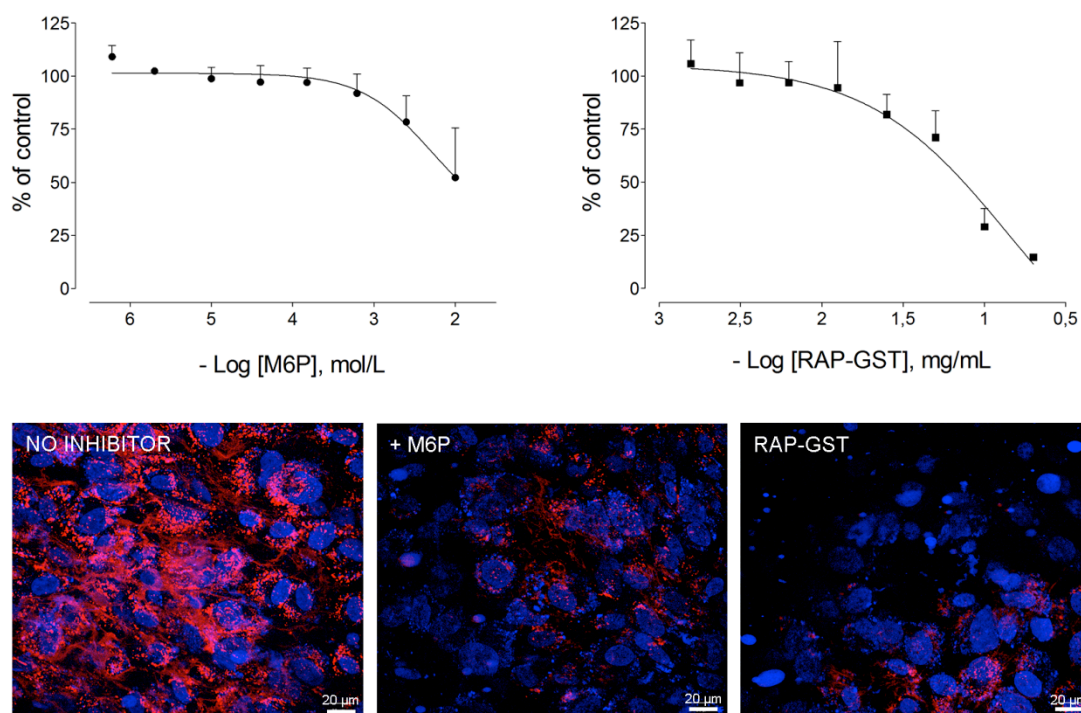


Figure 25. Inhibition of BSA uptake in ciPTEC by M6P and RAP-GST (top panels), and fluorescence staining representing BSA accumulation (bottom panels). Data (mean of 2 experiments) have been expressed as a percentage of control (cells incubated with BSA in the absence of inhibitor).

In summary, ciPTEC bind and internalize renin and prorenin in a time- and temperature-dependent manner. This process involves megalin and/or M6P receptors, and results in prorenin activation at 37°C. Both M6P and RAP-GST block this phenomenon to the same degree, most likely because M6P additionally blocks megalin-mediated uptake.

## 8 CONCLUSIONS AND PERSPECTIVES

More than a century has passed since the discovery of renin by Tigerstedt and Bergman in 1898. From that moment, research on the renin-angiotensin system (RAS) has never stopped growing, and notably, renin assumed a prominent position, as it is responsible for the first and rate-limiting step of the RAS cascade. It is now well-established that the RAS is a major player in blood pressure regulation and fluid electrolyte homeostasis, besides its participation in the pathophysiology of renal and cardiovascular diseases. Nevertheless, despite the extensive knowledge acquired so far, renin-producing cells (RPC) are still a conundrum, and only recently, these cells are starting to be deciphered. RPCs play a much more in-depth role than simply producing and releasing renin. Their huge phenotypical plasticity, exemplified in the “recruitment phenomenon”, allows them to work as pluripotent progenitors for different kidney cell types.

Just recently, RPCs have been connected to tissue regeneration, inflammation and possibly fibrosis. Interestingly, our findings have revealed the PDGF  $\beta$  - PDGF  $\beta$  receptor signaling pathway as a potential regulator of the RPCs expression, able to shift their classical renin phenotype into an inflammatory phenotype. Yet, PDGF  $\beta$  is a pericyte marker, and the latter cells are known to wrap vascular walls and to possess a high phenotypical plasticity. Not surprisingly, RPCs are able to differentiate into pericytes and vice versa.

It's noteworthy that our findings do not support the concept of extrarenal sites of renin production, in particular in the brain. Multiple papers have speculated about (pro)renin production in the brain, possibly intracellularly, and about locally synthesized prorenin displaying activity following its binding to the brain (pro)renin receptor. However, no paper actually quantified brain (pro)renin in an appropriate manner. Our data now support that there is no (pro)renin in the brain except for the small amounts of renin and prorenin in trapped blood in brain tissue (which disappeared after buffer perfusion), thus arguing strongly against angiotensin production at brain tissue sites. Even if prorenin is released locally (e.g., in the ovary), we were unable to show that such prorenin would display activity at its site of release. Together with the recent insight that the (pro)renin receptor has functions beyond the RAS, and is unrelated to prorenin activation, this implies that we need to

find novel mechanisms supporting a role for prorenin, if any, in local angiotensin generation. Thus, JGC firmly remain the only source of renin in the body, on which angiotensin generation depends, and whether prorenin generates angiotensins locally under physiological or even pathological conditions remains to be proven.

Within the kidney, apart from JGC, also tubular cells have been proposed to synthesize prorenin. Surprisingly, angiotensin stimulates rather than inhibits this production (positive feedback, as opposed to its negative feedback in JGC), and there is no evidence for tubular renin production. To what degree this prorenin truly contributes to intrarenal angiotensin generation is still controversial; it was even suggested to act on angiotensinogen of tubular origin, for instance when bound to the (pro)renin receptor. Yet, making use of transgenic rodents not expressing renal angiotensinogen it became clear that renal angiotensin production depends entirely on plasma-derived angiotensinogen, i.e., angiotensinogen of hepatic origin. Studies in patients with defective proximal tubular reabsorption support megalin-dependent reabsorption of filtered angiotensinogen, renin and prorenin. Most likely, changes in urinary (pro)renin and angiotensinogen levels reflect changes in megalin-dependent reabsorption (regulated, among others, by angiotensin!) instead of independent tubular release of RAS components.

The benefit of RAS blockade in cardiovascular and renal disease is undisputed, but what is still controversial, is the optimal degree of RAS blockade. A high degree of RAS blockade may have additional beneficial effects, but also results in a higher incidence of side effects. The degree of blockade can be estimated from the increase in circulating renin, depicting the “recruitment” of new RPC along the afferent arterioles. The long-term consequences of this process are still unknown, nor do we know if it contributes to renal impairment in the future. Besides renin production, RPC would participate directly in the concentric vascular hypertrophy, despite the control of the blood pressure levels. Furthermore, many questions remain unanswered. Would these cells contribute to a fibrosis process, leading to architecture disruption and extracellular matrix production? If these cells possess tissue repair mechanisms, why are they switched off or dysfunctional? To what degree is tissue regeneration truly effective to restore the normal function? Would such regeneration be persistent or transient? Answering these questions, combined with a full understanding of local (renal) angiotensin production will ultimately allow more effective anti-hypertensive therapies, and better outcomes in patients with

cardiovascular and renal pathologies.

## REFERENCES

1. Phillips MI, Schmidt-Ott KM. The discovery of renin 100 years ago. *News Physiol Sci*. 1999;14:271-4.
2. Basso N, Terragno NA. History about the discovery of the renin-angiotensin system. *Hypertension*. 2001;38(6):1246-9.
3. Sparks MA, Crowley SD, Gurley SB, Mirotso M, Coffman TM. Classical Renin-Angiotensin system in kidney physiology. *Compr Physiol*. 2014;4(3):1201-28.
4. Weber KT. Aldosterone in congestive heart failure. *N Engl J Med*. 2001;345(23):1689-97.
5. Williams JS, Williams GH. 50th anniversary of aldosterone. *J Clin Endocrinol Metab*. 2003;88(6):2364-72.
6. Hackenthal E, Paul M, Ganten D, Taugner R. Morphology, physiology, and molecular biology of renin secretion. *Physiol Rev*. 1990;70(4):1067-116.
7. Schweda F, Friis U, Wagner C, Skott O, Kurtz A. Renin release. *Physiology (Bethesda)*. 2007;22:310-9.
8. Castrop H, Hocherl K, Kurtz A, Schweda F, Todorov V, Wagner C. Physiology of kidney renin. *Physiol Rev*. 2010;90(2):607-73.
9. Campbell DJ. Critical review of prorenin and (pro)renin receptor research. *Hypertension*. 2008;51(5):1259-64.
10. Danser AHJ, Deinum J. Renin, prorenin and the putative (pro)renin receptor. *Hypertension*. 2005;46:1069-76.
11. Neves FA, Duncan KG, Baxter JD. Cathepsin B is a prorenin processing enzyme. *Hypertension*. 1996;27(3 Pt 2):514-7.
12. Saris JJ, Derkx FHM, Lamers MJM, Saxena PR, Schalekamp MADH, Danser AHJ. Cardiomyocytes bind and activate native human prorenin: role of soluble mannose 6-phosphate receptors. *Hypertension*. 2001;37(2 Part 2):710-5.
13. Saris JJ, Derkx FHM, de Bruin RJA, Dekkers DHW, Lamers MJM, Saxena PR, et al. High-affinity prorenin binding to cardiac man-6-P/IGF-II receptors precedes proteolytic activation to renin. *Am J Physiol*. 2001;280(4):H1706-H115.
14. Saris JJ, van den Eijnden MMED, Lamers MJM, Saxena PR, Schalekamp MADH, Danser AHJ. Prorenin-induced myocyte proliferation: no role for intracellular angiotensin II. *Hypertension*. 2002;39(2 Pt 2):573-7.
15. Nguyen G, Delarue F, Burcklé C, Bouzahir L, Giller T, Sraer J-D. Pivotal role of the renin/prorenin receptor in angiotensin II production and cellular responses to renin. *J Clin Invest*. 2002;109:1417-27.
16. Nguyen G, Contrepas A. The (pro)renin receptors. *J Mol Med (Berl)*. 2008;86(6):643-6.

17. Nguyen G, Danser AH. Prorenin and (pro)renin receptor: a review of available data from in vitro studies and experimental models in rodents. *Exp Physiol*. 2008;93(5):557-63.
18. Danser AHJ. (Pro)renin receptors: are they biologically relevant? *Curr Opin Nephrol Hypertens*. 2009;18(1):74-8.
19. Contrepas A, Walker J, Koulakoff A, Franek KJ, Qadri F, Giaume C, et al. A role of the (pro)renin receptor in neuronal cell differentiation. *Am J Physiol Regul Integr Comp Physiol*. 2009;297(2):R250-7.
20. Benigni A, Cassis P, Remuzzi G. Angiotensin II revisited: new roles in inflammation, immunology and aging. *EMBO Mol Med*. 2010;2(7):247-57.
21. Ferrao FM, Lara LS, Lowe J. Renin-angiotensin system in the kidney: What is new? *World J Nephrol*. 2014;3(3):64-76.
22. Singh KD, Karnik SS. Angiotensin Receptors: Structure, Function, Signaling and Clinical Applications. *J Cell Signal*. 2016;1(2).
23. Zhuo JL, Ferrao FM, Zheng Y, Li XC. New frontiers in the intrarenal Renin-Angiotensin system: a critical review of classical and new paradigms. *Front Endocrinol (Lausanne)*. 2013;4:166.
24. Carey RM, Siragy HM. Newly recognized components of the renin-angiotensin system: potential roles in cardiovascular and renal regulation. *Endocr Rev*. 2003;24(3):261-71.
25. Burrell LM, Johnston CI, Tikellis C, Cooper ME. ACE2, a new regulator of the renin-angiotensin system. *Trends Endocrinol Metab*. 2004;15(4):166-9.
26. Turner AJ, Tipnis SR, Guy JL, Rice G, Hooper NM. ACEH/ACE2 is a novel mammalian metalloprotease and a homologue of angiotensin-converting enzyme insensitive to ACE inhibitors. *Can J Physiol Pharmacol*. 2002;80(4):346-53.
27. Gironacci MM, Adamo HP, Corradi G, Santos RA, Ortiz P, Carretero OA. Angiotensin (1-7) induces MAS receptor internalization. *Hypertension*. 2011;58(2):176-81.
28. Ferrario CM, Chappell MC, Tallant EA, Brosnihan KB, Diz DI. Counterregulatory actions of angiotensin-(1-7). *Hypertension*. 1997;30(3 Pt 2):535-41.
29. Santos RA, Ferreira AJ, Simoes ESAC. Recent advances in the angiotensin-converting enzyme 2-angiotensin(1-7)-Mas axis. *Exp Physiol*. 2008;93(5):519-27.
30. Yugandhar VG, Clark MA. Angiotensin III: a physiological relevant peptide of the renin angiotensin system. *Peptides*. 2013;46:26-32.
31. Chai SY, Fernando R, Peck G, Ye SY, Mendelsohn FA, Jenkins TA, et al. The angiotensin IV/AT4 receptor. *Cell Mol Life Sci*. 2004;61(21):2728-37.
32. Stragier B, De Bundel D, Sarre S, Smolders I, Vauquelin G, Dupont A, et al. Involvement of insulin-regulated aminopeptidase in the effects of the renin-angiotensin fragment angiotensin IV: a review. *Heart Fail Rev*. 2008;13(3):321-37.
33. Villela DC, Passos-Silva DG, Santos RA. Alamandine: a new member of the angiotensin family. *Curr Opin Nephrol Hypertens*. 2014;23(2):130-4.

34. Etelvino GM, Peluso AA, Santos RA. New components of the renin-angiotensin system: alamandine and the MAS-related G protein-coupled receptor D. *Curr Hypertens Rep.* 2014;16(6):433.
35. Kumar R, Thomas CM, Yong QC, Chen W, Baker KM. The intracrine renin-angiotensin system. *Clin Sci (Lond).* 2012;123(5):273-84.
36. Paul M, Poyan Mehr A, Kreutz R. Physiology of local renin-angiotensin systems. *Physiol Rev.* 2006;86(3):747-803.
37. Brewster UC, Perazella MA. The renin-angiotensin-aldosterone system and the kidney: effects on kidney disease. *Am J Med.* 2004;116(4):263-72.
38. Unger T, Li J. The role of the renin-angiotensin-aldosterone system in heart failure. *J Renin Angiotensin Aldosterone Syst.* 2004;5 Suppl 1:S7-10.
39. Gomez RA, Norwood VF. Developmental consequences of the renin-angiotensin system. *Am J Kidney Dis.* 1995;26(3):409-31.
40. Campbell DJ. Clinical relevance of local Renin Angiotensin systems. *Front Endocrinol (Lausanne).* 2014;5:113.
41. De Mello WC, Frohlich ED. Clinical perspectives and fundamental aspects of local cardiovascular and renal Renin-Angiotensin systems. *Front Endocrinol (Lausanne).* 2014;5:16.
42. Wright JW, Harding JW. The brain angiotensin system and extracellular matrix molecules in neural plasticity, learning, and memory. *Prog Neurobiol.* 2004;72(4):263-93.
43. Aroor AR, Demarco VG, Jia G, Sun Z, Nistala R, Meininger GA, et al. The role of tissue Renin-Angiotensin-aldosterone system in the development of endothelial dysfunction and arterial stiffness. *Front Endocrinol (Lausanne).* 2013;4:161.
44. Herr D, Bekes I, Wulff C. Local Renin-Angiotensin system in the reproductive system. *Front Endocrinol (Lausanne).* 2013;4:150.
45. Kurtz A, Wagner C. Regulation of renin secretion by angiotensin II-AT1 receptors. *J Am Soc Nephrol.* 1999;10 Suppl 11:S162-8.
46. Pohl M, Kaminski H, Castrop H, Bader M, Himmerkus N, Bleich M, et al. Intrarenal renin angiotensin system revisited: role of megalin-dependent endocytosis along the proximal nephron. *J Biol Chem.* 2010;285(53):41935-46.
47. van Esch JHM, Gembardt F, Sterner-Kock A, Heringer-Walther S, Le T, Lassner D, et al. Cardiac phenotype and angiotensin II levels in AT1a, AT1b and AT2 receptor single, double and triple knockouts *Cardiovasc Res.* 2010;86:401-9.
48. Gonzalez-Villalobos RA, Janjoulia T, Fletcher NK, Giani JF, Nguyen MT, Riquier-Brison AD, et al. The absence of intrarenal ACE protects against hypertension. *J Clin Invest.* 2013;123(5):2011-23.
49. Lu X, Roksnoer LC, Danser AH. The intrarenal renin-angiotensin system: does it exist? Implications from a recent study in renal angiotensin-converting enzyme knockout mice. *Nephrol Dial Transplant.* 2013;28(12):2977-82.
50. Matsusaka T, Niimura F, Pastan I, Shintani A, Nishiyama A, Ichikawa I. Podocyte injury enhances filtration of liver-derived angiotensinogen and renal angiotensin II generation. *Kidney Int.* 2014;85(5):1068-77.

51. Matsusaka T, Niimura F, Shimizu A, Pastan I, Saito A, Kobori H, et al. Liver angiotensinogen is the primary source of renal angiotensin II. *J Am Soc Nephrol.* 2012;23(7):1181-9.
52. Krop M, de Bruyn JH, Derkx FH, Danser AH. Renin and prorenin disappearance in humans post-nephrectomy: evidence for binding? *Front Biosci.* 2008;13:3931-9.
53. Jennette JC, Heptinstall RH. *Heptinstall's pathology of the kidney.* 6th ed. Philadelphia, PA: Lippincott Williams & Wilkins; 2007.
54. Karginova EA, Pentz ES, Kazakova IG, Norwood VF, Carey RM, Gomez RA. Zis: a developmentally regulated gene expressed in juxtaglomerular cells. *Am J Physiol.* 1997;273(5 Pt 2):F731-F8.
55. Castellanos-Rivera RM, Pentz ES, Lin E, Gross KW, Medrano S, Yu J, et al. Recombination signal binding protein for Ig-kappaJ region regulates juxtaglomerular cell phenotype by activating the myo-endocrine program and suppressing ectopic gene expression. *J Am Soc Nephrol.* 2015;26(1):67-80.
56. Sequeira Lopez ML, Gomez RA. Novel mechanisms for the control of renin synthesis and release. *Curr Hypertens Rep.* 2010;12(1):26-32.
57. Pan L, Gross KW. Transcriptional regulation of renin: an update. *Hypertension.* 2005;45(1):3-8.
58. Gomez RA, Pupilli C, Everett AD. Molecular and cellular aspects of renin during kidney ontogeny. *Pediatr Nephrol.* 1991;5(1):80-7.
59. Reddi V, Zaglul A, Pentz ES, Gomez RA. Renin-expressing cells are associated with branching of the developing kidney vasculature. *J Am Soc Nephrol.* 1998;9(1):63-71.
60. Pentz ES, Moyano MA, Thornhill BA, Sequeira Lopez ML, Gomez RA. Ablation of renin-expressing juxtaglomerular cells results in a distinct kidney phenotype. *Am J Physiol Regul Integr Comp Physiol.* 2004;286(3):R474-R83.
61. Sequeira Lopez ML, Gomez RA. Development of the renal arterioles. *J Am Soc Nephrol.* 2011;22(12):2156-65.
62. Michos O. Kidney development: from ureteric bud formation to branching morphogenesis. *Curr Opin Genet Dev.* 2009;19(5):484-90.
63. Gilbert SF. *Developmental biology.* 6th ed. Sunderland, Mass.: Sinauer Associates; 2000. xviii, 749 p. p.
64. Hohenstein P, Pritchard-Jones K, Charlton J. The yin and yang of kidney development and Wilms' tumors. *Genes Dev.* 2015;29(5):467-82.
65. Sequeira Lopez ML, Pentz ES, Robert B, Abrahamson DR, Gomez RA. Embryonic origin and lineage of juxtaglomerular cells. *Am J Physiol Renal Physiol.* 2001;281(2):F345-F56.
66. Gomez RA, Belyea B, Medrano S, Pentz ES, Sequeira-Lopez ML. Fate and plasticity of renin precursors in development and disease. *Pediatr Nephrol.* 2014;29(4):721-6.

67. Sequeira-Lopez ML, Lin EE, Li M, Hu Y, Sigmund CD, Gomez RA. The earliest metanephric arteriolar progenitors and their role in kidney vascular development. *Am J Physiol Regul Integr Comp Physiol*. 2015;308(2):R138-R49.
68. Gomez RA, Sequeira-Lopez ML. Novel Functions of Renin Precursors in Homeostasis and Disease. *Physiology (Bethesda)*. 2016;31(1):25-33.
69. Gomez RA, Chevalier RL, Everett AD, Elwood JP, Peach MJ, Lynch KR, et al. Recruitment of renin gene-expressing cells in adult rat kidneys. *Am J Physiol*. 1990;259(4 Pt 2):F660-F5.
70. Matsushita K, Zhang Z, Pratt RE, Dzau VJ. Molecular mechanism of juxtaglomerular cell hyperplasia: a unifying hypothesis. *J Am Soc Hypertens*. 2007;1(3):164-8.
71. Everett AD, Carey RM, Chevalier RL, Peach MJ, Gomez RA. Renin release and gene expression in intact rat kidney microvessels and single cells. *J Clin Invest*. 1990;86(1):169-75.
72. Cantin M, Araujo-Nascimento MD, Benchimol S, Desormeaux Y. Metaplasia of smooth muscle cells into juxtaglomerular cells in the juxtaglomerular apparatus, arteries, and arterioles of the ischemic (endocrine) kidney. An ultrastructural-cytochemical and autoradiographic study. *Am J Pathol*. 1977;87(3):581-602.
73. Sequeira Lopez ML, Pentz ES, Nomasa T, Smithies O, Gomez RA. Renin cells are precursors for multiple cell types that switch to the renin phenotype when homeostasis is threatened. *Dev Cell*. 2004;6(5):719-28.
74. Tamura K, Chen YE, Horiuchi M, Chen Q, Daviet L, Yang Z, et al. LXRalpha functions as a cAMP-responsive transcriptional regulator of gene expression. *Proc Natl Acad Sci U S A*. 2000;97(15):8513-8.
75. Martini AG, Xa LK, Lacombe MJ, Blanchet-Cohen A, Mercure C, Haibe-Kains B, et al. Transcriptome Analysis of Human Reninomas as an Approach to Understanding Juxtaglomerular Cell Biology. *Hypertension*. 2017;69(6):1145-55.
76. Matsushita K, Morello F, Wu Y, Zhang L, Iwanaga S, Pratt RE, et al. Mesenchymal stem cells differentiate into renin-producing juxtaglomerular (JG)-like cells under the control of liver X receptor-alpha. *J Biol Chem*. 2010;285(16):11974-82.
77. Wang H, Gomez JA, Klein S, Zhang Z, Seidler B, Yang Y, et al. Adult renal mesenchymal stem cell-like cells contribute to juxtaglomerular cell recruitment. *J Am Soc Nephrol*. 2013;24(8):1263-73.
78. Yang Y, Gomez JA, Herrera M, Perez-Marco R, Repenning P, Zhang Z, et al. Salt restriction leads to activation of adult renal mesenchymal stromal cell-like cells via prostaglandin E2 and E-prostanoid receptor 4. *Hypertension*. 2015;65(5):1047-54.
79. Qian H, Le Blanc K, Sigvardsson M. Primary mesenchymal stem and progenitor cells from bone marrow lack expression of CD44 protein. *J Biol Chem*. 2012;287(31):25795-807.
80. Della Bruna R, Kurtz A, Schricker K. Regulation of renin synthesis in the juxtaglomerular cells. *Curr Opin Nephrol Hypertens*. 1996;5(1):16-9.

81. Klar J, Sandner P, Muller MW, Kurtz A. Cyclic AMP stimulates renin gene transcription in juxtaglomerular cells. *Pflugers Arch.* 2002;444(3):335-44.
82. Beierwaltes WH. The role of calcium in the regulation of renin secretion. *Am J Physiol Renal Physiol.* 2010;298(1):F1-F11.
83. Alberts B. *Molecular biology of the cell.* 5th ed. New York: Garland Science; 2008.
84. Chen L, Kim SM, Oppermann M, Faulhaber-Walter R, Huang Y, Mizel D, et al. Regulation of renin in mice with Cre recombinase-mediated deletion of G protein G $\alpha$  in juxtaglomerular cells. *Am J Physiol Renal Physiol.* 2007;292(1):F27-F37.
85. Neubauer B, Machura K, Chen M, Weinstein LS, Oppermann M, Sequeira-Lopez ML, et al. Development of vascular renin expression in the kidney critically depends on the cyclic AMP pathway. *Am J Physiol Renal Physiol.* 2009;296(5):F1006-F12.
86. Pentz ES, Lopez ML, Cordaillat M, Gomez RA. Identity of the renin cell is mediated by cAMP and chromatin remodeling: an in vitro model for studying cell recruitment and plasticity. *Am J Physiol Heart Circ Physiol.* 2008;294(2):H699-H707.
87. Schweda F, Kurtz A. Cellular mechanism of renin release. *Acta Physiol Scand.* 2004;181(4):383-90.
88. Grünberger C, Obermayer B, Klar J, Kurtz A, Schweda F. The calcium paradoxon of renin release: calcium suppresses renin exocytosis by inhibition of calcium-dependent adenylate cyclases AC5 and AC6. *Circ Res.* 2006;99(11):1197-206.
89. Ortiz-Capisano MC, Ortiz PA, Harding P, Garvin JL, Beierwaltes WH. Decreased intracellular calcium stimulates renin release via calcium-inhibitable adenylyl cyclase. *Hypertension.* 2007;49(1):162-9.
90. Klar J, Sigl M, Obermayer B, Schweda F, Kramer BK, Kurtz A. Calcium inhibits renin gene expression by transcriptional and posttranscriptional mechanisms. *Hypertension.* 2005;46(6):1340-6.
91. Ortiz-Capisano MC, Liao TD, Ortiz PA, Beierwaltes WH. Calcium-dependent phosphodiesterase 1C inhibits renin release from isolated juxtaglomerular cells. *Am J Physiol Regul Integr Comp Physiol.* 2009;297(5):R1469-R76.
92. Friis UG, Madsen K, Stubbe J, Hansen PB, Svenningsen P, Bie P, et al. Regulation of renin secretion by renal juxtaglomerular cells. *Pflugers Arch.* 2013;465(1):25-37.
93. Neubauer B, Machura K, Kettl R, Lopez ML, Friebe A, Kurtz A. Endothelium-derived nitric oxide supports renin cell recruitment through the nitric oxide-sensitive guanylate cyclase pathway. *Hypertension.* 2013;61(2):400-7.
94. Wang Z, Qin G, Zhao TC. HDAC4: mechanism of regulation and biological functions. *Epigenomics.* 2014;6(1):139-50.
95. Gomez RA, Pentz ES, Jin X, Cordaillat M, Sequeira Lopez ML. CBP and p300 are essential for renin cell identity and morphological integrity of the kidney. *Am J Physiol Heart Circ Physiol.* 2009;296(5):H1255-H62.
96. Pentz ES, Cordaillat M, Carretero OA, Tucker AE, Sequeira Lopez ML, Gomez RA. Histone acetyl transferases CBP and p300 are necessary for maintenance of

renin cell identity and transformation of smooth muscle cells to the renin phenotype. *Am J Physiol Heart Circ Physiol*. 2012;302(12):H2545-H52.

97. Bartel DP. MicroRNAs: genomics, biogenesis, mechanism, and function. *Cell*. 2004;116(2):281-97.

98. Ambros V. The functions of animal microRNAs. *Nature*. 2004;431(7006):350-5.

99. Watson JD. Molecular biology of the gene. Seventh edition ed. Boston: Pearson; 2014. xxxiv, 872 pages p.

100. Sequeira-Lopez ML, Weatherford ET, Borges GR, Monteagudo MC, Pentz ES, Harfe BD, et al. The microRNA-processing enzyme dicer maintains juxtaglomerular cells. *J Am Soc Nephrol*. 2010;21(3):460-7.

101. Medrano S, Monteagudo MC, Sequeira-Lopez ML, Pentz ES, Gomez RA. Two microRNAs, miR-330 and miR-125b-5p, mark the juxtaglomerular cell and balance its smooth muscle phenotype. *Am J Physiol Renal Physiol*. 2012;302(1):F29-F37.

102. Brunskill EW, Sequeira-Lopez ML, Pentz ES, Lin E, Yu J, Aronow BJ, et al. Genes that confer the identity of the renin cell. *J Am Soc Nephrol*. 2011;22(12):2213-25.

103. Liu MJ, Takahashi Y, Wada T, He J, Gao J, Tian Y, et al. The aldo-keto reductase *Akr1b7* gene is a common transcriptional target of xenobiotic receptors pregnane X receptor and constitutive androstane receptor. *Mol Pharmacol*. 2009;76(3):604-11.

104. Machura K, Iankilevitch E, Neubauer B, Theuring F, Kurtz A. The aldo-keto reductase *AKR1B7* coexpresses with renin without influencing renin production and secretion. *Am J Physiol Renal Physiol*. 2013;304(5):F578-F84.

105. Lai EC. Notch signaling: control of cell communication and cell fate. *Development*. 2004;131(5):965-73.

106. Borggreffe T, Oswald F. The Notch signaling pathway: transcriptional regulation at Notch target genes. *Cell Mol Life Sci*. 2009;66(10):1631-46.

107. Castellanos Rivera RM, Monteagudo MC, Pentz ES, Glenn ST, Gross KW, Carretero O, et al. Transcriptional regulator RBP-J regulates the number and plasticity of renin cells. *Physiol Genomics*. 2011;43(17):1021-8.

108. Lin EE, Sequeira-Lopez ML, Gomez RA. RBP-J in *FOXD1*+ renal stromal progenitors is crucial for the proper development and assembly of the kidney vasculature and glomerular mesangial cells. *Am J Physiol Renal Physiol*. 2014;306(2):F249-F58.

109. Rider SA, Mullins LJ, Verdon RF, MacRae CA, Mullins JJ. Renin expression in developing zebrafish is associated with angiogenesis and requires the Notch pathway and endothelium. *Am J Physiol Renal Physiol*. 2015;309(6):F531-F9.

110. Belyea BC, Xu F, Pentz ES, Medrano S, Li M, Hu Y, et al. Identification of renin progenitors in the mouse bone marrow that give rise to B-cell leukaemia. *Nat Commun*. 2014;5:3273.

111. Kurtz L, Schweda F, de Wit C, Kriz W, Witzgall R, Warth R, et al. Lack of connexin 40 causes displacement of renin-producing cells from afferent arterioles to the extraglomerular mesangium. *J Am Soc Nephrol*. 2007;18(4):1103-11.

112. Pippin JW, Kaverina NV, Eng DG, Krofft RD, Glenn ST, Duffield JS, et al. Cells of renin lineage are adult pluripotent progenitors in experimental glomerular disease. *Am J Physiol Renal Physiol*. 2015;309(4):F341-F58.
113. Kurt B, Paliege A, Willam C, Schwarzensteiner I, Schucht K, Neymeyer H, et al. Deletion of von Hippel-Lindau protein converts renin-producing cells into erythropoietin-producing cells. *J Am Soc Nephrol*. 2013;24(3):433-44.
114. Kurt B, Gerl K, Karger C, Schwarzensteiner I, Kurtz A. Chronic hypoxia-inducible transcription factor-2 activation stably transforms juxtaglomerular renin cells into fibroblast-like cells in vivo. *J Am Soc Nephrol*. 2015;26(3):587-96.
115. Martini AG, Xa LK, Lacombe M-J, Blanchet-Cohen A, Mercure C, Haibe-Kains B, et al. Transcriptome analysis of human reninomas as an approach to understanding juxtaglomerular cell biology. *Hypertension*. 2017;69:1145-55.
116. Pippin JW, Sparks MA, Glenn ST, Buitrago S, Coffman TM, Duffield JS, et al. Cells of renin lineage are progenitors of podocytes and parietal epithelial cells in experimental glomerular disease. *Am J Pathol*. 2013;183(2):542-57.
117. Kaverina NV, Kadoya H, Eng DG, Rusiniak ME, Sequeira-Lopez ML, Gomez RA, et al. Tracking the stochastic fate of cells of the renin lineage after podocyte depletion using multicolor reporters and intravital imaging. *PLoS One*. 2017;12(3):e0173891.
118. Starke C, Betz H, Hickmann L, Lachmann P, Neubauer B, Kopp JB, et al. Renin lineage cells repopulate the glomerular mesangium after injury. *J Am Soc Nephrol*. 2015;26(1):48-54.
119. Stefanska A, Kenyon C, Christian HC, Buckley C, Shaw I, Mullins JJ, et al. Human kidney pericytes produce renin. *Kidney Int*. 2016;90(6):1251-61.
120. Bergers G, Song S. The role of pericytes in blood-vessel formation and maintenance. *Neuro Oncol*. 2005;7(4):452-64.
121. Rider SA, Christian HC, Mullins LJ, Howarth AR, MacRae CA, Mullins JJ. Zebrafish mesonephric renin cells are functionally conserved and comprise of two distinct morphological populations. *Am J Physiol Renal Physiol*. 2017;312:F778-F90.
122. Gomez RA, Chevalier RL, Everett AD, Elwood JP, Peach MJ, Lynch KR, et al. Recruitment of renin gene-expressing cells in adult rat kidneys. *Am J Physiol*. 1990;259(4 Pt 2):F660-5.
123. Laframboise M, Reudelhuber TL, Jutras I, Brechler V, Seidah NG, Day R, et al. Prorenin activation and prohormone convertases in the mouse As4.1 cell line. *Kidney Int*. 1997;51(1):104-9.
124. Pinet F, Mizrahi J, Laboulandine I, Menard J, Corvol P. Regulation of prorenin secretion in cultured human transfected juxtaglomerular cells. *J Clin Invest*. 1987;80(3):724-31.
125. Gottardo F, Cesari M, Morra A, Gardiman M, Fassina A, Dal Bianco M. A kidney tumor in an adolescent with severe hypertension and hypokalemia: an uncommon case--case report and review of the literature on reninoma. *Urol Int*. 2010;85(1):121-4.
126. Wong L, Hsu TH, Perloth MG, Hofmann LV, Haynes CM, Katznelson L. Reninoma: case report and literature review. *J Hypertens*. 2008;26(2):368-73.

127. Mercure C, Prescott G, Lacombe MJ, Silversides DW, Reudelhuber TL. Chronic increases in circulating prorenin are not associated with renal or cardiac pathologies. *Hypertension*. 2009;53(6):1062-9.
128. Bolger AM, Lohse M, Usadel B. Trimmomatic: a flexible trimmer for Illumina sequence data. *Bioinformatics*. 2014;30(15):2114-20.
129. Kim D, Pertea G, Trapnell C, Pimentel H, Kelley R, Salzberg SL. TopHat2: accurate alignment of transcriptomes in the presence of insertions, deletions and gene fusions. *Genome Biol*. 2013;14(4):R36.
130. Legendre F, Cody N, Iampietro C, Bergalet J, Lefebvre FA, Moquin-Beaudry G, et al. Whole mount RNA fluorescent in situ hybridization of *Drosophila* embryos. *J Vis Exp*. 2013(71):e50057.
131. Krop M, van Veghel R, Garrelds IM, de Bruin RJA, van Gool JMG, van den Meiracker AH, et al. Cardiac renin levels are not influenced by the amount of resident mast cells. *Hypertension*. 2009;54:315-21.
132. Martin SA, Mynderse LA, Lager DJ, Chevillie JC. Juxtaglomerular cell tumor: a clinicopathologic study of four cases and review of the literature. *Am J Clin Pathol*. 2001;116(6):854-63.
133. Machura K, Iankilevitch E, Neubauer B, Theuring F, Kurtz A. The Aldo-keto reductase AKR1B7 coexpresses with renin without influencing renin production and secretion. *Am J Physiol Renal Physiol*. 2013;304(5):F578-84.
134. Berg AC, Chernavvsky-Sequeira C, Lindsey J, Gomez RA, Sequeira-Lopez ML. Pericytes synthesize renin. *World J Nephrol*. 2013;2(1):11-6.
135. Lin EE, Sequeira-Lopez ML, Gomez RA. RBP-J in FOXD1+ renal stromal progenitors is crucial for the proper development and assembly of the kidney vasculature and glomerular mesangial cells. *Am J Physiol Renal Physiol*. 2014;306(2):F249-58.
136. Morello F, de Boer RA, Steffensen KR, Gneccchi M, Chisholm JW, Boomsma F, et al. Liver X receptors alpha and beta regulate renin expression in vivo. *J Clin Invest*. 2005;115(7):1913-22.
137. Machura K, Neubauer B, Steppan D, Kettl R, Grobeta A, Kurtz A. Role of blood pressure in mediating the influence of salt intake on renin expression in the kidney. *Am J Physiol Renal Physiol*. 2012;302(10):F1278-85.
138. Nistala R, Zhang X, Sigmund CD. Differential expression of the closely linked KISS1, REN, and FLJ10761 genes in transgenic mice. *Physiol Genomics*. 2004;17(1):4-10.
139. Franchimont N, Durant D, Rydzziel S, Canalis E. Platelet-derived growth factor induces interleukin-6 transcription in osteoblasts through the activator protein-1 complex and activating transcription factor-2. *J Biol Chem*. 1999;274(10):6783-9.
140. Gianni-Barrera R, Bartolomeo M, Vollmar B, Djonov V, Banfi A. Split for the cure: VEGF, PDGF-BB and intussusception in therapeutic angiogenesis. *Biochem Soc Trans*. 2014;42(6):1637-42.
141. Suzuki N, Yamamoto M. Roles of renal erythropoietin-producing (REP) cells in the maintenance of systemic oxygen homeostasis. *Pflugers Arch*. 2016;468(1):3-12.

142. Neubauer B, Machura K, Rupp V, Tallquist MD, Betsholtz C, Sequeira-Lopez ML, et al. Development of renal renin-expressing cells does not involve PDGF-B-PDGFR-beta signaling. *Physiol Rep*. 2013;1(5):e00132.
143. Johns DW, Carey RM, Gomez RA, Lynch K, Inagami T, Saye J, et al. Isolation of renin-rich rat kidney cells. *Hypertension*. 1987;10(5):488-96.
144. Motegi S, Garfield S, Feng X, Sardy M, Udey MC. Potentiation of platelet-derived growth factor receptor-beta signaling mediated by integrin-associated MFG-E8. *Arterioscler Thromb Vasc Biol*. 2011;31(11):2653-64.
145. Liu Y, Long L, Yuan F, Liu F, Liu H, Peng Y, et al. High glucose-induced Galectin-1 in human podocytes implicates the involvement of Galectin-1 in diabetic nephropathy. *Cell Biol Int*. 2015;39(2):217-23.
146. Sato W, Sato Y. Midkine in nephrogenesis, hypertension and kidney diseases. *Br J Pharmacol*. 2014;171(4):879-87.
147. LeBleu VS, Teng Y, O'Connell JT, Charytan D, Muller GA, Muller CA, et al. Identification of human epididymis protein-4 as a fibroblast-derived mediator of fibrosis. *Nat Med*. 2013;19(2):227-31.
148. Hayakawa S, Ohashi K, Shibata R, Kataoka Y, Miyabe M, Enomoto T, et al. Cardiac myocyte-derived follistatin-like 1 prevents renal injury in a subtotal nephrectomy model. *J Am Soc Nephrol*. 2015;26(3):636-46.
149. Matsuba H, Watanabe T, Watanabe M, Ishii Y, Waguri S, Kominami E, et al. Immunocytochemical localization of prorenin, renin, and cathepsins B, H, and L in juxtaglomerular cells of rat kidney. *J Histochem Cytochem*. 1989;37(11):1689-97.
150. Wang PH, Do YS, Macaulay L, Shinagawa T, Anderson PW, Baxter JD, et al. Identification of renal cathepsin B as a human prorenin-processing enzyme. *J Biol Chem*. 1991;266(19):12633-8.
151. Ganten D, Minnich JL, Granger P, Hayduk K, Brecht HM, Barbeau A, et al. Angiotensin-forming enzyme in brain tissue. *Science*. 1971;173(3991):64-5.
152. Lee-Kirsch MA, Gaudet F, Cardoso MC, Lindpaintner K. Distinct renin isoforms generated by tissue-specific transcription initiation and alternative splicing. *Circ Res*. 1999;84(2):240-6.
153. Mercure C, Thibault G, Lussier-Cacan S, Davignon J, Schiffrin EL, Reudelhuber TL. Molecular analysis of human prorenin prosegment variants in vitro and in vivo. *J Biol Chem*. 1995;270(27):16355-9.
154. Peters J. Secretory and cytosolic (pro)renin in kidney, heart, and adrenal gland. *J Mol Med (Berl)*. 2008;86(6):711-4.
155. Grobe JL, Xu D, Sigmund CD. An intracellular renin-angiotensin system in neurons: fact, hypothesis, or fantasy. *Physiology (Bethesda)*. 2008;23:187-93.
156. Wanka H, Staar D, Lutze P, Peters B, Hildebrandt J, Beck T, et al. Anti-necrotic and cardioprotective effects of a cytosolic renin isoform under ischemia-related conditions. *J Mol Med (Berl)*. 2016;94(1):61-9.
157. Grobe JL, Rahmouni K, Liu X, Sigmund CD. Metabolic rate regulation by the renin-angiotensin system: brain vs. body. *Pflugers Arch*. 2013;465(1):167-75.

158. Shinohara K, Liu X, Morgan DA, Davis DR, Sequeira-Lopez ML, Cassell MD, et al. Selective deletion of the brain-specific isoform of renin causes neurogenic hypertension. *Hypertension*. 2016;68:1385-92.
159. Li W, Sullivan MN, Zhang S, Worker CJ, Xiong Z, Speth RC, et al. Intracerebroventricular infusion of the (pro)renin receptor antagonist PRO20 attenuates deoxycorticosterone acetate-salt-induced hypertension. *Hypertension*. 2015;65(2):352-61.
160. Li W, Peng H, Mehaffey EP, Kimball CD, Grobe JL, van Gool JMG, et al. Neuron-specific (pro)renin receptor knockout prevents the development of salt-sensitive hypertension. *Hypertension*. 2014;63(2):316-23.
161. Batenburg WW, Lu X, Leijten F, Maschke U, Müller DN, Danser AHJ. Renin- and prorenin-induced effects in rat vascular smooth muscle cells overexpressing the human (pro)renin receptor: does (pro)renin-(pro)renin receptor interaction actually occur? *Hypertension*. 2011;58(6):1111-9.
162. Batenburg WW, van den Heuvel M, van Esch JHM, van Veghel R, Garrelds IM, Leijten F, et al. The (pro)renin receptor blocker handle region peptide upregulates endothelium-derived contractile factors in aliskiren-treated diabetic transgenic (mREN2)27 rats. *J Hypertens*. 2013;31:292-302.
163. Takahashi N, Lopez ML, Cowhig JE, Jr., Taylor MA, Hatada T, Riggs E, et al. Ren1c homozygous null mice are hypotensive and polyuric, but heterozygotes are indistinguishable from wild-type. *J Am Soc Nephrol*. 2005;16(1):125-32.
164. Roksnoer LCW, van Veghel R, de Vries R, Garrelds IM, Bhaggoe UM, Friesema ECH, et al. Optimum AT1 receptor-nephrilysin inhibition has superior cardioprotective effects compared with AT1 receptor blockade alone in hypertensive rats. *Kidney International*. 2015;88:109-20.
165. Fraune C, Lange S, Krebs C, Holzel A, Baucke J, Divac N, et al. AT1 antagonism and renin inhibition in mice: pivotal role of targeting angiotensin II in chronic kidney disease. *Am J Physiol Renal Physiol*. 2012;303(7):F1037-F48.
166. Danser AHJ, van Kesteren CAM, Bax WA, Tavenier M, Derkx FHM, Saxena PR, et al. Prorenin, renin, angiotensinogen, and angiotensin-converting enzyme in normal and failing human hearts. Evidence for renin binding. *Circulation*. 1997;96(1):220-6.
167. Campbell DJ, Kladis A, Duncan AM. Nephrectomy, converting enzyme inhibition, and angiotensin peptides. *Hypertension*. 1993;22(4):513-22.
168. Su AI, Wiltshire T, Batalov S, Lapp H, Ching KA, Block D, et al. A gene atlas of the mouse and human protein-encoding transcriptomes. *Proc Natl Acad Sci U S A*. 2004;101(16):6062-7.
169. Wood JM, Maibaum J, Rahuel J, Grutter MG, Cohen NC, Rasetti V, et al. Structure-based design of aliskiren, a novel orally effective renin inhibitor. *Biochem Biophys Res Commun*. 2003;308(4):698-705.
170. Lu H, Rateri DL, Feldman DL, Jr RJ, Fukamizu A, Ishida J, et al. Renin inhibition reduces hypercholesterolemia-induced atherosclerosis in mice. *J Clin Invest*. 2008;118(3):984-93.

171. Batenburg WW, de Bruin RJA, van Gool JM, Müller DN, Bader M, Nguyen G, et al. Aliskiren-binding increases the half life of renin and prorenin in rat aortic vascular smooth muscle cells. *Arterioscler Thromb Vasc Biol.* 2008;28:1151-7.
172. Gregory TJ, Wallis CJ, Printz MP. Regional changes in rat brain angiotensinogen following bilateral nephrectomy. *Hypertension.* 1982;4(6):827-38.
173. Migliarini S, Pacini G, Pelosi B, Lunardi G, Pasqualetti M. Lack of brain serotonin affects postnatal development and serotonergic neuronal circuitry formation. *Mol Psychiatry.* 2013;18(10):1106-18.
174. Lange S, Fraune C, Alenina N, Bader M, Danser AHJ, Frenay AR, et al. Aliskiren accumulation in the kidney: no major role for binding to renin or prorenin. *J Hypertens.* 2013;31(4):713-9.
175. de Lannoy LM, Danser AHJ, van Kats JP, Schoemaker RG, Saxena PR, Schalekamp MADH. Renin-angiotensin system components in the interstitial fluid of the isolated perfused rat heart. Local production of angiotensin I. *Hypertension.* 1997;29(6):1240-51.
176. Heller LJ, Opsahl JA, Wernsing SE, Saxena R, Katz SA. Myocardial and plasma renin-angiotensinogen dynamics during pressure-induced cardiac hypertrophy. *Am J Physiol.* 1998;274(3 Pt 2):R849-R56.
177. Danser AHJ, van Kats JP, Admiraal PJJ, Derkx FHM, Lamers JMJ, Verdouw PD, et al. Cardiac renin and angiotensins. Uptake from plasma versus in situ synthesis. *Hypertension.* 1994;24(1):37-48.
178. Deinum J, Derkx FHM, Danser AHJ, Schalekamp MADH. Identification and quantification of renin and prorenin in the bovine eye. *Endocrinology.* 1990;126(3):1673-82.
179. Xu D, Borges GR, Davis DR, Agassandian K, Sequeira Lopez ML, Gomez RA, et al. Neuron- or glial-specific ablation of secreted renin does not affect renal renin, baseline arterial pressure, or metabolism. *Physiol Genomics.* 2011;43(6):286-94.
180. Xu D, Borges GR, Grobe JL, Pelham CJ, Yang B, Sigmund CD. Preservation of intracellular renin expression is insufficient to compensate for genetic loss of secreted renin. *Hypertension.* 2009;54(6):1240-7.
181. Lavoie JL, Liu X, Bianco RA, Beltz TG, Johnson AK, Sigmund CD. Evidence supporting a functional role for intracellular renin in the brain. *Hypertension.* 2006;47(3):461-6.
182. Bader M, Ganten D. It's renin in the brain: transgenic animals elucidate the brain renin angiotensin system. *Circ Res.* 2002;90(1):8-10.
183. Lippoldt A, Fuxe K, Luft FC. A view of renin in the brain. *J Mol Med (Berl).* 2001;79(2-3):71-3.
184. Saavedra JM. Brain angiotensin II: new developments, unanswered questions and therapeutic opportunities. *Cell Mol Neurobiol.* 2005;25(3-4):485-512.
185. Kubo T, Ikezawa A, Kambe T, Hagiwara Y, Fukumori R. Renin antisense injected intraventricularly decreases blood pressure in spontaneously hypertensive rats. *Brain Res Bull.* 2001;56(1):23-8.

186. Campbell DJ, Duncan AM, Kladis A. Angiotensin-converting enzyme inhibition modifies angiotensin but not kinin peptide levels in human atrial tissue. *Hypertension*. 1999;34(2):171-5.
187. van Kats JP, Danser AHJ, van Meegen JR, Sassen LM, Verdouw PD, Schalekamp MADH. Angiotensin production by the heart: a quantitative study in pigs with the use of radiolabeled angiotensin infusions. *Circulation*. 1998;98(1):73-81.
188. Klotz S, Burkhoff D, Garrelds IM, Boomsma F, Danser AHJ. The impact of left ventricular assist device-induced left ventricular unloading on the myocardial renin-angiotensin-aldosterone system: therapeutic consequences? *Eur Heart J*. 2009;30(7):805-12.
189. Davisson RL, Yang G, Beltz TG, Cassell MD, Johnson AK, Sigmund CD. The brain renin-angiotensin system contributes to the hypertension in mice containing both the human renin and human angiotensinogen transgenes. *Circ Res*. 1998;83(10):1047-58.
190. Thomas WG, Sernia C. Immunocytochemical localization of angiotensinogen in the rat brain. *Neuroscience*. 1988;25(1):319-41.
191. Ito T, Eggena P, Barrett JD, Katz D, Metter J, Sambhi MP. Studies on angiotensinogen of plasma and cerebrospinal fluid in normal and hypertensive human subjects. *Hypertension*. 1980;2(4):432-6.
192. Schelling P, Muller S, Clauser E. Regulation of angiotensinogen in cerebrospinal fluid and plasma of rats. *Am J Physiol*. 1983;244(4):R466-71.
193. Schinke M, Baltatu O, Bohm M, Peters J, Rascher W, Bricca G, et al. Blood pressure reduction and diabetes insipidus in transgenic rats deficient in brain angiotensinogen. *Proc Natl Acad Sci U S A*. 1999;96(7):3975-80.
194. Intebi AD, Flaxman MS, Ganong WF, Deschepper CF. Angiotensinogen production by rat astroglial cells in vitro and in vivo. *Neuroscience*. 1990;34(3):545-54.
195. Milsted A, Barna BP, Ransohoff RM, Brosnihan KB, Ferrario CM. Astrocyte cultures derived from human brain tissue express angiotensinogen mRNA. *Proc Natl Acad Sci U S A*. 1990;87(15):5720-3.
196. van Kats JP, Chai W, Duncker DJ, Schalekamp MADH, Danser AHJ. Adrenal angiotensin. Origin and site of generation. *Am J Hypertens*. 2005;18:1045-51.
197. van Kats JP, Schalekamp MADH, Verdouw PD, Duncker DJ, Danser AHJ. Intrarenal angiotensin II: interstitial and cellular levels and site of production. *Kidney Int*. 2001;60:2311-7.
198. Campbell DJ, Kladis A, Duncan AM. Effects of converting enzyme inhibitors on angiotensin and bradykinin peptides. *Hypertension*. 1994;23(4):439-49.
199. van Kats JP, de Lannoy LM, Danser AHJ, van Meegen JR, Verdouw PD, Schalekamp MADH. Angiotensin II type 1 (AT1) receptor-mediated accumulation of angiotensin II in tissues and its intracellular half-life in vivo. *Hypertension*. 1997;30(1 Pt 1):42-9.
200. van Kats JP, van Meegen JR, Verdouw PD, Duncker DJ, Schalekamp MADH, Danser AHJ. Subcellular localization of angiotensin II in kidney and adrenal. *J Hypertens*. 2001;19:583-9.

201. Pelisch N, Hosomi N, Ueno M, Nakano D, Hitomi H, Mogi M, et al. Blockade of AT1 receptors protects the blood-brain barrier and improves cognition in Dahl salt-sensitive hypertensive rats. *Am J Hypertens*. 2011;24(3):362-8.
202. Morales R, Watier Y, Böcskei Z. Human prorenin structure sheds light on a novel mechanism of its autoinhibition and on its non-proteolytic activation by the (pro)renin receptor. *J Mol Biol*. 2012;421(1):100-11.
203. Schalekamp MADH, Derkx FHM, Deinum J, Danser AHJ. Newly developed renin and prorenin assays and the clinical evaluation of renin inhibitors. *J Hypertens*. 2008;26:928-37.
204. Krop M, van Gool JM, Day D, Hollenberg NK, Danser AHJ. Evaluation of a direct prorenin assay making use of a monoclonal antibody directed against residues 32-39 of the prosegment. *J Hypertens*. 2011;29:2138-46.
205. Derkx FHM, Deinum J, Lipovski M, Verhaar M, Fischli W, Schalekamp MADH. Nonproteolytic "activation" of prorenin by active site-directed renin inhibitors as demonstrated by renin-specific monoclonal antibody. *J Biol Chem*. 1992;267(32):22837-42.
206. Krop M, Lu X, Verdonk K, Schalekamp MADH, van Gool JM, McKeever BM, et al. New renin inhibitor VTP-27999 alters renin immunoreactivity and does not unfold prorenin. *Hypertension*. 2013;61(5):1075-82.
207. Rahuel J, Priestle JP, Grütter MG. The crystal structures of recombinant glycosylated human renin alone and in complex with a transition state analog inhibitor. *J Struct Biol*. 1991;107(3):227-36.
208. Batenburg WW, Krop M, Garrelds IM, de Vries R, de Bruin RJA, Burcklé C, et al. Prorenin is the endogenous agonist of the (pro)renin receptor. Binding kinetics of renin and prorenin in rat vascular smooth muscle cells overexpressing the human (pro)renin receptor. *J Hypertens*. 2007;25:2441-53.
209. Chu WN, Baxter JD, Reudelhuber TL. A targeting sequence for dense secretory granules resides in the active renin protein moiety of human preprorenin. *Mol Endocrinol*. 1990;4(12):1905-13.
210. Markoff E, Zeitler P, Peleg S, Handwerker S. Characterization of the synthesis and release of prolactin by an enriched fraction of human decidual cells. *J Clin Endocrinol Metab*. 1983;56(5):962-8.
211. Galen FX, Devaux C, Atlas S, Guyenne T, Menard J, Corvol P, et al. New monoclonal antibodies directed against human renin. Powerful tools for the investigation of the renin system. *J Clin Invest*. 1984;74(3):723-35.
212. Campbell DJ, Nussberger J, Stowasser M, Danser AHJ, Morganti A, Frandsen E, et al. Activity assays and immunoassays for plasma renin and prorenin: information provided and precautions necessary for accurate measurement. *Clin Chem*. 2009;55(5):867-77.
213. Krop M, Garrelds IM, de Bruin RJA, van Gool JMG, Fisher ND, Hollenberg NK, et al. Aliskiren accumulates in renin secretory granules and binds plasma prorenin. *Hypertension*. 2008;52(6):1076-83.
214. Schweda F, Friis U, Wagner C, Skott O, Kurtz A. Renin release. *Physiology*. 2007;22:310-9.

215. Deinum J, Derkx FHM, Schalekamp MADH. Probing epitopes on human prorenin during its proteolytic and non-proteolytic activation. *Biochim Biophys Acta*. 1998;1388(2):386-96.
216. Derkx FHM, Schalekamp MPA, Schalekamp MADH. Two-step prorenin-renin conversion. Isolation of an intermediary form of activated prorenin. *J Biol Chem*. 1987;262(6):2472-7.
217. Sealey JE. Plasma renin activity and plasma prorenin assays. *Clin Chem*. 1991;37(10 Pt 2):1811-9.
218. van Kesteren CAM, Saris JJ, Dekkers DHW, Lamers JMJ, Saxena PR, Schalekamp MADH, et al. Cultured neonatal rat cardiac myocytes and fibroblasts do not synthesize renin or angiotensinogen: evidence for stretch-induced cardiomyocyte hypertrophy independent of angiotensin II. *Cardiovasc Res*. 1999;43(1):148-56.
219. Kinouchi K, Ichihara A, Sano M, Sun-Wada GH, Wada Y, Kurauchi-Mito A, et al. The (pro)renin receptor/ATP6AP2 is essential for vacuolar H<sup>+</sup>-ATPase assembly in murine cardiomyocytes. *Circ Res*. 2010;107(1):30-4.
220. Lu X, Meima ME, Nelson JK, Sorrentino V, Loregger A, Scheij S, et al. Identification of the (pro)renin receptor as a novel regulator of low-density lipoprotein metabolism. *Circ Res*. 2016;118:222-9.
221. Riediger F, Quack I, Qadri F, Hartleben B, Park J-K, Potthoff SA, et al. Prorenin receptor is essential for podocyte autophagy and survival *J Am Soc Nephrol*. 2011;22:2193-202.
222. Trepiccione F, Gerber SD, Grahammer F, Lopez-Cayuqueo KI, Baudrie V, Paunescu TG, et al. Renal ATP6ap2/(pro)renin receptor is required for normal vacuolar H<sup>+</sup>-ATPase function but not for the renin-angiotensin system. *J Am Soc Nephrol*. 2016.
223. Rose BD, Post TW. *Clinical physiology of acid-base and electrolyte disorders*. 5th ed. New York: McGraw-Hill, Medical Pub. Division; 2001. x, 992 p. p.
224. Curthoys NP, Moe OW. Proximal tubule function and response to acidosis. *Clin J Am Soc Nephrol*. 2014;9(9):1627-38.
225. Garcia NH, Ramsey CR, Knox FG. Understanding the Role of Paracellular Transport in the Proximal Tubule. *News Physiol Sci*. 1998;13:38-43.
226. Christensen EI, Birn H, Storm T, Weyer K, Nielsen R. Endocytic receptors in the renal proximal tubule. *Physiology (Bethesda)*. 2012;27(4):223-36.
227. Nielsen R, Christensen EI, Birn H. Megalin and cubilin in proximal tubule protein reabsorption: from experimental models to human disease. *Kidney Int*. 2016;89(1):58-67.
228. Dickson LE, Wagner MC, Sandoval RM, Molitoris BA. The proximal tubule and albuminuria: really! *J Am Soc Nephrol*. 2014;25(3):443-53.
229. Bokenkamp A, Ludwig M. Disorders of the renal proximal tubule. *Nephron Physiol*. 2011;118(1):p1-6.
230. Roksnoer LC, Heijnen BF, Nakano D, Peti-Peterdi J, Walsh SB, Garrelds IM, et al. On the Origin of Urinary Renin: A Translational Approach. *Hypertension*. 2016;67(5):927-33.

231. Wilmer MJ, Saleem MA, Masereeuw R, Ni L, van der Velden TJ, Russel FG, et al. Novel conditionally immortalized human proximal tubule cell line expressing functional influx and efflux transporters. *Cell Tissue Res.* 2010;339(2):449-57.
232. Caetano-Pinto P, Janssen MJ, Gijzen L, Verscheijden L, Wilmer MJ, Masereeuw R. Fluorescence-Based Transport Assays Revisited in a Human Renal Proximal Tubule Cell Line. *Mol Pharm.* 2016;13(3):933-44.
233. Krop M, Garrelds IM, de Bruin RJ, van Gool JM, Fisher ND, Hollenberg NK, et al. Aliskiren accumulates in Renin secretory granules and binds plasma prorenin. *Hypertension.* 2008;52(6):1076-83.
234. Batenburg WW, de Bruin RJ, van Gool JM, Muller DN, Bader M, Nguyen G, et al. Aliskiren-binding increases the half life of renin and prorenin in rat aortic vascular smooth muscle cells. *Arterioscler Thromb Vasc Biol.* 2008;28(6):1151-7.
235. Yamamoto T, Nakagawa T, Suzuki H, Ohashi N, Fukasawa H, Fujigaki Y, et al. Urinary angiotensinogen as a marker of intrarenal angiotensin II activity associated with deterioration of renal function in patients with chronic kidney disease. *J Am Soc Nephrol.* 2007;18(5):1558-65.
236. van den Heuvel M, Batenburg WW, Jainandunsing S, Garrelds IM, van Gool JM, Feelders RA, et al. Urinary renin, but not angiotensinogen or aldosterone, reflects the renal renin-angiotensin-aldosterone system activity and the efficacy of renin-angiotensin-aldosterone system blockade in the kidney. *J Hypertens.* 2011;29(11):2147-55.
237. Kobori H, Alper AB, Jr., Shenava R, Katsurada A, Saito T, Ohashi N, et al. Urinary angiotensinogen as a novel biomarker of the intrarenal renin-angiotensin system status in hypertensive patients. *Hypertension.* 2009;53(2):344-50.
238. van den Eijnden MM, Saris JJ, de Bruin RJ, de Wit E, Sluiter W, Reudelhuber TL, et al. Prorenin accumulation and activation in human endothelial cells: importance of mannose 6-phosphate receptors. *Arterioscler Thromb Vasc Biol.* 2001;21(6):911-6.
239. Saris JJ, Derkx FH, De Bruin RJ, Dekkers DH, Lamers JM, Saxena PR, et al. High-affinity prorenin binding to cardiac man-6-P/IGF-II receptors precedes proteolytic activation to renin. *Am J Physiol Heart Circ Physiol.* 2001;280(4):H1706-15.
240. Saris JJ, Derkx FH, Lamers JM, Saxena PR, Schalekamp MA, Danser AH. Cardiomyocytes bind and activate native human prorenin : role of soluble mannose 6-phosphate receptors. *Hypertension.* 2001;37(2 Pt 2):710-5.
241. Saris JJ, van den Eijnden MM, Lamers JM, Saxena PR, Schalekamp MA, Danser AH. Prorenin-induced myocyte proliferation: no role for intracellular angiotensin II. *Hypertension.* 2002;39(2 Pt 2):573-7.
242. Batenburg WW, Krop M, Garrelds IM, de Vries R, de Bruin RJ, Burckle CA, et al. Prorenin is the endogenous agonist of the (pro)renin receptor. Binding kinetics of renin and prorenin in rat vascular smooth muscle cells overexpressing the human (pro)renin receptor. *J Hypertens.* 2007;25(12):2441-53.
243. Christensen EI, Verroust PJ, Nielsen R. Receptor-mediated endocytosis in renal proximal tubule. *Pflugers Arch.* 2009;458(6):1039-48.

